

Syracuse University

**SURFACE**

---

Dissertations - ALL

SURFACE

---

June 2017

## Early universe cosmology as a probe of fundamental physics

Ogan Ozsoy  
*Syracuse University*

Follow this and additional works at: <https://surface.syr.edu/etd>



Part of the [Physical Sciences and Mathematics Commons](#)

---

### Recommended Citation

Ozsoy, Ogan, "Early universe cosmology as a probe of fundamental physics" (2017). *Dissertations - ALL*. 737.

<https://surface.syr.edu/etd/737>

This Dissertation is brought to you for free and open access by the SURFACE at SURFACE. It has been accepted for inclusion in Dissertations - ALL by an authorized administrator of SURFACE. For more information, please contact [surface@syr.edu](mailto:surface@syr.edu).

# Abstract

Cosmology, together with cosmological and astrophysical observations of ever increasing precision, represents a unique opportunity to study physics at energies far beyond the reach of terrestrial laboratories. In particular, observations of the cosmic microwave background radiation supports the idea for an early phase of accelerated expansion called inflation. While the simplest inflationary models provide a consistent theoretical framework in explaining observational data, we are yet to understand the microscopic details of the inflationary dynamics, the process of how the inflation ends and how the evolution in the post-inflationary era proceeds. In this dissertation, we will explore observational consequences of well-motivated scenarios in the early universe both from a top-down and bottom-up perspective. In particular, motivated by the null results of low energy searches of supersymmetry at Large Hadron Collider, we will first focus on the so-called Split Supersymmetry scenarios including a stable dark matter candidate and study observational signatures/constraints of (on) these models. Next, we investigate the phenomenology of particle production events during inflation focusing on cases that are well motivated both by UV physics and bottom-up EFT considerations. Considering the cosmological correlators in the presence of particle production, we explore the viability of scenarios in light of recent data on the Cosmic Microwave Background radiation. Finally, we take some small steps towards understanding the dynamics at the end of inflation from an Effective Field Theory perspective and discuss a possible observational effects that might arise in this formalism.

# Early universe cosmology as a probe of fundamental physics

by

Ogan Özsoy

B.Sc. (Physics) Istanbul Technical University, Istanbul, 2009

M.Sc. (Physics) Boğaziçi University, Istanbul, 2011

DISSERTATION

Submitted in partial fulfillment of the requirements for the degree of  
Doctor of Philosophy in Physics

Syracuse University

June 2017

Copyright 2017 Ogan Özsoy

All rights reserved

*To Yasemin, Can, and Beliz*

*In loving memory of Ali Fuat Kundak*

*and*

*Muzaffer Özsoy.*

*“A person can spend his whole life between four walls. If he doesn’t think or feel that he’s a prisoner, then he’s not a prisoner. But then there are people for whom the whole planet is a prison, who see the infinite expanse of the universe, the millions of stars and galaxies that remain forever inaccessible to them. And that awareness makes them the greatest prisoners of time and space.”*

*-Vladimir Bartol, Alamut*

# Acknowledgements

This dissertation is a result of six years of a journey, during which I had the chance to interact with so many great people. I am extremely grateful to all the people who made this possible.

First and foremost, I am indebted to my advisor, *Scott Watson*, for his guidance and generous support throughout my studies. Without his continous encouragement and faith in me, I could never made it.

I would like to thank *JiJi Fan* who was practically a second advisor for me. JiJi was involved in some of the research presented in this dissertation and has been very generous with her time. I admire JiJi's quick but detailed back of the envelope calculations and technical knowledge in particle physics.

I wish to thank the greatest teachers that any graduate student could hope for: *Cristian Armendariz-Picon* and *Mark Bowick*. Their deep knowledge in fundamental aspects of physics and style of tackling problems have been very influencial on my studies. Special thanks to *Mark Bowick*, for showing me *more is actually different*.

Thank you to all my friends and colleagues in the physics department—*Swetha Baghwat, Michael Czajkowski, Bithika Jain, Raghav Govind Jha, Prayush Kumar, Brandon Melcher, Prashant Mishra, Jayanth Neelakanta, Adam Patch, Riccardo Penco, Francesco Serafin, Suraj Shankar, Gizem Şengör, Kazage Utuje* for interesting and insightful conversations on pretty much everything and for all the fun we have shared.

I also want to express my gratitude to all the staff in the Department of Physics and especially to *Penny Davis, Diane Sanderson, Yudaisy Salomón Sargentón, Linda Terramiggi, Cindy Urtz* and *Patty Whitmore* for their constant help at the administrative level, regardless of my ignorance of bureaucratic affairs.

Finally, I would like to thank my parents who always value education more than anything. I am thankful for their open mindedness, understanding and encouragment during the past few years.

# List of Papers

Chapters 2, 3, 4, 5 and 6 of the dissertation are comprised of the work carried out in the following papers, respectively:

1. *Supersymmetry, Nonthermal Dark Matter and Precision Cosmology*, Phys. Rev. D **89**, no. 2, 023522 (2014), Richard Easther, Richard Galvez, Ogan Özsoy and Scott Watson
2. *Heavy Gravitino and Split SUSY in the Light of BICEP2*, JHEP **1407**, 073 (2014), JiJi Fan, Bithika Jain, Ogan Özsoy
3. *Nonthermal histories and implications for structure formation*, Phys. Rev. D **90** (2014) no.4, 043536, JiJi Fan, Ogan Özsoy and Scott Watson
4. *How Well Can We Really Determine the Scale of Inflation?*, Phys. Rev. D **91**, no. 10, 103509 (2015), Ogan Özsoy, Kuver Sinha, and Scott Watson
5. *Toward an Effective Field Theory Approach to Reheating*, [arXiv:1507.06651 [hep-th]], Ogan Özsoy, Tom Giblin, Eva Nesbit, Gizem Şengör and Scott Watson

# Contents

<b>1</b>	<b>Introduction</b>	<b>1</b>
1.1	Hot Big Bang Cosmology . . . . .	2
1.1.1	Problems of the Hot Big Bang Model . . . . .	9
1.1.2	A simple solution to the horizon problem . . . . .	13
1.2	Slow-roll Inflation . . . . .	14
1.3	Reheating . . . . .	18
1.4	Inflation in the CMB sky . . . . .	20
1.4.1	Cosmological Perturbations . . . . .	20
1.4.2	Contact with Observations . . . . .	26
1.5	$\Lambda$ CDM model . . . . .	34
1.6	Open Problems and Outline of the Dissertation . . . . .	38
	<b>Appendices</b>	<b>41</b>
1.A	Perturbed Einstein Equations . . . . .	41
<b>2</b>	<b>Supersymmetry, Non-thermal Dark Matter and Precision Cosmology</b>	<b>43</b>
2.1	Introduction . . . . .	43
2.2	CMB Uncertainties from the Post-Inflationary Expansion . . . . .	45
2.3	Thermal vs Non-thermal Dark Matter . . . . .	47
2.3.1	Non-thermal DM: A Realization Through Scalar Decay . . . . .	50



2.3.2	Non-thermal Histories and CMB Observables . . . . .	55
2.4	Constraining Nonthermal Dark Matter . . . . .	57
2.4.1	Nonthermal Wino-like Neutralinos . . . . .	58
2.4.2	Neutralino WIMPs: The General Case . . . . .	61
2.5	Conclusion . . . . .	63
<b>3</b>	<b>Split SUSY and the Scale Inflation</b>	<b>65</b>
3.1	Introduction . . . . .	65
3.2	Gravitino and Wino Relic Abundance . . . . .	67
3.2.1	Primordial Gravitino Relic Abundance . . . . .	68
3.2.2	Wino Relic Abundance from Gravitino Decays . . . . .	70
3.3	Indirect Detection Constraints . . . . .	73
3.4	Implications of the BICEP2 Result . . . . .	75
3.4.1	Basics of Tensor-to-Scalar Ratio . . . . .	76
3.4.2	Implication for Reheating Temperature . . . . .	78
3.5	Implications for SUSY . . . . .	81
3.6	Conclusions and Outlook . . . . .	82
	<b>Appendices</b>	<b>83</b>
3.A	Gravitino from Inflaton Decay . . . . .	83
<b>4</b>	<b>Non-thermal histories and Implications for Structure Formation</b>	<b>85</b>
4.1	Introduction . . . . .	85
4.2	Non-thermal Cosmologies . . . . .	87
4.2.1	Background Evolution . . . . .	90
4.3	Cosmological Perturbations . . . . .	93
4.3.1	Initial Conditions . . . . .	95
4.3.2	Evolution of the Perturbations during Moduli Domination . . . . .	96
4.4	Determining the Scale of the Smallest Dark Matter Structures . . . . .	106
4.4.1	Free Streaming and Kinetic Decoupling of Dark Matter . . . . .	106

4.4.2	Determining the Relevant Scale . . . . .	107
4.5	Neutralino Dark Matter in the Moduli Scenario . . . . .	111
4.6	Conclusions . . . . .	114
<b>Appendices</b>		<b>117</b>
4.A	Derivation of Perturbation Equations . . . . .	117
4.B	Adiabatic Initial Conditions . . . . .	120
4.C	Solution for Radiation Density Perturbation During Scalar Domination	122
<b>5</b>	<b>Alternative sources of Gravitational Waves and the Scale of Inflation</b>	<b>125</b>
5.1	Introduction . . . . .	125
5.2	Gravity Waves from Inflation and Particle Production . . . . .	128
5.2.1	Quantum Vacuum Fluctuations and Gravity Waves . . . . .	129
5.2.2	Gravity Waves from Particle Production during Inflation . . . . .	130
5.3	Particle Production Mechanisms with Direct Inflaton Coupling . . . . .	134
5.3.1	Scalar Production During Inflation . . . . .	135
5.3.2	Pseudo-scalar Inflaton and Vector Production . . . . .	143
5.3.3	Summary of Direct Coupling Case . . . . .	147
5.4	Particle Production Mechanisms with Gravitational Coupling . . . . .	148
5.5	Towards a UV Completion and the Resulting Constraints from String Theory . . . . .	152
5.5.1	Axions in Type IIB String Theory . . . . .	152
5.5.2	Orientifold Compactification Data and Axion Decay Constant	154
5.5.3	Stable Five-brane-Anti-brane Systems and Axion Potentials . . . . .	157
5.6	A String Model of Gauge Field Production . . . . .	160
5.6.1	Magnetized 5-Branes in Orientifold Compactifications . . . . .	163
5.6.2	Microscopic Parameters in the Inflaton and Hidden Sector . . . . .	166
5.6.3	Consistency Conditions . . . . .	168
5.7	Conclusions . . . . .	170

<b>Appendices</b>	<b>172</b>
5.A ADM formalism . . . . .	172
5.B Gauge Field Production . . . . .	177
5.C Gravity Waves sourced by Gauge Fields . . . . .	181
5.D Microscopic Conditions for Slow Roll and Back Reaction . . . . .	184
<b>6 Toward an Effective Field Theory Approach to Reheating</b>	<b>186</b>
6.1 Introduction . . . . .	186
6.2 Challenges for Inflationary Reheating . . . . .	188
6.3 Reheating in Weinberg’s Covariant formulation of the EFT of Inflation	191
6.3.1 Construction of the EFT . . . . .	191
6.3.2 Analysis of Reheating in the EFT . . . . .	195
6.4 The EFT of (p)Reheating . . . . .	202
6.4.1 Construction of the EFT of Fluctuations . . . . .	205
6.4.2 Background Evolution During Reheating and Symmetries of the Action . . . . .	213
6.4.3 Capturing Existing Models . . . . .	216
6.4.4 A New Class of Reheating Models . . . . .	226
6.5 Challenges and Outlook . . . . .	229
<b>Appendices</b>	<b>233</b>
6.A Terms proportional to $\chi$ in the unitary gauge action . . . . .	233
6.B ADM Formalism and Mixing with Gravity . . . . .	234
6.C Relating Unitary Gauge to the Scalar Potential . . . . .	237
<b>Bibliography</b>	<b>238</b>

# List of Figures

1.1	Distribution of galaxies found by the 2dF Galaxy Redshift Survey (1998-2003). The distribution is clumpy on small scales and late times, but becomes more uniform on large scales and early times. . . . .	3
1.2	Evolution of different energy components in the Universe. . . . .	7
1.3	Schematic representation of the horizon problem in standard Big Bang cosmology. Photons that are reaching us from the CMB decoupling surface originates from causally disconnected parts in the early universe. The same situation applies to any two points at the CMB surface that are separated by more than the particle horizon size, corresponding to more than 1 degree on the sky today. . . . .	12
1.4	The CMB temperature anisotropy power spectrum measured by Planck satellite [1]. Red lines represent the experimental error bars. The green line represents the best-fit curve of the $\Lambda$ CDM model (See Table 1.1).	36
2.1	The lefthand timeline represents the thermal history of the early universe when dark matter is populated in the thermal bath that emerges shortly after after inflation. The right timeline represents a possible nonthermal history where dark matter production occurs directly from scalar decay. . . . .	48

2.2 Evolution of physical wavelengths as labelled by their inverse wavenumber  $k_p^{-1}$  during inflation (below the x-axis) and during the post-inflationary epoch (above the x-axis). The solid (blue) line represents the Hubble radius,  $H_r^{-1}$  in a Universe dominated by a radiation fluid  $w = 1/3$ , the dashed (red) line is the Hubble radius,  $H_m^{-1}$  in a post-inflationary era dominated by a pressure-less fluid,  $w = 0$ . We compare the evolution of a physical mode  $k_*$  that re-enters at CMB decoupling in the standard scenario (Radiation  $\rightarrow$  Matter  $\rightarrow$  Dark energy) with a mode  $k'_*$  that re-enters at CMB decoupling in the nonthermal scenario (Matter  $\rightarrow$  Radiation  $\rightarrow$  Matter  $\rightarrow$  Dark Energy). These modes exit the Hubble radius at different times during inflation,  $t_*$  and  $t'_*$ , which translates into a shift in the number of e-folds  $\Delta N = H\Delta t$ . The corresponding shift in the pivot scale or any co-moving mode is given by  $k'_* = k_* e^{-\Delta N}$ . 56

2.1 The thermally average annihilation rate  $\langle\sigma v\rangle$  for a dominantly wino neutralino to annihilate to a pair of  $W$ -bosons, as a function of mass. The Fermi constraint comes from two years of data from 10 Dwarf spheroidal galaxies [2]. These results have been obtained using DarkSUSY [3], but the general shape of the curve is in good agreement with the analytic expression (2.23). For this scan we took the MSSM parameters to vary over:  $M_2 = 100$  GeV to 2 TeV,  $\mu = 100$  GeV to 2 TeV, and  $\tan\beta = 5$  to 50. We applied all LEP2 constraints and color charged particles were taken to decouple by setting their masses to be above 2 TeV, allowing agreement with LHC constraints. . . . . 59

2.2	The thermally average annihilation rate $\langle\sigma v\rangle$ for a general neutralino to annihilate to a pair of $W$ -bosons, with a bino fraction of less than 10%, to realize a nonthermal history. The constraint from Fermi comes from two years of data from 10 Dwarf spheroidal galaxies [2]. These results have been obtained using DarkSUSY [3], however the general shape of the upper curve is in good agreement with the analytic expression (2.23) and the shape of the lower, higgsino curve agrees with the expectation that $\langle\sigma v\rangle \sim 1/\mu^2$ . Other parameter choices match those in Figure 2.1. . . . .	60
2.3	The WIMP-nucleon (proton) scattering cross-section as a function of WIMP mass. For wino-higgsino mixtures we find that most models are excluded by the Xenon 2011 / 2012 data. For purified WIMPs (dominantly wino or higgsino) many models escape existing constraints and for models with wino fractions 90% we must wait until Xenon1T for meaningful constraints to be established. However, for the dominantly higgsino models many are already disfavored. For this scan we took the MSSM parameters to vary over: $M_2 = 100$ GeV to 2 TeV, $\mu = 100$ GeV to 2 TeV, and $\tan\beta = 5$ to 50. We have applied all LEP2 constraints and color charged particles were taken to decouple by setting their masses to be above 2 TeV – allowing agreement with LHC constraints.	61
3.1	Upper bounds on inflaton reheating temperature $T_R$ as a function of wino mass for $m_{3/2} = 100$ TeV (left) and $m_{3/2} = 10^4$ TeV (right). The blue, purple, green curves with bands around them correspond to constraints from Fermi galactic center continuum, Fermi line search and HESS line search respectively. The bands are derived by varying parameters of NFW (Einasto) dark matter profiles in the $2\sigma$ range [4]. The burgundy dot-dashed line corresponds to the upper bound derived from requiring $\Omega_{\tilde{W}}h^2 = 0.12$ .	74

3.2	Upper bounds on scalar mass $m_s$ as a function of wino mass for $m_{3/2} = 100$ TeV(left) and $m_{3/2} = 10^4$ TeV (right). The blue, purple, green curves with bands around them correspond to constraints from Fermi galactic center continuum, Fermi line search and HESS line search respectively. The bands are derived by varying parameters of NFW (Einasto) dark matter profiles in the $2\sigma$ range [4]. The burgundy dot-dashed line corresponds to the upper bound derived from requiring $\Omega_{\tilde{W}} h^2 = 0.12$ . . . . .	76
4.1	Evolution of the logarithm of normalized energy densities (as discussed in the text), $\log(\rho_\alpha/\rho)$ for two different non-thermal cosmologies. In both figures we take $m_\chi = 500$ GeV, $B_\chi = 1/3$ , $g_* = 30$ , and $\langle\sigma v\rangle = 3 \times 10^{-8}$ GeV $^{-2}$ . On the left we chose an initial dimensionless decay rate $\Gamma_\sigma/H_0 \simeq 2 \times 10^{-7}$ and the moduli mass $m_\sigma = 10^6$ GeV. On the left the universe becomes radiation dominated at $N_{rh} \simeq 10.6$ and the reheat temperature is $T_r \simeq 707$ MeV. Whereas on the right we have $\Gamma_\sigma/H_0 = 0.5 \times 10^{-12}$ and $m_\sigma = 10^5$ GeV, with $N_{rh} \simeq 19$ at reheating and $T_r \simeq 22$ MeV. . . . .	93
4.1	Evolution of the density perturbations in radiation fluid for modes with $k/H_0 = 0.1$ and for different rates of decay and annihilation. The bottom blue curve corresponds to the evolution of radiation perturbations in the absence of scalar decay and annihilation terms in a “matter” dominated Universe, whereas green and red curves shows the evolution with enhanced decay and annihilations. Particularly, the values of $A$ and $\alpha$ for the red curve is implied by SUSY model building. . . .	101

- 4.2 Evolution of normalized radiation density contrast,  $|\delta_r|/\Phi_0$ , velocity perturbation  $\theta_r/(H_0\Phi_0)$  and gravitational potential  $\Phi/\Phi_0$  for the modes  $k/H_0 = 0.1$  (Left),  $k/H_0 = 0.04$  (Right). These modes enters the horizon at  $N_h = \ln(k/H_0)^{-2} \simeq 4.6$  (Left),  $N_h = \ln(k/H_0)^{-2} \simeq 6.4$  (Right). In this non-thermal cosmology the universe is effectively matter dominated until  $N_{rh} \simeq 10.6$  e-foldings after which the universe becomes radiation dominated. Well after reheating, the density perturbation oscillates with an amplitude  $A_{\delta_r} \simeq 0.0005\Phi_0$  (Left),  $A_{\delta_r} \simeq 1.7\Phi_0$  (Right). For these modes, the ratio of the size of the comoving horizon  $k_{rh}^{-1}$  at the time of reheating to the size  $k^{-1}$  of the fluctuation is given by,  $k/k_{rh} \simeq 20$  (Left) and  $k/k_{rh} \simeq 8$  (Right). . . . . 103
- 4.3 Evolution of DM density contrast (normalized) in a non-thermal cosmology for modes with  $k/H_0 = 0.1$  (Left) and  $k/H_0 = 0.04$  (Right). As the mode enters the horizon, it grows linearly with the scale factor  $e^N \sim a$ . We see that the solution (4.32) (red dot-dashed curve) we derived in the previous section is an excellent fit during the scalar dominated era. After the universe become radiation dominated at  $N_{rh} \simeq 10.6$ , the amplitude of the density contrast decreases due to rapid annihilations of DM particles. For  $N \gtrsim 12$ , the density contrast then begins to grow logarithmically as expected. . . . . 104
- 4.1 Elastic/inelastic scattering rates per Hubble (red/blue curves) as a function of the mass splittings fixing  $\mu = 200$  GeV. Left: energy of DM produced from decay is fixed to be 2 TeV. Right: energy of DM produced from decays is fixed to be 200 GeV. The solid curves correspond to the temperature of the thermal bath to be about  $T_{rh} = 0.4$  GeV; the dashed curves correspond to a much lower temperature 5 MeV. The gray dashed lines corresponds to  $\gamma/H = 1$ . . . . . 114



5.1	Change in the tensor power spectrum due to particle production $\Delta P_t$ (as defined in the text) vs Hubble rate $H$ during inflation for both the single ( $N_{\text{events}} = 1$ ) and multiple production cases ( $N_{\text{events}} > 1$ ). The lightly shaded region (red) represents a tension with the Planck upper-bound on equilateral type non-Gaussianity ( $ f_{\text{NL}}^{\text{equil}}  < 16$ ), whereas in the dark shaded region particle production is clearly not competitive with the vacuum contribution. We note that even in cases where the signal is competitive, this does not necessarily imply a dominant contribution. Thus, we see that in both cases (single or multiple production) non-Gaussianity puts strong constraints on the tensor contribution. The multiple production case is rather insensitive to the coupling, but in both cases we have plotted results for $g = 10^{-2}$ and $ f_{\text{NL}}^{\text{equil}}  < 16$ . . . . .	143
5.1	Change in the tensor power spectrum $\Delta P_t$ due to (gravitationally coupled) gauge field production as discussed in the text. The red region represents a tension with the Planck upperbound on equilateral type non-Gaussianity ( $ f_{\text{NL}}^{\text{equil}}  < 16$ ), whereas in the darkest shaded region gauge field production is not competitive with the vacuum contribution. The light Blue region corresponds to the constraint coming from the back reaction of the produced gauge fields on the spectator scalar $\chi$ . As plotted, the above graph is actually conservative as the real constraint requires the kinetic energy to be <i>much</i> greater than the gauge field energy $\dot{\chi}^2 \gg \langle \vec{E}^2 + \vec{B}^2 \rangle$ . Given this caveat, the two white regions represent the available parameter space for the choices $\epsilon_\chi = \epsilon$ and the more realistic value $\epsilon_\chi < \epsilon$ ( $\epsilon_\chi < \epsilon < 1$ is required for $\chi$ to remain a spectator field.) . . . . .	151
5.1	A cartoon of the model for gauge field production from a sector $\chi$ that is gravitationally coupled to the inflaton $\phi$ . . . . .	161

6.1	This figure gives the evolution of the background fields and Hubble parameter, where tildes imply we have normalized these quantities by $\sqrt{8\pi}m_{\text{pl}}$ , and time is in units of the inflaton mass. For this realization we take $m_\chi/m_\phi = 10$ , $m_{\text{pl}}/\Lambda = 14$ and initial conditions $\phi_0 = 1.038 m_{\text{pl}}$ , $\dot{\phi}_0 = -0.662 m_{\text{pl}}$ , $\chi_0 = \dot{\chi}_0 = 0.005 m_{\text{pl}}$ . The top panel gives the evolution of the inflaton. In the middle panel the solid black curve is $\tilde{\chi}_0(t)$ and below the dot-dashed blue horizontal line marks the region where the EFT of the background is valid. The bottom plot gives the Hubble rate where the red-dashed line represents a strictly matter dominated evolution. . . . .	196
6.2	Instability band structure for the model $V_{\text{tot}} = \frac{1}{2}m_\phi^2\phi^2 + \frac{1}{2}m_\chi^2\chi^2 - \frac{1}{2}\dot{\phi}_0^2 f\left(\frac{\chi}{\Lambda}\right)$ , where $f$ is given by (6.11). This density plot represents the real part of the scaled Floquet exponent, $\text{Re}(\mu_k)$ , where lighter regions represent larger values. The y-axis is the hierarchy between the Planck mass and the rescaled cut-off of the EFT, $\tilde{\Lambda} = \Lambda/\sqrt{8\pi}$ , while the x-axis corresponds to $K = \sqrt{k^2 + m_\chi^2}$ in units of $m_\phi$ . . . . .	200
6.1	Obtaining adequate inflation, ending inflation and then successful reheating in the EFT requires a complete knowledge of the inflationary potential. This presents a challenge when using Weinberg's EFT approach to capture reheating in many classes of models. . . . .	203
6.2	Relevant energy scales for the preheating models considered in Section 6.4.3. On the left, we have the hierarchy in energy scales associated with the dynamics of the Goldstone boson with a sound speed $c_\pi$ following our general discussion of self-resonant models. The right diagram shows the hierarchy of scales for the example of canonical two-field preheating models. . . . .	219

# List of Tables

1.1	Parameters of $\Lambda$ CDM baseline model (at 68 % CL). The first four parameters describe the composition of the universe, whereas the last two sets the initial conditions for CMB fluctuations. . . . .	37
-----	---	----

# List of conventions and symbols

Throughout this dissertation, we have adopted the following conventions:

- Greek indices  $\mu, \nu, \lambda, \dots$  label the components of tensors with respect to the coordinate basis and take values 0, 1, 2, 3.
- Latin indices  $i, j, k, \dots$  run over the spatial coordinates and take the values 1, 2, 3.
- Repeated indices are summed over.
- The metric has a  $(-, +, +, +)$  signature unless stated otherwise
- We work in units such that  $\hbar = c = k_B = 1$ . This results in units where  $[\text{Mass}] = [\text{Energy}] = [\text{Momentum}] = [\text{Length}^{-1}] = [\text{Time}^{-1}]$ .
- Torsion-free, metric compatible Christoffel Connection is defined as

$$\Gamma_{\mu\nu}^{\sigma} = \frac{1}{2}g^{\sigma\rho} \left( \partial_{\mu}g_{\nu\rho} + \partial_{\nu}g_{\mu\rho} - \partial_{\rho}g_{\mu\nu} \right) \quad (1)$$

- The Riemann tensor is defined as  $R_{\mu\sigma\nu}^{\lambda} \equiv \partial_{\sigma}\Gamma_{\mu\nu}^{\lambda} - \partial_{\nu}\Gamma_{\mu\sigma}^{\lambda} + \Gamma_{\sigma\rho}^{\lambda}\Gamma_{\mu\nu}^{\rho} - \Gamma_{\nu\rho}^{\lambda}\Gamma_{\mu\sigma}^{\rho}$ .
- The Ricci tensor is defined as  $R_{\mu\nu} \equiv R_{\mu\lambda\nu}^{\lambda}$ .
- The energy momentum tensor  $T_{\mu\nu}$  is related to the matter action  $S_m$  by

$$T_{\mu\nu} = -\frac{2}{\sqrt{-g}} \frac{\delta S_m}{\delta g^{\mu\nu}}.$$

- We use the reduced Planck mass  $M_{\text{pl}} = (8\pi G)^{-1/2} \approx 2 \times 10^{18} \text{ GeV}$  unless stated otherwise.
- We denote cosmic time with  $t$  and conformal time with  $\tau$ . The relation between these two time variables is  $d\tau = dt/a(t)$ , and we use the following abbreviations  $\dot{f} \equiv \partial_t f$  and  $f' \equiv \partial_{\tau} f$ .

Throughout this dissertation, we have used the following abbreviations:

- AdS: Anti-de Sitter
- BSM: Beyond the Standard Model
- CC: Cosmological Constant
- CDM: Cold Dark Matter
- CMB: Cosmic Microwave Background
- GW: Gravitational Waves
- DM: Dark matter
- EFT: Effective Field Theory
- FLRW: Friedmann-Lemaître-Robertson-Walker
- GR: General Relativity
- KK: Kaluza-Klein
- LSP: Lightest Supersymmetric Partner
- MSSM: Minimally Supersymmetric Standard Model
- PNGB: Pseudo-Nambu-Goldstone Boson
- QED: Quantum Electrodynamics
- QCD: Quantum Chromodynamics
- QFT: Quantum field theory
- SM: Standard Model
- SUSY: Supersymmetry
- vev: vacuum expectation value

# Chapter 1

## Introduction

The pursuit to understand the origin and structure of the universe has been an important human endeavor throughout history. For thousands of years, ancient civilizations have wondered and speculated about the true nature of the “celestial sphere”. The first radical ideas, that shook the common views about our privileged position in the Universe, emerged by the invention of the first telescope and led us to the acceptance of Copernicus’ heliocentric model. It was not until the beginning of the twentieth century that the technological advances reached to a level to provide evidence for the existence of galaxies apart from our own. Moreover, some earlier results in this era suggested that these galaxies are moving away from us [5]. In 1929, Edwin Hubble gathered further evidence [6] for an expanding Universe and proposed an empirical formula that establishes a relationship between the recessional velocity  $v$  and the distance  $d$  of the galaxies,  $v = Hd$ . This is the famous Hubble’s law where  $H$  is a measure for the rate of expansion and known as the Hubble constant. This discovery was one of the corner stones in cosmology as it provided strong evidence for the dynamical Universe picture.

Over the past few decades, modern cosmology was in a better position to seek answers to the more fundamental questions given the rapid technological progress. The observational and theoretical advances have improved our understanding regarding

the composition and evolution of the Universe to a remarkable degree. One of the most important tools that has contributed significantly to this understanding is the Cosmic Microwave Background (CMB) radiation. Until its discovery, astronomers were primarily using light from astrophysical objects to obtain information on the Universe's recent past. The discovery by Penzias and Wilson [7] was one of the great triumphs of modern cosmology in the sense that it opened a new window into the physical processes prior to the formation of compact objects. Further investigations showed that these relic photons follow a blackbody distribution and has a uniform temperature of  $T_{\gamma,0} \approx 2.7K$  (today), corresponding to the microwave part of the electromagnetic spectrum. Importantly, this discovery together with the dynamical Universe picture presented by Hubble and our understanding of particle physics to date, have led us to the Hot Big Bang Model as the right framework to study cosmology [8, 9].

Due to its central importance in modern cosmology, we therefore intend to present a short review of the Hot Big Bang model and state some of the conceptual problems that arise in this standard picture in the following section.

## 1.1 Hot Big Bang Cosmology

The central premise in modern cosmology is that as we look at the Universe on large enough scales, it appears to be simpler and more uniform compared to the small scales. It is clear from the night sky that matter is clumped into stars and galaxies. However if we focus on sufficiently large scales, the distribution of galaxies becomes isotropic and homogeneous (See Figure 1.1). Homogeneity and isotropy has been tested by a variety of observations of the Large Scale Structure (LSS) surveys [10, 11] but perhaps the most important evidence supporting this claim is the almost uniform temperature of the CMB originating from different parts of the sky. To first approximation, we can therefore take the Universe to be isotropic and homogeneous.

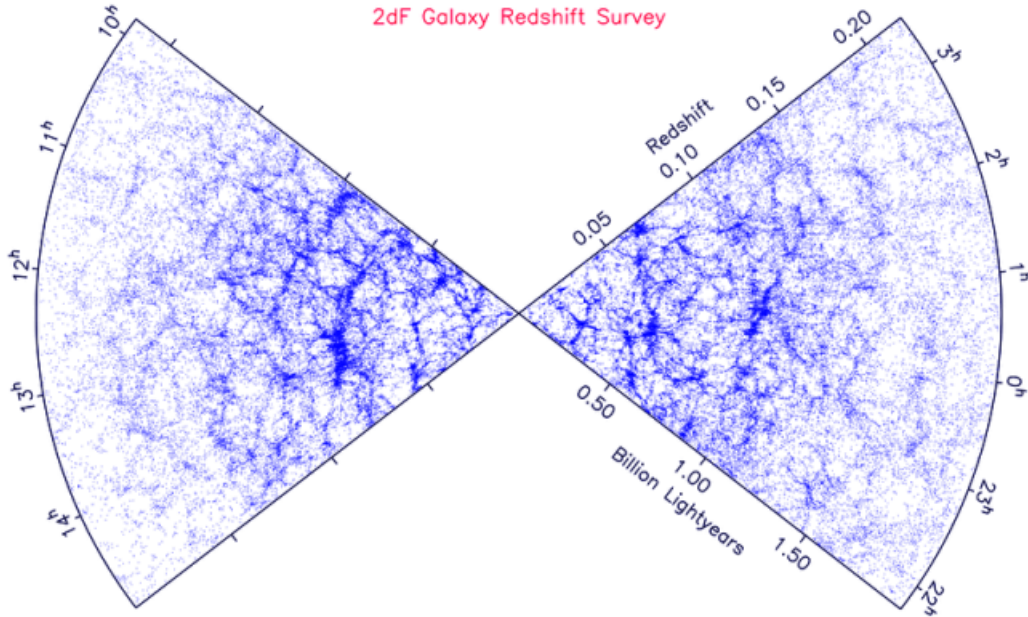


Figure 1.1: Distribution of galaxies found by the 2dF Galaxy Redshift Survey (1998-2003). The distribution is clumpy on small scales and late times, but becomes more uniform on large scales and early times.

Due to the high degree of spatial symmetry, the line element describing the universe takes the simple FLRW form,

$$ds^2 = -dt^2 + a^2(t) \left( \frac{dr^2}{1 - Kr^2} + r^2 d\Omega_2 \right), \quad (1.1)$$

where  $d\Omega_2 = (d\theta^2 + \sin^2\theta d\phi^2)$  is the line element on the 2-sphere  $S_2$  and  $K = \{-1, 0, 1\}$  represents negative, zero and positive curvature of constant-time hypersurfaces, respectively. Note that the symmetries of the Universe allow us to describe the metric by just a single function of time  $a(t)$  and a constant parameter  $K$ . The function  $a(t)$  is called the scale factor which parametrizes the size of the spatial slices at a given moment in time and the Hubble's "constant" describing the speed of expansion is given by  $H(t) = \dot{a}/a$ . Here, an expanding universe  $H(t) > 0$  corresponds to a monotonically increasing scale factor  $a(t)$ . This line element in (1.1) was independently derived by Friedmann [12, 13], Lemaître [14], Robertson [15] and Walker



[16].

The evolution of the universe is governed by the Einstein field equations

$$R_{\mu\nu} - \frac{1}{2}g_{\mu\nu}R = \frac{1}{M_{\text{pl}}^2}T_{\mu\nu}, \quad (1.2)$$

where  $R_{\mu\nu}$  is the Ricci tensor build out of the metric field tensor  $g_{\mu\nu}$ ,  $R \equiv R^\mu{}_\mu$  is the Ricci scalar and  $T_{\mu\nu}$  is the energy-momentum tensor for the matter content of the universe. Using the metric in (1.1), these field equations determine the evolution of the scale factor

$$H^2 = \frac{\rho}{3M_{\text{pl}}^2} - \frac{K}{a^2}, \quad (1.3)$$

$$\frac{\ddot{a}}{a} = -\frac{1}{6M_{\text{pl}}^2}(\rho + 3P). \quad (1.4)$$

In deriving these equations (also known as Friedmann equations) we have used an energy momentum tensor on the right hand side of the field equations in (1.2) that has the perfect fluid form consistent with homogeneity and isotropy,

$$T_{\mu\nu} = (\rho + P)U_\mu U_\nu + Pg_{\mu\nu}. \quad (1.5)$$

where  $\rho$  and  $P$  are the energy density and the pressure in the rest frame of the fluid and  $U^\mu$  is the relative 4-velocity between the fluid and the observer. The evolution equation for the energy density driving the expansion of the universe can be derived by either combining the two equations in (1.3) or from the  $\nu = 0$  part of the covariant conservation of the energy-momentum tensor  $\nabla_\mu T^\mu{}_\nu = 0$ ,

$$\nabla_\mu T^\mu{}_0 = 0 \quad \Rightarrow \quad \dot{\rho} + 3H(\rho + P) = 0. \quad (1.6)$$

For each fluid that contributes to this evolution, the continuity equation in (1.6) can be imposed independently since we can decompose the energy momentum tensor as

$T_{\mu\nu} = \sum_I T_{\mu\nu}^I$ , where  $I$  labels different fluids. In this sense, the  $\rho$  and  $P$  in (1.6) should be understood as the sum of all contributions to the energy density and the pressure in the universe. For each of these individual components, we can define an equation of state as

$$w \equiv \frac{P_I}{\rho_I}. \quad (1.7)$$

Now, for a constant equation of state  $w_I$ , the continuity equation (1.6) can be solved easily in terms of the scale factor

$$\rho_I \propto a^{-3(1+w_I)}, \quad (1.8)$$

and if this form of matter dominates the total energy density of the universe, we can solve for the time dependence of the scale factor using the first Friedmann equation in (1.3). In a spatially flat universe  $k = 0$ , this gives

$$a(t) \propto \begin{cases} t^{2/3(1+w_I)} & w_I \neq -1, \\ e^{Ht} & w_I = -1 \end{cases} \quad (1.9)$$

We can classify important sources of energy content by their contribution to the pressure : (i) Ultra-relativistic gas (radiation)  $w = 1/3$ , (ii) Non-relativistic pressureless dust (matter)  $w = 0$ , (iii) Cosmological constant  $w = -1$  with the corresponding scaling of the energy densities,  $\rho \propto a^{-4}$  radiation,  $\rho \propto a^{-3}$  matter and  $\rho \propto \text{const.}$  for vacuum energy, respectively. The physical meaning for these scalings can be understood by considering the scaling of the spatial volume in FLRW cosmology,  $V \propto a^3$ . Therefore the energy density of non-relativistic matter is diluted by the same proportion whereas the energy density of radiation picks up one extra factor  $a^{-1}$  due to the energy loss through the stretching of their wavelength by expansion.

Let us use subscripts ‘0’ to denote the quantities evaluated today  $t = t_0$  and define

the critical density today in a flat universe by using Friedmann equation (1.3),

$$\rho_{c,0} = 3H_0^2 M_{\text{pl}}^2. \quad (1.10)$$

For each energy component, using the critical energy density, we can define dimensionless density parameters today  $\Omega_{I,0} = \rho_{I,0}/\rho_{c,0}$ . We can then re-write the Friedmann equation in terms of the dimensionless density parameters today,

$$\frac{H^2(a)}{H_0^2} = \Omega_{r,0}a^{-4} + \Omega_{m,0}a^{-3} + \Omega_{K,0}a^{-2} + \Omega_{\Lambda}, \quad (1.11)$$

where we have denoted  $\Omega_{\Lambda,0}$  as the contribution of the cosmological constant and defined a spatial curvature density parameter,  $\Omega_{K,0} \equiv -K/(a_0 H_0)^2$  using the conventional normalization of the scale factor today,  $a_0 = 1$ .

It is clear from the scalings of different energy content in the expression (1.11) that through most of the Universe's history a single component dominates the expansion. For example, assuming a nearly flat<sup>1</sup> universe  $\Omega_{K,0} \ll 1$ , as  $a \rightarrow 0$  first radiation starts to dominate, then matter and eventually cosmological constant will take over the evolution (See Figure 1.2). Another observation that can be made from these results is that unless the cosmological constant term dominates the energy density in the beginning, at some initial time, say  $t = 0$ , the scale factor vanishes (See *e.g.* (1.9)) and the energy density (hence the Hubble rate  $H$  in (1.11)) becomes infinite. This implies a cosmological singularity, called the Big Bang, in the finite past. This should not lead us to an immediate concern because we expect that at these high energies, we have to replace our EFT (*e.g.* General Relativity) description with a yet to be discovered quantum theory of gravity that comes to the rescue.

In our discussion so far, we have focused on the time evolution of the the universe in the Big Bang model without mentioning the origin of its ‘‘Hotness’’. Now consider a primordial plasma that is made up only of electrons, protons and photons where

---

<sup>1</sup>As we will see later, this is actually the case established by various observations.

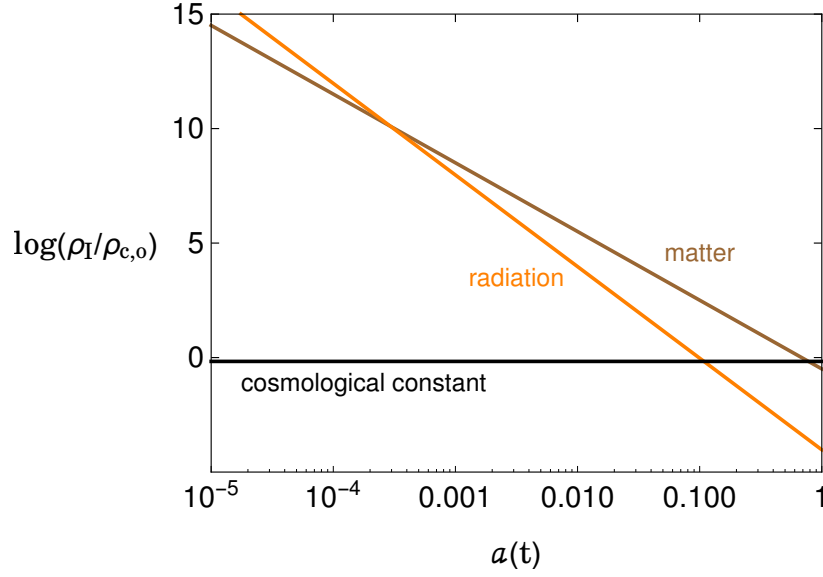


Figure 1.2: Evolution of different energy components in the Universe.

photons are assumed to follow a blackbody spectrum. This simply means that the distribution functions of the photons can be characterized by only using the temperature of the spectrum. In an expanding universe, it can be shown that the temperature  $T_\gamma$  of this spectrum decreases with scale factor as  $T_\gamma = T_{\gamma,0} a^{-1}$  which implies that the average energy of photons are larger as we go back in time. If we go back enough in time, we will reach an epoch where the average energy of photons is larger than that of the ionization energy of the Hydrogen atom (proton + electron). Therefore, prior to this time, neutral Hydrogen atom cannot exist. Moreover, efficient interactions in the plasma, such as Compton scattering between electrons and photons and Thompson scattering between electrons and protons keep these particles at the same temperature (*i.e.* in thermal equilibrium). This is why we call the evolution described by an FLRW universe, the Hot Big Bang Model. To represent the logic we presented so far in the actual chronological order: the early universe was made up of a hot plasma that was opaque as the mean free path of photons was very small. As the universe expands and cools down, the average energy of photons drops below

the ionization energy of Hydrogen and photons decouple from the rest of the plasma allowing the formation of neutral Hydrogen atoms. This phenomenon is called *recombination*. Due to our assumptions about homogeneity and isotropy, this process must have occurred everywhere in different patches of the universe. The decoupled photons move freely through space without interactions and should reach us today. This is why the observation made by Penzias and Wilson in 1965 is an indication of the Hot Big Bang Model as the correct description of the early universe because it predicts this “relic” radiation from the early universe.

The physics describing the Hot Big Bang model can be extended to higher temperatures by considering the particle content of Standard Model of particle physics such as quarks, leptons, gauge bosons, Higgs bosons, as well as Beyond the Standard Model (BSM) particles. At high enough temperatures, *i.e.* for  $T \gg m_i$  where  $m_i$  is the mass of the individual particles, we have a relativistic plasma that is in thermal equilibrium due to efficient interactions between constituents. Denoting the interaction rate by  $\Gamma$ , we can describe equilibrium in an expanding universe by the condition  $\Gamma > H$  at some initial temperature  $T_i$ . As the universe expands and cools two important things can happen: First, interaction rates may drop below the Hubble rate at some later time, leading to departure from equilibrium. Second, coupling constants between particles may vary and phase transitions can occur. The former is especially crucial in obtaining cosmological relic abundances for massive species because if the universe was in thermal equilibrium in all its history, the abundance of any massive species would be eventually suppressed by the Boltzmann factor  $e^{-m_i/T}$  when the temperature drops below the mass,  $m_i$ . This would single out radiation (*i.e.* massless photons) as the only relic that can reach until today, leading to a truly uninteresting universe. Below we list some of the important events in the thermal history of the universe that are essential for understanding the world we see today:

- **Electroweak (EW) phase transition.** At around  $T \sim 100$  GeV particles obtain masses through the Higgs mechanism.

- **QCD phase transition.** At high temperatures  $T \gg 150$  MeV, quarks behave like free particles, while below  $T < 150$  MeV strong interactions between the quarks and the gluons become important. Quarks and gluons then form bound three-quark states called baryons, and quark-antiquark pairs called mesons. These are the relevant low energy degrees of freedom below the scale of QCD phase transition.
- **Big Bang Nucleosynthesis (BBN).** BBN is the process ( $T \sim 100$  keV) through which abundance of light elements such as helium, deuterium and lithium are set and has central importance in modern cosmology [17].
- **Recombination.** Neutral Hydrogen atoms form through the reaction  $e^- + p^+ \rightarrow H + \gamma$  when the average energy of the photons are low enough that the reverse reaction is energetically disfavored ( $T \sim 0.33 - 0.26$  eV).
- **Photon decoupling.** The release of the CMB photons are not simultaneous with the formation of the first Hydrogen atoms. Before recombination, photons are tightly coupled to electrons through Thomson scattering,  $e^- + \gamma \rightarrow e^- + \gamma$ . The free electron density decreases as recombination proceeds everywhere in the universe such that the Thomson process becomes inefficient and photons decouple from the rest of the plasma ( $T \sim 0.28 - 0.23$  eV).

### 1.1.1 Problems of the Hot Big Bang Model

While Hot Big Bang cosmology gained widespread acceptance immediately after the discovery of the CMB and has since then provided an essentially correct picture of the cosmological evolution, it suffers several conceptual difficulties, along with the uncertainties in the initial conditions of the universe.

**Flatness Problem:**

Using the time dependent critical energy density  $\rho_c = 3H^2(t)M_{\text{pl}}^2$  we re-write the Friedmann equation in (1.3) in terms of a time dependent total density parameter  $\Omega \equiv \rho/\rho_c$ ,

$$\Omega_{\text{tot}} - 1 = \frac{K^2}{a^2 H^2}. \quad (1.12)$$

Note that in an exactly flat universe with  $k = 0$ , the total density parameter is constant and remains to be  $\Omega = 1$ . The difference of this quantity from unity is a measure of the spatial curvature and in a universe dominated by conventional matter sources with equation of state  $-1/3 < w < -1$  scales as,  $|\Omega - 1| \propto a^{(1+3w)}$ . This implies that  $|\Omega - 1|$  should decrease as we go back in time. Recent observations of the CMB [18] tells us that the spatial curvature is quite small today,

$$1 - \Omega_{\text{tot},0} \equiv \Omega_{K,0} = -0.0005_{-0.0066}^{+0.0065}, \quad (1.13)$$

at 95% CL. The smallness of the quantity  $|\Omega_{\text{tot},0} - 1|$  today implies that, it must have been even smaller at earlier times, *e.g.*  $|\Omega_{\text{tot},0} - 1| \leq 10^{-16}$  at the time of BBN. The miniscule value of the curvature  $\Omega_K$  in the past is not an issue in itself, but the naturalness of this finely tuned initial condition raises an immediate question: What kind of mechanism can set these initial conditions that appears to be unlikely within the Hot Big Bang picture ?

**Horizon Problem:**

The horizon problem can be understood by studying the propagation of light in an expanding space-time given by the line element (1.1). Due to spatial isotropy we can always define a coordinate system such that light travels purely in the radial direction  $r$ , where  $\theta = \phi = \text{constant}$ . Therefore, in a spatially flat<sup>2</sup> space-time,  $K = 0$ , the

---

<sup>2</sup>In what follows, we will assume flatness  $K = 0$  in light of CMB data.

evolution of light rays can be described by the two-dimensional line element,

$$ds^2 = -dt^2 + a^2(t) dr^2. \quad (1.14)$$

Since light rays follow null geodesics,  $ds^2 = 0$ , incoming and outgoing light rays at a given point are defined by  $\Delta r = \pm \Delta \tau$  where we have defined the conformal time as  $d\tau = dt/a(t)$ . The coordinates,  $r$  and  $\tau$  is particularly useful as the light rays can be described by straight lines with  $45^\circ$  angles in the  $r - \tau$  plane.

The comoving distance that a light ray can travel from an initial time  $t_i$  (say Big Bang) to  $t$  is given by the following integral

$$\Delta r(t) = \int_{t_i}^t \frac{dt'}{a(t')} \equiv \tau - \tau_i, \quad (1.15)$$

Equation (1.15) sets the maximum comoving distance from which an observer at a time  $t$  will be able to receive light signals since the Big Bang and therefore it is known as comoving particle horizon. It is the relevant quantity in describing the horizon problem in Big Bang cosmology. Using  $d \ln a = H dt$ , we can re-write equation (1.15) as

$$\Delta r(t) = \int_{a_i}^a d \ln a' (a' H')^{-1}. \quad (1.16)$$

In this way, we have related the causal structure of space-time to the evolution of the comoving Hubble radius,  $(aH)^{-1}$ . If the expansion is dominated by a fluid with an equation of state  $w$ , then the comoving Hubble radius is given by

$$(aH)^{-1} = H_0^{-1} a^{(1+3w)/2}. \quad (1.17)$$

For sources that satisfy the Strong Energy Condition (SEC),  $\rho + 3P = \rho(1 + 3w) > 0$ , *e.g.* radiation  $w = 1/3$  or pressurless dust,  $w = 0$ , from equation (1.17) we conclude that comoving Hubble radius grows monotonically in time. This implies that the integral in (1.16) will get most of its contribution at late times and hence will be



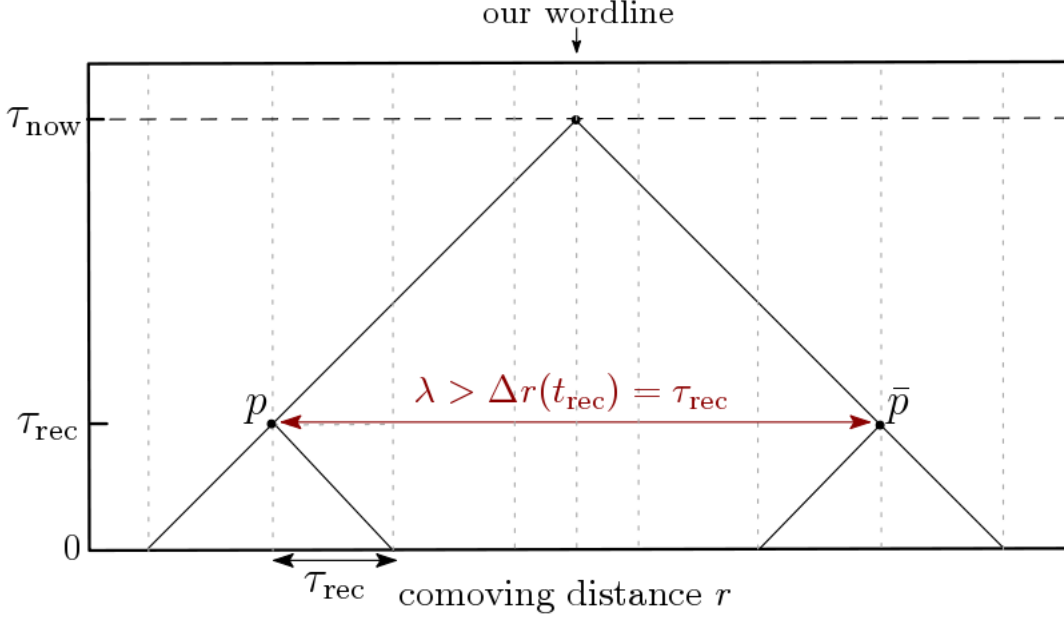


Figure 1.3: Schematic representation of the horizon problem in standard Big Bang cosmology. Photons that are reaching us from the CMB decoupling surface originates from causally disconnected parts in the early universe. The same situation applies to any two points at the CMB surface that are separated by more than the particle horizon size, corresponding to more than 1 degree on the sky today.

dominated by the upper limit. Plugging (1.17) inside the integral we have

$$\Delta r(t) = \frac{2H_0^{-1}}{(1+3w)} \left( a^{(1+3w)/2} - a_i^{(1+3w)/2} \right) \equiv \tau - \tau_i, \quad (1.18)$$

where we can send  $\tau_i \propto a_i^{(1+3w)/2}$  to zero by  $a_i \rightarrow 0$  for  $w \geq 0$ . Noting that  $(aH)^{-1} = H_0^{-1} a^{(1+3w)/2}$ , the comoving particle horizon at time  $t$  is simply given by

$$\Delta r(t) = \frac{2}{(1+3w)} (aH)^{-1} \equiv \tau. \quad (1.19)$$

This expression tells us that in the standard Big Bang cosmology, the comoving particle horizon grows proportional to the comoving Hubble radius. Now, consider two separate points  $p$  and  $\bar{p}$  at the time of CMB decoupling and the comoving particle horizon associated with them,  $\Delta_r(t_{\text{rec}}) = \tau_{\text{rec}}$ . By definition of the comoving particle

horizon, if these points are separated by a comoving length  $\lambda > \tau_{\text{rec}} \sim (aH)_{\text{rec}}^{-1}$ , then these points could never have been in causal contact with each other in the past. In other words, there is no point that lies inside the particle horizons of both  $p$  and  $\bar{p}$ . This is illustrated in 1.3. So the question is: If there is not enough time in the past for these points to send signals to each other, how can the CMB temperature be so uniform? The same question applies to any two points at the recombination surface that are separated by more than  $1^\circ$  degree in the sky today. How do photons originating from the CMB decoupling surface know that they should have almost the same temperature? This is the horizon problem in standard Big Bang cosmology.

In addition to the issues we have discussed, there are also magnetic monopoles that can be generated through symmetry breaking processes in the early universe and the inefficiency of the standard Big Bang evolution in diluting such relics poses an important problem [19].

The most serious issue among these issues we have presented here is the horizon problem as other ones can be addressed in other ways. Therefore, in the next section, we will focus on a possible solution to the horizon problem, which relies on an early accelerated ( $\ddot{a} > 0$ ) phase of expansion known as *inflation*.

### 1.1.2 A simple solution to the horizon problem

It is clear from the discussion in the previous section that, at the heart of the horizon problem resides the smallness of the particle horizon when the CMB radiation released. Therefore, in the search for a solution, we need to find a mechanism that can naturally lead to a much larger particle horizon, *i.e.*  $\Delta r(t_{\text{rec}}) \gg \lambda$ . This can simply be done by considering a phase of shrinking (comoving) Hubble radius  $(aH)^{-1}$  prior to the CMB decoupling such that integral representing the particle horizon takes most of its contribution from earlier times. Let us look at this argument more closely. First,

a decreasing comoving Hubble radius implies a perfect fluid with SEC violation,

$$\frac{d}{dt}(aH)^{-1} < 0 \Rightarrow \ddot{a} > 0 \Rightarrow (1 + 3w) < 0. \quad (1.20)$$

In this case the integral (1.15) describing the particle horizon is dominated by the lower limit and in the limit  $a_i \rightarrow 0$ , the particle horizon in (1.18) becomes infinitely large,

$$\Delta r(t) \rightarrow \infty, \quad \text{for } a_i \rightarrow 0. \quad (1.21)$$

In other words, if we consider a phase of accelerated expansion  $\ddot{a} > 0$  (or  $1 + 3w < 0$ ), there is much more conformal time between the singularity and the time of CMB decoupling as the Big Bang singularity is now pushed back to very large negative values

$$\tau_i = \frac{2H_0^{-1}}{(1 + 3w)} a_i^{(1+3w)/2} \rightarrow -\infty, \quad (1.22)$$

as  $a_i \rightarrow 0$ . This means that the photons that are released at the time of the CMB decoupling have enough time to communicate with each other in the past. This is how an inflationary early universe addresses the horizon problem.

In the following section, we will briefly review the physics of inflation together with its observational predictions in the simplest versions of the inflationary paradigm.

## 1.2 Slow-roll Inflation

We have seen that the shrinking comoving Hubble radius corresponds to an accelerated expansion  $\ddot{a} > 0$  and a universe dominated by a perfect fluid with negative pressure  $w < -1/3$ .

In the context of a microscopic theory, these conditions can be achieved by con-

sidering a minimally coupled scalar field to GR,

$$S = \int d^4x \sqrt{-g} \left\{ \frac{M_{\text{Pl}}^2}{2} R - \frac{1}{2} g^{\mu\nu} \partial_\mu \phi \partial_\nu \phi - V(\phi) \right\}, \quad (1.23)$$

where  $g^{\mu\nu}$  is the inverse of the metric  $g_{\mu\nu}$ ,  $R$  is the Ricci scalar derived from this metric and  $V(\phi)$  is the inflaton potential. The stress-energy tensor for the scalar field derived from this action is given by

$$T_{\mu\nu} = \partial_\mu \phi \partial_\nu \phi - \frac{1}{2} g_{\mu\nu} \left\{ \frac{1}{2} g^{\rho\sigma} \partial_\rho \phi \partial_\sigma \phi - V(\phi) \right\}. \quad (1.24)$$

If we assume that this energy-momentum tensor is the only source of the Einstein equations in (1.2), it can lead to a FLRW expansion. We are interested in conditions that can give rise to an accelerating solution in this framework. Consistent with the symmetries of FLRW evolution, let's consider the equation of state of homogeneous<sup>3</sup> inflaton  $\bar{\phi}$  field,

$$w_\phi \equiv \frac{P_\phi}{\rho_\phi} = \frac{\dot{\bar{\phi}}^2 - 2V(\bar{\phi})}{\dot{\bar{\phi}}^2 + 2V(\bar{\phi})}. \quad (1.25)$$

This immediately shows that negative pressure leading to  $\ddot{a} > 0$ , *e.g.*  $w_\phi \simeq -1 < -1/3$ , can be achieved if  $\dot{\bar{\phi}}^2 \ll 2V(\bar{\phi})$ . Inflation will last as long as  $\rho_\phi + 3P_\phi < 0$ , *i.e.*  $\dot{\bar{\phi}}^2 < 2V(\bar{\phi})$ . The exact equation of state with  $w_\phi = -1$  can be considered as a limiting case of accelerating expansion solutions. In this case, the scalar field does not roll, *i.e.*  $\dot{\bar{\phi}} = 0$  and such a FLRW solution is called de-Sitter space-time. As we have shown before in section 1.1, this corresponds to a universe dominated by a cosmological constant where the scale factor takes the exponential form with an constant Hubble rate (See *e.g.* equations (1.8) and (1.9)). In order to understand the departure from a cosmological constant (hence a stationary field configuration  $\dot{\bar{\phi}} \neq 0$ ), we first note that as long as universe undergoes an accelerated expansion,

---

<sup>3</sup>Later on, we will consider departures from exact homogeneity,  $\phi(\vec{x}, t) = \bar{\phi}(t) + \delta\phi(\vec{x}, t)$  to establish observational predictions of inflation.

the spatial curvature term will diminish quickly and hence we take  $K = 0$  in the first Friedmann equation in (1.3). Then, using  $\ddot{a}/a = \dot{H} + H^2$  in the second line of (1.3), we have  $-2\dot{H}M_{\text{pl}}^2 = \rho_\phi + P_\phi$ . Therefore, we can parametrize inflationary solutions with a rolling field in the following way

$$w_\phi = -1 - \frac{2\dot{H}}{3H^2} \equiv -1 + \frac{2}{3}\epsilon, \quad (1.26)$$

where we have defined the *slow-roll* parameter for the Hubble rate as  $\epsilon \equiv -\dot{H}/H^2 = \dot{\phi}^2/2H^2M_{\text{pl}}^2$ . It is clear from this expression that an accelerated solution with a rolling scalar, *i.e.*  $-1 < w_\phi < -1/3$ , requires

$$\epsilon = -\frac{\dot{H}}{H^2} = -\frac{d \ln H}{dN} < 1. \quad (1.27)$$

Here, we have defined  $dN = d \ln a = H dt$  which measures the number of e-foldings during the accelerated expansion. CMB data suggests that the universe would have had undergone at least 60 e-folds of inflation if the horizon problem is to be solved. In order to achieve this, we therefore require  $\epsilon$  to remain small for a sufficiently large number of e-folds. This can be parametrized by defining a second slow-roll parameter,

$$\eta \equiv \frac{d \ln \epsilon}{dN} = \frac{\dot{\epsilon}}{\epsilon H}. \quad (1.28)$$

For  $|\eta| < 1$ , fractional change of  $\epsilon$  is small per Hubble time and inflation continues for a sufficiently large amount of time.

The Hubble slow-roll conditions we have described can be related to the microphysics of inflationary models through the potential  $V(\phi)$  and its derivatives. For this purpose, we need to make use of the slow-roll approximations in the Friedmann

equation and Klein-Gordon<sup>4</sup> equation of the scalar field,

$$\ddot{\bar{\phi}} + 3H\dot{\bar{\phi}} + V'(\bar{\phi}) = 0 \quad \rightarrow \quad 3H\dot{\bar{\phi}} = -V', \quad (1.29)$$

$$H^2 = \frac{1}{3M_{\text{pl}}^2} \left( \frac{\dot{\bar{\phi}}^2}{2} + V(\bar{\phi}) \right) \quad \rightarrow \quad H^2 \simeq \frac{V}{3M_{\text{pl}}^2}, \quad (1.30)$$

where we have assumed  $\epsilon, \eta \ll 1$ . Here, note that  $\eta \ll 1$  implies that the dimensionless acceleration parameter of the scalar field is also small, namely  $\delta \equiv -\ddot{\bar{\phi}}/(\dot{\bar{\phi}}H) \ll 1$  as second slow-roll parameter is given by  $\eta = -2\delta + 2\epsilon$  by definition.

Using (1.30) in (1.29) provides a relationship between the kinetic energy and the gradient of the potential

$$\epsilon = \frac{\dot{\bar{\phi}}^2}{2H^2M_{\text{pl}}^2} \simeq \frac{M_{\text{pl}}^2}{2} \left( \frac{V'}{V} \right)^2. \quad (1.31)$$

On the other hand, taking a time derivative of (1.29) and again using (1.30) in the resulting expression leads to

$$\delta + \epsilon = 2\epsilon - \frac{\eta}{2} = M_{\text{pl}}^2 \frac{V''}{V}. \quad (1.32)$$

The form of these expressions suggest that the following potential slow-roll parameters are convenient in describing inflationary solutions,

$$\epsilon_v = \frac{M_{\text{pl}}^2}{2} \left( \frac{V'}{V} \right)^2, \quad |\eta_v| = M_{\text{pl}}^2 \frac{|V''|}{V}, \quad (1.33)$$

where we require  $\{\epsilon_v, |\eta_v|\} \ll 1$ .

As we have mentioned previously, the number of e-foldings can be considered as a measure of time during the accelerated expansion. Particularly, it can be thought as the amount of inflation that has to occur at a given time  $t$  before inflation terminates.

---

<sup>4</sup>Equation of motion for the scalar field can be derived by using the continuity equation (1.6) with the energy momentum tensor (1.24).

Under the slow-roll conditions, it can be written as

$$N(t) = \int_a^{a_{\text{end}}} d \ln a = \int_t^{t_{\text{end}}} H(t) dt \simeq \frac{1}{M_{\text{pl}}^2} \int_{\bar{\phi}_{\text{end}}}^{\bar{\phi}(t)} \frac{V'}{V} d\bar{\phi}, \quad (1.34)$$

where we have denoted  $\bar{\phi}_{\text{end}}$  as the value of the field at the end point of inflation defined by  $\epsilon_v(\bar{\phi}_{\text{end}}) = 1$ . For inflationary models with monomial potential, *e.g.*  $V = \lambda M_{\text{pl}}^{4-p} \phi^p/p$ , the number of e-folds can be related to the value of the field or equivalently the value of the slow-roll parameter at a given time,

$$N(t) \simeq \frac{\bar{\phi}^2(t) - \bar{\phi}_{\text{end}}^2}{2pM_{\text{pl}}^2} \simeq \frac{p}{4\epsilon(t)}, \quad (1.35)$$

where we assumed  $\epsilon \simeq \epsilon_v \ll 1$ . As typically the value of the field is larger than the value at the end of inflation, the expression above implies that the value of the field is large compared to the Planck mass,  $\bar{\phi}(N) \simeq M_{\text{pl}}\sqrt{2pN}$ , *i.e.* for  $2pN > 1$ .

### 1.3 Reheating

Considering the end of inflation, we are challenged by another problem: During inflation, the energy density of the universe would have been dominated by a slowly rolling scalar field. In this phase, the energy density of the scalar field is almost constant, whereas, that of any pre-existing standard matter (*i.e.* radiation, non-relativistic matter including your toothbrush) gets diluted by a factor  $e^{-60}$  (also known as zero) by the exponential expansion. Recall that existence of matter is crucial in understanding the successes of Hot Big Bang Model through processes such as BBN and CMB decoupling. Therefore, we need a way to convert the energy in the scalar field at the end of inflation to that of normal matter. In particular, nucleosynthesis (See for example [20]) and evidence for cosmological neutrino background [21] imply that universe was in thermal equilibrium at MeV temperatures. This implies that universe has to be filled with relativistic particles some time between the end of inflation and  $T \sim \text{MeV}$ .

This process is called *reheating*.

Typically reheating proceeds as follows: at the end of inflation the scalar field starts oscillating around the minimum of its potential. If we approximate the shape of the potential around the minimum as quadratic, the energy density during this phase scales as  $\rho \propto a^{-3}$  and the universe effectively behaves as ordinary matter. Depending on the couplings between the inflaton and daughter fields, decays of inflaton might proceed perturbatively [22, 23] or through a very efficient process called *preheating* (also known as parametric resonance) [24, 25]. Finally, produced particles should interact and reach thermal equilibrium [26]. The details of reheating are highly model-dependent, but this series of phases we described ultimately determines the temperature at which the universe becomes in equilibrium and enters the standard Hot Big Bang behavior.

The main unattractive features of reheating are its inability to leave direct imprints on observable scales [27] and its strong model dependence. Though several coarse grained features of the reheating phase, such as its equation of state and duration, can have an indirect effect on inflationary observables [28].

In this thesis, reheating will be one of our main focuses. In the following chapters, we will study scenarios where reheating dynamics can lead to observable effects when considered in conjunction with dark matter<sup>5</sup> (DM) physics. In the last chapter, we will also present a framework that may be helpful in reducing the model dependence in reheating studies. Our main aim in this section was to introduce the importance of this era in understanding Hot Big Bang evolution. Therefore, we will leave important details to the relevant chapters as our discussion proceeds.

---

<sup>5</sup>An essential component within the standard Hot Big Bang cosmology that we will discuss later on.



## 1.4 Inflation in the CMB sky

So far, we have mainly dealt with background dynamics of inflationary cosmology and its success in explaining the observed flatness, isotropy and homogeneity of the universe. However, as first shown by the COBE mission [29], there are small inhomogeneities (at the level of  $\delta T/T_{\gamma,0} \sim 10^{-5}$ ) in the CMB temperature. Moreover, interpreted as density perturbations at later epochs, the time evolution of these inhomogeneities in GR lead to the formation of LSS structure we see today (See *e.g.* Figure 1.1). It was first realized by Chibisov and Mukhanov [30] that quantization of inflaton fluctuations can indeed account for small, scale invariant inhomogeneities we observe on the CMB. This is one of the main attractive features of inflation since the idea was first introduced; The structure we see today originates from tiny quantum fluctuations during inflation!

A complete treatment of fluctuations from inflation requires the introduction of some technical details related to cosmological perturbation theory. We will therefore digress into these issues first.

### 1.4.1 Cosmological Perturbations

The main philosophy behind cosmological perturbation theory is to expand all quantities of interest around their homogeneous background values,  $X(\vec{x}, t) = \bar{X}(t) + \delta X(\vec{x}, t)$  where  $X(\vec{x}, t)$  can be the metric and matter fields,  $X \equiv \{g_{\mu\nu}, \phi, \rho, P\}$ . Since the fluctuations are small,  $\delta X \ll \bar{X}$ , dynamics of the space-time, *i.e.*  $\delta g_{\mu\nu}$  can be accurately described by the linearized Einstein equations,

$$\delta G_{\mu\nu} = M_{\text{pl}}^{-2} \delta T_{\mu\nu}. \quad (1.36)$$

The high degree of symmetry of the background allows us to decompose the metric and stress-energy perturbations into its irreducible parts. At linear order in perturbations

the decomposition of the metric is given by [31, 32]

$$\delta g_{\mu\nu} = \begin{pmatrix} -2\Phi & a(\partial_i B + \hat{B}_i) \\ a(\partial_i B + \hat{B}_i) & a^2(-2\Psi\delta_{ij} + 2D_{ij}E + 2\partial_{(i}\hat{E}_{j)} + h_{ij}) \end{pmatrix}, \quad (1.37)$$

where  $D_{ij} \equiv \partial_i\partial_j - \frac{1}{3}\delta_{ij}\nabla^2$ . Here, hatted vectors are divergence free (transverse),  $\partial_i\hat{A}_i = 0$  and  $h_{ij}$  is transeverse and traceless tensor,  $\partial_i h_{ij} = h_{ii} = 0$ . The metric in (1.37) contains 10 degrees of freedom: 4 scalars  $\{\Phi, \Psi, B, E\}$ , 4 vectors  $\{\hat{B}_i, \hat{E}_i\}$  (2 independent component for each vector) and 2 tensors in  $h_{ij}$ . In single field inflationary models, vector fields are not produced and even if they are produced they decay away with the expansion. Therefore, from now on we will focus on scalar and tensor perturbations.

For matter sources that have the perfect fluid form (1.5), perturbations in the stress-energy tensor are given by

$$\delta T^\mu_\nu = \begin{pmatrix} -\delta\rho & a(\bar{\rho} + \bar{P})v_i \\ a^{-1}\delta^{ij}(\bar{\rho} + \bar{P})(v_j - \partial_j B) & \delta P\delta^i_j + \Pi^i_j \end{pmatrix}, \quad (1.38)$$

where  $\Pi^i_j$  is the traceless anisotropic stress and  $v_i$  is the spatial component of the perturbed 4-velocity of the fluid,  $\delta U_\mu = (-\Phi, av_i)$ . The velocity  $v_i$  and the anisotropic stress  $\Pi^i_j$  can be further decomposed into their irreducible parts,

$$v_i = \partial_i v + \hat{v}_i, \quad (1.39)$$

$$\Pi_{ij} = D_{ij}\Pi + \partial_{(i}\hat{\Pi}_{j)} + \hat{\Pi}_{ij}. \quad (1.40)$$

Given the form of the perturbed stress-tensor, it is also convenient to define the scalar 3-momentum density as  $(\bar{\rho} + \bar{P})av \equiv \delta q$ , where we took into account the decomposition in (1.39).

*Gauge Freedom.* An important subtlety in the study of cosmological perturbations is that the splitting of quantities into the background and perturbations is not unique

but depends on the choice of coordinates. This freedom is referred to as a gauge choice akin to the terminology in particle physics. To illustrate the dependence on the choice of coordinates, consider an infinitesimal change in the coordinates,  $x^\mu \rightarrow \tilde{x}^\mu = x^\mu + \xi^\mu(\vec{x}, t)$  and the inflaton field  $\phi(\vec{x}, t) = \bar{\phi}(t) + \delta\phi(\vec{x}, t)$ . By definition a 4-scalar,  $\phi$  has to be invariant under  $x \rightarrow \tilde{x}$ , *i.e.*  $\phi(x) = \tilde{\phi}(\tilde{x})$ . Expanding both sides of this equation, to linear order in  $\xi$ , we have the following transformation rule for the perturbation  $\delta\phi$ ,

$$\delta\tilde{\phi} = \delta\phi - \dot{\bar{\phi}}(t)\xi^0. \quad (1.41)$$

Now, even if we have a physical situation where original perturbation of the field vanishes  $\delta\phi = 0$ , by our coordinate choice, we have introduced a fake perturbation  $\delta\tilde{\phi} \neq 0$ . Similarly, we can remove a real perturbation by choosing  $\xi^0 = \delta\phi/\dot{\bar{\phi}}$ , *i.e.*  $\delta\tilde{\phi} = 0$ . In other words, a perturbation that is present in one coordinate system can be made to vanish in another; by choosing appropriate coordinates, a perturbation can be “gauged away”. In order to resolve this ambiguity between real and fake perturbations, we need to consider matter fluctuations, *i.e.*  $\delta\phi, \delta\rho$ , *etc.* simultaneously with metric fluctuations. Neglecting the former, or the latter might lead to gauge modes being treated as physical perturbations and vice versa. When we handle both types of perturbations, a physical perturbation<sup>6</sup> never disappears from the dynamics, it is just hidden in a different degree of freedom after we fix the gauge (choose a coordinate system). In other words, we can trade one for the other using the gauge freedom.

*Gauge transformations.* Under an infinitesimal coordinate transformations  $x^\mu \rightarrow x^\mu + \xi^\mu$ , perturbations of a rank- $n$  tensor  $T_{\mu_1 \dots \mu_n}$  around its background value  $\bar{T}_{\mu_1 \dots \mu_n}$  transform as

$$\delta\tilde{T}_{\mu_1 \dots \mu_n} = \delta T_{\mu_1 \dots \mu_n} - \xi^\nu \partial_\nu \bar{T}_{\mu_1 \dots \mu_n} - \bar{T}_{\nu \dots \mu_n} \partial_{\mu_1} \xi^\nu - \dots - \bar{T}_{\mu_1 \dots \nu} \partial_{\mu_n} \xi^\nu. \quad (1.42)$$

Now we exploit this general fact to derive transformation rules for the scalar<sup>7</sup> metric

---

<sup>6</sup>See the discussion below on gauge invariant perturbations.

<sup>7</sup>Note that tensorial part of the any perturbed quantity is by definition gauge invariant, *e.g.*  $h_{ij}$ .

perturbations and the perturbed scalar quantities associated with the stress energy tensor. For an infinitesimal vector  $\xi^\mu = (\xi^0, \epsilon^i)$ , further decomposing  $\epsilon_i = \partial_i \epsilon + \hat{\epsilon}_i$ , scalar metric perturbations transform as

$$\begin{aligned}\Phi &\rightarrow \Phi - \dot{\xi}^0(x), & B &\rightarrow B + \frac{\xi^0(x)}{a(t)} - a(t) \dot{\epsilon}(x), \\ E &\rightarrow E - \epsilon(x), & \Psi &\rightarrow \Psi + H(t) \xi^0(x).\end{aligned}\tag{1.43}$$

Similarly, from the transformation law of perturbed stress tensor, we can obtain

$$\begin{aligned}\delta\rho &\rightarrow \delta\rho - \dot{\bar{\rho}} \xi^0(x), & \delta P &\rightarrow \delta P - \dot{\bar{P}} \xi^0, \\ v &\rightarrow v + \frac{\xi^0(x)}{a(t)} \Rightarrow \delta q &\rightarrow \delta q + (\bar{\rho} + \bar{P}) \xi^0(x).\end{aligned}\tag{1.44}$$

By considering the linear combinations of the scalar metric and matter fluctuations, we can build scalar perturbations that are invariant under gauge transformations.

*Gauge invariant perturbations.* Two important gauge-invariant variables are called Bardeen potentials [33],

$$\begin{aligned}\Phi_{\text{B}} &\equiv \Phi - \frac{d}{dt}[a^2(\dot{E} - B/a)] \\ \Psi_{\text{B}} &\equiv \Psi + a^2 H(\dot{E} - B/a).\end{aligned}\tag{1.45}$$

Another gauge invariant quantity is the curvature perturbation on uniform-density hypersurfaces [34],

$$-\zeta \equiv \Psi + \frac{H}{\dot{\bar{\rho}}} \delta\rho.\tag{1.46}$$

By definition,  $\zeta$  can be considered as a measure of the spatial curvature on constant density hypersurfaces (*i.e.*  $\delta\rho = 0$ ),  $R^{(3)} = \nabla^2 \Psi / a^2$  where  $R^{(3)}$  is the Ricci curvature scalar of the spatial hypersurfaces. Another useful property of this quantity is; in a gauge defined by vanishing  $\Psi = 0$ ,  $\zeta$  can be directly related to the dimensionless density perturbation  $\delta\rho/3(\bar{\rho} + \bar{P})$  and hence with temperature fluctuations in the

CMB. For super-horizon scales  $(k/aH) \rightarrow 0$ , it coincides (up to a sign) with another gauge invariant scalar called comoving curvature perturbation

$$\mathcal{R} \equiv \Psi - \frac{H}{\bar{\rho} + \bar{p}} \delta q. \quad (1.47)$$

$\mathcal{R}$  measures spatial curvature on comoving hypersurfaces. Arguably, the most important property of  $\zeta$  and  $\mathcal{R}$  is that they remain constant outside the horizon for adiabatic matter perturbations. This can be seen from writing the following expression for the time evolution of comoving curvature scalar  $\mathcal{R}$ ,

$$\dot{\mathcal{R}} \simeq \frac{H}{\bar{\rho} + \bar{P}} \delta P_{\text{nad}}, \quad (1.48)$$

where

$$\delta P_{\text{nad}} \equiv \delta P - \frac{\bar{P}}{\bar{\rho}} \delta \rho \quad (1.49)$$

is the gauge invariant non-adiabatic pressure [35]. For example, in single field inflationary models  $\delta P_{\text{nad}} = 0$  and conservation of  $\mathcal{R}$  is firmly established. However, in the case of multiple fluids or scalar fields this is not guaranteed. In the following chapters, we will further discuss this issue in a multi-field inflationary model. For now we assume that both curvature perturbations are conserved on large scales outside the horizon. An immediate consequence of this is that, since inflation can be characterized by a shrinking comoving Hubble radius  $(aH)^{-1}$ , modes with comoving wavelength  $k^{-1}$  that is smaller than the horizon will eventually cross the horizon,  $k = aH$  and freeze. From this time on, they will remain constant and continue their super-horizon evolution during the Big Bang phase until they re-enter the horizon (*i.e.* at the time of CMB decoupling). This tells us that the initial conditions for the small temperature fluctuations in the CMB are essentially set at the horizon exit during inflation, which we denote by  $k_* = a(t_*)H(t_*)$ .

We note that for single field slow-roll inflation the definitions of  $-\zeta$  and  $\mathcal{R}$  match

exactly. This can be realized by using  $\delta\rho = V'\delta\phi \simeq -3H\dot{\phi}\delta\phi$  and  $\delta T_0^i = -\dot{\phi}\partial_i\delta\phi = \partial_i\delta q$  in (1.46) and (1.47),

$$-\zeta \simeq \mathcal{R} = \Psi + \frac{H}{\dot{\phi}}\delta\phi. \quad (1.50)$$

*Gauge Fixing.* A common way to deal with gauge freedom is to use it to our advantage by removing some of the scalar perturbations. For example, we can determine the slicing and threading of space-time by fixing  $\xi^0(x)$  and  $\epsilon(x)$  to set some perturbations to zero. Here, we mention two important gauges we will make use of parallel to some of our discussions in this thesis.

Without specifying the sources of the expansion, we can consider the following set for the scalar perturbations  $\{\Phi, \Psi, E, B, \delta\rho, \delta q\}$ . First by a spatial coordinate transformation  $x^i \rightarrow x^i + \delta^{ij}\partial_j\epsilon$  with  $\epsilon(x) = E(x)$ , we can set  $E \rightarrow 0$  (See equation (1.43)). Then by choosing an appropriate slicing, *e.g.*  $\xi^0 = -aB + a^2\dot{E}$ , we can set  $B \rightarrow 0$ . The remaining variables in the matter sector, *i.e.*  $\delta\rho, \delta q$  can be related to  $\Phi$  and  $\Psi$  by the Einstein constraint equations (See Appendix 1.A). Therefore we are left with one independent scalar degree of freedom as expected and this set up is called *Newtonian gauge* (or longitudinal gauge) where the metric takes the following form

$$ds^2 = -(1 + 2\Phi)dt^2 + a^2(t)(1 - 2\Psi)\delta_{ij}dx^i dx^j. \quad (1.51)$$

Moreover, if the anisotropic stress vanishes<sup>8</sup>, we can further simplify the metric by  $\Phi = \Psi$  [32]. Note also that in the Newtonian gauge,  $E = B = 0$ , gauge invariant Bardeen potentials coincide with potentials in the Newtonian gauge,  $\Psi_B \rightarrow \Psi, \Phi_B \rightarrow \Phi$ .

In the context of inflation, we can consider the following set of scalar perturbations  $\{\Phi, \Psi, E, B, \delta\phi\}$ . By setting  $E = 0$  in the same way we did before, we can now relate the  $\Phi$  and  $B$  to  $\Psi$  and  $\delta\phi$  through the energy and momentum constraint equations, therefore we are left with two independent perturbations where  $\Psi$  parametrizes

---

<sup>8</sup>Indeed this is the case for perfect fluids including scalar fields

the curvature perturbation of spatial hypersurfaces and  $\delta\phi$  is the fluctuations in the matter sector;

$$g_{ij} = a^2(t)e^{-2\Psi(x)}\delta_{ij}, \quad \phi = \bar{\phi}(t) + \delta\phi(x). \quad (1.52)$$

We can utilize left over time-reparametrization to set the inflaton fluctuations to zero,  $\delta\phi \rightarrow 0$  by requiring  $\xi^0 = \delta\phi/\dot{\bar{\phi}}$ . Since the scalar momentum density vanishes with this choice of slicing,  $\delta q \rightarrow \delta q + (\bar{\rho} + \bar{P})\xi^0 = 0$ , this coordinate choice is called the *comoving gauge*. In this gauge we have

$$g_{ij} = a^2(t)e^{-2\mathcal{R}(x)}\delta_{ij} = a^2(t)e^{2\zeta(x)}\delta_{ij}, \quad \phi = \bar{\phi}(t) \quad (1.53)$$

where  $\mathcal{R} = \Psi + (H/\dot{\bar{\phi}})\delta\phi$ . As we claimed before, a physical perturbation never disappears from the dynamics, in the comoving gauge, inflaton fluctuations are hidden inside the comoving curvature perturbation  $\mathcal{R}$ .

## 1.4.2 Contact with Observations

We are now ready to extract predictions from inflation by quantizing the fluctuations in the theory given by the action (1.23). To properly take into account the metric fluctuations in the theory, it is convenient to use the metric in the ADM form [36] where the space-time is sliced into three dimensional hypersurfaces,

$$ds^2 = -N^2 dt^2 + \hat{g}_{ij}(dx^i + N^i dt)(dx^j + N^j dt). \quad (1.54)$$

Here, the lapse function  $N(x)$  and the shift function  $N_i(x)$  essentially contain the same information as the metric perturbations  $\Phi$  and  $B$  in (1.85) in the sense that they are non-dynamical<sup>9</sup> variables that can be solved in terms of the dynamical ones and  $\hat{g}_{ij}$  is the three-dimensional metric on constant time  $t$  hypersurfaces. Using (1.54), the action (1.23) takes the following form

---

<sup>9</sup>This correspondence is also clear by noticing that,  $\Phi$  and  $B$  in the linearized Einstein equations (1.87),(1.88) appear with at most with single time derivative

$$S = \frac{1}{2} \int d^4x \sqrt{\hat{g}} \left\{ M_{\text{pl}}^2 [NR^{(3)} + N^{-1}(E_{ij}E^{ij} - E^2)] \right. \\ \left. + N^{-1}(\dot{\phi} - N^i \partial_i \phi)^2 - N \hat{g}^{ij} \partial_i \phi \partial_j \phi - 2NV \right\}, \quad (1.55)$$

where we have used the following inverse metric components in terms of  $N, N^i$  and  $\hat{g}^{ij}$   $g^{00}$ ,

$$g^{00} = -\frac{1}{N^2}, \quad g^{0i} = g^{i0} = \frac{N^i}{N^2}, \quad g^{ij} = \hat{g}^{ij} - \frac{N^i N^j}{N^2}. \quad (1.56)$$

In (1.55),  $E_{ij}$  is related to the extrinsic curvature of the three-dimensional spatial slices  $K_{ij} = N^{-1}E_{ij}$  and is given by

$$E_{ij} \equiv \frac{1}{2}(\dot{\hat{g}}_{ij} - \hat{\nabla}_i N_j - \hat{\nabla}_j N_i), \quad E = E^i{}_i. \quad (1.57)$$

To describe the leading action for the perturbations, we fix time and spatial reparameterizations to focus on the comoving gauge for the dynamical fields  $g_{ij}$  and  $\phi$ ,

$$\delta\phi = 0, \quad \hat{g}_{ij} = a^2[e^{2\zeta}\delta_{ij} + h_{ij}], \quad \partial_i h_{ij} = h^i{}_i = 0, \quad (1.58)$$

where we described the curvature perturbation on constant  $\phi$  surfaces with  $\zeta$ . As we have mentioned in the previous section, this gauge choice removes two of five scalar perturbations in the theory and the remaining two can be eliminated in favor of the gauge invariant  $\zeta$  and  $h_{ij}$  by varying the action (1.55) with respect to lapse and the shift  $N, N^i$  and plugging these constraint equations back into the action.

*Scalar Power Spectrum (a.k.a scalar 2-pt function).* Following the lengthy procedure we described above leads to the following 2nd order action for the curvature



perturbation  $\zeta$  [37]

$$S_s^{(2)} = \frac{1}{2} \int d^4x a^3 \frac{\dot{\phi}^2}{H^2} \left[ \dot{\zeta}^2 - a^{-2} (\partial_i \zeta)^2 \right]. \quad (1.59)$$

Written in this form, the second order action is not suitable for standard canonical quantization methods in QFT. For this purpose, we introduce the *Mukhanov-Sasaki* variable  $v = z\zeta$  with  $z \equiv a\dot{\phi}/H$  by switching to conformal time  $d\tau = dt/a$ . This leads to the following action for  $v$  [31]

$$S_s^{(2)} = \frac{1}{2} \int d\tau d^3x \left[ (v')^2 + (\partial_i v)^2 + \frac{z''}{z} v^2 \right], \quad (1.60)$$

which is essentially the action for a free scalar field with a time dependent mass,  $m_{\text{eff}}^2(\tau) = z''/z$ . We can now promote the field  $v$  to a quantum operator as a superposition of annihilation and creation operators,

$$v \rightarrow \hat{v} = \int \frac{d^3\mathbf{k}}{(2\pi)^3} \left[ v_{\mathbf{k}}(\tau) \hat{a}_{\mathbf{k}} e^{i\mathbf{k}\cdot\mathbf{x}} + v_{\mathbf{k}}^*(\tau) \hat{a}_{\mathbf{k}}^\dagger e^{-i\mathbf{k}\cdot\mathbf{x}} \right], \quad (1.61)$$

where  $\hat{a}_{\mathbf{k}}$  and  $a_{\mathbf{k}}^\dagger$  satisfies the algebra  $[\hat{a}_{\mathbf{k}}, a_{\mathbf{k}'}^\dagger] = (2\pi)^3 \delta(\mathbf{k} + \mathbf{k}')$  and the vacuum is defined by the standard relation  $\hat{a}_{\mathbf{k}}|0\rangle = 0$ . This decomposition leads to the following equation for the mode functions  $v_{\mathbf{k}}(\tau)$ ,

$$v_{\mathbf{k}}'' + \left( k^2 - \frac{z''}{z} \right) v_{\mathbf{k}} = 0, \quad (1.62)$$

where the effective mass term to first order in slow-roll parameters is given by

$$\frac{z''}{z} = \frac{\nu_s^2 - 1/4}{\tau^2}, \quad \nu_s \simeq \frac{3}{2} + 2\epsilon - \delta. \quad (1.63)$$

The solution for (1.62) that reduces the Bunch-Davies vacuum in the  $-k\tau \rightarrow \infty$  limit,

i. e. to  $v_{\mathbf{k}} = \frac{1}{\sqrt{2k}}e^{-ik\tau}$ , can be written as

$$v_{\mathbf{k}}(\tau) = \sqrt{\frac{\pi}{4k}} e^{i(\nu_s+1/2)\pi/2} (-k\tau)^{1/2} H_{\nu_s}^{(1)}(-k\tau). \quad (1.64)$$

Since we are interested in modes that exit the horizon during inflation, a useful limit to take in (1.64) is  $-k\tau \rightarrow 0$ ,

$$v_{\mathbf{k}}(\tau) \simeq e^{i(\nu_s-1/2)\pi/2} 2^{\nu_s-3/2} \frac{\Gamma[\nu_s]}{\Gamma[3/2]} \frac{(-k\tau)^{1/2-\nu_s}}{\sqrt{2k}}, \quad -k\tau \rightarrow 0. \quad (1.65)$$

Now, given the fourier decomposition (1.61) of the canonically normalized field  $v(x)$ , we are can ready to calculate the 2-point function of curvature perturbation  $\zeta$ ,

$$\langle \zeta_{\mathbf{k}} \zeta_{\mathbf{k}'} \rangle \equiv (2\pi)^3 \delta(\mathbf{k} + \mathbf{k}') \mathcal{P}_\zeta(\tau, k) = (2\pi)^3 \delta(\mathbf{k} + \mathbf{k}') \frac{|v_{\mathbf{k}}(\tau)|^2}{z^2}, \quad (1.66)$$

where  $\langle \dots \rangle$  denotes vacuum expectation value and the delta function follows from the fact that background is invariant under spatial translations. Since the modes freeze after the horizon exit at  $-k\tau = 1$ , and stay intact through the super-hubble evolution until horizon re-entry, the 2-point function of  $\zeta$  is suitable for comparison with CMB temperature anisotropies. For a reference comoving scale,  $k_*$ , that re-enters the horizon at CMB decoupling, the horizon exit condition at a time  $\tau_*$  during inflation can be written as  $k_*\tau_* = 1$ . Using this parametrization and the solution we found in (1.65), we can finally write the *dimensionless* power spectrum as

$$\Delta_s^2(k) = \frac{k^3}{2\pi^2} \mathcal{P}_\zeta(\tau_*, k) = \frac{1}{8\pi^2} \frac{H_*^2}{\epsilon_* M_{\text{pl}}^2} \left( \frac{k}{k_*} \right)^{n_s-1}, \quad (1.67)$$

where the scalar spectral tilt is given by  $n_s - 1 = 3 - 2\nu_s = -4\epsilon_* + 2\delta_*$  and  $*$  denotes that relevant quantities are evaluated at horizon crossing during inflation. Since slow-roll parameters are small, this result implies that inflation predicts an almost scale invariant (with a slightly red tilt) power spectrum. In other words, in the slow-roll

inflationary paradigm, the deviation from perfect scale invariance,  $n_s = 1$  can be realized as a departure from a perfect de-Sitter expansion parametrized by  $\epsilon, \delta$  etc. In recent years, this prediction has been confirmed by various CMB experiments. At a pivot scale  $k_*$ , the most recent measurements on the CMB anisotropies favors the following values for the amplitude and spectral index of the power spectrum [38]

$$n_s = 0.9645 \pm 0.0049 \quad (68\% \text{CL}), \quad (1.68)$$

$$A_s \equiv \frac{1}{8\pi^2} \frac{H_*^2}{\epsilon_* M_{\text{pl}}^2} = 2.2 \times 10^{-9}. \quad (1.69)$$

Note also that the small amplitude of the power-spectrum further justifies our perturbation theory approach at linear order.

*Tensor Power Spectrum.* Using the tensor part of the metric (1.54), the first line of the action (1.55) leads to the 2nd order action for  $h_{ij}$ . In conformal time, this procedure gives [39]

$$S_t^{(2)} = \frac{M_{\text{pl}}^2}{8} \int d\tau d^3x \ a^2 \left[ h'_{ij} h'_{ij} + \partial_k h_{ij} \partial_k h_{ij} \right]. \quad (1.70)$$

Similar to the scalar case, we decompose the tensor modes in fourier space as

$$h_{ij} = \sum_{\lambda} \int \frac{d^3\mathbf{k}}{(2\pi)^3} \left[ \epsilon_{ij}^{\lambda}(k) h_{\mathbf{k}}^{\lambda}(\tau) \hat{b}_{\mathbf{k}}^{\lambda} e^{i\mathbf{k}\cdot\mathbf{x}} + \text{h.c} \right], \quad (1.71)$$

where the polarization tensors satisfy  $e_{ii} = k^i \epsilon_{ij} = 0$ ,  $e_{ij}^{\lambda} e_{ij}^{\lambda'} = 2\delta^{\lambda\lambda'}$  and h.c stands for hermitian conjugate of the preceding expression. Annihilation and creation operators satisfies the algebra  $[\hat{b}_{\mathbf{k}}^{\lambda}, \hat{b}_{\mathbf{k}'}^{\lambda'\dagger}] = (2\pi)^3 \delta(\mathbf{k} + \mathbf{k}') \delta^{\lambda\lambda'}$  and the vacuum is defined by  $\hat{b}_{\mathbf{k}}^{\lambda}|0\rangle = 0$ .

By plugging the decomposition (1.71) into the action (1.70) one can obtain the equation of motion for the canonically normalized mode functions,  $v_{\mathbf{k}} \equiv a M_{\text{pl}} h_{\mathbf{k}}^{\lambda}(\tau)/2$ ,

$$v_{\mathbf{k}}^{\lambda \prime\prime} + \left( k^2 - \frac{a''}{a} \right) v_{\mathbf{k}}^{\lambda} = 0. \quad (1.72)$$

From the equations of motion above, it is clear that we have just two copies of the same equation we dealt with in the scalar perturbation case. The only difference is that the effective mass term is now given by

$$\frac{a''}{a} = \frac{\nu_t^2 - 1/4}{\tau^2}, \quad \nu_t \simeq \frac{3}{2} + \epsilon. \quad (1.73)$$

Following the same procedure as before, the 2-pt function for each polarization state is simply

$$\langle h_{\mathbf{k}}^\lambda h_{\mathbf{k}'}^{\lambda'} \rangle = (2\pi)^3 \delta(\mathbf{k} + \mathbf{k}') \mathcal{P}_t^\lambda(k, \tau) = (2\pi)^3 \delta(\mathbf{k} + \mathbf{k}') \frac{2H^2}{k^3 M_{\text{pl}}^2} (-k\tau)^{3-2\nu_t} \quad (1.74)$$

Summing over both polarizations, the dimensionless tensor power spectrum at horizon crossing  $\tau_* = k_*^{-1}$  reads [40],

$$\Delta_t^2(k) = \frac{k^3}{2\pi^2} \sum_\lambda \mathcal{P}_t^\lambda = \frac{2H_*^2}{\pi^2 M_{\text{pl}}^2} (-k\tau_*)^{n_t} = \frac{2H_*^2}{\pi^2 M_{\text{pl}}^2} \left( \frac{k}{k_*} \right)^{n_t}, \quad (1.75)$$

where  $n_t = 3 - 2\nu_t = -2\epsilon_*$ . This implies that tensors are also scale invariant, thanks to the appearance of the slow-roll parameter. In analogy with scalars we can identify the amplitude of the tensors as

$$A_t = \frac{2H_*^2}{\pi^2 M_{\text{pl}}^2}. \quad (1.76)$$

Note that the scalar power  $A_s$  has an extra factor of  $1/\epsilon_*$  compared to tensors at leading order in slow-roll. This implies that there is more scalar power than tensors in slow-roll models. For this reason, the tensor amplitude is often normalised with respect to the measured scalar amplitude by defining the *tensor to scalar ratio*,

$$r_* \equiv \left. \frac{\Delta_t^2(k)}{\Delta_s^2(k)} \right|_* = \left. \frac{A_t}{A_s} \right|_*. \quad (1.77)$$

It is also important to note the consistency condition between tensor to scalar ratio,  $r$  and the tensor tilt,  $n_t = -r_*/8 = 2\epsilon_*$ . An immediate conclusion that can be made

from this relation is that if we find a nearly scale invariant spectrum of tensor modes,  $|n_t| \ll 1$ , this would confirm that  $|\dot{H}| \ll H^2$  in the early universe and hence would be strong evidence that inflation took place in the early universe. There is another important implication of the observation of tensor modes during inflation. Using the definition (1.77), we can write

$$\frac{H_*}{M_{\text{pl}}} = \pi \Delta_s(k_*) \sqrt{\frac{r_*}{2}}. \quad (1.78)$$

Substituting the observed power in scalar fluctuations,  $\Delta_s(k_*) \simeq 4.7 \times 10^{-5}$ , it provides us a hierarchy between Hubble rate during inflation and the Planck scale,

$$\frac{H_*}{M_{\text{pl}}} \simeq 3 \times 10^{-5} \left( \frac{r_*}{0.1} \right)^{1/2}, \quad (1.79)$$

where we take a fiducial value for  $r$  considering the recent constraints from Planck:  $r < 0.10$  (95% CL) at  $k_* = 0.002 \text{ Mpc}^{-1}$ . Therefore, detection of the inflationary tensor modes at the level of  $r = 0.1$  would imply that the Hubble rate  $H_*$  during inflation was about  $10^{-5} M_{\text{pl}}$ . Another common way of expressing this result is through the energy scale of inflation,

$$E_{\text{inf}} \equiv (3H_* M_{\text{pl}})^{1/4} \simeq (V_*)^{1/4} \simeq 8 \times 10^{-3} \left( \frac{r_*}{0.1} \right)^{1/4} M_{\text{pl}}. \quad (1.80)$$

Notice that the energy scale does not depend strongly on tensor to scalar ratio, reducing  $r$  by four orders of magnitude reduces the energy scale only by one order of magnitude.

Gravitational waves are robust relics that are essential in our understanding of the inflationary era. Their detection through the CMB B-mode polarization [41] would provide strong evidence for inflation and the energy scale at which inflation takes place. It is therefore important to challenge the inflationary paradigm with future B-mode polarization experiments. In particular, the next generation CMB S4

experiment [42] will be able put bounds on the level of tensor modes at,  $r \lesssim 10^{-3}$ , hence it can significantly impact the way we think about inflationary models.

**Non-gaussianities from inflation.** So far, we have discussed the lowest order predictions that arise from quantum fluctuations in a free field theory, *e.g.* (1.59). If this was the full theory, fluctuations would be Gaussian and the theory could be completely described by its 2-pt functions, while all other n-point functions vanish. However, even in the simplest slow-roll models we are considering here, there are deviations from perfect Gaussianity [37]. In general, a wealth of information can be obtained by studying interactions on top of the free theory and we call this information *primordial non-Gaussianity* [43, 44].

The primary indicator of non-Gaussianity is the 3-point function (or bispectrum),

$$\langle \Omega | \zeta_{\mathbf{k}_1} \zeta_{\mathbf{k}_2} \zeta_{\mathbf{k}_3} | \Omega \rangle = (2\pi)^3 \delta(\mathbf{k}_1 + \mathbf{k}_2 + \mathbf{k}_3) B_\zeta(k_1, k_2, k_3), \quad (1.81)$$

where  $|\Omega\rangle$  is the vacuum of the interacting theory and the delta-function is due to the translation invariance of the background. The bispectrum can be factorized as  $B_\zeta(k_1, k_2, k_3) = f_{\text{NL}} \mathcal{S}(k_1, k_2, k_3)$  where  $f_{\text{NL}}$  is the dimensionless non-Gaussianity parameter and the function  $\mathcal{S}$  determines the shape of bispectrum associated with triangles of different shapes formed by the wavevectors  $\{\mathbf{k}_1, \mathbf{k}_2, \mathbf{k}_3\}$ . The most recent Planck analysis [45] has put the following constraints on the amplitudes of the different shapes

$$f_{\text{NL}}^{\text{local}} = 2.5 \pm 5.7, \quad f_{\text{NL}}^{\text{ortho}} = -34 \pm 33, \quad f_{\text{NL}}^{\text{equil}} = -16 \pm 70, \quad 68\% \text{ CL}, \quad (1.82)$$

where the equilateral shape peaks when  $k_1 = k_2 = k_3$  while the orthogonal shape peaks for both equilateral and flattened configurations  $k_1 = k_2 = k_3/2$ . The local signal peaks for squeezed triangles, *i.e.*  $k_1 \ll k_2 \simeq k_3$ . Particularly, in single field models of inflation, the bispectrum in the squeezed limit can be shown to lead an

important consistency relation [37, 46],

$$f_{\text{NL}}^{\text{local}} = \frac{5}{12}(n_s - 1). \quad (1.83)$$

This implies that primordial non-Gaussianity is expected to be very small in the canonical single field models. Therefore, observing  $f_{\text{NL}}^{\text{local}} > 1$  would rule out all models of single-field inflation! In light of the constraints from Planck above, this possibility seems to be constrained significantly.

## 1.5 $\Lambda$ CDM model

Before we introduce the standard model of cosmology, we need to talk about the two main components in the universe: *Dark Energy and Dark Matter*.

*Dark Energy.* Dark energy is essentially the energy density of the vacuum itself. If this vacuum energy arises due to the cosmological constant  $\Lambda$  of general relativity being nonzero, the energy density is a constant in space and time. We have already showed this in Section 1.1, where we described the cosmological constant by a perfect fluid with an equation of state  $w = -1$  and hence  $\rho_\Lambda \propto \text{constant}$ . Thus, a larger volume of space will have a larger amount of dark energy. So, as the universe expands, during very late times one would expect dark energy to dominate over all other forms of energy (See Figure 1.2).

*Dark Matter.* The CMB temperature anisotropies on the sky today are a consequence of the evolution of fluctuations from earlier epochs, and hence it is certainly clear that their distribution depends on a number of factors like the amount of matter in the universe, the rate at which the universe is expanding, the geometry of the spatial hypersurfaces, etc. For a given set of initial conditions at some time before recombination, we can make use of this set of parameters to calculate the distribution of the anisotropies on the sky today. Conversely, given the observed distribution of the anisotropies, we can estimate the values of these parameters.

Following the latter route, if we consider only the particles that we know from the Standard Model of Particle Physics (*e.g.* leptons, baryons, gauge bosons), it turns out that CMB data do not fit the theory for any values of parameters. At this point, we are left with two options; we either modify General Relativity (GR) or modify the particle content in the Standard Model of Particle Physics. Given the success of GR on a wide range of scales, it is acceptable to begin by doing the latter via the introduction of a new kind of particle. In 1933, Zwicky [47] proposed that the Coma Cluster had an dark mass density that does not interact with light as a solution to the observation that the mass of the galaxies that he estimated seemed to be much more than his calculations for the mass of the luminous matter in the cluster. If we follow Zwicky’s suggestion, we can propose two types of matter: baryonic matter which are a part of the Standard Model and dark matter, referring to matter that interacts very weakly with the Standard Model. Considering the distribution of the CMB anisotropies today, matter plays two different roles. First, the phenomenon of CMB decoupling depends on the non-gravitational interaction between photons, electrons and protons. Second, by having mass, matter influences how the universe evolves, and hence how photons propagate in and out of the gravitational potential wells created by matter. It turns out that considering an additional component of dark matter provides a much better fit of the model to the CMB data. In the context of FLRW cosmology, dark matter (DM) can be modeled as a perfect fluid, just like baryons are. Thus, energy density and pressure completely characterize the dark matter fluid. We can therefore decompose the dimensionless matter density parameter as  $\Omega_m = \Omega_b + \Omega_c$ .

The perturbations in the DM fluid also play a crucial role in the structure formation. As we will see, the CMB data prefers  $\Omega_{c,0} \gg \Omega_{b,0}$  so that at early times (recall that both fluids energy density scale as  $a^{-3}$ , *e.g.* see (1.11)), the pressureless matter dominated era is dominated primarily by the DM fluid. On the other hand, before the time of radiation and matter equality, the universe is dominated by ultra-relativistic particles which can be considered as a fluid with  $P_r = 1/3\rho_r$ . The pressure density of



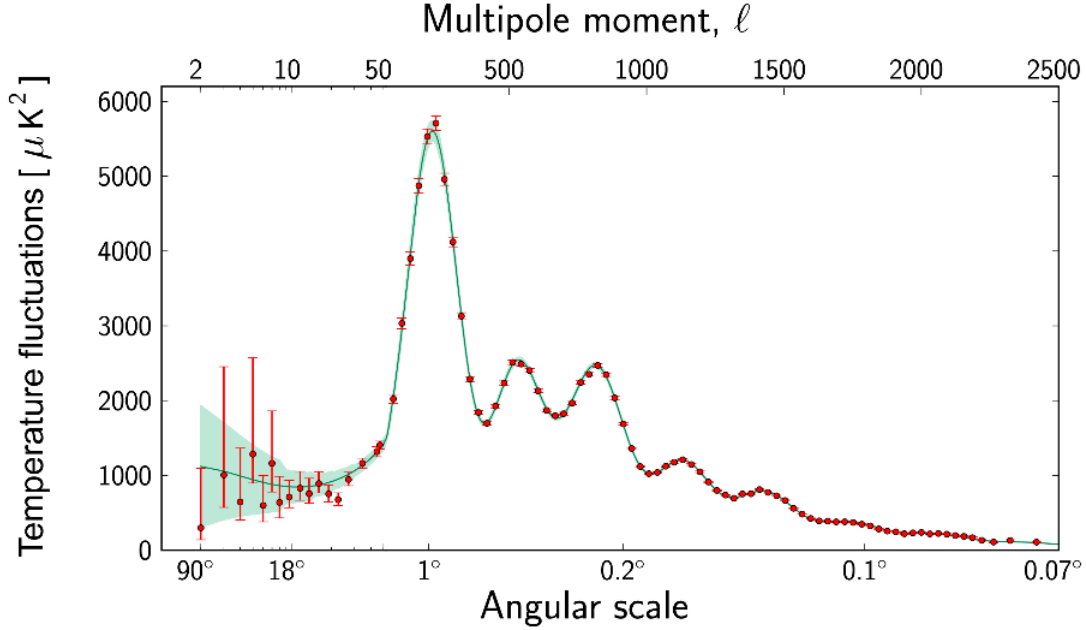


Figure 1.4: The CMB temperature anisotropy power spectrum measured by Planck satellite [1]. Red lines represent the experimental error bars. The green line represents the best-fit curve of the  $\Lambda$ CDM model (See Table 1.1).

the background fluid is crucial in understanding the growth of the perturbations in the DM fluid, in that it suppresses the growth of structures. For example, it is known that DM perturbations grow only logarithmically with the scale factor,  $\propto \ln a(t)$  in a radiation dominated universe ( $w_r = 1/3$ ), whereas in a DM dominated universe (or in a fluid with  $w = 0$  in general), it evolves linearly with  $a(t)$ .

Looking at the structure we see in the sky today, we can obtain important clues about the properties of DM. The temperature of DM is an important property that can effect structure formation in the universe. If the dark matter particles have large temperature, this would mean that they would have large velocity dispersions and thus large mean free paths. Large velocity dispersions of DM particles would decrease the ability of the growth of structure on scales smaller than the mean free path of the particles, simply because clumping of the particles would be inefficient at those scales. In this case, structure formation should proceed in a “top-down” manner, that is, first

Parameter	Planck
$\Omega_{b,0}h^2$	$0.02207 \pm 0.00067$
$\Omega_{c,0}h^2$	$0.1196 \pm 0.0061$
$\Omega_{\Lambda,0}$	$0.683 \pm 0.040$
$\tau$	$0.097 \pm 0.80$
$10^9 A_s$	$2.23 \pm 0.32$
$n_s$	$0.962 \pm 0.019$

Table 1.1: Parameters of  $\Lambda$ CDM baseline model (at 68 % CL). The first four parameters describe the composition of the universe, whereas the last two sets the initial conditions for CMB fluctuations.

structures on the largest scales (such as superclusters) should form first, subsequently fragmenting into smaller pieces like galaxies. In this case we would expect fluctuations on small scales would be erased over time. In the case of cold dark matter instead, the structure formation proceeds in a “bottom-up” manner: first small structures form and then continue to grow in bigger and bigger-sized objects.

Evidence from the CMB and other experimental probes have shown that structure formation proceeded in a bottom-up manner. Therefore, there is a big consensus in the cosmology community that there must be a significant amount of Cold Dark Matter (CDM).

The  $\Lambda$ CDM model has six free parameters: the physical baryon density,  $\Omega_{b,0}h^2$ , the physical density<sup>10</sup> of CDM,  $\Omega_{c,0}h^2$ , the dark energy density  $\Omega_{\Lambda,0}$ , the optical depth  $\tau$ , and the scalar amplitude  $A_s$  and the spectral index  $n_s$  of the primordial scalar power spectrum with the power-law ansatz,

$$\Delta_s^2(k) = A_s \left( \frac{k}{k_*} \right)^{n_s-1}. \quad (1.84)$$

This simple model provides an excellent fit to the CMB data. This can be seen in Figure 1.4 where we show the CMB temperature fluctuations measured by Planck

<sup>10</sup>Physical density parameters are obtained by multiplying density parameters,  $\Omega_X$  with the square of the reduced Hubble constant  $h \equiv H_0/(100 \text{ km s}^{-1}\text{Mpc}^{-1})$

satellite, and the best-fit curve of the  $\Lambda$ CDM model provided by the best-fit parameters [18] in Table 1.1.

## 1.6 Open Problems and Outline of the Dissertation

Supported by the inflationary paradigm, the  $\Lambda$ CDM model is incredibly successful in identifying the composition of the Universe and in explaining the observed CMB temperature anisotropies and LSS data. Despite its success, the standard model of cosmology on its own can not explain the true micro-physical origin of the different components (phases) in (of) the Universe. For example, while inflation provides us with a consistent, testable framework for understanding the origin of structure in our universe, we are yet to understand details of inflationary dynamics, how it ends (through reheating) and how the evolution in the post-inflationary era proceeds. Intriguingly, these stages are host to a number of interesting phenomena, including the generation of stable relics such as DM [48] and matter/anti-matter asymmetry [49], that are essential in understanding the world we observe today, as well as for establishing new physics. From this perspective, it is clear that the issues related to the standard model of cosmology are firmly interconnected with high energy particle physics. In this thesis, we therefore aim to investigate this connection further by focusing on the following topics from a cosmological perspective;

*DM and Reheating.* Apart from the properties of DM that we have discussed, little is known about the microphysical nature of DM. As we have discussed briefly, these properties are enough to explain phenomena such as CMB anisotropies and galaxy clustering that are essentially separated widely in scales. These lines of evidence for the existence of CDM is one of the most concrete reasons to believe in Beyond the Standard Model (BSM) physics. On the other hand, competitive bounds from collider searches, direct and indirect detection have made the DM puzzle enticing. On the

early universe side of this puzzle, BSM approaches can play a key role in the cosmological production of DM together with the associated micro-physics. Focusing on BSM physics within the Split-Supersymmetry (SUSY) framework, in Chapter 2, we will discuss low temperature reheating scenarios and investigate the correlation between the reheating temperature, non-thermal production of DM and the uncertainty inherent in inflationary observables due to post-inflationary evolution. In Chapter 3, we will study DM production from gravitino decays. Using the constraints from indirect DM detection together with the requirement of observed cosmological DM abundance, we will set upper bounds on the reheating temperature. In Chapter 4, we will focus on the DM perturbations in the low reheating temperature scenarios in order to shed light on the formation and survival of DM clumps within the Split SUSY framework.

*Inflation.* Despite the success of the simplest models of inflation in explaining the CMB data, the fundamental mechanism behind inflation continues to elude us. A unique experimental window that can help us explore these issues is by looking at the B-mode polarization pattern that GW's left on the CMB sky. As we have discussed in Section 1.4.2, a detection of GW's of primordial origin would provide us the energy scale of inflation, revealing a new energy scale of particle physics. In Chapter 5, considering constraints on the cosmological correlators, we will discuss if one can alter this connection between the scale of inflation and the detection of tensor modes in models where non-trivial multi-field dynamics including particle production events are present.

*Reheating.* In the presence of couplings to additional fields, the dynamics at the end of inflation is typically dominated by an explosive particle production process called *(p)reheating*. Despite its theoretical appeal, recent studies of (p)reheating rely on ad-hoc couplings between the relevant fields present. On the other hand, from the perspective of inflationary dynamics, it is not clear what values these couplings should take in order to agree with natural realizations of inflation. In the hope of clarifying these issues, in Chapter 6 we will first study the restrictions of efficient

particle production on the validity of the EFT of background fields. Later on, we will extend our analysis by focusing on the EFT of the fluctuations and comment on a possible enhancement of GW's during the linear regime of preheating.

# Appendix

## 1.A Perturbed Einstein Equations

The full metric containing scalar metric perturbations,  $\Phi, \Psi, E, B$  can be written as

$$ds^2 = -(1 + 2\Phi) dt^2 + 2a(t)B_{,i} dx^i dt + a^2(t)[(1 - 2\Psi)\delta_{ij} + 2\partial_i\partial_j E] dx^i dx^j, \quad (1.85)$$

where we have absorbed the  $\nabla^2 E \delta_{ij}$  part into the  $\Psi \delta_{ij}$  part. Metric perturbations are connected to stress-energy perturbations via linearized Einstein Equations

$$\delta G_{\mu\nu} = M_{\text{pl}}^{-2} \delta T_{\mu\nu}. \quad (1.86)$$

Using the scalar part of the perturbed energy momentum tensor (See *e.g.* (1.38)-(1.40)) we have the following *Einstein constraint equations* (or *energy and momentum constraint equations*) at linear order,

$$\begin{aligned} 3H(\dot{\Psi} + H\Phi) + \frac{k^2}{a^2} \left[ \Psi + H(a^2 \dot{E} - aB) \right] &= -\frac{\delta\rho}{2M_{\text{pl}}^2} \\ \dot{\Psi} + H\Phi &= -\frac{\delta q}{2M_{\text{pl}}^2}. \end{aligned} \quad (1.87)$$

On the other hand, the Einstein equations also yield two *dynamical equations*

$$\begin{aligned}\ddot{\Psi} + 3H\dot{\Psi} + H\dot{\Phi} + (3H^2 + 2\dot{H})\Phi &= \frac{1}{2M_{\text{pl}}^2} \left( \delta p - \frac{2}{3}k^2\Pi \right) \\ (\partial_t + 3H)(\dot{E} - B/a) + \frac{\Psi - \Phi}{a^2} &= \frac{\Pi}{M_{\text{pl}}^2}.\end{aligned}\tag{1.88}$$

Using the definition of the Bardeen potentials in (1.45), the last equation may be written as

$$\Psi_{\text{B}} - \Phi_{\text{B}} = 8\pi G a^2 \Pi.\tag{1.89}$$

In the absence of anisotropic stress this implies,  $\Psi_{\text{B}} = \Phi_{\text{B}}$ .

# Chapter 2

## Supersymmetry, Non-thermal Dark Matter and Precision Cosmology

### 2.1 Introduction

Cosmological observations allow us to determine the geometry, composition and age of the universe with great accuracy, and to tightly constrain the primordial perturbation spectrum. Big Bang Nucleosynthesis (BBN) and the recently revealed cosmological neutrino background imply that the universe was thermalized at MeV scales. Further, the correlation between temperature and E-mode polarization anisotropies in the Cosmic Microwave Background (CMB) gives strong evidence that primordial perturbations were laid down before recombination.

Standard Model physics cannot generate the primordial perturbations, drive baryogenesis or supply the dark matter content of the universe. Consequently, key processes occur at very high energies during the *primordial dark ages* in which the universe is dominated by physics beyond the Standard Model. This period is weakly constrained, given our ignorance of the underlying physics. Crucially, while the neutrino background and BBN require that the universe was thermalized at MeV scales, it need not be thermalized at higher energies. The equation of state during the primordial



dark age determines the expansion rate, and thus the rate at which modes (re)enter the horizon, modifying the observed power spectrum if the spectral index,  $n_s$ , is not strictly scale-invariant [50–58]. This issue has primarily been discussed in the context of inflation, but it arises in any mechanism generating perturbations well beyond Standard Model scales.

If the primordial universe is thermalized, massive long-lived particles may *freeze-out* with a final abundance determined primarily by their mass and annihilation cross-section [48]. This is the basis of thermal WIMP<sup>1</sup> dark matter, which assumes a weak-scale cross-section,  $\sigma$  and  $\langle\sigma v\rangle_{th} \simeq 10^{-26} \text{ cm}^3/\text{s}$ , where  $v$  is the typical velocity. Alternatively, *nonthermal* dark matter is produced via the decay of heavier particles into a long-lived final state and does not require thermal equilibrium [59–63] (for a review see [64], and for recent related work [65–67]). Dark matter models are constrained by both direct detection experiments and searches for astrophysical signals generated by their annihilation products. Nonthermal dark matter can have a higher self interaction cross-section than thermal dark matter so astrophysical signals are potentially stronger for these scenarios, particularly in indirect experiments such as FERMI and AMS-2 [68–73].

Simple supersymmetric (SUSY) versions of the Standard Model face considerable pressure from LHC data, but SUSY remains a candidate symmetry of high energy physics and SUSY models provide a wide range of dark matter candidates. In the Minimal SUSY Standard Model (MSSM), LHC data requires large scalar superpartner masses of 10 TeV or more [74] while the dark matter species can be lighter. This a situation that naturally leads to nonthermal dark matter production (e.g. [75, 76]) and a similar argument applies to anomaly mediated SUSY breaking [77]. Further, a primordial nonthermal phase may be generic in SUSY models with a high energy completion in the presence of gravity [64, 78]. This was seen explicitly in the *G2-MSSM* [79], and later generalized to models with *strong* moduli stabilization [80,

---

<sup>1</sup>Weakly Interacting Massive Particles

81]. In many cases nonthermal dark matter production is naturally favored in these scenarios.

Given LHC bounds on the SUSY spectrum in the MSSM, cosmological constraints – while indirect – are key to explorations of the SUSY parameter space at higher energies. In this paper we explore nonthermal dark matter production in the MSSM, quantifying the extent to which the nonthermal phase changes expectations for inflationary observables. For nonthermal production, the cross-sections are often larger than typical for thermal dark matter, increasing the sensitivity of astrophysical searches for dark matter decay products. In particular, we discuss constraints on the mass of neutralino dark matter and the allowed contributions to the neutralino mass from the bino, wino and higgsino.

The paper is organized as follows. In Section 2 we review uncertainties in inflationary observables derived from the unknown post-inflationary equation of state. In Section 3, we summarize nonthermal dark matter phenomenology and the associated expansion history. In Section 4, we explore the post-inflationary expansion history of the universe in an MSSM model with SUSY breaking above the TeV scale, and show how this is constrained by existing and future constraints from dark matter experiments. In the final section we conclude.

## 2.2 CMB Uncertainties from the Post-Inflationary Expansion

To determine the predictions of a specific inflationary model<sup>2</sup> we match the comoving wavenumber  $k$  to the instant it exits the Hubble horizon [50–58]. This occurs when  $k = a_k H_k$  where  $H$  and  $a$  denote the Hubble parameter and scale factor respectively, and a subscript  $k$  labels values at horizon crossing. We define  $N$ , the number of

---

<sup>2</sup>We focus on inflation, but our arguments apply to any mechanism which generates perturbations on super-Hubble scales with a power spectrum whose spectral index is not strictly scale-invariant.

e-folds before the end of inflation,

$$e^{N(k)} \equiv \frac{a_{\text{end}}}{a_k}, \quad (2.1)$$

where  $a_{\text{end}}$  denotes the scale factor at the end of inflation and rewrite  $N(k)$  as

$$N(k) = \ln \left( \frac{H_k}{H_{\text{end}}} \right) - \ln \left( \frac{k}{a_0 H_0} \right) + \ln \left( \frac{a_{\text{end}} H_{\text{end}}}{a_0 H_0} \right), \quad (2.2)$$

where  $(a_0 H_0)^{-1}$  is the value of the co-moving Hubble radius today [53]. The first term in equation (2.2) can be determined for any specific model, while the final term depends on the post-inflationary expansion history of the universe. We assume single-field slow-roll inflation for the purposes of illustration and characterize the post-inflationary expansion by an effective equation of state  $w$ . One finds the matching equation [50]

$$N(k, w) \simeq 71.21 - \ln \left( \frac{k}{a_0 H_0} \right) + \frac{1}{4} \ln \left( \frac{V_k}{M_{\text{pl}}^4} \right) + \frac{1}{4} \ln \left( \frac{V_k}{\rho_{\text{end}}} \right) + \frac{1 - 3w}{12(1 + w)} \ln \left( \frac{\rho_r}{\rho_{\text{end}}} \right), \quad (2.3)$$

where  $\rho_{\text{end}}$  is the value of the energy density at the end of inflation,  $V_k$  is the inflaton potential as the  $k$ th mode leaves the horizon, and  $\rho_r$  is the energy density at which the universe is assumed to become thermalized. The first two terms in (2.3) are model independent. For GUT scale inflation the third term is roughly  $-10$ . The fourth term is typically order unity given that the value of the inflaton potential necessarily evolves slowly as inflation proceeds. Finally, if the universe thermalizes promptly the last term is negligible, and we recover the familiar result that  $50 \lesssim N \lesssim 60$  for modes contributing to the CMB.

If  $\rho_{\text{end}}^{1/4} \gg \rho_r^{1/4}$  and  $w \neq 1/3$  then  $N$  differs from its benchmark value<sup>3</sup> by

$$\Delta N = \frac{1 - 3w}{12(1 + w)} \ln \left( \frac{\rho_r}{\rho_{\text{end}}} \right), \quad (2.4)$$

where  $\rho_{\text{end}} = 3V_{\text{end}}/2$  for a given potential. If  $w < 1/3$ ,  $\Delta N$  is negative, since  $\rho_r < \rho_{\text{end}}$ .

The equation of state during the primordial dark age induces uncertainties in inflationary predictions for the scalar tilt and tensor-to-scalar ratio  $n_s$  and  $r$ . The uncertainty in  $n_s$  is clearly associated with the running  $\alpha_s = dn_s/d \ln k$  and to lowest order in slow roll [82–84]

$$\begin{aligned} \Delta n_s &= (n_s - 1) \left[ -\frac{5}{16}r - \frac{3}{64} \frac{r^2}{n_s - 1} \right] \Big| \Delta N, \\ \Delta r &= r \left[ (n_s - 1) + \frac{r}{8} \right] \Big| \Delta N. \end{aligned} \quad (2.5)$$

The resulting fractional uncertainties  $\Delta r/r$ ,  $\Delta n_s/|n_s - 1|$  in these observables can be substantial [51, 53]. In particular, the theoretical uncertainty in  $n_s$  can be comparable to the precision with which it is measured by Planck [85]. Our primary focus is the implications for  $w$  and  $\rho_r$  of MSSM scenarios with nonthermal dark matter, which will lead to tighter predictions for the primordial spectrum of specific inflation models.

## 2.3 Thermal vs Non-thermal Dark Matter

In the early universe, the density in WIMPs relative to the critical density at freeze-out is [86]

$$\Omega_{dm}^{\text{th}} h^2 \simeq 8.63 \times 10^{-11} \left( \frac{m_X}{g_*^{1/2} \langle \sigma v \rangle T} \right) \text{GeV}^{-2}. \quad (2.6)$$

---

<sup>3</sup>In models that make an explicit prediction for  $\rho_r$  we can insert this value into equation (2.3). If the post-inflationary thermal history is unknown  $\rho_r^{1/4}$  is the energy scale by which thermalization is required to have occurred [55].

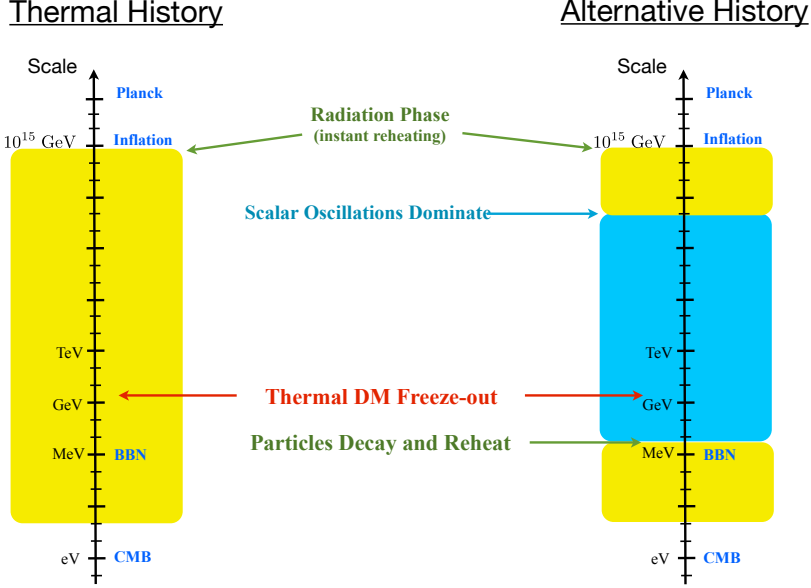


Figure 2.1: The lefthand timeline represents the thermal history of the early universe when dark matter is populated in the thermal bath that emerges shortly after after inflation. The right timeline represents a possible nonthermal history where dark matter production occurs directly from scalar decay.

where  $m_X$  is the dark matter particle's mass,  $\langle\sigma v\rangle$  is the *total* thermally averaged cross-section,  $g_*$  and  $T$  are the number of relativistic degrees of freedom and temperature at freeze-out and  $h$  is the present Hubble parameter in units of 100 km/s/Mpc. If the universe is thermalized, freeze-out occurs at  $T_f \simeq m_X/20$  and  $g_* \sim 100$ , assuming the effective number of degrees of freedom is similar to that of the Standard Model [87]. The abundance simplifies to

$$\Omega_{dm}^{\text{th}} h^2 \simeq 0.12 \left( \frac{1.63 \times 10^{-26} \text{ cm}^3 \text{ s}^{-1}}{\langle\sigma v\rangle} \right). \quad (2.7)$$

where we have used  $\text{GeV}^{-2} \cdot c \simeq 1.17 \times 10^{-17} \text{ cm}^3/\text{s}$ . WIMPs with typical speeds ( $v \simeq 0.3c$ ) and electroweak cross-sections ( $\approx 1 \text{ pb}$ ) yield  $\Omega_{dm}^{\text{th}} h^2 \simeq 0.12$  in agreement with the data, a coincidence often called the WIMP miracle.

Simple SUSY models with thermal WIMPs are in growing conflict with collider

data and direct detection experiments [88]. By contrast, nonthermal models posit that dark matter production occurs at temperatures below standard thermal freeze-out<sup>4</sup> leading to dark matter with novel and unexpected experimental signatures. For example, if a heavy relic comes to dominate the energy density following inflation and the dark matter particle is one its decay products, the resulting relic density is still given by (2.6) but with  $T = T_r$  and  $g_* = g_*(T_r)$ , the value at the time of reheating

$$\begin{aligned}\Omega_{dm}^{\text{nt}} h^2 &\simeq 8.60 \times 10^{-11} \left( \frac{m_X}{g_*(T_r)^{1/2} \langle \sigma v \rangle T_r} \right), \\ &\simeq 0.10 \left( \frac{m_X}{100 \text{ GeV}} \right) \left( \frac{10.75}{g_*} \right)^{1/2} \left( \frac{3 \times 10^{-23} \text{ cm}^3 \text{ s}^{-1}}{\langle \sigma v \rangle} \right) \left( \frac{10 \text{ MeV}}{T_r} \right)\end{aligned}\quad (2.8)$$

The similarity to the thermal freezeout result (2.6) arises because when the WIMPs are produced from scalar decay they will rapidly annihilate until their number density reduces to the point where annihilations can no longer occur. This process is essentially instantaneous (on cosmological time scales) and so this second “freeze-out” occurs at the reheat temperature  $T_r$  (see [64] for a review). Any thermally produced dark matter is diluted by the increase in entropy during the decay by a factor of  $(T_r/T_f)^3$ . Equation (2.8) demonstrates both the benefits and disadvantages of nonthermal dark matter. There is no longer a robust relationship between  $m_X$  and freeze-out temperature but there is more flexibility to satisfy the observational constraint  $\Omega_{dm} h^2 = 0.12$ , and the possibility of larger annihilation rates. The extreme case of MeV scale reheating enhances the annihilation rate by three orders of magnitude, relative to the thermal WIMP case. This would yield larger fluxes in indirect detection experiments, and modifies design strategies for direct detection and collider probes. This has led to new model building possibilities for SUSY neutralino dark matter, many of which are already tightly constrained by PAMELA and FERMI [69–73].

---

<sup>4</sup>If the particles were produced above their freeze-out threshold, they could thermalize via their mutual interactions.

There have been several phenomenological studies of nonthermal dark matter over the years. This option became more attractive when it was realized that in SUSY based solutions to the hierarchy problem – where gravity is important – the reheat temperature is not a free parameter, but is fixed by the high energy behavior of the theory [78, 79]. In combination with tightening collider and dark matter detection constraints on thermal dark matter there is thus considerable motivation for considering nonthermal dark matter.

A comparison of the thermal history of the universe for representative thermal and nonthermal scenarios appears in Figure 1. There are many possible alternatives to a strictly thermal history, which are generally associated with dark matter production that occurs at a temperature below that of thermal production, or out of equilibrium. These can include cosmic histories where there is a second phase of low-scale inflation (thermal inflation [89]), or if the decay of heavy particles leads to a significant source of dark matter and entropy production prior to BBN.

### 2.3.1 Non-thermal DM: A Realization Through Scalar Decay

Many Beyond the Standard Model (BSM) proposals contain scalar degrees of freedom beyond the minimal higgs. This is the case in supergravity and string theoretic approaches to BSM, where the vacuum expectation values of scalar fields determine the couplings of the low energy theory. However, these fields also lead to the cosmological moduli problem [90–92] – the fields are displaced from the low-energy minima in the early universe and undergo coherent oscillations, mimicking a matter dominated epoch<sup>5</sup> prior to BBN. The fields typically decay through gravitational strength couplings, and the universe reheats via the production of relativistic Standard Model and BSM particles – the lightest of which, if stable, may provide a WIMP candidate.

---

<sup>5</sup>This is strictly true only if the mass term in the potential gives the dominant contribution, otherwise the cosmological scaling of the energy density is determined by the dominant term in the potential [93].

For scalars of mass  $m_\sigma$  the decay rate typically scales as  $\Gamma \sim m_\sigma^3/M_{\text{pl}}^2$  and the corresponding reheat temperature is

$$T_r \simeq \left( \frac{m_\sigma}{10 \text{ TeV}} \right)^{3/2} \text{ MeV}. \quad (2.9)$$

If this temperature is below the thermal freeze-out scale  $T_f \simeq m_X/20$  and the field dominates the energy density at the time of decay we have a nonthermal dark matter scenario. Successful BBN and observations of neutrino decoupling require  $T_r \gtrsim 3 \text{ MeV}$  [94–97]. For dark matter with a mass not too far above the electroweak scale, fixing  $T_r < T_f \sim m_x/20$  provides an upper bound

$$20 \text{ TeV} \lesssim m_\sigma \lesssim 10^4 \text{ TeV}. \quad (2.10)$$

To give a specific example<sup>6</sup>, consider a supersymmetric model with a singlet scalar field  $\sigma$  with a shift symmetry  $\sigma \rightarrow \sigma + c$  where  $c$  is a constant, so the potential is independent of the field, or  $V(\sigma) = 0$ . If this remains a good symmetry until SUSY breaking and SUSY breaking is mediated by gravitational interactions the resulting mass is comparable that of the gravitino  $m_{3/2}$ . If SUSY addresses the electroweak hierarchy problem

$$m_{3/2} = \frac{\Lambda^2}{M_{\text{pl}}} \simeq 0.1 - 10^3 \text{ TeV}, \quad (2.11)$$

where  $\Lambda$  is the SUSY breaking scale, the electroweak hierarchy implies  $\Lambda \simeq 10^{11} - 10^{12} \text{ GeV}$ . Thus, SUSY theories can easily lead to masses in the range given by equation (2.10). The lower bound of 0.1 TeV is the origin of the term *cosmological moduli problem*, as it leads to scalar decay and a reheat temperature in conflict with the bounds set by BBN and neutrino decoupling. Within the MSSM, such low scales are already disfavored by LHC data since squarks in this mass range have not been

---

<sup>6</sup>The arguments that follow will not rely strongly on the presence of SUSY, and it would seem that the main ingredients in our argument – the existence of scalars and symmetry breaking associated with the electroweak scale – could be realized in other approaches to BSM physics.



detected, pushing up the mass scale of the gravitino.

A shift-symmetric scalar in a fundamental theory – such as supergravity or string theory – typically has additional geometric factors that lift its mass to larger values. For Type-IIB flux compactifications the mass is of order  $m_\sigma \sim \log(M_{\text{pl}}/m_{3/2})m_{3/2}$  [98] if the model accounts for both the electroweak hierarchy and the present-day vacuum energy. The authors of [78] argued that in supergravity and string frameworks the mass of a scalar which is stabilized and which meets the above requirements is typically within the range of equation (2.10), implying a nonthermal history.

In the early universe and during inflation, the shift symmetry is broken by both the finite energy density of the universe and quantum gravity effects, contributing a Hubble scale mass and a tower of non-renormalizable operators to the effective potential,

$$\Delta V(\sigma) = -c_1 H_{\text{inf}}^2 \sigma^2 + \frac{c_2}{M_{\text{pl}}^2} \sigma^6 + \dots, \quad (2.12)$$

where we expect the couplings  $c_1, c_2 \simeq \mathcal{O}(1)$ . During high scale inflation  $H > m_\sigma$  and  $\langle \sigma \rangle \simeq M_{\text{pl}}$ , as opposed to the low-energy minimum  $\langle \sigma \rangle \simeq 0$  resulting from SUSY breaking. The displacement from the low energy minima provides the initial amplitude for the coherently oscillating field  $\sigma$ . The energy density of the coherent field is

$$\rho_{\text{osc}}^\sigma(t) = \frac{1}{2} m_\sigma^2 \Delta \sigma^2 \left( \frac{a(t_{\text{osc}})}{a(t)} \right)^3. \quad (2.13)$$

Coherent oscillations begin as the expansion rate reaches  $H \simeq m_\sigma$ , corresponding to a temperature

$$T_{\text{osc}} = \left( \frac{\pi^2 g_*(T_{\text{osc}})}{90} \right)^{-1/4} (m_\sigma M_{\text{pl}})^{1/2} \simeq 2.25 \times 10^{11} \left( \frac{g_*(T_{\text{osc}})}{200} \right)^{-1/4} \left( \frac{m_\sigma}{100 \text{ TeV}} \right)^{1/2} \text{ GeV}. \quad (2.14)$$

The Universe remains effectively matter dominated until the field decays into Standard Model and SUSY particles when  $\Gamma_\sigma \simeq H$ . For a gravity mediated process, the

decay rate is

$$\Gamma_\sigma = c_3 \frac{m_\sigma^3}{M_{\text{pl}}^2}, \quad (2.15)$$

where  $c_3 = 1/(4\pi)$  is a typical value. At the time of decay the transfer of energy from the scalar field to Standard Model and SUSY particles will be instantaneous compared to the expansion rate and, because the scalar dominates the energy density, we expect a large yield of dark matter and radiation<sup>7</sup>. The radiation represents the relativistic Standard Model particles, whereas the dark matter results from rapid decays of SUSY particles down to the Lightest SUSY Particle (LSP). Due to the large production of LSPs, some annihilations take place, and these particles will achieve kinetic equilibrium quickly by scattering off the relativistic bath of Standard Model particles.

The reheat temperature of the universe is

$$T_r = \left( \frac{\pi^2 g_*}{90} \right)^{-1/4} (\Gamma_\sigma m_p)^{1/2} \simeq 20 c_3^{1/2} \left( \frac{g_*}{10.75} \right)^{-1/4} \left( \frac{m_\sigma}{100 \text{ TeV}} \right)^{3/2} \text{ MeV}. \quad (2.16)$$

and  $g_* \equiv g_*(T_r) = 10.75$  if  $T_r$  is low. Using this expression and (2.8), we estimate the relic density in nonthermal dark matter,

$$\begin{aligned} \Omega_{dm}^{\text{nt}} h^2 &\simeq 8.60 \times 10^{-11} \left( \frac{m_X}{g_*^{1/2} \langle \sigma v \rangle T_r} \right), \\ &\simeq 0.08 \left( \frac{m_X}{g_*^{1/4} \langle \sigma v \rangle m_\sigma^{3/2}} \right), \end{aligned} \quad (2.17)$$

which now depends only on the properties of the dark matter (mass and annihilation rate) and the mass of the decaying scalar resulting from SUSY breaking. As discussed above, in most models the scalar mass is not a free parameter, but similar to the gravitino mass  $m_{3/2}$ , which is related to the scale of SUSY breaking as  $\Lambda_{susy}^2 =$

---

<sup>7</sup>If the decay to SUSY particles was for some reason further suppressed compared to the Standard Model, amount of dark matter would be set by the corresponding branching ratio and the initial amount of scalar field condensate. Such a situation is difficult to arrange in practice.

$m_{3/2}M_{\text{pl}}$ . Thus, the mass of the scalar (and so the relic density of dark matter) is controlled by the need for SUSY to generate a hierarchy between the electroweak and Planck scale (i.e.  $\Lambda_{EW} \sim m_{3/2} \ll M_{\text{pl}}$ ). With a typical SUSY breaking scale of  $\Lambda = 10^{11}$  GeV, corresponding to a gravitino mass of around 4 TeV the resulting relic density is

$$\Omega_{dm}^{\text{nt}} h^2 \simeq 0.11 \left( \frac{m_X}{100 \text{ GeV}} \right) \left( \frac{10.75}{g_*} \right)^{1/4} \left( \frac{3 \times 10^{-23} \text{ cm}^3 \text{ s}^{-1}}{\langle \sigma v \rangle} \right) \left( \frac{4 \text{ TeV}}{m_{3/2}} \right)^{3/2} \left( \frac{34}{k} \right)^{3/2} \quad (2.18)$$

where we have set  $c_3 = 1/(4\pi)$ , and the ratio between the scalar and gravitino mass as  $k = m_\sigma/m_{3/2} \simeq \log(M_{\text{pl}}/m_{3/2})$  – which is only logarithmically sensitive to changes in the hierarchy. This constant is model dependent and typically between  $\mathcal{O}(1 - 100)$ . We have chosen a fiducial value for the annihilation rate that yields roughly the right amount of dark matter for the hierarchy set by the choice of low-scale SUSY breaking  $\Lambda = 10^{11}$  GeV. The cross-section is three orders of magnitude higher than expected with a thermal history with important experimental consequences, as discussed in Section 4.

The reheat temperature in this framework is not a free parameter, but a consequence of the hierarchy between the electroweak and Planck scale (determined by  $\Lambda_{susy}^2 = m_{3/2}M_{\text{pl}}$ ), which also helps determine the SUSY breaking masses of other sparticles in the theory. In both supergravity and string motivated approaches, the key lesson is that the reheat temperature is intimately connected to other aspects of the theory and not a free and tunable parameter. Given that gravitationally coupled scalars are generic in high energy completions of the Standard Model and in no sense exotic, we see that nonthermal histories are a feasible and robust possibility.

### 2.3.2 Non-thermal Histories and CMB Observables

For simplicity we assume inflationary (p)reheating was instantaneous (on gravitational time scales) and focus on the oscillations of the scalars, which come to dominate the energy density, as specified by equation (2.14). Following [50, 51, 53], we make the substitution  $\rho_{\text{end}} \rightarrow \rho_{\text{osc}} = \frac{1}{2}m_\sigma^2 \Delta\sigma^2$ , and use the fact that  $\rho_r = (\pi^2/30) g_*(T_r) T_r^4$  in equation (2.4) to write the uncertainty in e-folds as

$$\begin{aligned} \Delta N &= -0.04 + \frac{1}{12} \ln \left( \frac{g_*(T_r) T_r^4}{m_\sigma^2 \Delta\sigma^2} \right), \\ &= -10.75 + \frac{1}{12} \ln \left[ \left( \frac{g_*(T_r)}{10.75} \right) \left( \frac{T_r}{3 \text{ MeV}} \right)^4 \left( \frac{100 \text{ TeV}}{m_\sigma} \right)^2 \left( \frac{M_{\text{pl}}}{\Delta\sigma} \right)^2 \right], \end{aligned} \quad (2.19)$$

where we used  $w = 0$ , and the second line expresses the parameters relative to fiducial values. If scalar decay proceeds via a gravitational strength coupling, equation (2.15) eliminates the mass dependence in (2.19). With  $c_3 = 1/(4\pi)$  we find

$$\Delta N = -10.68 + \frac{1}{18} \ln \left[ \left( \frac{g_*(T_r)}{10.75} \right) \left( \frac{T_r}{3 \text{ MeV}} \right)^4 \left( \frac{M_{\text{pl}}}{\Delta\sigma} \right)^3 \right]. \quad (2.20)$$

This shift and its effect on physical modes is described qualitatively in Figure 2.2. We see that  $\Delta N$  is logarithmically sensitive to changes in parameters, including the reheat temperature. To generate nonthermal dark matter, the reheat temperature must typically be below about  $T_r \simeq 10 \text{ GeV}$ , but above the BBN and neutrino bounds of about  $T_r \simeq 3 \text{ MeV}$ . The range of possible temperatures is more than four orders of magnitude, but (2.20) the corresponding shift in  $\Delta N$  is  $-10.68 \lesssim \Delta N \lesssim -8.51$ . Thus, for the scenarios considered here we have a relatively robust  $|\Delta N| \simeq 10$ . Physically, a more massive field decays earlier while a lighter field decays later, but oscillations and the corresponding matter dominated phase also begin later as well (as seen from (2.14)), leading to similar values of  $\Delta N$ .

The change in inflationary observables is estimated by recalling that for most

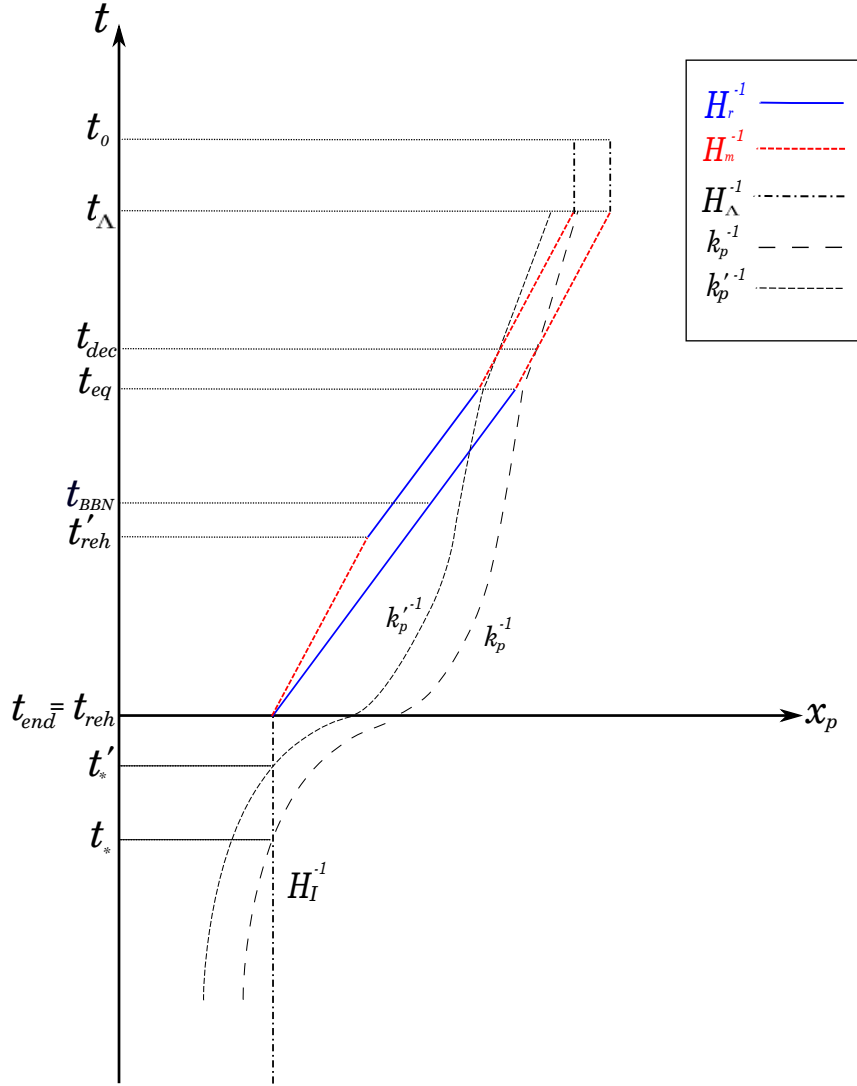


Figure 2.2: Evolution of physical wavelengths as labelled by their inverse wavenumber  $k_p^{-1}$  during inflation (below the x-axis) and during the post-inflationary epoch (above the x-axis). The solid (blue) line represents the Hubble radius,  $H_r^{-1}$  in a Universe dominated by a radiation fluid  $w = 1/3$ , the dashed (red) line is the Hubble radius,  $H_m^{-1}$  in a post-inflationary era dominated by a pressure-less fluid,  $w = 0$ . We compare the evolution of a physical mode  $k_*$  that re-enters at CMB decoupling in the standard scenario (Radiation  $\rightarrow$  Matter  $\rightarrow$  Dark energy) with a mode  $k'_*$  that re-enters at CMB decoupling in the nonthermal scenario (Matter  $\rightarrow$  Radiation  $\rightarrow$  Matter  $\rightarrow$  Dark Energy). These modes exit the Hubble radius at different times during inflation,  $t_*$  and  $t'_*$ , which translates into a shift in the number of e-folds  $\Delta N = H\Delta t$ . The corresponding shift in the pivot scale or any co-moving mode is given by  $k'_* = k_* e^{-\Delta N}$ .

simple models of inflation, the running of the spectral index  $\alpha_s \equiv dn_s/d\log k$  is typically  $-10^{-4} \gtrsim \alpha \gtrsim -10^{-3}$  [53], so  $\Delta n_s$  is between  $-10^{-3}$  and  $-10^{-2}$ , relative to the value seen with instant reheating. The remaining uncertainty in the  $n_s$  and  $r$  is significantly reduced, since these models predict that the universe is matter dominated through most of the primordial dark age.

## 2.4 Constraining Nonthermal Dark Matter

We focus on SUSY neutralinos as the WIMPs, but we expect our conclusions to be easily extended to other non-SUSY dark matter candidates. The neutralino is an electrically charge neutral state and linear combination of the superpartners of the Standard Model  $B$ ,  $W^3$ , and higgses<sup>8</sup>

$$\chi^0 = N_{10}\tilde{B} + N_{20}\tilde{W}^3 + N_{30}\tilde{H}_1^0 + N_{40}\tilde{H}_2^0, \quad (2.21)$$

where  $\tilde{B}$  and  $\tilde{W}^3$  are the bino and wino, and  $\tilde{H}_{1,2}$  are higgsinos. The  $N_{i0}$ 's denote the amount each component contributes to the neutralino. The neutralino or WIMP mass is determined by<sup>9</sup> diagonalizing a matrix which depends on the masses of the bino, wino, and higgsino ( $M_1$ ,  $M_2$ , and  $\mu$ , respectively), the Weinberg angle  $\theta_W$ , and  $\tan(\beta)$  which is the ratio of the vacuum expectation values of the higgs vevs.

When dark matter is composed of thermally produced neutralinos, the neutralino must be bino-dominated, which causes neutralinos to annihilate less efficiently, generating the correct relic density of dark matter [99]. However, if the reheat temperature following scalar decay is below thermal freeze-out, larger annihilation cross-sections are required. Likewise, because the decaying scalar gets a mass from SUSY breaking there is a natural relationship between the reheat temperature and the scale of SUSY breaking, which addresses the hierarchy problem and sets other sparticle masses. The

---

<sup>8</sup>The MSSM extension of the Standard Model higgs sector requires two higgs doublets.

<sup>9</sup>We refer the reader to [99] for more details.

hierarchy problem requires  $m_\sigma \sim m_{3/2} \sim \text{TeV}$ , which results in reheat temperatures below neutralino freeze-out temperature ( $T_f \simeq m_X/20$ ), favoring a nonthermal history. The resulting dark matter density is given by (2.8) as

$$\Omega_{dm}^{\text{nt}} h^2 \simeq 0.10 \left( \frac{m_X}{100 \text{ GeV}} \right) \left( \frac{10.75}{g_*} \right)^{1/2} \left( \frac{3 \times 10^{-23} \text{ cm}^3 \text{ s}^{-1}}{\langle \sigma v \rangle} \right) \left( \frac{10 \text{ MeV}}{T_r} \right) \quad (2.22)$$

requiring a larger annihilation cross-section. For neutralinos, the larger cross-section requires a more significant contribution from wino and higgsinos, changing expectations for colliders, and for direct and indirect detection experiments.

Existing data from these experiments place a lower bound on the reheat temperature. From (2.22), with Planck's central value  $\Omega_{dm} h^2 \simeq 0.12$  and constraints from indirect detection on  $\sigma v$  and solving for the reheat temperature we arrive at a minimum value which is typically above the hard lower bound of 3 MeV, further constraining the equation of state in the primordial dark ages.

### 2.4.1 Nonthermal Wino-like Neutralinos

The thermally averaged cross-section for the dominantly wino-like neutralino is given by [77]

$$\langle \sigma v \rangle = \frac{g_2^4}{2\pi M_2^2} \left( \frac{(1 - x_W)^{3/2}}{(2 - x_W)^2} \right) \quad (2.23)$$

where  $x_W \equiv m_W^2/M_2^2$  ( $m_W$  is the mass of the W-boson),  $g_2 \simeq 0.66$  is the  $SU_L(2)$  electro-weak gauge coupling (at the weak scale) in the MSSM,  $M_2$  is the wino mass, and we note that the result is independent of the velocity (s-wave channel). From (2.23), a wino of mass  $M_2 = 100 \text{ GeV}$ , the annihilation rate will be around  $\langle \sigma v \rangle = 4.06 \times 10^{-24} \text{ cm}^3 \text{ s}^{-1}$ , exceeding the cross-section expected for thermal WIMPs by about two orders of magnitude. The cosmological constraint (2.22) then requires a reheat temperature of around 67 MeV. From (2.23) we see that as the wino mass increases, the corresponding annihilation rate decreases, requiring larger reheat temperatures via (2.22). At this point it seems that the reheat temperature is a free and tunable

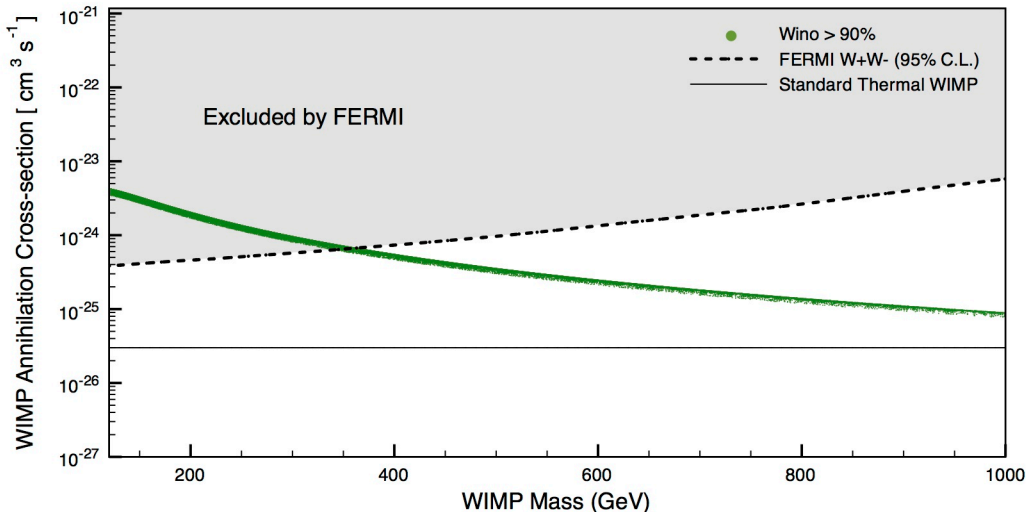


Figure 2.1: The thermally average annihilation rate  $\langle\sigma v\rangle$  for a dominantly wino neutralino to annihilate to a pair of  $W$ -bosons, as a function of mass. The Fermi constraint comes from two years of data from 10 Dwarf spheroidal galaxies [2]. These results have been obtained using DarkSUSY [3], but the general shape of the curve is in good agreement with the analytic expression (2.23). For this scan we took the MSSM parameters to vary over:  $M_2 = 100$  GeV to 2 TeV,  $\mu = 100$  GeV to 2 TeV, and  $\tan\beta = 5$  to 50. We applied all LEP2 constraints and color charged particles were taken to decouple by setting their masses to be above 2 TeV, allowing agreement with LHC constraints.

parameter. However, additional experimental constraints can be placed on the wino cross-section through the indirect detection of dark matter.

The wino annihilation rate is s-wave<sup>10</sup> so the annihilation rate above remains relevant for winos in the galaxy today, which are non-relativistic with  $v \simeq 10^{-3}c$ . Annihilation is dominantly into  $W$ -boson pairs, providing a source of anti-protons, positrons, and gamma rays. Indirect detection measurements constrain the cross-section, but suffer from a number of astrophysical complications, which includes un-

<sup>10</sup>We note that annihilations with other light MSSM states (coannihilations) can be crucial when calculating the relic density [100], and for high mass winos ( $m_X \gg \text{TeV}$ ) Sommerfeld enhancement may also play an important role [101]. However, for the range of masses and temperatures we will consider (in order to establish a *lower bound* on the reheat temperature) these effects are negligible.



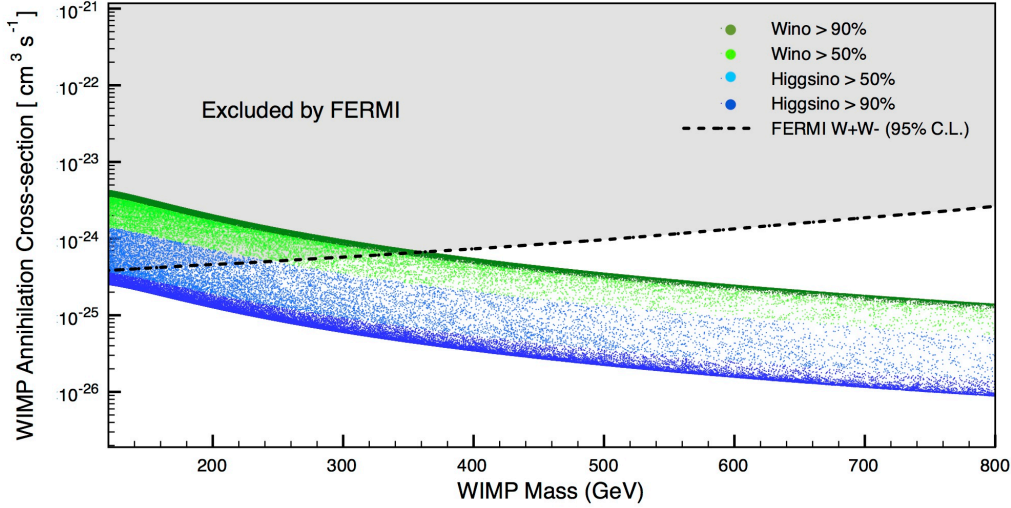


Figure 2.2: The thermally average annihilation rate  $\langle\sigma v\rangle$  for a general neutralino to annihilate to a pair of  $W$ -bosons, with a bino fraction of less than 10%, to realize a nonthermal history. The constraint from Fermi comes from two years of data from 10 Dwarf spheroidal galaxies [2]. These results have been obtained using DarkSUSY [3], however the general shape of the upper curve is in good agreement with the analytic expression (2.23) and the shape of the lower, higgsino curve agrees with the expectation that  $\langle\sigma v\rangle \sim 1/\mu^2$ . Other parameter choices match those in Figure 2.1.

certainties in the halo profile and propagation models [102]). Therefore, the best constraints on the wino arguably come from gamma rays as opposed to charged anti-matter, and we will use bounds from FERMI’s two year data from observations of 10 Dwarf Spheroidal galaxies [2], showing our results for the cross-section in Figure 2.1. For masses less than roughly 375 GeV the wino annihilation rate is too large, giving  $\langle\sigma v\rangle \lesssim 6.13 \times 10^{-25} \text{ cm}^3 \text{s}^{-1}$ . Using this in the cosmological constraint (2.22) we find  $T_r \gtrsim 696 \text{ MeV}$  (where  $g_* = 61.75$ ). Finally, the corresponding change in the number of e-folds from (2.20) is  $\Delta N = -9.37$ .

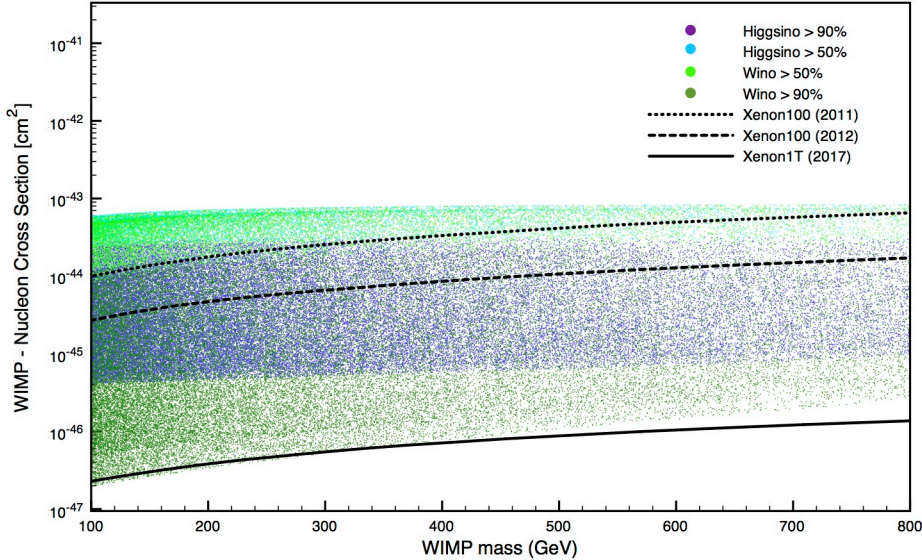


Figure 2.3: The WIMP-nucleon (proton) scattering cross-section as a function of WIMP mass. For wino-higgsino mixtures we find that most models are excluded by the Xenon 2011 / 2012 data. For purified WIMPs (dominantly wino or higgsino) many models escape existing constraints and for models with wino fractions 90% we must wait until Xenon1T for meaningful constraints to be established. However, for the dominantly higgsino models many are already disfavored. For this scan we took the MSSM parameters to vary over:  $M_2 = 100$  GeV to 2 TeV,  $\mu = 100$  GeV to 2 TeV, and  $\tan\beta = 5$  to 50. We have applied all LEP2 constraints and color charged particles were taken to decouple by setting their masses to be above 2 TeV – allowing agreement with LHC constraints.

## 2.4.2 Neutralino WIMPs: The General Case

Neutralinos can also contain bino and higgsinos in their composition as indicated in (2.21). We now consider more general neutralinos within the nonthermal framework. For a large bino contribution to (2.21) the annihilation rate is too small to allow a nonthermal history. Thus, we restrict the bino fraction to be less than 10% to ensure that a nonthermal history is realized<sup>11</sup>. On the other hand, a neutralino with a large

<sup>11</sup>We refer the reader to [103] for a recent account of the phenomenology of bino-mixed neutralinos as thermal dark matter and their observational consequences.

higgsino component is compatible with a nonthermal history. In Figure 2.2 we present the FERMI constraints on annihilations to  $W$ -bosons allowing for this possibility. We scan the MSSM parameter space using DarkSUSY [3] and present results for around 100,000 models. We restrict the bino-fraction to be less than 10%, and we take  $\mu$  and the wino mass ( $M_2$ ) to range from 100 GeV up to 2 TeV, and  $\tan\beta$  between 10 – 50.

We reject models that are incompatible with collider data, but properties of neutralino WIMPs are primarily determined by the gaugino masses ( $M_1$  and  $M_2$ ),  $\mu$  and  $\tan\beta$  – see e.g. the recent discussion in [104]. Thus, it is easy to obtain models consistent with LHC constraints on color charged super-partners. We also require a 126 GeV higgs<sup>12</sup>. From Figure 2.2, we see that our numeric results agree well with the analytic expectation that a pure wino annihilation rate should scale as  $1/M_2^2$  (top curve in Figure 2.2), whereas a pure higgsino would scale as  $1/\mu^2$  (bottom curve in Figure 2.2). Allowing for a higgsino contribution relaxes the bound on the reheat temperature provided by FERMI – with a pure higgsino being completely unconstrained.

We have restricted attention to the  $W$ -boson annihilation channel, which is typically dominant for well-mixed neutralinos, but we find similar constraints for annihilations to other common channels such as bottom quarks. Our key observation is that indirect detection alone does not put a useful bound on the reheat temperature when more general neutralinos are considered. However, bounds from direct searches partially remedy this situation. Recall that a pure wino-like neutralino gives little direct detection signal, as the WIMP-nucleon interaction is loop suppressed [104] but for more general neutralinos the situation changes and direct detection experiments provide meaningful constraints.

Consider the spin independent constraints provided by Xenon100 [106], as well as future constraints expected from Xenon1T [107]. In Figure 2.3 we use the Xenon 2011 and 2012 null results to constrain the nonthermal neutralino models considered above.

---

<sup>12</sup>There are constraints from LHC on light neutralinos, but because we are considering masses larger than around 100 GeV these constraints are not important here [105].

Although higgsino mixing relaxed the constraint on the reheat temperature coming from FERMI, many of these models are then ruled out by Xenon100. As seen in Figure 2.3, unless the neutralino is purely wino or higgsino, it is typically in tension with the Xenon100 data. Xenon1T will constrain these models even further, and would potentially bring the pure wino into tension if it yields a null result. Thus, for generically mixed neutralinos, the nonthermal history is in tension with direct detection data, and for the pure wino the lower bound on the reheat temperature is 696 MeV. The only exception is the pure higgsino, which in the low mass range is somewhat constrained by direct detection but does allow in some cases for a lower reheat temperature.

## 2.5 Conclusion

Current LHC constraints on scalar super-partner masses suggest a new mass scale  $m_{3/2} = \Lambda^2/M_{\text{pl}}$  around the 10 – 100 TeV range. When the MSSM is accompanied by additional singlets which receive SUSY breaking masses near this scale, this implies a nonthermal history for the early universe. We have shown that a nonthermal history modifies the predictions of inflationary models relative to those seen with a thermal history, and that these changes are comparable to the precision of parameter estimates made with Planck data.

A caveat to our analysis is provided by the recent work in [104] (see also [100, 108]), showing that there are certain regions of the neutralino parameter space ‘hidden’ to direct detection experiments. Although one may expect such points to be atypical, it has been argued for some time that special relations between parameters (e.g. in the case of well-tempered neutralinos [100]) may be the only way for SUSY based WIMPs to survive, given existing collider constraints. We leave a more detailed analysis – including these subtleties and constraints from spin-dependent interactions – to future work. In addition, perturbations grow in a matter dominated universe, so density

inhomogeneities with an initial amplitude of  $\delta\rho/\rho \sim 10^{-5}$  grow to be of order unity during the matter dominated phase, a phenomenon also seen in inflationary models with inefficient reheating [109]. Consequently, there will be large, short wavelength inhomogeneities in the moduli fields before thermalization, and the impact of this on their dynamics has not yet been properly explored.

More generally, these preliminary results show that within a complete theory of particle physics (in this case SUSY), understanding the origin of the present-day dark matter abundance can constrain the expansion history of the universe during the primordial dark age, and lead to more precise predictions for the primordial power spectrum.

*Note Added:* While this paper was in its final stages we received a draft from the authors of [110]. In their paper they perform a comprehensive study of the nonthermal wino, performing a careful analysis which takes into account astrophysical uncertainties associated with indirect detection and additional data from HESS [111]. In some instances they are able to arrive at more stringent constraints on the wino self-annihilation cross-section. This should lead to an improvement in the theoretical priors used for our analysis here and so stronger constraints on inflationary model building.

# Chapter 3

## Split SUSY and the Scale Inflation

### 3.1 Introduction

Supersymmetry (SUSY) has long been a favorite theoretical framework of physics beyond the Standard Model (SM). However, given the current null results of all SUSY searches, if SUSY is realized in Nature, it is unclear at what scale it will manifest itself. At the moment, theoretical studies of SUSY fall into two broad catalogues: one direction is to still focus on weak-scale natural SUSY and design non-trivial structures of flavor and Higgs sectors to evade the direct search constraints and explain the observed Higgs mass. The other direction is take seriously high-scale fine-tuned SUSY, in particular, split SUSY, with scalars heavier than gauginos. The virtues of this approach include simplicity, automatic amelioration of SUSY flavor and CP problems, preservation of gauge coupling unification and the lightest neutralino being a dark matter (DM) candidate. The idea of split SUSY, in particular, mini-split with scalars one-loop factor heavier than gauginos, was actually predicted a while ago by the simplest version of anomaly mediation [112, 113] (and later by a wide variety of moduli mediation scenarios [114–119]). Since 2003, split SUSY has started to be taken as a viable possibility despite the presence of a fine-tuned EWSB and gained more attention recently given the increasing tension between data and

naturalness [76, 118–131].

In split SUSY, the high SUSY breaking scale could naturally lead to a heavy unstable gravitino. In the mini-split scenario based on anomaly mediation, there is a loop factor separating the gravitino and gaugino mass scales with gravitino at about  $(10^2 - 10^3)$  TeV and gaugino at the TeV scale. In this scenario, the neutralino DM particles produced by late-time gravitino decays could not annihilate efficiently and thus inherit the number density of the gravitinos which adds to its thermal number density. During the reheating era, the thermal scattering of the SM superpartners contributes (at least part of) the gravitino primordial relic abundance, which is approximately proportional to the reheating temperature  $T_R$ . Consequently the requirement that the neutralino DM does not overclose the Universe sets an interesting upper bound on  $T_R$  as a function of DM mass. This upper bound could be tightened if wino is (a component of) DM. Indirect detection looking for excesses in the photon continuum spectrum or a monochromatic photon line sets a strong bound on allowed wino DM relic abundance for the whole mass range assuming NFW or Einasto DM profiles [110, 132]. The bound could be relaxed if the Milky Way DM distribution near the galactic center deviates considerably from the standard DM-only  $N$ -body simulation predictions. However, the bound does not necessarily disappear entirely. For example, even if the Milky Way DM profile has a significant core with a radius of 1 kpc, light non-thermal wino with mass below 400 GeV as a single-component DM is excluded [110]. We will present the derivation of the upper bound on  $T_R$  from the constraints of the relic abundance of neutralino DM, in particular, wino DM in Sec. 3.2 and Sec. 3.3.

On the other hand, the discovery of  $B$ -mode by the BICEP2 collaboration gives us some clues of the inflation scale [133]. The observation could be fit by a lensed  $\Lambda$ CDM plus tensor model with a tensor-to-scalar ratio  $r = 0.2^{+0.07}_{-0.05}$ . Such a large  $r$  prefers large field inflation with a heavy inflaton and very likely a high reheating temperature. We will present estimates of inflaton mass scale and reheating temperature in Sec. 3.4.

We find that in the mini-split scenario based on anomaly mediation,  $T_R$  is bounded to be at or below  $10^9 - 10^{10}$  GeV while the BICEP2 data prefers  $T_R$  to be around or above  $10^9$  GeV. The BICEP2 result has some tension with the mini-split scenario with a heavy gravitino. In other words, the BICEP2 result favors a splitting between gravitinos and gauginos larger than the loop factor predicted by anomaly mediation. Intriguingly, if SUSY breaking is tied up with gravity, e.g., through the Scherk-Schwarz mechanism, gravitinos could be as heavy as  $10^{13}$  GeV, which is the same mass scale of the inflaton inferred from the BICEP2 result while gauginos could still be light at the TeV scale. The implications for SUSY scales will be discussed in Sec. 3.5. See Refs. [134–142] for some other recent discussions of implications of the BICEP2 result for SUSY.

We conclude in Sec. 3.6 and present a discussion of gravitinos from inflaton decays in the appendix.

## 3.2 Gravitino and Wino Relic Abundance

In this section, we first review different mechanisms generating the primordial gravitino relic abundance in the early Universe. Then we discuss the relic abundance of wino DM from gravitino decays. Notice that most of the discussions also apply to other neutralino DM scenarios such as higgsino DM. The main point we want to emphasize is that: for gravitinos at or below the PeV scale, the neutralino DM relic abundance has an irreducible non-thermal contribution which scales linearly with the inflaton reheating temperature  $T_R$ ; **in particular, requiring DM relic abundance not overclose the Universe restricts the reheating temperature to be below  $(10^{10} - 10^9)$  GeV for DM mass in the range (100 GeV - 1 TeV)**; for gravitino much above the PeV scale, the neutralino DM relic abundance is almost UV insensitive, meaning that it is almost independent of  $T_R$ .



### 3.2.1 Primordial Gravitino Relic Abundance

As a superpartner of the graviton, the gravitino couples to all supermultiplets with gravitational interaction strength. In an  $R$ -parity conserving scenario, an unstable gravitino always decays to a particle and its superpartner. Decay of a gravitino will always produce a lightest superparticle (LSP) as all the other produced superparticles will cascade down to the LSP. The decay width of an unstable gravitino is given by

$$\Gamma_{3/2} \approx 2.0 \times 10^{-23} \text{ GeV} \left( \frac{N_G}{12} \right) \left( \frac{m_{3/2}}{100 \text{ TeV}} \right)^3, \quad (3.1)$$

where  $m_{3/2}$  is the gravitino mass and  $N_G$  is the number of degrees of freedom gravitino decays to. In the split SUSY scenarios with all gauginos lighter than the gravitino and the squarks heavier than the gravitino,  $N_G = 12$ .<sup>1</sup>

There could be several different origins of the primordial gravitino relic abundance,  $\Omega_{3/2} h^2$ . One comes from scattering processes of MSSM particles in the thermal bath [143–145]. This contribution approximately scales linearly with the inflaton reheating temperature  $T_R$ . The higher  $T_R$  is, the larger the gravitino relic abundance is. We will use the following approximate formula for the gravitino yield:

$$Y_{3/2}^{UV} \approx \sum_{i=1}^3 y_i g_i^2(T_R) \ln \left( \frac{k_i}{g_i(T_R)} \right) \left( \frac{T_R}{10^9 \text{ GeV}} \right), \quad (3.2)$$

where  $y_{1,2,3} = (0.653, 1.604, 4.276) \times 10^{-13}$ ,  $k_{1,2,3} = 1.266, 1.312, 1.271$  and  $g_{1,2,3}(T_R)$  are gauge couplings of SM gauge group  $U(1)_Y, SU(2)_W, SU(3)_c$  evaluated at  $T_R$  respectively [143]. The small  $y$ 's originate from  $T_R/M_p$  with  $M_p$  the reduced Planck scale. Compared to the formula given in [143], we neglected a contribution at the order of  $(M_i^2/m_{3/2}^2)$  with  $M_i$  the gaugino masses. The yield given in (3.2) leads to a

---

<sup>1</sup>The squarks could be lighter than the gravitino in the split SUSY scenarios and then  $N_G$  is larger. However, it will not change much our discussions and results.

gravitino relic abundance

$$\Omega_{3/2}^{UV} h^2 \approx 5.1 \times 10^{-2} \left( \frac{m_{3/2}}{1 \text{ TeV}} \right) \left( \frac{T_R}{10^9 \text{ GeV}} \right), \quad (3.3)$$

where we evaluated temperature dependent variables in Eq. (3.2) at  $T_R = 10^9 \text{ GeV}$ . In the numerical evaluation in Sec. 3.3, we include the full temperature dependence.

Another potential important contribution to the gravitino relic abundance comes from the decays of superpartners that are still in thermal equilibrium with the post-inflationary thermal bath [146].<sup>2</sup> When the temperature of the primordial plasma drops around the SUSY scalar masses, which we will take to be around the same scale, decays of the scalars to gravitinos could also generate a potentially non-negligible contribution to the gravitino relic abundance. This is the ‘‘freeze-in’’ mechanism [147]. When the temperature drops below the scalar masses, the number density of SUSY scalars is suppressed exponentially,  $e^{-m_s/T}$  and freeze-in stops. The freeze-in contribution is independent of the UV physics, particularly the reheating temperature  $T_R$  [148]. The gravitino yield from freeze-in is

$$\begin{aligned} Y_{3/2}^{FI} &\simeq \frac{405}{4\pi^4} \sqrt{\frac{5}{2}} \frac{M_p}{g_*^{3/2}} \sum_i g_i \frac{\Gamma_i}{m_i^2}, \\ &\approx 1.6 \times 10^{-16} \left( \frac{200}{g_*} \right)^{3/2} \left( \frac{100 \text{ TeV}}{m_{3/2}} \right)^2 \sum_i g_i \left( \frac{m_i}{1000 \text{ TeV}} \right)^3, \end{aligned} \quad (3.4)$$

where we approximated  $g_*(m_i) \simeq g_{S^*}(m_i)$  and  $\Gamma_i = (1/48\pi)(m_i^5/(m_{3/2}^2 M_p^2))$  as the partial decay width of scalar  $i$  to the gravitino. Here,  $g_i$  denotes degrees of freedom of SUSY scalar  $i$  with mass  $m_i$ . The yield in Eq. (3.4) leads to a gravitino relic abundance

$$\Omega_{3/2}^{FI} h^2 \approx 1.1 \times 10^{-2} \left( \frac{100 \text{ TeV}}{m_{3/2}} \right) \sum_i g_i \left( \frac{m_i}{1000 \text{ TeV}} \right)^3. \quad (3.5)$$

It is clear that the gravitino relic abundance  $\Omega_{3/2} h^2$  from the freeze-in contribution

---

<sup>2</sup>This contribution exists only when  $m_s > m_{3/2}$ , where  $m_s$  denotes the SUSY scalar mass. Besides, the thermal equilibrium requires reheating temperature to be  $T_R > m_s$ .

is highly sensitive to the scalar superpartner masses  $m_i$  as it scales as  $\sim m_i^3$ .

The total gravitino abundance is just a sum of the thermal scattering (Eq. (3.3)) and freeze-in (Eq. (3.5)) contributions

$$\Omega_{3/2} h^2 = \Omega_{3/2}^{UV} h^2 + \Omega_{3/2}^{FI} h^2. \quad (3.6)$$

Before ending this section, we want to mention that there could be other model-dependent sources of primordial gravitino relic abundance. For example, decay of inflaton itself could also produce a sizable gravitino relic abundance. The contribution to gravitino relic abundance from inflaton decays depends on the structure of the dynamical SUSY breaking sector and could be problematic [149, 150]. However, as discussed in [151, 152], gravitino production from inflaton decay can be suppressed if there exists a hierarchy between the mass scales of the inflaton and the field whose  $F$ -term VEV breaks SUSY spontaneously. In the discussions below, we will not include this model dependent contribution. We refer the reader to the Appendix 3.A for more details of gravitinos from inflaton decays.

### 3.2.2 Wino Relic Abundance from Gravitino Decays

In this section, we will specify the neutralino DM to be wino yet the discussions hold for other neutralino DM such as higgsino DM. We will also focus on gravitino with mass above 10 TeV so that its lifetime is shorter than a second and its decays do not spoil the successful Big Bang Nucleosynthesis [153].

The relic abundance of wino DM is a sum of the thermal contribution and the non-thermal contribution from gravitino decays. The non-thermal contribution could be computed numerically by solving the Boltzmann equations Eq. (2.1) - (2.3) in Ref [101]. The primordial gravitino relic abundance in Eq. (3.2) and (3.4) discussed in the previous section is an input to the Boltzmann equations. In solving the Boltzmann

equations, we took  $g_*(T)$  and  $g_{*,s}(T)$  from a table in the DarkSUSY code [3].<sup>3</sup> As the Sommerfeld effect becomes important for heavy winos [101, 154, 155], we computed the temperature-dependent value of  $\langle\sigma_{\text{eff}}v\rangle$  from a preliminary version 1.1 of the DarkSE code [156], taking into account not only the Sommerfeld effect but also co-annihilation among different wino species.<sup>4</sup> As an input to this code, we have used the two-loop splitting between the neutral and charged winos from Ref. [157]. For wino masses of about a TeV and temperatures around a GeV, the Sommerfeld enhancement can be as large as 3 in  $\langle\sigma_{\text{eff}}v\rangle$ .

The non-thermal contribution to wino relic abundance from gravitino decays changes parametrically when the gravitino mass  $m_{3/2}$  increases. For large gravitino mass, the wino LSP produced from the gravitino decays can annihilate effectively due to the high temperature of the plasma at the time of gravitino decay. More specifically, we find that DM annihilation is efficient for  $m_{3/2} \gtrsim 10^4$  TeV. This can be seen by estimating the “decay temperature” as in [101]

$$T_{3/2} \equiv \left( \frac{10}{g_*(T_{3/2})\pi^2} M_{\text{pl}}^2 \Gamma_{3/2}^2 \right)^{1/4} \approx 2.2 \text{ GeV} \left( \frac{75.75}{g_*(T_{3/2})} \right)^{1/4} \sqrt{\frac{N_G}{12}} \left( \frac{m_{3/2}}{10^4 \text{ TeV}} \right)^{3/2} \quad (3.7)$$

At such high temperature, winos produced from the gravitino decays annihilate rapidly, reducing the number density  $n_{\widetilde{W}}$  down to a critical value  $n_{c,\widetilde{W}} \simeq 3H/\langle\sigma_{\text{eff}}v\rangle|_{T=T_{3/2}}$  at which winos can no longer annihilate. This critical value  $n_{c,\widetilde{W}}$  behaves as an attractor in determining relic abundance of wino LSP, making it independent of the primordial gravitino relic abundance. In this case, the wino relic abundance is given as

$$\begin{aligned} \Omega_{\widetilde{W}}^{(a)} h^2 &\approx \frac{3m_{\widetilde{W}}H}{\langle\sigma_{\text{eff}}v\rangle s} \left( \frac{h^2}{\rho_{c,0}/s_0} \right), \\ &\approx 0.12 \left( \frac{75.75}{g_*(T_{3/2})} \right)^{1/4} \left( \frac{m_{\widetilde{W}}}{1 \text{ TeV}} \right) \left( \frac{1.2 \times 10^{-7} \text{ GeV}^{-2}}{\langle\sigma_{\text{eff}}v\rangle (T_{3/2})} \right) \left( \frac{m_{3/2}}{10^4 \text{ TeV}} \right)^{-3/2} \end{aligned} \quad (3.8)$$

<sup>3</sup>We keep factors involving  $\partial \log g_{*(s)}(T)/\partial \log T$  in the Boltzmann equation for  $\rho_{\text{rad}}$ .

<sup>4</sup>This version was kindly provided by Andrzej Hryczuk to JF in a previous project.

where we used Hubble parameter  $H(T) = (\pi^2 g_*(T)/90)^{1/2} T^2/M_p$ , entropy density  $s(T) = (2\pi^2 g_{*,s}(T)/45) T^3$ . We also assumed  $g_* \simeq g_{s,*}$  for the temperature of interest. We will present a more precise numerical evaluation in the following section.

For a lighter gravitino within the mass range,  $10 \text{ TeV} < m_{3/2} < 10^4 \text{ TeV}$ , the gravitino starts to decay at such a low temperature that the annihilation of wino DM is ineffective. In this case, almost all the winos produced from gravitino decays survive and hence, its relic abundance is proportional to the total gravitino abundance.

$$\begin{aligned} \Omega_{\widetilde{W}}^{(\text{na})} h^2 &= \frac{m_{\widetilde{W}}}{m_{3/2}} (\Omega_{3/2}^{UV} h^2 + \Omega_{3/2}^{FI} h^2) \\ &\approx 0.12 \left( \frac{m_{\widetilde{W}}}{1 \text{ TeV}} \right) \left[ \left( \frac{T_R}{2 \times 10^9 \text{ GeV}} \right) + 10^{-3} \left( \frac{10^2 \text{ TeV}}{m_{3/2}} \right)^2 \sum_i g_i \left( \frac{m_i}{10^3 \text{ TeV}} \right)^3 \right], \end{aligned} \quad (3.9)$$

where the first(second) term in the square brackets in the second line originates from decays of gravitino produced by the thermal scattering (freeze-in). We want to caution the reader that there is no sharp boundary value of  $m_{3/2}$  that separates the two cases with “effective” and “ineffective” wino annihilations in Eq. (3.8) and Eq. (3.9). In Sec. 3.3, we will derive more precise bounds by solving the Boltzmann equations numerically.

From Eq. (3.9), we could see that for gravitino at or below PeV scale as in the mini-split scenario, to avoid overproduction of DM from gravitino decays, the reheating temperature has to be below

$$T_R \lesssim 2 \times 10^9 \text{ GeV} \left( \frac{1 \text{ TeV}}{m_{\widetilde{W}}} \right), \quad (3.10)$$

assuming a negligible contribution from freeze-in. This upper bound would only be pushed even lower if the freeze-in contribution is comparable to or even dominate over the thermal scattering contribution. Similarly, one could obtain an upper bound

on the scalar soft mass

$$m_s \lesssim 10^4 \text{ TeV} \left( \frac{m_{3/2}}{100 \text{ TeV}} \right)^{2/3} \left( \frac{1 \text{ TeV}}{m_{\tilde{W}}} \right)^{1/3}. \quad (3.11)$$

Early discussions of reheating temperature in high-scale SUSY scenario with a decaying gravitino could be found in [80, 158].

### 3.3 Indirect Detection Constraints

As wino DM has a large annihilation rate, there are strong constraints on its relic abundance from indirect detection searches looking for its annihilation products [2, 111, 159, 160]. Thus in the wino DM case, one could obtain a stronger upper bound on the reheating temperature compared to Eq. (3.10) which holds for generic neutralino DM. In this section, we present a numerical evaluation of the constraints on the reheating temperature and SUSY scalar mass scale in the scenario with wino as (a component of) DM.

There are multiple indirect search channels for wino DM [161]. In general DM indirect detection searches for decay and annihilation products of DM in fluxes of cosmic rays containing charged particles or photons or neutrinos. We focus on searches looking for excesses in the photon continuum spectrum of satellite dwarf galaxies [2], or our galactic center [162] and monochromatic photon line [160, 163].<sup>5</sup> A continuum photon spectrum is generated from either the bremsstrahlung of charged particles or the hadronic fragmentation of the decay products of  $W/Z$ 's in the final state of tree-level processes  $\chi^0\chi^0 \rightarrow W^+W^-/ZZ$ . The gamma ray lines are generated from DM annihilation into  $\gamma\gamma/\gamma Z$ . Each photon in the final state carries away energy about the DM mass.

As demonstrated by Fig. 4 in Ref. [110], the thermal wino relic abundance (computed in [154, 164]) is ruled out by the indirect constraint for  $m_{\tilde{W}}$  above 1.5 TeV

---

<sup>5</sup>The first paper on the HESS search constraint for wino DM is Ref. [164].

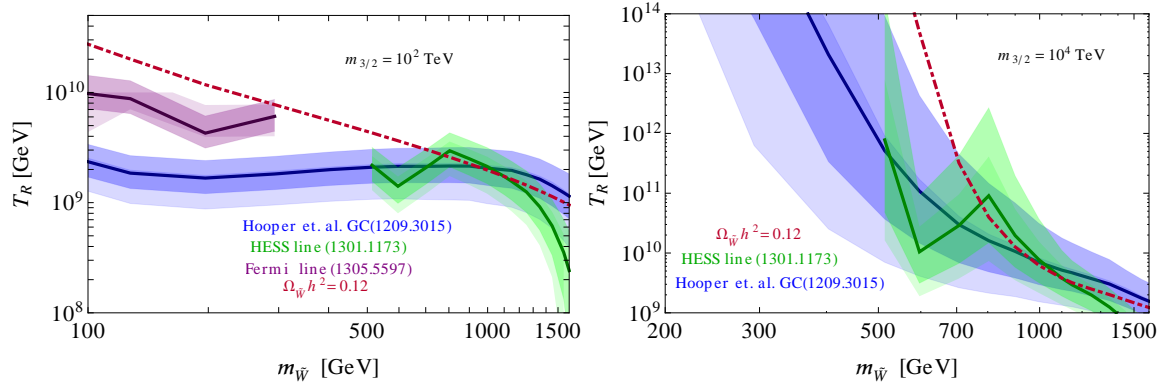


Figure 3.1: Upper bounds on inflaton reheating temperature  $T_R$  as a function of wino mass for  $m_{3/2} = 10^2$  TeV (left) and  $m_{3/2} = 10^4$  TeV (right). The blue, purple, green curves with bands around them correspond to constraints from Fermi galactic center continuum, Fermi line search and HESS line search respectively. The bands are derived by varying parameters of NFW (Einasto) dark matter profiles in the  $2\sigma$  range [4]. The burgundy dot-dashed line corresponds to the upper bound derived from requiring  $\Omega_{\tilde{W}} h^2 = 0.12$ .

assuming standard cuspy (NFW and Einasto) DM halo profiles. Since the wino relic abundance is a sum of the thermal contribution and the non-thermal contribution from gravitino decays, there is room for a non-thermal relic abundance only for wino with mass below 1.5 TeV.<sup>6</sup>

We express the constraints on allowed non-thermal  $\Omega_{\tilde{W}} h^2$  as an upper bound on the inflaton reheating temperature  $T_R$  as a function of wino mass for  $m_{3/2} = 100$  TeV and  $10^4$  TeV in Fig. 3.1. In this figure, we assumed that freeze-in contribution to the primordial gravitino relic abundance is negligible. As mentioned at the end of last section, taking into account of the freeze-in contribution will only make the upper bound stronger.

The left panel of Fig. 3.1 stays almost unmodified for  $10 \text{ TeV} < m_{3/2} < 10^4 \text{ TeV}$  as the wino annihilation is ineffective and the relic abundance is independent of  $m_{3/2}$  as can be seen from the first term in Eq. (3.9). The reheating temperature is bounded to be below  $3 \times 10^9$  GeV for the whole wino mass range. For wino mass close to

<sup>6</sup>There could be different non-thermal scenario such as moduli scenario [77]. The implications of indirect detection for moduli scenario have been discussed in [110, 165, 166].

1.5 TeV, the HESS constraint pushes the reheating temperature to be even lower to about a few times  $10^8$  GeV.

In the right panel of Fig. 3.1, the gravitino mass is set to be  $10^4$  TeV. In this case, for light wino with mass below 300 GeV, wino annihilation becomes effective and its relic abundance is insensitive to the reheating temperature as shown in Eq. (3.8). Therefore, the upper bound on the inflaton reheating temperature is lifted up entirely. For heavier wino, the annihilation rate drops with the increasing mass and the wino relic abundance interpolates between Eq. (3.8) and Eq. (3.9). In the whole wino mass range, the upper bound on  $T_R$  is above  $10^9$  GeV. For even heavier gravitino, the bound on  $T_R$  becomes even weaker.

One could also consider upper bound on the SUSY scalar masses,  $m_s$ , which is depicted in Fig. 3.2. In the left panel, we took  $m_{3/2} = 100$  TeV and  $T_R = 10^8$  GeV so that the thermal scattering contribution is negligible. Increasing the reheating temperature will only make the bound even stronger. In this case, indirect detection constraints restrict the scalar mass to be below  $(2 - 3) \times 10^3$  TeV for the whole wino mass range. In the right panel, we set  $m_{3/2} = 10^4$  TeV and  $T_R = 2 \times 10^9$  GeV. Since this is the case where wino annihilation becomes more effective, the upper bounds on the SUSY scalar mass depends less on  $T_R$  and are reduced significantly compared to the case with a lighter gravitino. More specifically, for wino above 300 GeV, indirect detection constraints restrict scalar masses to be below  $10^4 - 10^6$  TeV. For wino below 300 GeV, the upper bound is almost lifted up entirely.

### 3.4 Implications of the BICEP2 Result

Recently the BICEP2 collaboration reported a groundbreaking discovery of inflationary gravitational waves in the  $B$ -mode power spectrum in the range  $30 < l < 150$  [133]. The observed  $B$ -mode spectrum is well fit by a lensed  $\Lambda$ CDM plus tensor model with a tensor-to-scalar ratio  $r = 0.20^{+0.07}_{-0.05}$ . Such a large tensor-to-scalar ratio



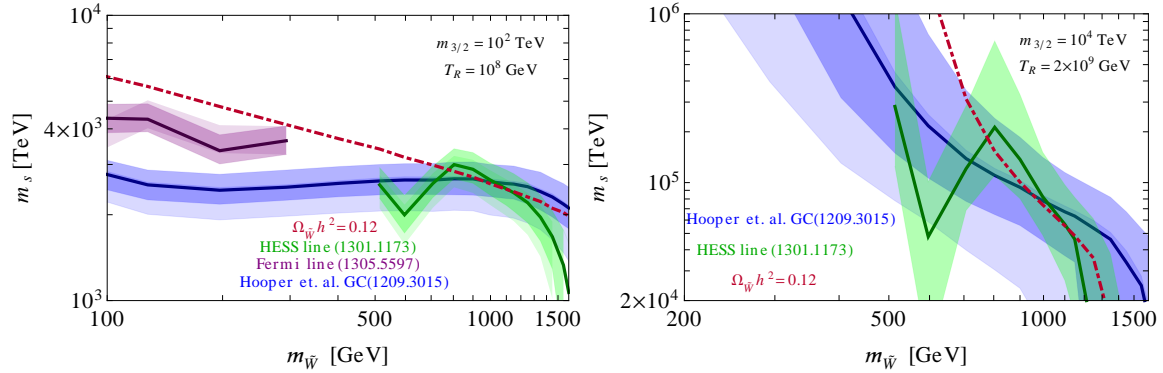


Figure 3.2: Upper bounds on scalar mass  $m_s$  as a function of wino mass for  $m_{3/2} = 100$  TeV (left) and  $m_{3/2} = 10^4$  TeV (right). The blue, purple, green curves with bands around them correspond to constraints from Fermi galactic center continuum, Fermi line search and HESS line search respectively. The bands are derived by varying parameters of NFW (Einasto) dark matter profiles in the  $2\sigma$  range [4]. The burgundy dot-dashed line corresponds to the upper bound derived from requiring  $\Omega_{\tilde{W}} h^2 = 0.12$ .

has a profound implication for the inflation paradigm. Notice that if running of the spectral index is allowed, the combined Planck and BICEP data could have a different best fit. In our paper, we will not explore this possibility as we don't expect  $r$  to change much. We will first review the basics of tensor-to-scalar ratio in the slow-roll inflation paradigm for completeness in Sec. 3.4.1. Readers who are familiar with this topic could skip this section. Then we will discuss the implications of BICEP2 result for the inflation mass scale and reheating temperature in Sec. 3.4.2.

### 3.4.1 Basics of Tensor-to-Scalar Ratio

We will follow closely Lecture 2 in Ref. [32] in this brief review. In slow-roll inflation models, the metric perturbation during the inflation period could be decomposed into scalar and tensor modes, which result in density and gravitational wave fluctuations respectively. Each mode could be characterized by a fluctuation amplitude

squared [39, 167]

$$\Delta_s^2(k) = \frac{H^4}{4\pi^2 \dot{\phi}^2} = \frac{1}{12\pi^2 M_p^6} \frac{V^3}{V'^2} \quad \text{scalar} \quad (3.12)$$

$$\Delta_t^2(k) = \frac{2H^2}{\pi^2 M_p^2} = \frac{2}{3\pi^2} \frac{V}{M_p^4}, \quad \text{tensor} \quad (3.13)$$

where the reduced Planck scale is  $M_p = 2.4 \times 10^{18}$  GeV. It should be understood that all the physical quantities above are evaluated at horizon crossing  $k = aH$  at which the relevant comoving scales for the CMB exits the Hubble radius.  $\dot{\phi}$  is the time derivative of the inflaton field  $\phi$  and  $V'$  is the derivative of the inflaton potential with respect to  $\phi$ . In deriving the second expression of the amplitude squared in each line, we used equation of motion for the inflaton  $H^2 \approx V/(3M_p^2)$  and  $\dot{\phi} \approx -V'/(3H)$ .<sup>7</sup>

Normalizing the scalar spectrum to the COBE [29] or WMAP [169] anisotropy measurement gives  $\Delta_s^2(k) \approx 2.2 \times 10^{-9}$ . Then one could define tensor-to-scalar ratio  $r \equiv \Delta_t^2(k)/\Delta_s^2(k)$ , which directly measures the inflation energy scale

$$V \approx (1.8 \times 10^{16} \text{ GeV})^4 \left( \frac{r}{0.1} \right). \quad (3.14)$$

$r$  also relates directly to the evolution of the inflaton as

$$r = \frac{8}{M_p^2} \left( \frac{d\phi}{dN} \right)^2, \quad (3.15)$$

where differential  $e$ -folds  $dN = Hdt$ . Then one could write the field displacement between the time when CMB fluctuations exited the horizon at  $N_{\text{cmb}}$  and the end of

---

<sup>7</sup>One easy way to understand the appearance of  $\dot{\phi}^2$  in the scalar perturbation amplitude squared is through effective field theory (EFT) [168]. The key insight of inflation EFT is that the inflaton spontaneously breaks time translation invariance and results in a Goldstone mode “eaten” by the graviton to appear in the scalar modes. Compared to the tensor mode, the kinetic term for the Goldstone (scalar) mode has an additional factor of  $\dot{H}$  in the kinetic term, which signals the break down of EFT in the limit of pure de Sitter space  $\dot{H} = 0$ . By equation of motion,  $\dot{H}$  is proportional to  $\dot{\phi}^2$  and consequently  $\dot{\phi}^2$  appear in the denominator of scalar fluctuation amplitude squared.

inflation at  $N_{\text{end}}$  in terms of an integral

$$\frac{\Delta\phi}{M_p} = \int_{N_{\text{end}}}^{N_{\text{cmb}}} dN \sqrt{\frac{r}{8}}. \quad (3.16)$$

Setting  $N_{\text{end}} = 0$  and given that  $N_{\text{cmb}} \approx (40 - 60)$  and  $r$  is approximately constant during the inflation era, one obtains the famous Lyth bound [170]

$$\frac{\Delta\phi}{M_p} \approx 6.7 \left( \frac{N_{\text{cmb}}}{60} \right) \sqrt{\frac{r}{0.1}}. \quad (3.17)$$

Inspecting Eq. (3.14) and (3.17), one could see immediately that the BICEP2 result points towards a large field displacement of order Planck scale during inflation or in other words, large field inflation. Existing examples of large-field inflation include chaotic inflation where a single power term dominates the potential [171, 172]

$$V(\phi) = \lambda_p \phi^p, \quad (3.18)$$

and natural inflation with a periodic potential resulting from a shift symmetry the inflaton enjoys [173]

$$V(\phi) = V_0 \left( 1 + \cos \left( \frac{\phi}{f} \right) \right). \quad (3.19)$$

### 3.4.2 Implication for Reheating Temperature

Now we want to estimate the inflaton mass scale. We start with a toy model of large field inflation  $V = m_\phi^2 \phi^2$ . In this model, the scalar fluctuation amplitude squared is

$$\Delta_s^2(k) = \frac{m_\phi^2}{M_p^2} \frac{N_{\text{cmb}}^2}{3\pi^2}, \quad (3.20)$$

where  $N_{\text{cmb}} = \phi_{\text{cmb}}^2/(4M_p^2)$ . Given the normalization to the CMB measurement,  $\Delta_s^2(k) \approx 2.2 \times 10^{-9}$ , the inflaton mass is

$$m_\phi \approx 10^{13} \text{ GeV} \left( \frac{60}{N_{\text{cmb}}} \right)^2. \quad (3.21)$$

One could check in more realistic models such as chaotic inflation and natural inflation that the inflaton mass scale is around  $10^{13} \text{ GeV}$  [134, 174, 175]. One crude estimate of the inflaton mass in all these large-field inflation model is

$$m_\phi^2 \sim \frac{V}{(\Delta\phi)^2} \approx (2 \times 10^{13} \text{ GeV})^2, \quad (3.22)$$

where we used Eq. (3.14) and (3.17) assuming  $N_{\text{cmb}} = 60$ .

After inflation ends, inflaton starts to oscillate around the minimal of the potential. Its coupling to other particles induce conversion of the inflationary energy into the SM degrees of freedom. The reheating temperature is then determined by the inflaton decay width  $\Gamma_\phi$  as

$$T_R = \left( \frac{10}{g_*(T_R)\pi^2} \right)^{1/4} \sqrt{\Gamma_\phi M_p} \approx 0.3 \sqrt{\Gamma_\phi M_p}, \quad (3.23)$$

where we took  $g_*(T_R) \approx 200$ . The simplest possibility is that inflatons decay through renormalizable couplings to lighter degrees of freedom. For example, the decay width is  $\Gamma_\phi = y^2 m_\phi / (8\pi)$  for inflaton coupling to fermions with a Yukawa coupling  $y$ . Then the reheating temperature is

$$T_R \approx 3 \times 10^{11} \text{ GeV} \left( \frac{y}{10^{-3}} \right) \sqrt{\frac{m_\phi}{10^{13} \text{ GeV}}}. \quad (3.24)$$

Notice that Yukawa coupling larger than  $10^{-5}$  only makes sense in supersymmetric scenarios where the one-loop quantum correction does not modify the inflaton potential much due to a cancelation between fermionic and bosonic contributions.

If the renormalizable couplings of inflaton to lighter particles are negligible (e.g.,  $y < 10^{-5}$ ), it would always decay through Planck-scale suppressed operators. At the leading order, the inflaton decay width and the corresponding reheating temperature are

$$\Gamma_\phi = \frac{cm_\phi^3}{M_p^2}, \quad T_R \approx 5 \times 10^9 \text{ GeV} \sqrt{c} \left( \frac{m_\phi}{10^{13} \text{ GeV}} \right)^{3/2}, \quad (3.25)$$

where  $c$  is some order one number determined by quantum gravity. From the point of view of operator analysis, this decay is induced by dimension five operators such as  $\phi F\tilde{F}/M_p$  with  $F$  the field strength of SM gauge interaction. In other words, the BICEP2 results imply a minimal reheating temperature at or above  $10^9$  GeV!

One should worry about the caveats of the very simple estimate above. One question is whether the leading order gravitational couplings through dimension five operators could be suppressed and the reheating temperature could be even lower. This could be true if the inflaton is charged under a gauge symmetry (global symmetry is not respected by quantum gravity) and then dimension five operators are forbidden. This is an interesting possibility but we will not explore it here further but leave it for future work. Another concern is that since reheating is a very complicated process (for a review, see [176]), our simple estimate of a minimal reheating temperature might be misleading. In particular, there could exist a preheating era in which particles coupled to the inflaton are resonantly produced by parametric resonance and the temperature of the plasma could be higher than the reheating temperature. Yet preheating might make the tension between the upper bound on  $T_R$  derived in Sec. 3.2 and Sec. 3.3 and the lower bound on  $T_R$  derived in this section even worse. The reason is that gravitinos could be over-produced non-thermally during the preheating era [177–181].<sup>8</sup> Nonetheless, it is interesting and important to carry out a thorough study of preheating/reheating in sound (stringy) inflation models.

---

<sup>8</sup>In certain supergravity models, the non-thermal production could be suppressed [182, 183].

### 3.5 Implications for SUSY

So far we have demonstrated a (mild) tension between mini-split SUSY with a heavy unstable gravitino at around the PeV scale and the BICEP2 result. In mini-split SUSY, the reheating temperature has to be below  $10^9$  GeV to avoid overproduction of DM particles from gravitino decay while the BICEP2 result prefers large-field inflation with a reheating temperature above  $10^9$  GeV. In other words, the BICEP2 results favor a larger splitting between the gravitino and the gauginos than the one-loop factor if the gauginos are fixed at around the TeV scale. Interestingly, **the requirement that gaugino mass does not exceed the TeV scale constrains the gravitino mass to be around or below  $10^{13}$  GeV, which is also the mass scale of the inflaton implied by BICEP2 !** Below we will review the derivation of this statement by operator analysis following Refs. [121, 122].

In supergravity, the easiest way to cancel the positive vacuum energy from SUSY breaking contribution is to have a non-zero VEV of the superpotential. As the superpotential  $W$  carries  $R$ -charge 2, its VEV  $W_0$  breaks  $U(1)_R$  symmetry spontaneously. It also gives a gravitino mass

$$m_{3/2} \approx \frac{W_0}{M_p^2} \approx \frac{|F_X|}{\sqrt{3}M_p}, \quad (3.26)$$

where  $F_X$  is the  $F$ -term VEV of the SUSY breaking spurion  $X$ . A non-zero gaugino mass is generated only when both  $U(1)_R$  and SUSY are broken. The lowest dimensional operator built out of SUSY breaking spurion  $X$ ,  $U(1)_R$  breaking spurion  $W$  and MSSM superfields arise in the Kähler potential

$$\int d^2\theta d^2\bar{\theta} \frac{X^\dagger X W W_\alpha W^\alpha}{M_*^6}, \quad (3.27)$$

where  $W_\alpha$  denotes the MSSM gauge supermultiplet. This operator could be generated by gravitational loops where  $M_* \sim M_p$  and gives a minimal contribution to the

gaugino mass

$$m_{1/2} \gtrsim \frac{|F_X|^2 W_0}{M_p^6} \approx \frac{3m_{3/2}^3}{M_p^2}. \quad (3.28)$$

Requiring  $m_{1/2}$  at or below TeV leads to  $m_{3/2} \lesssim 10^{13}$  GeV! This large hierarchy between gravitino and gaugino could be realized in no-scale supergravity which could arise from the Scherk-Schwarz mechanism [184, 185].

### 3.6 Conclusions and Outlook

In this paper, we study the implications of DM indirect detection and BICEP2 in the split SUSY scenario with a heavy unstable gravitino. In the mini-split spectrum with scalars/gravitinos only one-loop factor above the TeV-scale gauginos, the reheating temperature has to be low to avoid overproduction of DM particles from gravitino decays. In particular, we demonstrate that indirect detection requires the reheating temperature to be below about  $10^9$  GeV if the wino is (a component of) DM. On the other hand, the large tensor-to-scalar ratio observed by BICEP2 favors large-field-inflation with a reheating temperature around or above  $10^9$  GeV. Given this mild tension and the phenomenological upper bound on the gravitino mass derived by requiring the gauginos to be at the TeV scale, it is tempting to think more seriously of the (highly) split SUSY scenario in which inflaton/gravitino are at around  $10^{13}$  TeV and gauginos are still at the TeV scale with lightest neutralino being (part of) DM.<sup>9</sup> Indeed this picture has recently been discussed in the framework of Intermediate Scale SUSY [142].

Given the BICEP2 result, it is also interesting to use the scale of inflation to probe the full range of split SUSY scenarios through observables such as equilateral non-gaussianity [138]. It will also be of interest to study the implications of the BICEP2 result for baryogenesis. For example, thermal leptogenesis works for a reheating temperature above  $2 \times 10^9$  GeV [186], which fits well with the BICEP2 result.

---

<sup>9</sup>Axion could be the dominant DM component.

# Appendix

## 3.A Gravitino from Inflaton Decay

In this appendix, we review non-thermal gravitino production from inflaton decays. In general, decays of inflaton can overproduce gravitinos and subsequent decays can induce LSP overproduction [149, 150]. Consider the following simple model of SUSY breaking and inflation [152],

$$K = |\phi|^2 + |X|^2 + |z|^2 - \frac{|z|^4}{\tilde{\Lambda}^2}, \quad (3.29)$$

$$W = X \left( g \frac{\phi^n}{M_p^{n-2}} - v^2 \right) + \mu^2 z + W_0, \quad (3.30)$$

where  $z$  is the SUSY breaking spurion and  $\tilde{\Lambda}$  is the QCD scale of the dynamical SUSY breaking sector. Here,  $\mu$  is the SUSY breaking scale related to the  $F$ -term VEV of  $z$  through  $F_z \simeq -\mu^2 \simeq \sqrt{3}m_{3/2}M_p$  and  $W_0$  is the constant term introduced to cancel the positive vacuum energy contribution from  $F$ -terms.

The scalar potential in supergravity is given by

$$V = e^{K/M_{\text{pl}}^2} \left[ K_{i\bar{j}}^{-1} (D_i W) (D_{\bar{j}} W) - 3 \frac{|W|^2}{M_{\text{pl}}^2} \right], \quad (3.31)$$

where  $D_i$  is the covariant derivative with respect to field  $i$ . There is a mass mixing



between  $X$  and  $z$  arising from the following terms in the scalar potential above (3.31),

$$V \supset \left| \frac{Xng\phi^{n-1}}{M_p^{n-2}} + \frac{\phi^\dagger W}{M_p^2} \right|^2 \approx \frac{m_\phi \langle \phi \rangle \mu^2}{M_p^2} X z^\dagger + h.c., \quad (3.32)$$

where  $m_\phi = ng\langle\phi\rangle^{n-1}/M_p^{n-2}$ .

The operator  $|z|^4/\tilde{\Lambda}$  in the Kähler potential induces  $z$  decaying into the goldstino pair ( $\tilde{z}$ ) via

$$\mathcal{L} \supset \int d^2\theta d^2\bar{\theta} K \sim -2 \frac{F^\dagger}{\tilde{\Lambda}^2} z^\dagger \tilde{z} \tilde{z} + h.c., \quad (3.33)$$

where the decay rate is given by

$$\Gamma_{z \rightarrow \tilde{z}\tilde{z}} \simeq \frac{1}{96\pi} \frac{m_z^5}{m_{3/2}^2 M_p^2}. \quad (3.34)$$

Since the goldstino is “eaten” by the gravitino via the super-Higgs mechanism, the decay rate above can be expressed as the decay rate of the inflaton into a pair of gravitinos via the mass mixing with  $z$ :

$$\begin{aligned} \Gamma_{\phi \rightarrow \tilde{z}\tilde{z}} &\sim \left( \frac{\theta}{\sqrt{2}} \right)^2 \frac{m_\phi}{m_z} \Gamma_{z \rightarrow \tilde{z}\tilde{z}}, \\ &\sim \left( \frac{\theta}{\sqrt{2}} \right)^2 \left( \frac{m_z}{m_\phi} \right)^4 \frac{m_\phi^5}{m_{3/2}^2 M_p^2} \end{aligned} \quad (3.35)$$

where the mixing angle between inflaton  $\phi$  and  $z$ ,  $\theta$ , is given by  $\sqrt{3}(m_{3/2}\langle\phi\rangle)/(m_\phi M_p)$  for  $m_\phi \gg m_z$ ,  $\sqrt{3}(m_{3/2}m_\phi\langle\phi\rangle)/(m_z^2 M_p)$  for  $m_\phi \ll m_z$ . Therefore, in the case that  $m_\phi \gg m_z$ , the decay rate (3.35) of inflaton into a pair of gravitino is suppressed by  $(m_z/m_\phi)^4$ . If  $z$  is only charged under some global symmetry, one could not forbid operators such as  $|\phi|^2 z$  and  $|\phi|^2 z z$  in the Kähler potential (3.29). These operators will always be induced by Planck scale physics as it only respects local symmetries [187]. These operators are dangerous as they would enhance the decay rate of inflaton to gravitinos by  $m_\phi^2/m_{3/2}^2$ . Thus in addition to the hierarchy  $m_{3/2} \ll m_z \ll m_\phi$ , the SUSY breaking spurion cannot be a gauge singlet!

# Chapter 4

## Non-thermal histories and Implications for Structure Formation

### 4.1 Introduction

Cosmological observations have led to an impressive level of constraint on inflationary model building. However, the post-inflationary universe prior to Big Bang Nucleosynthesis (BBN) remains elusive. The lack of direct observations at this time is unfortunate, since it is precisely during this epoch that we would hope to probe Beyond the Standard Model (BSM) physics. Even though direct probes on this cosmic period are lacking, we can try and establish some aspects of BSM physics by understanding how new particles and fields may change the expansion history and perhaps alter the inflationary seeds that led to the growth of structure.

In this paper we investigate non-thermal cosmologies and the effects they can have on the growth of density perturbations during the cosmic dark ages – the post-inflationary universe prior to BBN. These non-standard cosmologies (in particular those associated with high-scale supersymmetry) are motivated by both fun-

damental theory [64, 78, 79] and experimentally given rising tensions for natural BSM models [188–192]. Past investigations into the implications of a non-thermal post-inflationary history on cosmological perturbations have already demonstrated there can be important consequences for interpreting Cosmic Microwave Background (CMB) observations and for the restrictions CMB observations place on inflationary model building [165, 193]. Here we examine in detail the evolution of perturbations during the non-thermal period and address the question of whether the extra matter dominated phase predicted by these models can lead to an enhancement in the growth of structure on small scales. Because sub-Hubble matter perturbations grow linearly during a matter dominated phase (and only logarithmically during a thermal / radiation dominated phase), this suggests a new scale that could prove interesting for the primordial matter power spectrum. The relevance of this scale for determining the smallest allowed primordial dark matter (DM) structures depends on the reheat temperature at the end of the non-thermal phase, as well as on the free streaming length and kinetic decoupling of the DM. In this paper we address all of these issues within non-thermal cosmologies and establish in which situations interesting phenomenology may result. In addition to the general consideration, we also investigate the particular scenario with neutralino DM and heavy moduli in the context of Split Supersymmetry [76, 120–124, 126, 127].

The paper is organized as follows. In Section 4.2 we present a brief review of non-thermal cosmologies and establish the background evolution. In Section 4.3 we present a general discussion of the evolution of cosmological perturbations in these non-thermal cosmologies. We discuss in detail how the extra matter dominated phase can alter both sub-Hubble and super-Hubble matter and radiation perturbations during this time. We also discuss the different production mechanisms for DM in non-thermal cosmologies and how this relates to expectations for whether structure should be enhanced or suppressed. One key result from this section is the emergence of a new scale associated with the Hubble radius at the end of the non-thermal phase,

which suggests a new possible minimal scale for the smallest allowed primordial DM structures. In Section 4.4 we compare this scale with other important effects for removing DM structure on small scales, namely the effects of free streaming and kinetic decoupling. Within our discussion we also discuss how the scalar decay at the end of the non-thermal history can lead to a free-streaming effect that must be taken into account when establishing the relevant scale for the smallest substructures. In Section 4.5 we consider neutralino DM in the moduli scenario and discuss whether an enhanced growth of small scale structure is a natural expectation in this scenario. In Section 4.6 we conclude and relegate more technical details of our analysis to the appendices.

We note that some of our results have overlap with existing papers found in the literature. Many of our results in the perturbation analysis have overlap with that of Erickcek and Sigurdson in [194]. However, we have included the effect of DM annihilations and considered a broader class of non-thermal cosmologies – as we discuss in Section 4.2. We will also emphasize that after reheating, the scattering of DM off radiation could couple DM to radiation and thus wipe out the matter perturbation growth. In summary, we consider the effect of interactions between DM particles and between DM and radiation, which are generally non-negligible in well-motivated particle DM models. We also try to emphasize closely the connection to the microscopic parameters of the underlying theory, which helps to establish which parameter regions prove most relevant. For our considerations of SUSY neutralinos in Section 4.5 we note the work of Arcadi and Ullio in [195] where they considered strictly wino DM in the context of the  $G2$ -MSSM.

## 4.2 Non-thermal Cosmologies

In this section we begin by reviewing non-thermal cosmologies and their implications for the primordial DM abundance. We then present the background equations to

model the non-thermal epoch, to be followed in the next section with a study of the perturbations.

There are two assumptions leading to a non-thermal history following inflationary reheating; the existence of shift symmetric scalars (or moduli), and both high and low energy sources that break that symmetry. The former is a generic expectation of BSM physics, whereas low-scale symmetry breaking is motivated by the hierarchy problem and inflation provides a gravity mediated source of breaking at the high scale<sup>1</sup> [64, 78]. Given these assumptions the scalar will typically be displaced from its low energy minimum and its oscillations can lead to an effectively matter dominated universe (see e.g. [79] and references within). For moduli with masses around 100 TeV and which decay through gravitationally suppressed couplings, this will lead to a late stage of reheating shortly before the time of BBN [79]. Since oscillations begin roughly when  $H \sim m_\sigma \sim 100$  TeV, this implies a long period of matter domination prior to BBN and a modification to the usually assumed radiation dominated post-inflationary universe.

Depending on the specifics of the non-thermal history (the exact couplings and masses of the fields) there are a few possible predictions for the primordial origin of DM. If the energy density of oscillations remains subdominant compared to radiation, this can lead to interesting cosmological predictions [193], but the cosmic evolution will remain thermal. This will not lead to any change in the growth of structure, so for the remainder of the paper we will assume this is not the case. Moreover, top-down approaches to model building typically imply that the moduli will come to dominate the energy density almost immediately following the onset of oscillations [79]. Given that the moduli dominate at the time of decay, this implies a large generation of entropy and so any previous DM abundance will be diluted.

---

<sup>1</sup>In fact, further motivation is provided by inflation itself, where a shift symmetry for the inflaton is not enough to obtain adequate inflation, but one must introduce an additional symmetry (such as SUSY) to protect the flatness of the potential against corrections. In the SUSY case, this leads to an additional scalar playing the same role as the moduli that we are discussing here (see e.g. [138]).

This leads to the following possible cases [62]:

- Branching Scenario: In this case the moduli decay into radiation (standard model particles) and DM particles with no DM annihilations occurring during the process. The final abundance of DM will then be the (diluted) primordial amount  $\sim \Omega_\chi^{(0)}(T_r/T_f)^3$  where  $T_r$  and  $T_f$  are the reheat and freeze-out temperatures, respectively ( $T_r < T_f$ ), and the decays can lead to a non-thermal source of DM  $\Omega_\chi^{NT} \sim B_\chi \rho_\sigma m_\chi / (m_\sigma \rho_c)$  where  $B_\chi$  is the branching ratio,  $\rho_\sigma \sim H^2 M_{\text{pl}}^2$  is the energy density of the moduli at decay,  $\rho_c \sim H_0^2 M_{\text{pl}}^2$  is the critical density today, and  $m_\chi$  and  $m_\sigma$  are the masses of the DM and the moduli, respectively. Within this scenario there is the possibility that the branching ratio could be negligible ( $B_\chi \simeq 0$ ) and so all of the DM is produced during freeze-out before decay<sup>2</sup>. Requiring that the non-thermal production provides all of the DM today leads to the constraint [62]

$$B_\chi = 6.4 \times 10^{-8} \left( \frac{5 \text{ MeV}}{T_r} \right) \left( \frac{10.75}{g_{*s}} \right)^{1/3}, \quad (4.1)$$

which we see is quite suppressed for low reheat temperatures.

- Annihilation Scenario: In this case when the DM is produced from the moduli decay, the abundance results in enough DM so that rapid self annihilations of the DM is possible. In this case one typically finds that the abundance of DM is primarily of non-thermal origin and the amount of DM today is then  $\Omega_\chi^{NT} \sim \Omega_\chi^{std}(T_f/T_r)$ . That is, because of the annihilations the abundance is related to the standard thermal result  $\Omega_\chi^{std}$  except that the freeze-out temperature is replaced by the reheating temperature. Requiring that this provides the totality of DM today forces a relationship between the reheat temperature and DM annihilation cross-section (see e.g. [110]). For a reheat temperature around

---

<sup>2</sup>In this case the freeze-out process can actually occur during the matter dominated phase. This leads to a slightly more involved calculation (e.g. modified freeze-out temperature) than we have presented here [62], however the differences will be irrelevant for our analysis in this paper.

5 MeV this results in an enhanced DM interaction rate  $\langle\sigma v\rangle \sim 10^{-23} \text{ cm}^3\text{s}^{-1}$  implying the possibility of interesting predictions for the indirect detection of DM [110, 132, 161].

Given these two possible scenarios we next consider the evolution of the cosmological background. We note that in [194] the authors only considered the ‘branching scenario’ where DM annihilations are negligible. Here we extend their analysis to consider both cases, noting that motivation from fundamental theory so far seems to favor the ‘annihilation scenario’.

### 4.2.1 Background Evolution

The treatment of the background equations has appeared in many places in the past, and we find our results to be in close agreement with those of [196]. We are interested in the background evolution following the end of inflationary reheating, assuming a high-scale model of inflation with reheating temperatures near the GUT scale. Once the expansion rate becomes comparable to the moduli mass, coherent oscillations of the scalar will lead to a matter dominated phase. Within this regime we can describe the cosmological background as a system of three interacting fluids as

$$\dot{\rho}_\sigma = -3H\rho_\sigma - \Gamma_\sigma\rho_\sigma, \quad (4.2)$$

$$\dot{\rho}_r = -4H\rho_r + (1 - B_\chi)\Gamma_\sigma\rho_\sigma + \frac{\langle\sigma v\rangle}{m_\chi} [\rho_\chi^2 - \rho_{\chi,\text{eq}}^2], \quad (4.3)$$

$$\dot{\rho}_\chi = -3H\rho_\chi + B_\chi\Gamma_\sigma\rho_\sigma - \frac{\langle\sigma v\rangle}{m_\chi} [\rho_\chi^2 - \rho_{\chi,\text{eq}}^2], \quad (4.4)$$

where  $\Gamma_\sigma \sim (m_\sigma^3/M_{\text{pl}}^2)$  is the decay rate of the scalar with  $M_{\text{pl}} = 2.44 \times 10^{18} \text{ GeV}$  the reduced Planck mass,  $\langle\sigma v\rangle$  is the self annihilation cross section of DM particles with mass  $m_\chi$  and  $B_\chi$  is the branching ratio for scalar to decay to DM. We assume all other decays result in relativistic particles. We will be interested in the non-relativistic regime of DM where  $T \ll m_\chi$  and so we can neglect the equilibrium density terms

$\rho_{\chi,\text{eq}}^2 \sim e^{-m_\chi/T}$  in (4.3) and (4.4). The temperature is related to the radiation energy density as  $\rho_r = (\pi^2 g_*/30) T^4$ , and we take care to track the non-standard relation between the temperature and expansion rate during the entropy production within the matter (moduli) dominated phase [196].

The Hubble and Friedmann equations are

$$3H^2 M_{\text{pl}}^2 = \sum_{\alpha} \rho_{\alpha}, \quad (4.5)$$

$$2\dot{H} M_{\text{pl}}^2 = -\sum_{\alpha} (\rho_{\alpha} + p_{\alpha}), \quad (4.6)$$

where  $\alpha$  runs over the values  $\alpha = \{\sigma, r, \chi\}$  for each fluid and dot denotes differentiation with respect to cosmological time  $t$ . Instead of working with time it is convenient to express the equations in the number of e-folds,  $Hdt = dN = d(\ln a)$ , so that the dynamical equations (4.2)-(4.4) and (4.6) become

$$\frac{d\rho_{\sigma}}{dN} = -3\rho_{\sigma} - \frac{\Gamma_{\sigma}}{H} \rho_{\sigma}, \quad (4.7)$$

$$\frac{d\rho_{\chi}}{dN} = -3\rho_{\chi} + B_{\chi} \frac{\Gamma_{\sigma}}{H} \rho_{\sigma} - \frac{\langle\sigma v\rangle}{m_{\chi} H} \rho_{\chi}^2, \quad (4.8)$$

$$\frac{d\rho_r}{dN} = -4\rho_r + (1 - B_{\chi}) \frac{\Gamma_{\sigma}}{H} \rho_{\sigma} + \frac{\langle\sigma v\rangle}{m_{\chi} H} \rho_{\chi}^2, \quad (4.9)$$

$$\frac{dH}{dN} = -\frac{1}{2HM_{\text{pl}}^2} (\rho_{\sigma} + \rho_{\chi} + \frac{4}{3}\rho_r), \quad (4.10)$$

subject to the energy constraint (4.5).

We begin studying the behavior of the system well within the matter dominated phase resulting from the coherent oscillations of the moduli, i.e.  $t \sim H^{-1} \gg m_{\sigma}^{-1}$ . Moduli decays into both DM (which is by this time non-relativistic) and radiation do not significantly reduce the abundance of moduli until the time of decay  $t_d \sim H^{-1} \simeq \Gamma_{\sigma}^{-1}$ , however the decays do affect the scaling behavior as discussed in e.g. [196]. Indeed, we find that prior to reheating the moduli evolve as expected but that the



DM and radiation scale differently

$$\rho_\sigma(N) \simeq \rho_\sigma^{(0)} e^{-3N}, \quad (4.11)$$

$$\rho_\chi(N) = \rho_\chi^{(0)} e^{-3N/2}, \quad (4.12)$$

$$\rho_r(N) = \rho_r^{(0)} e^{-3N/2}, \quad (4.13)$$

where we choose initial values so that  $\rho_\chi^{(0)}, \rho_r^{(0)} \ll \rho_\sigma^{(0)}$  and DM will be primarily of non-thermal origin<sup>3</sup>. The scaling behavior in (4.12) and (4.13) is similar to the case studied recently in [194], where the annihilations of DM were not taken into account. However, (as we have checked numerically) the behavior here is due to a near cancelation between the decay and annihilation terms on the right hand side of equations (4.8) and (4.9), which allows the DM density to track quasi-static equilibrium [148, 195] and so it dilutes more slowly than the standard  $\sim 1/a^3$  as seen in (4.12). This characterizes the behavior of the system until near  $H^{-1} \sim \Gamma_\sigma^{-1}$  when the decays become significant enough to reduce the scalar abundance. The evolution during this time is described well by the sudden decay approximation, and given a large enough yield of DM rapid annihilations will occur – see [64] for more details.

The dynamics of the entire system is easily solved numerically, and the evolution of the background energy densities as a fraction of total  $\rho = \rho_\sigma + \rho_r + \rho_\chi$  for two different non-thermal cosmologies is presented in Figure 4.1. For both sets of parameters the DM and radiation is found to evolve as  $\sim e^{-3N/2} \sim a^{-3/2}$ , until the time of reheating at  $H^{-1} \sim \Gamma_\sigma^{-1}$ . Then, the scalar energy density becomes exponentially suppressed,  $\rho_\sigma \sim e^{-2\Gamma_\sigma/3H(N)}$  and most of the energy density deposited in the coherent scalar oscillations will be transferred to radiation and DM fluids in a very short time interval as seen in both figures above. The sudden decay will increase the DM density to a critical value such that DM annihilations terms in (4.8) will be more important than the Hubble expansion terms, resulting in rapid annihilations of DM into radiation

---

<sup>3</sup>In explicitly constructed models with moduli and TeV scale (gravity or anomaly mediated) SUSY breaking this is typically found to be the case – see e.g. [79].

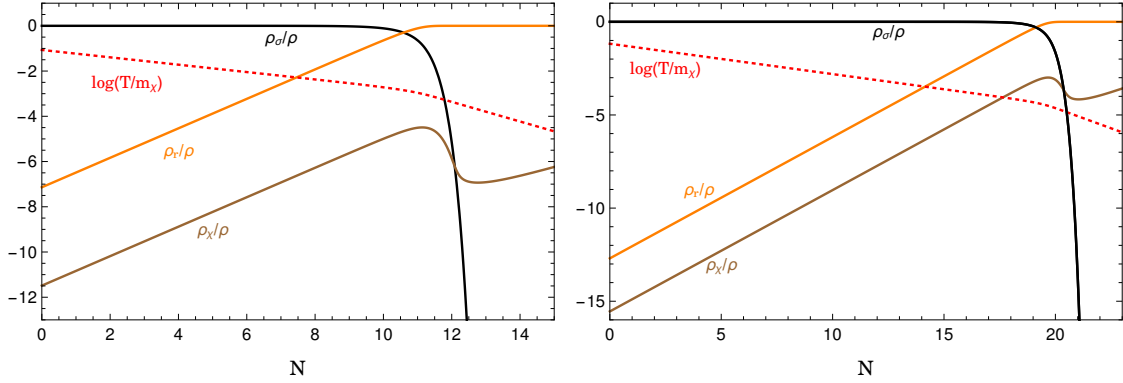


Figure 4.1: Evolution of the logarithm of normalized energy densities (as discussed in the text),  $\log(\rho_\alpha/\rho)$  for two different non-thermal cosmologies. In both figures we take  $m_\chi = 500$  GeV,  $B_\chi = 1/3$ ,  $g_* = 30$ , and  $\langle\sigma v\rangle = 3 \times 10^{-8}$  GeV $^{-2}$ . On the left we chose an initial dimensionless decay rate  $\Gamma_\sigma/H_0 \simeq 2 \times 10^{-7}$  and the moduli mass  $m_\sigma = 10^6$  GeV. On the left the universe becomes radiation dominated at  $N_{rh} \simeq 10.6$  and the reheat temperature is  $T_r \simeq 707$  MeV. Whereas on the right we have  $\Gamma_\sigma/H_0 = 0.5 \times 10^{-12}$  and  $m_\sigma = 10^5$  GeV, with  $N_{rh} \simeq 19$  at reheating and  $T_r \simeq 22$  MeV.

until these two terms balance each other. On the other hand, DM pair annihilations do not have an observable effect on the radiation fluid due to the large hierarchy between the energy densities of these fluids at reheating. Once all the energy in scalar oscillations is transferred into DM and radiation, all the source terms in background equations are negligible and the fluids evolve as  $\rho_r \sim e^{-4N}$  and  $\rho_\chi \sim e^{-3N}$ . Given both an analytic and numeric description of the system we now turn to a study of the evolution of cosmological perturbations.

### 4.3 Cosmological Perturbations

The evolution equations for the scalar perturbations can be derived by perturbing covariant versions of the background equations presented in Section 4.2 – details appear in Appendix 4.A. Consistent with our analysis in that section, we will drop terms the equilibrium terms  $\rho_{\chi,\text{eq}}$  in equations (4.16)-(4.18) focusing on the evolution

after DM has become non-relativistic. We work in longitudinal gauge where the scalar metric perturbations are

$$ds^2 = -(1 + 2\Phi) dt^2 + a(t)^2 (1 - 2\Psi) \delta_{ij} dx^i dx^j. \quad (4.14)$$

In the absence of anisotropic stress for the fluid sources we have  $\Phi = \Psi$  and working in momentum space (and suppressing the wave number) the time-time component of the perturbed Einstein equation is

$$\left( \frac{k^2}{3a^2 H^2} + 1 \right) \Phi + \Phi' = -\frac{1}{6H^2 M_{\text{pl}}^2} \sum_{\alpha} \delta\rho_{\alpha}, \quad (4.15)$$

where prime denotes derivatives with respect to number of e-folds and  $\delta\rho_{\alpha}$  is scalar density perturbation for each fluid. Introducing fractional density perturbations  $\delta_{\alpha} \equiv \delta\rho_{\alpha}/\rho_{\alpha}$  and re-defining the velocity perturbation for each fluid as  $\theta_{\alpha} = a^{-1}\nabla^2 v_{\alpha}$ , the continuity equations in momentum space are given by

$$\begin{aligned} \delta'_{\sigma} + \frac{\theta_{\sigma}}{aH} - 3\Phi' &= -\frac{\Gamma_{\sigma}}{H} \Phi, \\ \delta'_{\chi} + \frac{\theta_{\chi}}{aH} - 3\Phi' &= B_{\chi} \frac{\Gamma_{\sigma}}{H} \left( \frac{\rho_{\sigma}}{\rho_{\chi}} \right) [\delta_{\sigma} - \delta_{\chi} + \Phi] - \frac{\langle \sigma v \rangle \rho_{\chi}}{m_{\chi} H} [\delta_{\chi} + \Phi], \\ \delta'_{r} + \frac{4}{3} \frac{\theta_r}{aH} - 4\Phi' &= (1 - B_{\chi}) \frac{\Gamma_{\sigma}}{H} \left( \frac{\rho_{\sigma}}{\rho_r} \right) [\delta_{\sigma} - \delta_r + \Phi] + \frac{\langle \sigma v \rangle \rho_{\chi}}{m_{\chi} H} \left( \frac{\rho_{\chi}}{\rho_r} \right) [2\delta_{\chi} - \delta_r + \Phi], \end{aligned} \quad (4.16)$$

Similarly, the equations for velocity perturbations are

$$\begin{aligned} \theta'_{\sigma} + \theta_{\sigma} - \frac{k^2}{aH} \Phi &= 0, \\ \theta'_{\chi} + \theta_{\chi} - \frac{k^2}{aH} \Phi &= B_{\chi} \frac{\Gamma_{\sigma}}{H} \left( \frac{\rho_{\sigma}}{\rho_{\chi}} \right) [\theta_{\sigma} - \theta_{\chi}], \\ \theta'_{r} - \frac{k^2}{aH} \left( \frac{\delta_r}{4} + \Phi \right) &= (1 - B_{\chi}) \frac{\Gamma_{\sigma}}{H} \left( \frac{\rho_{\sigma}}{\rho_r} \right) \left[ \frac{3}{4} \theta_{\sigma} - \theta_r \right] + \frac{\langle \sigma v \rangle \rho_{\chi}}{m_{\chi} H} \left( \frac{\rho_{\chi}}{\rho_r} \right) \left[ \frac{3}{4} \theta_{\chi} - \theta_r \right]. \end{aligned} \quad (4.17)$$

In deriving the equations in (4.16) and (4.17), we have assumed each fluid has a definite equation of state with  $p_{\alpha} = w_{\alpha} \rho_{\alpha}$  which also implies  $\delta p_{\alpha} = c_{s,\alpha}^2 \delta \rho_{\alpha}$  with

$c_{s,\chi}^2 = c_{s,\sigma}^2 = 0, c_{s,r}^2 = 1/3$ . The set of differential equations in (4.16) and (4.17) can be closed by using the perturbed Einstein equation (4.15).

### 4.3.1 Initial Conditions

In order to calculate the evolution of perturbations we need to specify initial conditions. We set these initial conditions are well after the scalar dominated era has begun and when all modes of interest are super-Hubble,  $k/aH \rightarrow 0$ . Given the multiple fluid setup and the presence of decays, one concern may be a substantial contribution to an isocurvature component that could then be in conflict with CMB observations [197]. However, here we will be interested in the case when the modulus completely dominates the energy density before decay, and so any existing isocurvature carried by the moduli will be eliminated as the moduli evolve to dominate – see [193] and references within. Moreover, any DM or radiation that exists prior to moduli domination is found to be insignificant compared to that coming from decay, and so this does not lead to a constraint from observations<sup>4</sup>. We elaborate on the role of isocurvature in Appendix B, but given these considerations we are interested in strictly adiabatic initial conditions for the multi-fluid perturbations so that

$$\frac{\delta\rho_\alpha^{(0)}}{\rho'_\alpha} = \frac{\delta\rho_\beta^{(0)}}{\rho'_\beta}. \quad (4.18)$$

Using the background fluid equations (4.7)-(4.9) with the ansatz (4.11)-(4.13) and remembering that during scalar domination  $\Gamma_\sigma/H \ll 1$ , from (4.18) we obtained the following relation for fluid perturbations

$$\delta_\sigma^{(0)} = 2\delta_\chi^{(0)} = 2\delta_r^{(0)}. \quad (4.19)$$

---

<sup>4</sup>In fact, it was found in [193] that the interesting case corresponds to when the modulus does not completely dominate, and even then it was demonstrated that the importance of isocurvature constraints depends sensitively on the theoretical priors of the model.

This relation differs from the standard relation ( $\delta_\chi^{(0)} = (3/4)\delta_r^{(0)}$ ) due to the presence of decays and entropy production. Taking the super-horizon limit  $k/aH \rightarrow 0$  of (4.15) in a scalar dominated universe  $\rho_\sigma \gg \rho_r, \rho_\chi$ , we have

$$\Phi \simeq -\frac{1}{6H^2 M_{\text{pl}}^2} \rho_\sigma \delta_\sigma, \quad (4.20)$$

where we used that the gravitational potential  $\Phi$  is conserved on super-Hubble scales. Since  $\rho_\sigma \simeq 3H^2 M_{\text{pl}}^2$  during scalar domination (4.20) implies the following initial condition for long wavelength gravitational perturbations  $\delta_\sigma^{(0)} = -2\Phi_0$  and it follows from (4.18) that  $\delta_\chi^{(0)} = \delta_r^{(0)} = -\Phi_0$ . Finally, because scalar velocity perturbations quickly decay outside of the Hubble radius, we will set their initial value to vanish on large scales when solving the set of equations in (4.17).

### 4.3.2 Evolution of the Perturbations during Moduli Domination

In this section, we examine the evolution of the perturbations for modes that enter the Hubble radius during moduli domination. We note that these modes will be small compared to the size of the horizon at reheating,  $k^{-1} < k_{rh}^{-1}$ , and thus it will be important for determining the growth of structure at that time. Our results for this part of the analysis are in general agreement with [194], but here we will include the effect of annihilation terms on the evolution of the perturbations. Moreover, we emphasize again that our primary interest is in examining the consequences of Split-SUSY motivated phenomenology. Thus, we have in mind electroweak scale dark matter  $\sim 100$  GeV, whereas the moduli masses can be parametrically higher.

#### Moduli Perturbations

We have seen that moduli domination leads to an effectively matter dominated universe, and so the gravitational potential  $\Phi$  will be constant on both super and sub-

Hubble scales (neglecting the second decaying mode) [198]. Therefore, we can set  $\Phi = \Phi_0$  during the scalar dominated era for both super and sub-Hubble scales. Using this, we can rewrite the first line of (4.17) as

$$\theta'_\sigma + \theta_\sigma = \frac{k^2}{H_0} \Phi_0 e^{N/2}, \quad (4.21)$$

where we used  $H = H_0 e^{-3N/2}$  in a matter dominated Universe. This equation can be solved to give the behavior for all wavelengths, concentrating on the growing mode we have

$$\theta_\sigma(k, N) = \frac{2}{3} \frac{k^2}{H_0} \Phi_0 e^{N/2}, \quad (4.22)$$

which confirms that long wavelength vector modes are unimportant. From (4.22), we can derive the evolution of the scalar perturbation  $\delta_\sigma$  during the scalar dominated era subject to the initial condition  $\delta_\sigma^{(0)} = -2\Phi_0$ . Noting that until the time of reheating we have  $\Gamma_\sigma/H \ll 1$  and  $\Phi$  is constant, we can rewrite the first line of (4.16) as

$$\delta'_\sigma(k, N) \simeq -\frac{\theta_\sigma}{H_0} e^{N/2} \quad (4.23)$$

and using the result in (4.22), we integrate (4.23) to find

$$\delta_\sigma(k, N) \simeq -2\Phi_0 - \frac{2}{3} \frac{k^2}{H_0^2} \Phi_0 e^N, \quad (4.24)$$

which is again valid on all scales.

## Dark Matter and Radiation Perturbations

In the absence of the terms on the right hand side of the fluid perturbation equations (4.16)-(4.18) the perturbations would just evolve as expected in a matter dominated universe. However, these additional terms will be important during the period of scalar domination and solutions for the complete system can be found by noting that the background dependent quantities on the right hand side of these equations are

time independent constants. This can be seen by using the background solutions (4.11) - (4.13) to determine the coefficients on the right hand side of (4.16) which scale as

$$B_\chi \frac{\Gamma_\sigma}{H} \left( \frac{\rho_\sigma}{\rho_\chi} \right) \longrightarrow B_\chi \frac{\Gamma_\sigma}{H_0} \left( \frac{\rho_\sigma^{(0)}}{\rho_\chi^{(0)}} \right) \equiv A_1, \quad (4.25)$$

$$\frac{\langle \sigma v \rangle}{m_\chi H} \rho_\chi \longrightarrow \frac{\langle \sigma v \rangle}{m_\chi H_0} \rho_\chi^{(0)} \equiv A_2. \quad (4.26)$$

where we have used that  $H = H_0 e^{-3N/2}$  during the scalar dominated epoch and  $A_1$  and  $A_2$  are constants. While for density perturbations of radiation, from (4.17) and (4.18) we again find that the scaling cancels and the coefficients are determined by their initial values,

$$(1 - B_\chi) \frac{\Gamma_\sigma}{H} \left( \frac{\rho_\sigma}{\rho_r} \right) \longrightarrow (1 - B_\chi) \frac{\Gamma_\sigma}{H_0} \left( \frac{\rho_\sigma^{(0)}}{\rho_r^{(0)}} \right) \equiv A_3, \quad (4.27)$$

$$\frac{\langle \sigma v \rangle}{m_\chi H} \left( \frac{\rho_\chi}{\rho_r} \right) \rho_\chi \longrightarrow \frac{\langle \sigma v \rangle}{m_\chi H_0} \left( \frac{\rho_\chi^{(0)}}{\rho_r^{(0)}} \right) \rho_\chi^{(0)} \equiv A_4. \quad (4.28)$$

Using this information and selecting a range of initial values motivated from SUSY model building we find that the annihilation and decay terms are of comparable importance. We can first solve for the DM perturbations. The velocity perturbations of the DM fluid during scalar domination can be found by using (4.22) in (4.17),

$$\theta'_\chi + (1 + A_1)\theta_\chi = \left(1 + \frac{2A_1}{3}\right) \frac{k^2}{H_0} \Phi_0 e^{N/2}. \quad (4.29)$$

Integrating (4.29), we find

$$\theta_\chi(k, N) = \frac{2}{3} \frac{k^2}{H_0} \Phi_0 e^{N/2}. \quad (4.30)$$

Similarly, using (4.24) and (4.30) in (4.16) and remembering that the background coefficients are constants we have

$$\delta'_\chi + (A_1 + A_2)\delta_\chi = -(A_1 + A_2)\Phi_0 - \frac{2}{3}(1 + A_1)\frac{k^2}{H_0^2}\Phi_0 e^N. \quad (4.31)$$

Integrating the above equation gives

$$\delta_\chi(k, N) = -\Phi_0 - \frac{2}{3} \left( \frac{1 + A_1}{1 + A_1 + A_2} \right) \frac{k^2}{H_0^2} \Phi_0 e^N, \quad (4.32)$$

which again is valid on both super-Hubble and sub-Hubble scales, and we have used the initial conditions  $\delta_\sigma^{(0)} = 2\delta_\chi^{(0)} = -2\Phi_0$ .

Given the solutions for the scalar field and DM perturbations we can solve for the radiation fluid perturbations. Using the solutions (4.22), (4.24), (4.30), and (4.32) in (4.18) and (4.17) we have

$$\theta'_r - \frac{k^2}{4H_0} e^{\frac{N}{2}} \delta_r + A\theta_r = \left(1 + \frac{A}{2}\right) \frac{k^2}{H_0} e^{\frac{N}{2}} \Phi_0, \quad (4.33)$$

$$\delta'_r + \frac{4}{3H_0} e^{\frac{N}{2}} \theta_r + A\delta_r = -A\Phi_0 - \alpha \frac{k^2}{H_0^2} e^N \Phi_0, \quad (4.34)$$

where we defined  $A \equiv A_3 + A_4$  and

$$\alpha = \frac{2}{3} \left( \frac{A_1 A_3 + 2A_1 A_4 + A_2 A_3 + 2A_4 + A_3}{1 + A_1 + A_2} \right), \quad (4.35)$$

Differentiating (4.34), using (4.33) to eliminate  $\theta'_r$  and (4.34) to eliminate  $\theta_r$  in the result, we have

$$\delta''_r + \left(2A - \frac{1}{2}\right) \delta'_r + \left(A^2 - \frac{A}{2} + \frac{k^2}{3H_0^2} e^N\right) \delta_r = S(N), \quad (4.36)$$



where the source term is given by

$$S(N) \equiv - \left( A^2 - \frac{A}{2} \right) \Phi_0 - \left( \frac{\alpha}{2} (2A + 1) + \frac{2}{3} (A + 2) \right) \frac{k^2}{H_0^2} \Phi_0 e^N. \quad (4.37)$$

In the absence of decays and annihilations (corresponding to  $A = \alpha = 0$  above) the exact solution to (4.36) can be easily found for all scales

$$\delta_r = -4\Phi_0 + 3\Phi_0 \cos \left( \frac{2k}{\sqrt{3}H_0} (e^{N/2} - 1) \right). \quad (4.38)$$

The modes are initial taken to be super-Hubble and have constant amplitude. As they pass through the Hubble scale, they begin to oscillate with fixed amplitude and rapidly increasing frequency as can be seen in Figure 4.1. The maximum amplitude of  $|\delta_r^{max}| = 7\Phi_0$  is reached when the lone source term in (4.37) is in phase with the oscillations resulting from the homogenous solution. There are two important differences when the scalar decay and DM annihilations are included (i.e.  $A \neq 0$ ) as can be seen from (4.36). Firstly, we see that if  $A > 1/4$  the homogeneous equation (with  $S(N) = 0$ ) becomes that of a damped oscillator. This damping is the result of radiation being pumped into the system from decays of the scalar, as well as from DM annihilations. The exact amount of damping depends on the relative abundances of the different fluids, the branching ratios, decay rate, and annihilation rate all given by (4.27) and (4.28). For typical initial values of radiation and DM, as well as decay rates and branching ratios as required by a successful SUSY non-thermal DM scenario, we find that typically  $A > 1/4$  and the oscillations in the scalar dominated phase will be over damped. A comparison of this situation as compared with the case where annihilations and decays are absent is presented in Figure 4.1. A second important effect resulting from decays and annihilations is that this provides additional source terms in (4.37), which act to boost the amplitude of the density perturbations. As can be seen from (4.36) and (4.37), unlike the  $A = 0$  case, the first two source terms in (4.37) will lead to an immediate boost to the perturbation as it enters the

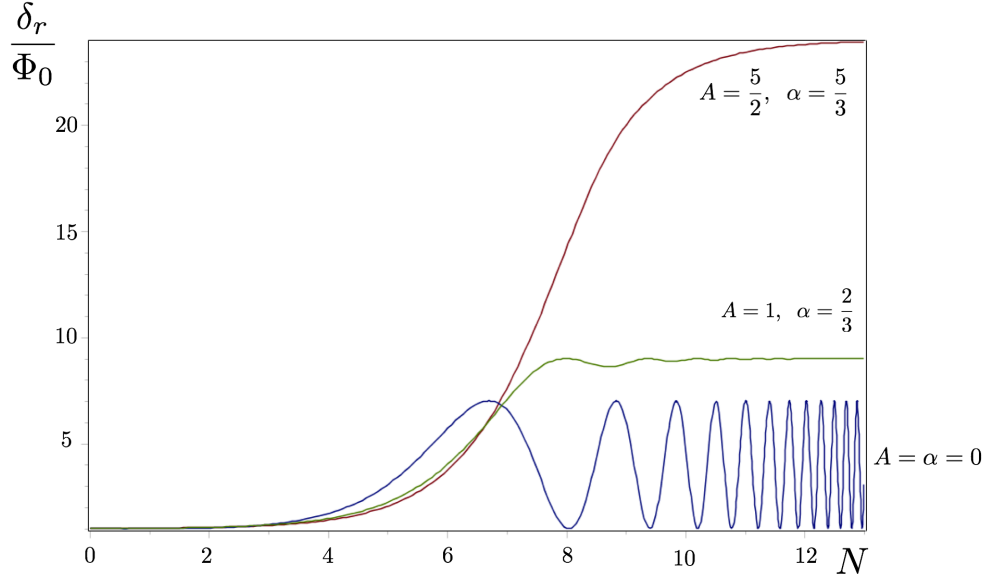


Figure 4.1: Evolution of the density perturbations in radiation fluid for modes with  $k/H_0 = 0.1$  and for different rates of decay and annihilation. The bottom blue curve corresponds to the evolution of radiation perturbations in the absence of scalar decay and annihilation terms in a “matter” dominated Universe, whereas green and red curves shows the evolution with enhanced decay and annihilations. Particularly, the values of  $A$  and  $\alpha$  for the red curve is implied by SUSY model building.

Hubble radius. The enhancement of the amplitude is again controlled by the decay and annihilation rates given by (4.27) and (4.28). In addition, although these new source terms with  $A \neq 0$  provide additional enhancement, for typical values of the parameters the damping overcomes this effect before one oscillation can complete as can again be seen in Figure 4.1.

Saturation of the radiation density perturbation at late times in the presence of decays and annihilations ( $A \neq 0$ ) can be also understood considering the first order equations (4.33) and (4.34). As we mentioned before, upon horizon entry the radiation density perturbation gets a kick and grows considerably. From (4.33), this growth began to contribute as an additional source for the velocity perturbation, causing a spatial dispersion of the radiation fluid. As the radiation velocity perturbation grows, this slows down the growth of radiation density perturbation through (4.34).

Eventually, the growth in the velocity perturbation will balance the source terms in (4.34) and saturate the growth in the radiation perturbation, giving that the radiation density perturbation is constant. For the full solutions of the radiation velocity and density perturbations during scalar decay we refer the reader to the Appendix C where we provide exact solutions using Green’s function methods.

To summarize, in this section we have derived the analytic solutions for the DM and radiation perturbations during the scalar dominated epoch prior to reheating<sup>5</sup>. Note that the solutions we found are valid on all scales and the behavior of perturbations in different regimes can be inferred by considering the limits  $k/aH \ll 1$  or  $k/aH \gg 1$ . In the next section we consider the evolution of perturbations by focusing on the reheating era during which the decay term for the scalar will significantly influence the evolution of the cosmological background.

### Evolution of Perturbations through Reheating

Thus far we have neglected the effect of decays on the moduli energy density  $\rho_\sigma$  and so also the effect on the Hubble expansion. We find that this approximation will remain valid until a time near  $t_d \sim H_d^{-1} \sim \Gamma^{-1}$  (or in e-folds  $0 < N < N_{rh}$ ). As mentioned above, this effective matter dominated phase is what allowed us to simplify the background dependent source terms in (4.16), (4.17), (4.17) and (4.18) (due to the scaling in (4.25) – (4.28)). However, as the scalar decays become important the constant scaling is no longer valid and the evolution of these terms must be considered. In this regime we perform the analysis numerically with our results appearing in Figures 3 and 4. We now discuss the behavior of these solutions and their connection to the perturbation equations.

First we consider the behavior of the radiation perturbations, which is given in

---

<sup>5</sup>We have seen that decay of the scalar to radiation and DM is important (e.g. it changes the scaling of both radiation and DM), however the energy density of the scalar field is only reduced appreciably near the time of ‘reheating’  $t_{rh} \sim H^{-1} \sim \Gamma_\sigma^{-1}$  as usually assumed in models of *instant* reheating.

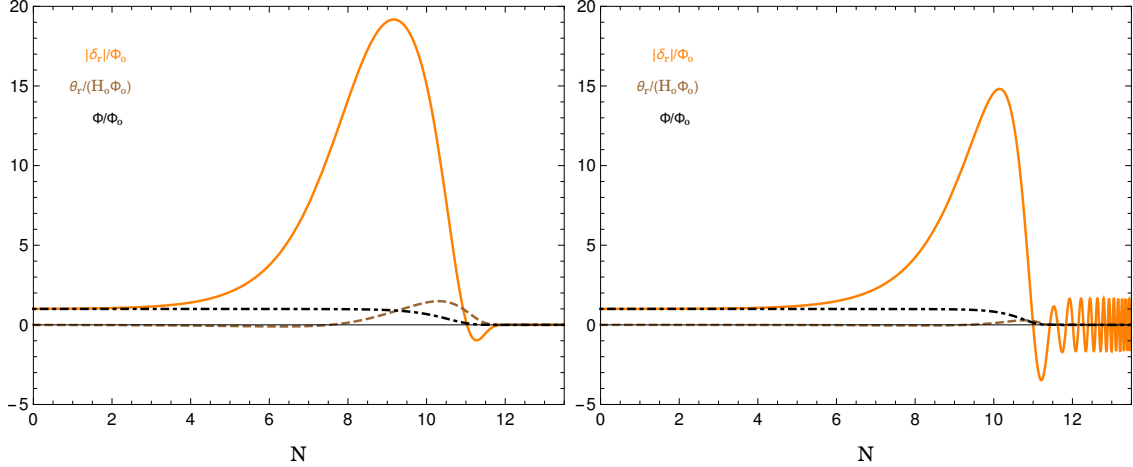


Figure 4.2: Evolution of normalized radiation density contrast,  $|\delta_r|/\Phi_0$ , velocity perturbation  $\theta_r/(H_0\Phi_0)$  and gravitational potential  $\Phi/\Phi_0$  for the modes  $k/H_0 = 0.1$  (Left),  $k/H_0 = 0.04$  (Right). These modes enters the horizon at  $N_h = \ln(k/H_0)^{-2} \simeq 4.6$  (Left),  $N_h = \ln(k/H_0)^{-2} \simeq 6.4$  (Right). In this non-thermal cosmology the universe is effectively matter dominated until  $N_{rh} \simeq 10.6$  e-foldings after which the universe becomes radiation dominated. Well after reheating, the density perturbation oscillates with an amplitude  $A_{\delta_r} \simeq 0.0005\Phi_0$  (Left),  $A_{\delta_r} \simeq 1.7\Phi_0$  (Right). For these modes, the ratio of the size of the comoving horizon  $k_{rh}^{-1}$  at the time of reheating to the size  $k^{-1}$  of the fluctuation is given by,  $k/k_{rh} \simeq 20$  (Left) and  $k/k_{rh} \simeq 8$  (Right).

Figure 4.2. In the figure we show the evolution for two different modes with  $k/k_{rh} = 20$  and  $k/k_{rh} = 8$ , where  $k_{rh}^{-1} = 1/(a_{rh}H_{rh})$  is the size of the comoving horizon at reheating. As discussed above, the radiation density perturbation gets an initial kick at Hubble radius crossing and grows considerably until it levels out due to the balance between the source terms in (4.17) at around  $N \simeq 9$  e-foldings. For  $9 < N < N_{rh}$ , radiation velocity perturbations continue to grow which leads to a dispersion of the radiation density perturbations through its effect given by (4.17). Equivalently this can be understood as the importance of the friction term and sources appearing in (4.36), acting to balance each other. The source terms lead to rapid growth of the density perturbation, but the friction term eventually saturates this growth depending on the amount of decay and annihilations.

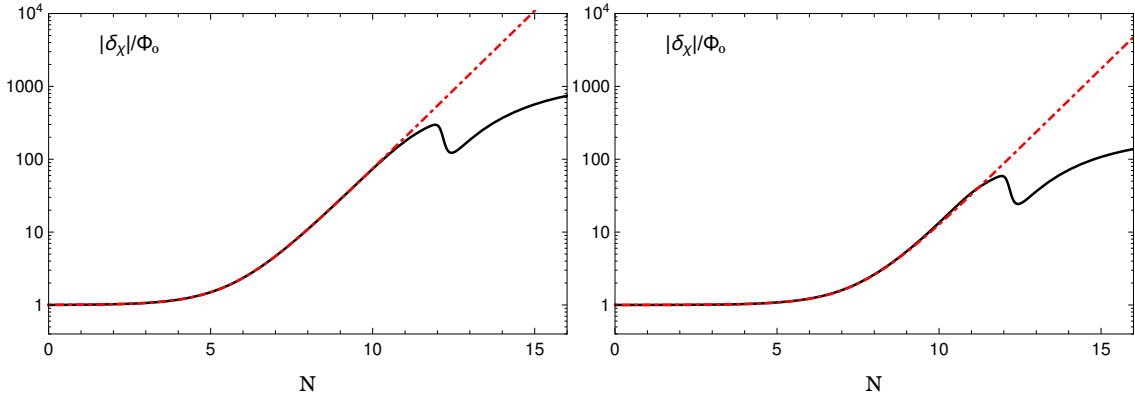


Figure 4.3: Evolution of DM density contrast (normalized) in a non-thermal cosmology for modes with  $k/H_0 = 0.1$  (Left) and  $k/H_0 = 0.04$  (Right). As the mode enters the horizon, it grows linearly with the scale factor  $e^N \sim a$ . We see that the solution (4.32) (red dot-dashed curve) we derived in the previous section is an excellent fit during the scalar dominated era. After the universe become radiation dominated at  $N_{rh} \simeq 10.6$ , the amplitude of the density contrast decreases due to rapid annihilations of DM particles. For  $N \gtrsim 12$ , the density contrast then begins to grow logarithmically as expected.

Once moduli decay becomes significant to change the expansion history at  $t_d$  the moduli density then scales as  $\rho_\sigma \sim e^{-2\Gamma_\sigma/3H}$  for  $N > N_{rh} \simeq 10.6$ , which leads to quick decay of the moduli in less than a Hubble time. This rapid decay results in a termination of the source terms in (4.17), while the relativistic conversion of scalar particles to radiation acts to wipe out the growth prior to decay. Thus, the only remnant of the moduli epoch is an extra suppression in the amplitude of radiation perturbations (as a consequence of the decay), which as discussed in [194] could lead to damping of dark matter perturbations on small scales if dark matter is not kinetically decoupled [199]. We find that the addition of DM annihilations to radiation does not change this conclusion. In fact, we saw above that both annihilations and decays enter (4.36) in a similar way (through the parameter  $A = A_3 + A_4$ , see also (4.27) and (4.28)). We find that the key effect of adding DM annihilations to the system is to effectively add an additional source of radiation complementary to that provided by scalar decay. As can be seen from both Figures 4.2 and 4.1, this increases the

rate of initial growth and the importance of the friction effect. This addition also leads to a larger suppression at the time  $t_d$  as the rapid decay of moduli to DM leads to annihilations in the super-critical case and these annihilations pump additional radiation into the system acting to further dilute the amplitude of radiation density perturbations.

We now consider the evolution of DM perturbations. Figure 4.3 shows the evolution for the DM density perturbations again for two different modes with  $k/k_{rh} = 20$  and  $k/k_{rh} = 8$ . As seen from the figure, the density contrast begins to grow linearly with the scale factor upon horizon entry until reheating  $N_{rh} \simeq 10.6$ . The solution (4.32) we obtained in the previous section is an excellent fit (red-dashed line) to the numerical solution for typical values of  $A_1$  and  $A_2$  motivated by SUSY model building. Briefly after reheating  $N > N_{rh}$  the DM annihilation terms become the main source in (4.16) and this along with the radiation production from decay leads to a power loss in DM density contrast. The annihilations happen in much less than a Hubble time and the resulting density contrast begins to grow logarithmically as expected in a radiation dominated universe [198]. In the absence of annihilations we find agreement with the analysis in [194], whereas in the case of super-critical non-thermal DM production – when annihilations are important – we find this acts to further reduce the strength of the perturbations following reheating.

We conclude this section by noting that the DM perturbations on scales that enter the Hubble-horizon during the early “matter” dominated epoch can experience a significant growth. This growth might lead to formation of substructure in the form of compact mini-halos or other objects [194], which could provide an important observational prediction of non-thermal cosmologies. To investigate this possibility one needs to take into account cut-off scales that arise due to kinetic decoupling and free-streaming of DM candidates. We address these questions in the next two sections.

## 4.4 Determining the Scale of the Smallest Dark Matter Structures

### 4.4.1 Free Streaming and Kinetic Decoupling of Dark Matter

In the standard WIMP paradigm, while freeze-out signals the departure from *chemical* equilibrium it does not signal the end of WIMP interactions. Scattering processes of the form  $\chi^l \rightarrow \chi^l$  (elastic) or  $\chi^l \rightarrow \chi'^{l'}$  (inelastic) keep WIMPs in *kinetic* equilibrium until later times and therefore to lower temperatures [200–202]. Here  $l$  and  $l'$  are the light degrees of freedom in the thermal bath, while  $\chi'$  is an unstable state that carries the same conserved quantum number as  $\chi$ . As the Universe expands and cools these scattering processes cease to be in effect and DM particles  $\chi$  kinetically decouple at a temperature  $T_{kd}$  when the scattering rate  $\gamma$  of the DM species becomes comparable to the Hubble expansion rate,  $\gamma(T_{kd}) \simeq H(T_{kd})$ .

The temperature  $T_{kd}$  at kinetic decoupling determines the length scale at which linear density perturbations of DM get damped, setting the scale of the smallest structures in the universe. In general, there are two important scales associated with kinetic decoupling below which the perturbations in the DM get suppressed:

- i. The free streaming distance of DM particles after kinetic decoupling,  $k_{fs}^{-1}$ ,
- ii. The size of the comoving horizon at kinetic decoupling,  $k_d^{-1}$ .

For temperatures  $T < T_{kd}$ , scattering of DM particles from the relativistic plasma cease to occur and WIMPs can stream from over-dense regions to under-dense regions freely, causing damping of the perturbations [203–206],

$$k_{fs}^{-1} = \int_{t_{kd}}^{t_0} \frac{\langle v \rangle}{a} dt, \quad (4.39)$$

where  $\langle v \rangle$  is the average velocity of DM particles after kinetic decoupling and  $t_{kd}$  is the time of kinetic decoupling. However, kinetic decoupling is not an instantaneous

process: coupling of the DM fluid to acoustic oscillations in the radiation bath induces both oscillations and damping of perturbations that crosses the horizon before kinetic decoupling [199, 203]. This leads to an additional source of damping, as so critical scale as modes with comoving wavelengths  $k^{-1} < k_d^{-1} = (a_{kd}H_{kd})^{-1}$  will be damped while  $k^{-1} > k_d^{-1} = (a_{kd}H_{kd})^{-1}$  continue to grow logarithmically. We emphasize that this damping due to acoustic oscillations is most important in a universe that is dominated by the radiation bath.

#### 4.4.2 Determining the Relevant Scale

We now consider the different possible cases for DM kinetic decoupling as compared to the reheating effects discussed in Section 4.3 and establish the implications for the formation of primordial substructures. We can capture the enhanced growth of perturbations discussed in Section 4.3 by introducing a Gaussian cutoff into the matter power spectrum<sup>6</sup>:

$$\delta_\chi \rightarrow \exp \left[ -\frac{k^2}{2k_{rh}^2} \frac{k_{rh}^2}{k_{cut}^2} \right] \delta_\chi(N_{rh}), \quad (4.40)$$

where the damping scale is given by  $k_{cut}^{-1} = \max(k_{fs}^{-1}, k_d^{-1})$  – where  $k_{fs}^{-1}, k_d^{-1}$  are the free-streaming and kinetic decoupling scales discussed above. This expression implies that any fluctuation of size  $k^{-1}$  must be larger than both of these scales to form structure.

DM particles produced from the scalar decays can thermalize with the relativistic plasma if the scattering rate is larger than the expansion rate  $\gamma(T_{rh}) > H(T_{rh})$ . Here, we assume that the decay populates DM almost instantaneously as can be verified from Figure 4.1. In this case, the kinetic decoupling temperature is lower than the reheat temperature  $T_{kd} < T_{rh}$  and the damping scale is typically given by  $k_{cut}^{-1} = k_d^{-1}$  as  $k_d^{-1} > k_{fs}^{-1}$  [199]. In this scenario, DM particles will lose their memory to the

---

<sup>6</sup>In the simplest case of DM produced from two-body decays, we approximate the damping effects on the growth of DM perturbations by a Gaussian cut-off (See also [207]).



growth (4.32) prior to reheating and will follow the tiny oscillations in the radiation perturbation after reheating (see figure 4.2). Therefore, the growth during the scalar dominated era will be erased. This is simply because the size of the horizon at kinetic decoupling  $k_d^{-1}$  is greater than the characteristic scale  $k_{rh}^{-1}$  in non-thermal cosmology. The hierarchy between these scales combined with the scales of interest during the scalar dominated epoch,  $k_d^{-1} > k_{rh}^{-1} > k^{-1}$  directly translate into the suppression of DM perturbations which can be seen from (4.40) by noting  $\delta_\chi(N_{rh}) \sim (k/k_{rh})^2$  from (4.32).

On the other hand, DM picks up a momentum when produced from heavy scalar decays after reheating and then their free streaming may erase structures on scales smaller than the free-streaming horizon  $k_{fs}^{-1}$  if they don't thermalize with radiation bath. This case corresponds to  $T_{kd} > T_{rh}$  where DM decouples kinetically prior reheating. In the following, we will derive the free-streaming horizon and discuss in which cases the free-streaming effect could become important.

We denote the average momentum of DM particles produced from decays by  $\langle p_{rh} \rangle$ . The momentum redshifts as  $a^{-1}$  assuming that there is negligible interaction to change the momentum, which is true in the case  $T_{kd} > T_{rh}$ :

$$\langle p(t) \rangle = \frac{\langle p_{rh} \rangle a_{rh}}{a(t)}. \quad (4.41)$$

In general, the DM particles produced from decays will have a continuum spectrum and  $\langle p_{rh} \rangle$  is model dependent. In the simplest case where DM particles all come from two-body decay  $\sigma \rightarrow \chi\chi$ ,  $\langle p_{rh} \rangle = \sqrt{\left(\frac{m_\sigma}{2}\right)^2 - m_\chi^2}$ .

For DM particles produced from scalar decays, the free-streaming horizon in (4.39)

is an integration from the reheating time  $t_{rh}$  till now  $t_0$

$$\begin{aligned}
k_{fs}^{-1} &= \int_{t_{rh}}^{t_0} \frac{\langle v \rangle}{a} dt \\
&= \int_{a_{rh}}^1 \left\langle \frac{p}{E} \right\rangle \frac{1}{a^2 H} da = \int_{a_{rh}}^1 \left\langle \frac{p}{\sqrt{p^2 + m_\chi^2}} \right\rangle \frac{1}{a^2 H} da, \\
&= \frac{a_{rh}}{\sqrt{\Omega_R} H_0} \int_{a_{rh}}^1 \left\langle \frac{p_{rh}}{\sqrt{p_{rh}^2 a_{rh}^2 + m_\chi^2 a^2}} \right\rangle \frac{1}{\sqrt{1 + a/a_{eq}}} da, \tag{4.42}
\end{aligned}$$

where in the second line, we changed variable from time to scale factor and used the kinematic relations  $v = p/E$  and  $E = \sqrt{p^2 + m_\chi^2}$ . In the third line, we used Eq. (4.41). We also used the facts that the scale factor at matter-radiation equality could be written as  $a_{eq} = \Omega_R/\Omega_M$  with  $\Omega_R(\Omega_M)$  being the current radiation (matter) density of the Universe and

$$\frac{H(a)}{H_0} = \sqrt{\Omega_R a^{-4} + \Omega_M a^{-3}} = a^{-2} \sqrt{\Omega_R} \sqrt{1 + a/a_{eq}}, \tag{4.43}$$

where  $H_0$  is the current Hubble rate and we neglect the dark energy contribution.

Knowing the momentum distribution of DM after reheating, one could carry out the integration in Eq. (4.42) either analytically or numerically. Below we will consider two interesting limits to obtain simple illustrative analytic results. In the case with  $\langle p_{rh} \rangle \ll m_\chi$ , where the DM particles produced from decays are non-relativistic,  $p_{rh} \approx m_\chi v_{rh}$  with  $v_{rh}$  the DM velocity after reheating, Eq. (4.42) is reduced to the result in [194],

$$k_{fs}^{-1} \approx \frac{2\langle v_{rh} \rangle a_{rh}}{\sqrt{\Omega_R} H_0} \left( \sinh^{-1} \sqrt{\frac{a_{eq}}{a_{rh}}} - \sinh^{-1} \sqrt{a_{eq}} \right). \tag{4.44}$$

In the case with  $\langle p_{rh} \rangle \gg m_\chi$ , where the DM particles produced from decays are relativistic, the dominating contribution to  $k_{fs}^{-1}$  is the integration over the period

when DM particles are relativistic,

$$k_{fs}^{-1} \approx \frac{1}{\sqrt{\Omega_R} H_0} (a_{nr} - a_{rh}), \quad (4.45)$$

where we approximated the integrand in Eq. (4.42) to be unity and integrated from  $a_{rh}$  till  $a_{nr}$  when DM is red-shifted and becomes non-relativistic with momentum of order  $m_\chi$ .

If  $k_{rh}/k_{fs} > 1$ , the free-streaming of the DM particles will completely erase the growth of density perturbation in the scalar domination period ( See eq. (4.40)). In the two limiting cases we considered, the ratio  $k_{rh}/k_{fs}$  is given by

$$\frac{k_{rh}}{k_{fs}} \approx \begin{cases} 2\langle v_{rh} \rangle \left( \sinh^{-1} \sqrt{\frac{\sqrt{2}k_{rh}}{k_{eq}}} - \sinh^{-1} \sqrt{a_{eq}} \right), & \langle p_{rh} \rangle \ll m_\chi \\ \frac{a_{nr}}{a_{rh}} - 1 \approx \frac{\langle p_{rh} \rangle}{m_\chi}, & \langle p_{rh} \rangle \gg m_\chi. \end{cases} \quad (4.46)$$

In deriving the formulas above, we used  $k_{rh}a_{rh} = H(a_{rh})a_{rh}^2 = H_0\sqrt{\Omega_R}$  and  $a_{eq}/a_{rh} = \sqrt{2}k_{rh}/k_{eq}$ . We also chose  $a_{nr} \equiv \langle p_{rh} \rangle a_{rh}/m_\chi$ . To obtain more accurate numerical results in a general case, one should use Eq. (4.42). Yet the approximate formulas already tell us the conditions in which case the free-streaming effect is important. If there is a large mass splitting between scalar and DM,  $\langle p_{rh} \rangle \gg m_\chi$ , then  $k_{rh} \gg k_{fs}$  and the free-streaming effect will definitely wipe out the growth of perturbation in the scalar domination phase. Only when DM particles produced from decays are non-relativistic,  $k_{rh}$  could be smaller than  $k_{fs}$ . Since

$$\frac{k_{rh}}{k_{eq}} = 1.2 \times 10^6 \frac{T_{rh}}{1 \text{ MeV}} \left( \frac{10.75}{g_{*,s}} \right)^{1/3} \left( \frac{g_*}{10.75} \right)^{1/2} \quad (4.47)$$

and  $\sinh^{-1} x$  behaves as  $\log x$  for  $x \gg 1$ ,  $k_{rh}/k_{fs}$  depends weakly on  $T_{rh}$  and for reheating temperatures above 10 MeV,  $k_{rh}/k_{fs} < 1$  leads to  $\langle v_{rh} \rangle < 0.06$  [194]. This could only occur in scenarios where the scalar mass is very close to the total mass of all decays products (a situation not favored by SUSY motivated phenomenology).

## 4.5 Neutralino Dark Matter in the Moduli Scenario

In this section we consider SUSY neutralino DM in the Split SUSY / moduli framework, which provides an explicit realization of the non-thermal histories discussed above. We will be interested in wino or higgsino DM and we begin by summarizing the picture of kinetic decoupling.

In the moduli scenario, immediately after the moduli decay at about  $T_{rh}$ , the produced DM particles would have a energy distribution which peaks at high energy and most of them are relativistic. Through scattering with SM particles,  $e^-$ ,  $\nu_e$ ,  $\nu_\mu$ ,  $\nu_\tau$  in the thermal bath, they will deposit energy into radiation. Because the scattering rate of either wino or higgsino is large enough (compared to Hubble), the DM particles will thermalize with the radiation quickly. When the temperature decreases and the DM particles become non-relativistic, the rate of the thermal scattering drops and eventually the DM particles would be kinetically decoupled from radiation. One key quantity that will determine whether thermalization happens or not is  $\gamma/H$  where  $\gamma$  is the scattering rate of DM particles off radiation. In this section, we will demonstrate thermalization indeed happens for either wino or higgsino DM by computing their scattering rates  $\gamma/H$ 's.

Light wino DM with mass of about a few hundred GeV fits very nicely into the moduli scenario [77]. However, indirect detection searching for excesses in the photon spectrum of our galactic center have already put strong constraints<sup>7</sup> on the wino as the only component of DM [110, 132]. In particular,  $T_{rh} > 1$  GeV in the moduli scenario even if the wino is only one component of DM [110]<sup>8</sup>. The cosmological history of winos after reheating has already been worked out in detail in Ref. [195]. It is

---

<sup>7</sup>Weaker constraints on the reheat temperature were found in [165], but this analysis only took into account FERMI observations of dwarf spheroidal galaxies. Reach of future dwarf spheroidal galaxies observations has been studied in [208].

<sup>8</sup>The constraint could be relaxed if the branching fraction of moduli decaying to winos are suppressed as in the branching scenario [166].

demonstrated that winos lose energy efficiently after production through the inelastic process  $\widetilde{W}^0 + e^\pm \rightarrow \widetilde{W}^\pm + \nu_e$  and thermalize with the radiation almost instantaneously. At low temperature  $T_{kd} \approx 10$  MeV, the wino DM will kinetically decouple from the thermal bath. Notice that  $T_{kd}$  is almost independent of the wino mass and is mostly set by the mass splitting between the charged and neutral components of wino DM, which is about  $\Delta m \approx 160$  MeV at the two-loop level [157]. This is because at low temperature, the scattering rate will be suppressed by the Boltzmann factor  $\exp(-\Delta m/T)$ .

Now we turn to the higgsino DM scenario. When DM is mostly higgsinos, or in other words,  $\mu < M_1, M_2$ , unlike the wino case, the tree-level mass splitting is only suppressed by one power of the larger mass scale  $M_1$  or  $M_2$ ,

$$\Delta m_{\widetilde{H}} \approx \frac{m_Z^2}{2M_1} c_W^2 (1 - \sin 2\beta) + \frac{m_Z^2}{2M_2} s_W^2 (1 + \sin 2\beta) \approx 0.5 \text{ GeV} \frac{4.5 \text{ TeV}}{M_s}, \quad (4.48)$$

where in the second step, we assume that  $\tan \beta \gg 1$  and  $M_2 = 2M_1 = M_s$ . Traditionally one could diagonalize the neutralino/chargino mass matrices and expand the formulas to obtain the result above. However, this could also be understood easily from an effective operator analysis. Integrating out a heavy bino or wino at tree-level, one gets dimension-five operators such as

$$\frac{g'^2}{M_1} H_u^\dagger \widetilde{H}_u H_d^\dagger \widetilde{H}_d, \quad \frac{g^2}{M_2} H_u^\dagger \sigma^a \widetilde{H}_u H_d^\dagger \sigma^a \widetilde{H}_d \quad (4.49)$$

where  $\sigma^a$  with  $a = 1, 2, 3$  are the three  $SU(2)_w$  generators.  $g$  and  $g'$  are the SM  $SU(2)_w$  and  $U(1)_B$  gauge couplings correspondingly. The operators above will lead to a charged/neutral mass splitting after electroweak symmetry breaking. Notice that the operators above also lead to an effective coupling between Higgsinos and  $Z$  gauge boson.

In the moduli scenario, the relic abundance of higgsino DM is estimated to be,

assuming order one branching fraction of moduli decaying to higgsinos,

$$\begin{aligned}\Omega_{\tilde{H}}h^2 &= 0.12 \frac{\langle\sigma v\rangle_{th}}{\langle\sigma v\rangle_{\tilde{H}\tilde{H}\rightarrow ZZ,WW}} \frac{T_f}{T_{rh}}, \\ T_{rh} &\approx 0.4 \text{ GeV} \left(\frac{\mu}{200 \text{ GeV}}\right)^3 \left(\frac{0.12}{\Omega_{\tilde{H}}h^2}\right),\end{aligned}\quad (4.50)$$

where we took  $\langle\sigma v\rangle_{th} = 3 \times 10^{-26} \text{ cm}^3/\text{s}$  and the thermal freeze-out temperature  $T_f \approx \mu/20$ . In deriving the second line, we used  $\langle\sigma v\rangle_{\tilde{H}\tilde{H}\rightarrow ZZ,WW} \approx g^4/(512\pi\mu^2)(21 + 3 \tan^2\theta_W + 11 \tan^4\theta_W)$  [100].

The elastic scattering rate of higgsino DM per expansion rate is [209]

$$\begin{aligned}\frac{\gamma_{el}}{H} &= \frac{45\sqrt{5}}{16\pi^{9/2}} \frac{1}{\sqrt{g_*(T)}} \frac{g^4}{m_W^4} c_{\tilde{H}\tilde{H}Z}^2 (1 - s_W^2 + 2s_W^4) \frac{m_p E^2 T^3}{\mu^2}, \quad (4.51) \\ \text{where } c_{\tilde{H}\tilde{H}Z} &= \frac{m_Z^2}{2\mu} \left(\frac{s_W^2}{M_1} + \frac{c_W^2}{M_2}\right) \cos(2\beta) \\ &= \frac{\Delta m}{\mu} \frac{(s_W^2 + c_W^2/r) \cos(2\beta)}{(c_W^2 + s_W^2/r) + (s_W^2/r - c_W^2) \sin(2\beta)}, \quad (4.52)\end{aligned}$$

where  $E$  is the energy of the DM particles,  $T$  is the temperature of the radiation bath and  $r = M_2/M_1$ . One could see that the elastic scattering rate per Hubble scales as  $(\Delta m)^2$  and increases when  $\Delta m$  increases. The inelastic scattering of higgsino DM per Hubble is

$$\frac{\gamma_{in}}{H} = \frac{6\sqrt{5}}{\pi^{3/2}} \frac{1}{\sqrt{g_*(T)}} \frac{g^4}{m_W^4} m_p E T^2 e^{-\frac{\mu\Delta m}{2ET}} \left(\frac{\Delta m}{\mu} + 6\frac{ET}{\mu^2}\right), \quad (4.53)$$

where  $e^{-\frac{\mu\Delta m}{2ET}}$  is the Boltzmann factor. Thus inelastic scattering would be more efficient at small  $\Delta m$ . In Fig. 4.1, we demonstrated the higgsino elastic/inelastic scattering rates per Hubble as a function of the mass splittings for different choices of the DM energy and thermal bath's temperature. From Fig. 4.1, the inelastic scattering rate always dominates over elastic scattering rate at the reheating temperature for the whole range of mass splitting. It is also much larger than Hubble rate and thus the

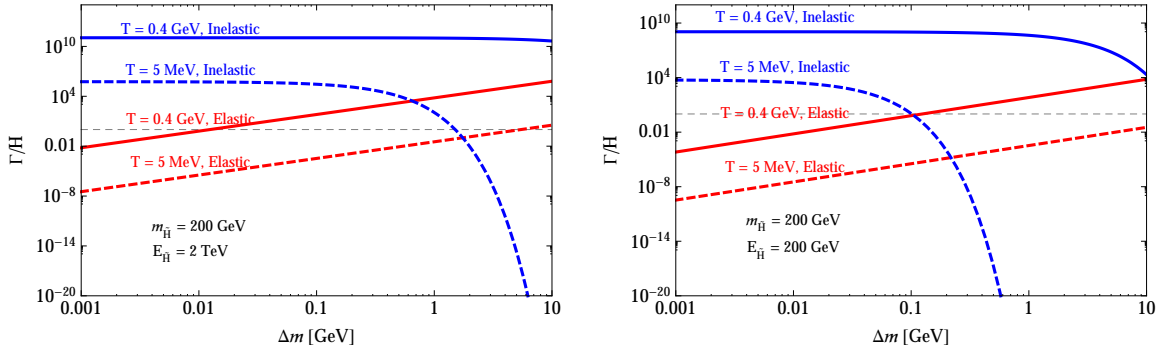


Figure 4.1: Elastic/inelastic scattering rates per Hubble (red/blue curves) as a function of the mass splittings fixing  $\mu = 200$  GeV. Left: energy of DM produced from decay is fixed to be 2 TeV. Right: energy of DM produced from decays is fixed to be 200 GeV. The solid curves correspond to the temperature of the thermal bath to be about  $T_{rh} = 0.4$  GeV; the dashed curves correspond to a much lower temperature 5 MeV. The gray dashed lines corresponds to  $\gamma/H = 1$ .

higgsino DM particles would quickly thermalize with the radiation immediately after reheating. When the temperature drops,  $\gamma/H$  decreases and eventually higgsinos decouple kinetically.

In summary, we find that for neutralino dark matter with a non-thermal history that any enhancement of dark matter perturbations arising from the moduli epoch are washed out by kinetic decoupling effects following reheating.

## 4.6 Conclusions

In this paper we have investigated the result of a matter (moduli) dominated phase prior to BBN on the growth of cosmological perturbations. We have seen that matter and radiation perturbations grow during this epoch, with dark matter perturbations being enhanced and radiation perturbations first growing and then eventually oscillating with an amplitude suppressed relative to the usual thermal case. We saw that this suppression arises at the peak of scalar decay when most of the radiation is created by both dark matter annihilations and decays of the moduli. In agreement

with [194] we find that the matter perturbations remain enhanced following reheating (with the growth inherited from the growth of scalar fluctuations during moduli domination), and we showed that this remains true even in the presence of dark matter annihilations to radiation. Whereas the suppression of the radiation perturbations can lead to damping of dark matter perturbations on small scales if dark matter is not kinetically decoupled [199] – again in agreement with [194].

However, we have also seen that for non-thermal models motivated by BSM physics – such as those motivated by moduli in the presence of SUSY breaking with a split spectrum – that these effects are lost since the kinetic decoupling temperature of neutralinos is typically below that of reheating. This is discouraging for establishing new signatures for the dark ages following inflation, because it means that the matter power spectrum (and enhanced small scale structure such as compact mini-halos) can not be used to distinguish a non-thermal history from the standard thermal case. Moreover, because the effects of the moduli decays to dark matter are local (sub-horizon) and dark matter is subdominant before, during, and after the decays, we should not expect any associated CMB signatures (e.g. from dark matter annihilations). That is, as far as observations are concerned, the cosmic dark ages remain elusive.

There are some exceptions to this conclusion. As discussed in [194], if dark matter is produced thermally after reheating (and kinetic decoupling and free-streaming effects are not important) the suppression of the radiation perturbations resulting from the non-thermal phase can lead to an erasure of dark matter structure (establishing a cutoff in the matter power spectrum). For typical SUSY WIMP models this seems to present model building challenges given the need for a large reheat temperature, and so the matter dominated phase would be short or even comparable to that of a thermal history. Another possibility is if dark matter is produced non-thermally but with a mass comparable to the moduli mass (so it is not relativistic at production). This possibility again seems rather exotic from a SUSY model building viewpoint, partic-



ularly in models with moduli masses associated with PeV-scale symmetry breaking.

Taking a more optimistic view, our results suggest the robustness of typical non-thermal histories (or early matter dominated phases) prior to BBN and provide further evidence that such models offer a realistic alternative to the standard thermal WIMP paradigm.

# Appendix

## 4.A Derivation of Perturbation Equations

We take the scalar field, radiation and the DM as perfect fluids with energy-momentum tensors

$$T^\mu{}_\nu = (\rho + p)u^\mu u_\nu + \delta^\mu{}_\nu p, \quad (4.54)$$

where four-velocities in the rest frame of each fluid is  $u^\mu = (1, \vec{0})$ . In this Appendix, we will work with the background metric  $g_{\mu\nu} = \text{diag}(-1, a^2, a^2, a^2)$  and use cosmic time  $t$  to be proper time. In the reheating model we are considering, there are energy transfer between different fluids which can be captured in a covariant manner by writing,

$$\nabla_\mu T^\mu{}_\nu^{(\alpha)} = Q_\nu^{(\alpha)} + Y_\nu^{(\alpha)}, \quad (4.55)$$

where  $Q_\nu^{(\alpha)}$  denotes the energy transfer due to scalar decay and  $Y_\nu^{(\alpha)}$  stands for the transfer of energy due to annihilations. Note that the total energy conservation  $\sum_\alpha \nabla_\mu T^\mu{}_\nu^{(\alpha)} = 0$  implies the constraint

$$\sum_\alpha Q_\nu^{(\alpha)} + Y_\nu^{(\alpha)} = 0. \quad (4.56)$$

The covariant form of energy transfer terms on the R.H.S of (4.55) can be written as,

$$Q_\nu^{(\alpha)} = \Gamma_\sigma^{(\alpha)} T_{\mu\nu}^{(\sigma)} u_{(\sigma)}^\mu, \quad (4.57)$$

$$Y_\nu^{(\alpha)} = \frac{\langle \sigma v \rangle^{(\alpha)}}{m_\chi} [\rho_\chi^2 - \rho_{\chi,eq}^2] u_\nu^{(\chi)}, \quad (4.58)$$

from which one can easily obtain,

$$\dot{\rho}_\alpha + 3H\rho_\alpha(1 + w_\alpha) = -\Gamma_\sigma^{(\alpha)}\rho_\sigma + \frac{\langle \sigma v \rangle^{(\alpha)}}{m_\chi}[\rho_\chi^2 - \rho_{\chi,eq}^2]. \quad (4.59)$$

Then, the fluid evolution equations (4.2)-(4.4) can be recast using the following conventions for the decay rate and annihilation cross section between scalar, radiation and DM fluids:  $\langle \sigma v \rangle^{(\sigma)} = 0$ ,  $\langle \sigma v \rangle^{(\chi)} = -\langle \sigma v \rangle$ ,  $\langle \sigma v \rangle^{(r)} = \langle \sigma v \rangle$  and  $\Gamma_\sigma^{(\sigma)} = \Gamma_\sigma$ ,  $\Gamma_\sigma^{(\chi)} = -B_\chi\Gamma_\sigma$ ,  $\Gamma_\sigma^{(r)} = -(1 - B_\chi)\Gamma_\sigma$ .

We now write the perturbed metric in the longitudinal gauge as

$$ds^2 = -(1 + 2\Phi) dt^2 + a(t)^2 (1 - 2\Psi) \delta_{ij} dx^i dx^j. \quad (4.60)$$

In the absence of anisotropic stress, from (4.54) we write perturbed energy-momentum tensor;

$$\delta T_\nu^{\mu(\alpha)} = \begin{pmatrix} -\delta\rho_\alpha & \rho_\alpha(1 + w_\alpha)\partial_i v_\alpha \\ -g^{ij}\rho_\alpha(1 + w_\alpha)\partial_j v_\alpha & \delta_j^i c_{s,\alpha}^2 \delta\rho_\alpha \end{pmatrix}, \quad (4.61)$$

where we have used  $p_\alpha = w_\alpha\rho_\alpha$ ,  $\delta p_\alpha = c_{s,\alpha}^2\delta\rho_\alpha$  and  $v_\alpha$  denotes the longitudinal part of the spatial velocity perturbation of each fluid,  $\delta u_{j,\alpha} = \partial_j v_\alpha$ . To first order in scalar

perturbations, components of energy transfer terms in (4.57) and (4.58) reads

$$\begin{aligned}
\delta Q_0^{(\alpha)} &= \Gamma_\sigma^{(\alpha)} [\delta \rho_\sigma + \rho_\sigma \Phi], \\
\delta Y_0^{(\alpha)} &= -\frac{\langle \sigma v \rangle^{(\alpha)}}{m_\chi} (2\rho_\chi \delta \rho_\chi - 2\rho_{\chi,eq} \delta \rho_{\chi,eq} + [\rho_\chi^2 - \rho_{\chi,eq}^2] \Phi), \\
\delta Q_j^{(\alpha)} &= -\Gamma_\sigma^{(\alpha)} \rho_\sigma \partial_j v_{(\sigma)}, \\
\delta Y_j^{(\alpha)} &= \frac{\langle \sigma v \rangle^{(\alpha)}}{m_\chi} [\rho_\chi^2 - \rho_{\chi,eq}^2] \partial_j v_{(\chi)},
\end{aligned} \tag{4.62}$$

where we used the fact that  $\delta u_\alpha^0 = -\Phi$ . Finally, we can obtain evolution equations for the density and velocity perturbations using perturbed stress-energy conservation equation (4.55) with (4.62), setting  $\Psi = \Phi$  in the absence of anisotropic stress. For temporal components we have,

$$\dot{\delta}_\alpha + 3H(c_{s,\alpha}^2 - w_\alpha) \delta_\alpha + (1 + w_\alpha) \left( \frac{\theta_\alpha}{a} - 3\dot{\Phi} \right) = \mathcal{S}_\delta(\delta_\alpha, \delta_\sigma, \delta_\chi, \delta_{\chi,eq}, \Phi),$$

where the source term on the RHS is given by

$$\mathcal{S}_\delta \equiv -\Gamma_\sigma^{(\alpha)} \frac{\rho_\sigma}{\rho_\alpha} [\delta_\sigma - \delta_\alpha + \Phi] + \frac{\langle \sigma v \rangle^{(\alpha)}}{m_\chi \rho_\alpha} (\rho_\chi^2 [2\delta_\chi - \delta_\alpha + \Phi] - \rho_{\chi,eq}^2 [2\delta_{\chi,eq} - \delta_\alpha + \Phi]).$$

Similarly, for spatial components

$$\dot{\theta}_\alpha + H\theta_\alpha + \frac{c_{s,\alpha}^2}{1 + w_\alpha} \frac{\nabla^2 \delta_\alpha}{a} - 3Hw_\alpha \theta_\alpha + \frac{\nabla^2 \Phi}{a} = \mathcal{S}_\theta(\theta_\alpha, \theta_\sigma, \theta_\chi),$$

where

$$\mathcal{S}_\theta \equiv -\Gamma_\sigma^{(\alpha)} \frac{\rho_\sigma}{\rho_\alpha} \left[ \frac{\theta_\sigma}{1 + w_\alpha} - \theta_\alpha \right] + \frac{\langle \sigma v \rangle^{(\alpha)}}{m_\chi \rho_\alpha} [\rho_\chi^2 - \rho_{\chi,eq}^2] \left( \frac{\theta_\chi}{1 + w_\alpha} - \theta_\alpha \right). \tag{4.63}$$

In deriving these equations we have defined  $\delta_\alpha \equiv \delta \rho_\alpha / \rho_\alpha$ ,  $\theta_\alpha \equiv a^{-1} \nabla^2 v_\alpha$  and made use of the background fluid equations (4.59).

## 4.B Adiabatic Initial Conditions

Before we start our discussion on adiabatic initial conditions, we would like to briefly review isocurvature perturbations and point out the non-existence of isocurvature modes in our reheating model after the decay of modulus.

On super-horizon scales, one can define a gauge invariant curvature perturbation for each species  $\alpha$  of the universe, which is conserved in the adiabatic limit when the Hubble expansion is dominated by a single species [34]

$$\zeta_\alpha = -\Psi - H \frac{\delta\rho_\alpha}{\dot{\rho}_\alpha}, \quad (4.64)$$

from which one can find the total curvature perturbation as a weighted sum of  $\zeta_\alpha$ ;

$$\zeta = \frac{\sum_\alpha (\rho_\alpha + p_\alpha) \zeta_\alpha}{\sum_\alpha (\rho_\alpha + p_\alpha)}. \quad (4.65)$$

The definition of isocurvature perturbation between two species is given by

$$S_{\alpha\beta} = 3(\zeta_\alpha - \zeta_\beta). \quad (4.66)$$

During inflation, in the model we are considering, the mass of the modulus at the high energy minima satisfies,

$$m_\sigma^2 \lesssim H_{\text{inf}}^2, \quad (4.67)$$

with an average amplitude of long wavelength fluctuations [210];

$$\delta\sigma \sim H_{\text{inf}}/2\pi. \quad (4.68)$$

The existence of such a mode can lead to isocurvature perturbations: while radiation and matter created from inflationary reheating carries the inflaton's fluctuation  $\zeta_{inf}$ , those produced from the moduli decay will inherit  $\delta\sigma$ . However, if the modulus dominates the energy density of the universe, all existing isocurvature modes will be

washed out as shown in [193] recently. Therefore, consistent with CMB anisotropy probes, we will consider adiabatic perturbations in our reheating model. We will consider the issue of adiabatic modes in the presence of moduli decay and DM annihilations in some detail below.

In the case of energy transfer between the constituents of the universe, it has been showed that perturbation equations allow for an adiabatic solution in the long wavelength limit with

$$\frac{\delta\rho_\alpha}{\dot{\rho}_\alpha} = \frac{\delta\rho_\beta}{\dot{\rho}_\beta}, \quad (4.69)$$

if the total intrinsic non-adiabatic energy transfer perturbation of each individual species  $\delta Q_T^{(\alpha)} = \delta Q_0^{(\alpha)} + \delta Y_0^{(\alpha)}$  vanishes [211]. For the reheating model we consider, these are given by

$$\delta Q_T^{(\sigma)} = 0, \quad (4.70)$$

$$\delta Q_T^{(\chi)} = -B_\chi \frac{\Gamma_\sigma}{3H} \dot{\rho}_\sigma S_{\sigma\chi}, \quad (4.71)$$

$$\delta Q_T^{(r)} = -(1 - B_\chi) \frac{\Gamma_\sigma}{3H} \dot{\rho}_\sigma S_{\sigma r} - \frac{2\langle\sigma v\rangle^{(r)}}{3m_\chi H} \rho_\chi \dot{\rho}_\chi S_{\chi r}, \quad (4.72)$$

where again we set  $\rho_{\chi,eq} = 0$  in the era we consider the fluid perturbation equations. Therefore, from (4.70)-(4.72), we see that an adiabatic mode with  $\zeta = constant$ ,  $\Psi = constant$  and  $S_{\alpha\beta} = 0$  [211] exist on large-scales where we ignored the decaying mode of gravitational potential  $\Psi$ .

## 4.C Solution for Radiation Density Perturbation During Scalar Domination

We are interested in finding the solution for the density perturbation during scalar domination. The equation of motion derived in the text is

$$\delta_r'' + \left(2A - \frac{1}{2}\right) \delta_r' + \left(A^2 - \frac{A}{2} + \frac{k^2}{3H_0^2} e^N\right) \delta_r = S(N), \quad (4.73)$$

where the source term is given by

$$S(N) \equiv - \left(A^2 - \frac{A}{2}\right) \Phi_0 - \left(\frac{\alpha}{2} (2A + 1) + \frac{2}{3} (A + 2)\right) \frac{k^2}{H_0^2} e^N \Phi_0. \quad (4.74)$$

The homogeneous solution is

$$\delta_r^{(h)} = c_1 e^{-AN} \sin\left(\frac{2k}{\sqrt{3}H_0} e^{\frac{N}{2}}\right) + c_2 e^{-AN} \cos\left(\frac{2k}{\sqrt{3}H_0} e^{\frac{N}{2}}\right) \quad (4.75)$$

From this we can construct the Green's function

$$\begin{aligned} G(N, \tilde{N}) &= \frac{s_1(N)s_2(\tilde{N}) - s_1(\tilde{N})s_2(N)}{s_1'(\tilde{N})s_2(\tilde{N}) - s_1(\tilde{N})s_2'(\tilde{N})} \\ &= \frac{\sqrt{3}H_0}{k} e^{(A-\frac{1}{2})\tilde{N}-AN} \sin\left[\frac{2k}{\sqrt{3}H_0} \left(e^{\frac{N}{2}} - e^{\frac{\tilde{N}}{2}}\right)\right] \end{aligned} \quad (4.76)$$

and so the full solution is

$$\delta_r = \delta_r^{(h)} + \int_0^N G(N, \tilde{N}) S(\tilde{N}) d\tilde{N}, \quad (4.77)$$

The integral gives a negligible contribution for super-Hubble modes initially, and so using the initial conditions  $\delta_r(N=0) = \delta_r^{(0)} = -\Phi_0$  and  $\delta_r'(N=0) = 0$  for  $k < aH$

we find  $c_1 = \sqrt{3}AH_0\delta_r^{(0)}/k$  and  $c_2 = (1 - 2A)\delta_r^{(0)}$ . The full solution is then

$$\delta_r = c_1 e^{-AN} \sin\left(\frac{2k}{\sqrt{3}H_0} e^{\frac{N}{2}}\right) + c_2 e^{-AN} \cos\left(\frac{2k}{\sqrt{3}H_0} e^{\frac{N}{2}}\right) + \delta_r^{(p)}, \quad (4.78)$$

where the particular solution is given by

$$\begin{aligned} \delta_r^{(p)} &= \int_0^N G(N, \tilde{N}) S(\tilde{N}) d\tilde{N}, \\ &= \frac{\sqrt{3}H_0}{k} e^{-AN} \Phi_0 \int_0^N e^{(A-\frac{1}{2})\tilde{N}} \sin\left[\frac{2k}{\sqrt{3}H_0} \left(e^{\frac{N}{2}} - e^{\frac{\tilde{N}}{2}}\right)\right] \left(\beta_1 - \beta_2 \frac{k^2}{H_0^2} e^{\tilde{N}}\right) d\tilde{N}, \end{aligned} \quad (4.79)$$

and we have defined

$$\begin{aligned} \beta_1 &= \frac{A}{2} - A^2, \\ \beta_2 &= \left(\frac{1}{2}\alpha(2A+1) + \frac{2}{3}(A+2)\right). \end{aligned} \quad (4.80)$$

Let  $\omega \equiv \frac{2}{\sqrt{3}H_0}$  and then (4.80) becomes

$$\begin{aligned} \delta_r^{(p)} &= -\frac{\sqrt{3}H_0}{k} e^{-AN} \Phi_0 \int_0^N e^{(A-\frac{1}{2})\tilde{N}} \sin\left[\omega k \left(e^{\frac{N}{2}} - e^{\frac{\tilde{N}}{2}}\right)\right] \left(\beta_1 - \beta_2 \frac{k^2}{H_0^2} e^{\tilde{N}}\right) d\tilde{N}, \\ &= \frac{\sqrt{3}H_0}{k} e^{-AN} \cos\left(\omega k e^{\frac{N}{2}}\right) \Phi_0 \int_0^N e^{(A-\frac{1}{2})\tilde{N}} \sin\left(\omega k e^{\frac{\tilde{N}}{2}}\right) \left(\beta_1 - \beta_2 \frac{k^2}{H_0^2} e^{\tilde{N}}\right) d\tilde{N} \\ &\quad - \frac{\sqrt{3}H_0}{k} e^{-AN} \sin\left(\omega k e^{\frac{N}{2}}\right) \Phi_0 \int_0^N e^{(A-\frac{1}{2})\tilde{N}} \cos\left(\omega k e^{\frac{\tilde{N}}{2}}\right) \left(\beta_1 - \beta_2 \frac{k^2}{H_0^2} e^{\tilde{N}}\right) d\tilde{N}, \end{aligned}$$

We need to solve the integrals

$$I_1 = \int_0^N e^{a\tilde{N}} \sin\left(b e^{\frac{\tilde{N}}{2}}\right) d\tilde{N} \quad (4.81)$$

$$I_2 = \int_0^N e^{a\tilde{N}} \cos\left(b e^{\frac{\tilde{N}}{2}}\right) d\tilde{N} \quad (4.82)$$

$$(4.83)$$



consider the change of variables,

$$x = be^{\frac{\tilde{N}}{2}}, \quad (4.84)$$

$$dx = \frac{b}{2}e^{\frac{\tilde{N}}{2}}d\tilde{N} \longrightarrow d\tilde{N} = \frac{2dx}{x} \quad (4.85)$$

we then have

$$I_1 = \int_{x(0)}^{x(N)} \left(\frac{x}{b}\right)^{2a} \sin x \left(\frac{2dx}{x}\right) = c \int_{x(0)}^{x(N)} x^m \sin x dx, \quad (4.86)$$

$$I_2 = \int_{x(0)}^{x(N)} \left(\frac{x}{b}\right)^{2a} \cos x \left(\frac{2dx}{x}\right) = c \int_{x(0)}^{x(N)} x^m \cos x dx, \quad (4.87)$$

where  $c \equiv 2b^{-2a}$  and  $m \equiv 2a - 1$ . We then have

$$\int x^m \sin x dx = -\frac{i^{m+1}}{2} [\Gamma(m+1, -ix) - (-1)^m \Gamma(m+1, ix)] \quad (4.88)$$

$$\int x^m \cos x dx = -\frac{i^{m+1}}{2} [\Gamma(m+1, -ix) + (-1)^m \Gamma(m+1, ix)] \quad (4.89)$$

where we must have  $m > 0$ . It is also useful to note the asymptotic form as  $x \rightarrow \infty$

$$\Gamma(m+1, \pm ix) = e^{\mp ix} x^m (\pm i)^m \left(1 - \frac{\pm im}{x} + \mathcal{O}\left(\frac{1}{x^2}\right)\right) \quad (4.90)$$

With these solutions we can now solve for the complete solution in (4.78), and this can then be used to solve for the velocity perturbations. This solution for different values of the parameters appears in Figure 4.1.

# Chapter 5

## Alternative sources of Gravitational Waves and the Scale of Inflation

### 5.1 Introduction

A positive detection of B-mode polarization in the Cosmic Microwave Background (CMB) – if identified as being of primordial origin – has been argued to provide *smoking gun* evidence for the existence of inflation [212]. It has been further argued that the signal would provide us with the scale at which inflation took place. Given the current and projected sensitivity of polarization experiments [212], a positive detection of primordial B-modes would then imply inflation occurred near the GUT scale, or slightly below. Indeed, if the results from BICEP2 [133] are confirmed, this would be the first direct evidence for physics beyond the Standard Model at a scale nearly a billion times that probed at the Large Hadron Collider (LHC).

In this paper we revisit the question; *Does a detection of primordial B-modes necessarily provide us with the scale of inflation?* In [213] it was argued that the answer is no. In that paper, the authors considered additional sources of gravity waves

arising from non-adiabaticity and particle production during inflation and claimed that in some cases this source of B-modes could exceed those coming from the quantum fluctuations of the quasi-de Sitter background. Related ideas have appeared in [214–225], although the primary focus of these papers was different. In this paper we will review both approaches and explicitly demonstrate their relation for the case of on-shell particle production. In many of these works it was also pointed out that the same effects leading to a significant level of gravity waves would also lead to a substantial level of equilateral type non-Gaussianity (NG) – a prediction that was important for Planck. Utilizing the current Planck data [45] we can now revisit these models utilizing the constraints on the level of equilateral type NG  $f_{\text{NL}}^{\text{equil}} < -16 \pm 70$ . Using this constraint, and demanding successful inflation and self consistent model building, in this paper we examine these models to see if particle production can lead to a competitive source for primordial B-modes.

We first consider the case of an inflaton directly coupled to spectator fields. This captures models with on-shell particle production such as Trapped Inflation and Moduli Trapping [226–228], and we also consider production of pseudo scalar and gauge fields during inflation [222]. In all of these models we find that the direct coupling typically leads to a high level of NG, rendering these alternatives for generating primordial B-modes irrelevant. We next consider the production of spectator fields with gravitational coupling to the inflaton sector [214, 219]. Because of the suppressed couplings, in some cases these models can lead to a lower level of NG and an alternative B-mode source is possible. However, additional constraints from back-reaction and isocurvature perturbations severely restrict the parameter space. We identify the most promising case as gauge field production resulting from a tachyonic and time dependent mass term resulting from the interaction of the gauge field with an additional spectator scalar field (not the inflaton). Given the elaborate nature of this model, after constraining the parameter space we turn to the question of UV completing the model. We construct an inflationary sector utilizing Axion Monodromy,

and then we realize the additional spectator fields needed within the framework of  $O3/O7$  orientifold compactifications of Type IIB string theory. We find that a UV embedding can be realized in the weakly coupled string theory if the compactification volume is taken parametrically larger than the Planck scale and if the axion decay constant is sub-Planckian. Our embedding also demonstrates that dangerous sinusoidal corrections to the gauge field production models can be suppressed through the compactification geometry.

The remainder of the paper is as follows. In the next section we review both the classical and quantum production of gravity waves during inflation. This section is primarily to establish notation and to address a few subtle points in the literature regarding the production of gravity waves from on-shell particle production. In Section 5.3, we consider the case of particle production of fields directly coupled to the inflationary sector. In Section 5.4, we consider the gravitationally coupled case. Unlike the direct coupling case, we find that some of these models do result in B-modes although the parameter space is severely restricted<sup>1</sup>. In the remainder of the paper, we consider the UV completion of these models. First, in Section 5.5 we review the relevant details of Type IIB orientifold compactifications and their role in Inflationary model building. Then in Section 5.6 we present an explicit model including the particle production and establish the model building constraints. In the final section we conclude. In appendix A we list a number of concerns for string model building with moduli stabilization and their possible resolutions.

---

<sup>1</sup>For a recent paper that considered constraints on these models from isocurvature perturbations see [229].

## 5.2 Gravity Waves from Inflation and Particle Production

In this section we review the general formalism for establishing the amount of gravity waves produced during inflation from both quantum fluctuations of the metric and classical sources from particle production events during inflation. For readers familiar with these types of calculations this section may be skipped, however it does serve to set our notation and conventions.

Gravity waves produced during inflation can perturb the homogeneous and isotropic background metric. These tensor fluctuations are described by the metric

$$ds^2 = a(\tau)^2[-d\tau^2 + (\delta_{ij} + h_{ij})dx^i dx^j], \quad (5.1)$$

where Latin indices denote spatial co-ordinates<sup>2</sup>,  $h_{ij}$  is the transverse ( $\partial_i h_{ij} = 0$ ) and traceless ( $h_{ii} = 0$ ) metric perturbation and we work in conformal time where the scale factor is  $a \simeq -1/(H\tau)$  for a quasi-dS background.

The mode equation for gravity waves in the cosmological background (working in Fourier space) is

$$\bar{h}_{ij}'' + \left(k^2 - \frac{a''}{a}\right) \bar{h}_{ij} = \frac{2}{M_{\text{pl}}^2} a T_{ij}^{TT}, \quad (5.2)$$

where we introduced canonical modes  $\bar{h}_{ij} = a(\tau)h_{ij}$  and  $T_{lm}^{TT}$  is the transverse and traceless components of the stress energy tensor for any sources which are present. The transverse, traceless components of the stress tensor can be obtained by introducing the projector  $\Pi_{ij}^{lm} = P_i^l P_j^m - \frac{1}{2} P_{ij} P^{lm}$  where  $P_{ij} = \delta_{ij} - k_i k_j / k^2$  so that  $T_{ij}^{TT} = \Pi_{ij}^{lm} T_{lm}$  (cf. [230]).

---

<sup>2</sup>We will follow metric signature  $(-, +, +, +)$  and work with the reduced Planck mass  $M_{\text{pl}} = 2.44 \times 10^{18}$  GeV.

We can formally solve (5.2) to find

$$\bar{h}_{ij}(\mathbf{k}, \tau) = \frac{2}{M_{\text{pl}}^2} \int d\tau' G_k(\tau, \tau') a(\tau') T_{ij}^{TT}(\mathbf{k}, \tau'), \quad (5.3)$$

where  $G_k(\tau, \tau')$  is the Green function satisfying the source free version of (5.2) with appropriate boundary conditions. For the quasi-dS background we find

$$G_k(\tau, \tau') = \frac{k(\tau' - \tau) \cos(k(\tau' - \tau)) - (1 + k^2\tau'\tau) \sin(k(\tau' - \tau))}{k^3\tau\tau'} \Theta(\tau - \tau'), \quad (5.4)$$

where  $\Theta(\tau - \tau') = 0$  for  $\tau < \tau'$  signaling that the source only produces gravity waves after its creation. This expression along with a source in (5.3) then allows us to find the resulting gravitational radiation.

### 5.2.1 Quantum Vacuum Fluctuations and Gravity Waves

For inflationary vacuum fluctuations and in the absence of sources ( $T_{lm} = 0$ ) equation (5.2) can be easily solved (see e.g. [31] or [231]) and one finds that the inflationary background generates a nearly scale invariant spectrum of gravitation waves. We can relate the correlation function to the tensor power spectrum for each helicity as,

$$\frac{1}{a^2} \langle \bar{h}_{ij}^s(\mathbf{k}) \bar{h}_{ij}^{s'}(\mathbf{k}') \rangle = (2\pi)^3 \delta(\mathbf{k} + \mathbf{k}') \delta^{ss'} \mathcal{P}_h, \quad (5.5)$$

where  $s$  refers to the polarization. The dimensionless tensor power-spectrum resulting from quantum vacuum fluctuations of the graviton is then

$$\Delta_t^2(k) = 2 \cdot \frac{k^3}{2\pi^2} \cdot \mathcal{P}_h = \frac{8}{M_{\text{pl}}^2} \left( \frac{H}{2\pi} \right)^2 \quad (5.6)$$

evaluated at  $k = aH$  and the tilt of the spectrum is  $n_t = d \ln \mathcal{P}_h / d \ln k$ . In the absence of any other primordial sources of gravity waves, a measurement of the tensor-to-scalar ratio (along with existing measurements of the scalar power spectrum) then allow us

to determine the scale of inflation  $H_I$  through (5.6). In terms of the scalar power spectrum  $\Delta_s^2$  we can then define the tensor to scalar ratio

$$r \equiv \frac{\Delta_t^2}{\Delta_s^2}. \quad (5.7)$$

where near-term and future experiments can be optimistically expected to probe as low as  $r \simeq 10^{-3}$  [212]. Using the COBE normalization  $\Delta_s^2 = 2.2 \times 10^{-9}$  this can be re-expressed as a determination of the scale of inflation (cf. [231])

$$H_I \simeq 3 \times 10^{-5} \left( \frac{r}{0.1} \right)^{1/2} M_{\text{pl}}. \quad (5.8)$$

Thus, given an observation of  $r$  and knowledge that the only source of gravity waves resulted from primordial vacuum fluctuations, we can determine the scale of inflation  $H_I \sim V^{1/2}/M_{\text{pl}}$ .

## 5.2.2 Gravity Waves from Particle Production during Inflation

We will first consider gravity wave sources from scalar field production during inflation and later generalize this to vector fields. To calculate the effect of the produced particles on gravity wave production we note that the contribution of the particles to the spatial part of the stress tensor will be of the form  $T_{ij} = \partial_i \chi \partial_j \chi + \delta_{ij}(\dots)$ . This implies that in Fourier space the transverse, traceless source is the convolution [232]

$$T_{ij}^{TT}(\mathbf{k}, \tau) = \Pi_{ij}^{lm}(\mathbf{k}) \int \frac{d^3 \mathbf{p}}{(2\pi)^{3/2}} p_l p_m \chi(\mathbf{p}, \tau) \chi(\mathbf{k} - \mathbf{p}, \tau). \quad (5.9)$$

Using this result, along with (5.3) we can construct the two point, equal time correlator

$$\begin{aligned}
\langle \bar{h}_{ij} \bar{h}_{ij}^* \rangle &= \frac{4}{M_{\text{pl}}^4} \int d\tau' a(\tau') G_k(\tau, \tau') \int d\tau'' a(\tau'') G_{k'}(\tau, \tau'') \langle T_{ij}^{TT}(\mathbf{k}, \tau') T_{ij}^{TT*}(\mathbf{k}', \tau'') \rangle \\
&= \frac{4}{M_{\text{pl}}^4} \int d\tau' \frac{G_k(\tau, \tau')}{a(\tau')} \int d\tau'' \frac{G_{k'}(\tau, \tau'')}{a(\tau'')} \Pi_{ij}^{lm}(\mathbf{k}) \Pi_{ij}^{no}(\mathbf{k}') \\
&\times \int \frac{d^3\mathbf{p}}{(2\pi)^3} \frac{d^3\mathbf{p}'}{(2\pi)^3} p_l p_m p'_n p'_o \langle \hat{\chi}(\mathbf{p}, \tau') \hat{\chi}(\mathbf{k} - \mathbf{p}, \tau') \hat{\chi}^*(\mathbf{p}', \tau'') \hat{\chi}^*(\mathbf{k}' - \mathbf{p}', \tau'') \rangle.
\end{aligned} \tag{5.10}$$

where we have introduced the canonical field  $\hat{\chi} = a(\tau)\chi$ .

As discussed in [232] if we now assume that the fields are well approximated by statistically homogeneous, random Gaussian fields then the four-point function can be written in terms of two-point functions by Wick's theorem<sup>3</sup>. Using that

$$\langle \hat{\chi}(\mathbf{p}, \tau') \hat{\chi}^*(\mathbf{p}', \tau'') \rangle = f(|\mathbf{p}|, \tau', \tau'') \delta(\mathbf{p} - \mathbf{p}'), \tag{5.11}$$

for statistically homogeneous and isotropic fields and keeping only the connected pieces of the correlator we have

$$\begin{aligned}
\langle \hat{\chi}(\mathbf{p}, \tau') \hat{\chi}(\mathbf{k} - \mathbf{p}, \tau') \hat{\chi}^*(\mathbf{p}', \tau'') \hat{\chi}^*(\mathbf{k}' - \mathbf{p}', \tau'') \rangle_c = \\
\delta(\mathbf{k} - \mathbf{k}') f(p, \tau', \tau'') f(k - p, \tau', \tau'') \left[ \delta(\mathbf{p}' - \mathbf{p}) + \delta(\mathbf{p}' - \mathbf{k} + \mathbf{p}) \right]
\end{aligned}$$

Using this result and the property of the projectors that  $\Pi_{ij}^{lm} \Pi_{ij}^{no} p_l p_m p_n p_o = \Pi^{lmno} p_l p_m p_n p_o = p^4 \sin^4(\theta)/2$  where  $\theta$  is the angle between  $\mathbf{k}$  and  $\mathbf{p}$ , we can perform one of the momentum integrals in (5.10) and we find

---

<sup>3</sup>The authors of [232] pointed out that this is a good approximation at both the beginning and end of inflationary preheating and is in good agreement with lattice simulations. Here we consider these events during inflation and will work within the same approximation. We will see that any strong coupling of the spectator field  $\chi$  will tend to generate a large level of non-Gaussianity making this approximation justified given existing CMB constraints.



$$\begin{aligned} \langle \bar{h}_{ij}(\mathbf{k}, \tau) \bar{h}_{ij}^*(\mathbf{k}', \tau) \rangle &= \frac{2\delta(\mathbf{k} + \mathbf{k}')}{M_{\text{pl}}^4} \int \frac{d\tau'}{a^2(\tau')} G_k(\tau, \tau') \int \frac{d\tau''}{a^2(\tau'')} G_{k'}(\tau, \tau'') \\ &\times \int \frac{d^3\mathbf{p}}{(2\pi)^3} |\mathbf{p}|^4 \sin^4(\theta) f(|\mathbf{p}|, \tau', \tau'') f(|\mathbf{k} - \mathbf{p}|, \tau', \tau'') \end{aligned} \quad (5.12)$$

It remains to determine the functions in the two-point correlator (5.11). We are interested in cases where quanta of the  $\hat{\chi}$  field become excited due to the interaction with the inflaton and particle production. To calculate this contribution to (5.11) we will follow the treatment in [25].

The mode equation for the canonical normalized particles  $\chi$  have generically the following form,

$$\chi_k'' + \omega_k^2(\tau)\chi_k = 0, \quad (5.13)$$

where we make the change of notation  $\hat{\chi} \rightarrow \chi$ . The time dependent frequency is given by

$$\omega_k^2(\tau) = k^2 + a^2 m_{\text{eff}}^2(\tau) - a^2 \Delta. \quad (5.14)$$

where  $\Delta \sim a''/a$  is typically negligible compared to the effective time-dependent mass  $m_{\text{eff}}$ . The WKB solution to this equation

$$\chi_k(\tau) = \frac{1}{\sqrt{2\omega_k}} \left( \alpha_k(\tau) e^{-i \int^\tau \omega_k(\tilde{\tau}) d\tilde{\tau}} + \beta_k(\tau) e^{i \int^\tau \omega_k(\tilde{\tau}) d\tilde{\tau}} \right) \quad (5.15)$$

is valid as long as  $\omega' < \omega^2$  and all higher order adiabatic invariants remain small. The condition that initially there are no quanta of the field present requires  $\alpha = 1$  and  $\beta = 0$ , i.e. only positive frequency modes are present. When the adiabatic conditions fails, particle production results, and the Bogolyubov coefficients above give the mode mixing that occurs due to the time dependence of the system. The creation and annihilation operators after production can be expanded in terms of the

initial creation  $\hat{a}_k^\dagger$  and annihilation operators  $\hat{a}_k$  of the field as

$$\hat{b}_k(\tau) = \alpha_k(\tau)\hat{a}_k + \beta_k^*(\tau)\hat{a}_{-k}^\dagger, \quad \hat{b}_k^\dagger(\tau) = \alpha_k(\tau)\hat{a}_k + \beta_k^*(\tau)\hat{a}_{-k}^\dagger, \quad (5.16)$$

where although  $\hat{a}_k$  annihilates the vacuum initially,  $\hat{b}_k$  does not, and if the system returns to adiabatic evolution the number density of particles produced is  $n_k \sim |\beta_k|^2$ . Proper renormalization requires that one normal orders the correlators with respect to the  $\hat{b}_k$  basis and then uses that  $\hat{a}_k$  annihilates the vacuum to find the surviving terms (see e.g. [214, 220]). Expanding the field and performing the normal ordering we find that the unknown function in (5.11) is

$$f(p, \tau', \tau'') = \frac{1}{2\sqrt{\omega_p(\tau')\omega_p(\tau'')}} \left\{ \beta_p(\tau')\beta_p^*(\tau'')e^{-i\int_{\tau'}^{\tau''}\omega_k(\tilde{\tau})d\tilde{\tau}} + \beta_p^*(\tau')\beta_p(\tau'')e^{i\int_{\tau'}^{\tau''}\omega_k(\tilde{\tau})d\tilde{\tau}} \right. \\ \left. + \alpha_p(\tau')\beta_p^*(\tau'')e^{-i\int^{\tau'}\omega_k(\tilde{\tau})d\tilde{\tau}-i\int^{\tau''}\omega_k(\tilde{\tau})d\tilde{\tau}} + c.c. (\tau' \rightarrow \tau'') \right\}, \quad (5.17)$$

where we just switched to notation  $|\mathbf{p}| \equiv p$ . We then use this expression in (5.12) to find the amount of gravitational radiation. However, as shown in [214] the arguments of the exponentials above lead to rapidly oscillating phases and don't give a significant contribution to the final correlator (5.12). Neglecting the phases, using the result above in (5.12) and keeping only the leading terms we find

$$\langle \bar{h}_{ij} \bar{h}_{ij}^* \rangle = \frac{2\delta(\mathbf{k} + \mathbf{k}')}{M_{\text{pl}}^4} \int \frac{d\tau'}{a^2(\tau')} G_k(\tau, \tau') \int \frac{d\tau''}{a^2(\tau'')} G_{k'}(\tau, \tau'') \\ \times \int \frac{d^3\mathbf{p}}{(2\pi)^3} p^4 \sin^4(\theta) \left( \frac{|\beta_p|^2(|\alpha_p|^2 + |\beta_p|^2)}{2\omega_p(\tau')\omega_p(\tau'')} + \dots \right), \quad (5.18)$$

where the missing terms are sub-leading and we refer to [214] for a more detailed discussion. The result (5.18) will allow us in the remainder of the paper to connect particle production and non-adiabaticity during inflation with the generation of grav-

itational waves. Given the Green function (5.4), we simply calculate the Bogolyubov coefficients for a given model and this gives us the associated gravity waves produced via (5.18). Given this contribution to the tensor power spectrum we can then compare to the vacuum source in (5.6) to determine if particle production can lead to a larger signal.

### 5.3 Particle Production Mechanisms with Direct Inflaton Coupling

Any contribution to the production of gravitational waves during inflation, if competitive to vacuum fluctuations, could obstruct the use of observations to determine both the scale of inflation and whether the waves are of classical or quantum mechanical origin – with quasi-dS fluctuations exemplifying the latter. In this section we consider the gravitational waves resulting from the production of fields directly coupled to the inflaton, and establish constraints for whether such effects can be competitive.

Inflation models in best agreement with existing data are necessarily sensitive to high energy (UV) physics. Thus, consistent model building requires these models to be embedded in a UV complete theory, with string theories currently providing the most developed approach. String theories come with additional fields, strings and branes, and the importance of these degrees of freedom on the inflation process has been demonstrated in a number of contexts (see [231] for a review). Among the anticipated effects, if these states couple to the inflaton during inflation this can lead to particle production, which in some cases may be expected to generate a large background of gravitational waves.

Following [233] (see also [213]) our starting point is the action

$$S = \int d^4x \sqrt{-g} \left\{ \frac{1}{2} M_{\text{pl}}^2 R - \frac{1}{2} (\partial\phi)^2 - V(\phi) \right\} + S_p + S_s + S_{\text{int}}, \quad (5.19)$$

where for particle sources we have

$$S_p = - \sum_p \int d^4x \int d\tau \delta^{(4)}(x^\mu - x_p^\mu(\tau)) \theta(t - t_p) m(\phi) \sqrt{-g_{\mu\nu}(\tau) \frac{dx^\mu}{d\tau} \frac{dx^\nu}{d\tau}}, \quad (5.20)$$

and the mass  $m(\phi)$  of the particle depends on the inflaton (and so co-ordinate time  $t$ ),  $t_p$  is the time at which a particle is created, and the argument of the square root is given by the world line trajectory of the particle and so depends on the proper time  $\tau$ . Similarly for string sources one has

$$S_s = - \sum_s \int d^4x \int d^2\sigma \delta^{(4)}(x^\mu - x_s^\mu(\sigma)) \theta(t - t_s) T(\phi) \sqrt{-\det\left(g_{\mu\nu}(\sigma) \frac{dx^\mu}{d\sigma^\alpha} \frac{dx^\nu}{d\sigma^\beta}\right)} \quad (5.21)$$

where the string tension  $T(\phi)$  can depend on the inflaton and  $\sigma = (\tau, \sigma_1)$  are the induced coordinates on the string world volume and  $t_s$  is the time of string production.  $S_{int}$  accounts for any interactions between the inflationary sector and the particles and strings.

In the rest of the section, we go through several examples of how couplings in (5.20) can lead to particle and string production during inflation. Our examples will cover the cases of a scalar and pseudo-scalar inflaton, producing scalar or vector particles. We will then go on to describe gravity wave production in these models, and finally constraints from non-Gaussianity and back-reaction.

### 5.3.1 Scalar Production During Inflation

The time dependent mass and tension appearing in (5.20) and (5.21) can lead to interesting cosmological implications. In models of moduli trapping [226, 227, 234, 235] the particle production resulting from the scalar's time dependence was shown to lead to dynamical stabilization of moduli (massless scalars) that would otherwise have little or no potential and remain unstabilized. When identified as the inflaton, it was shown in [228, 236] that when accounting for the effects of particle production

one can obtain slow-roll inflation from potentials that would otherwise not satisfy the slow-roll conditions. Taking the scalar in (5.20) and (5.21) to be the inflaton we can capture the dynamics of this production through an effective interaction

$$\mathcal{L}_{\text{int}} = g^2(\phi - \phi_0)^2\chi^2. \quad (5.22)$$

Here  $\phi$  is the inflaton and  $\chi$  the spectator field to be produced. Although this interaction is much simpler than what one might expect from (5.20) and (5.21), since we are treating  $\chi$  as a simple scalar, it was shown in [233] that this also provides an adequate description of string and brane production within the low-energy effective theory.

*How generic is such an interaction?* Interactions captured by (5.22) generically occur within the context of string theory and M-theory model building. Common examples include the presence of new light states (here represented as  $\chi$ ) as the size of a compact dimension or internal cycle (parametrized by  $\phi$ ) shrink and the symmetries of the theory become enhanced [227, 234] – i.e. there is an inverse string Higgs effect. Other examples include when D-branes become coincident, as in models of brane inflation, and new light states appear<sup>4</sup> [226], or near locations in field space associated with changes in topology [235]. In these and other cases the interaction is effectively captured by (5.22) where far from the location  $\phi = \phi_0$  the quanta of  $\chi$  can be quite heavy and so don't effect the dynamics. However, as the inflaton  $\phi$  approaches  $\phi_0$  quanta of the  $\chi$  field can become excited leading to on-shell<sup>5</sup> particle production<sup>6</sup>.

Given this motivation we are now interested in determining the amount of gravitational waves that could be generated during the creation process, while still allowing

---

<sup>4</sup>These new states correspond to open strings stretching between the branes becoming light.

<sup>5</sup>In this paper we will focus on on-shell production, whereas the interaction (5.22) can also lead to important off-shell (virtual) effects as discussed first in [237]. Which effect is dominant depends on whether the theory is in the strong or weak coupling regime as discussed in [226].

<sup>6</sup>This is analogous to Schwinger pair production in a strong electromagnetic field.

for successful inflation and being consistent with bound on non-Gaussianity. We first emphasize that scalar field waves do not produce an appreciable amount of gravitational radiation [232]. Instead, here the expectation of gravity waves comes from both the creation process and the existence of the particles following creation as they provide a classical source in (5.3). We emphasize that the created particles are inhomogeneously distributed, on-shell, and are not perturbations<sup>7</sup> [232]. Moreover, the creation process is non-perturbative and cannot be described within standard methods of linearized perturbation theory<sup>8</sup> [25].

Following the formalism reviewed in Section 2, the interaction (5.22) provides a time dependent mass in (5.14) where  $m_{\text{eff}}^2(\tau) = g^2(\phi - \phi_0)^2$ . As discussed there, particle production occurs when the adiabatic condition fails<sup>9</sup>, which in this case implies  $\omega'_k/\omega_k^2 \sim m'_{\text{eff}}/m_{\text{eff}}^2 \gtrsim \mathcal{O}(1)$ . As shown in e.g. [226] the production occurs on time scales small compared to the Hubble time so that gravitation effects are negligible and if we denote the time of production as  $\tau_0$  the Bogolyubov coefficients above for  $\tau > \tau_0$  are

$$\begin{aligned} |\alpha_k|^2 &= 1 + \exp\left(-\pi \frac{k^2}{m'_{\text{eff}}(\tau_0)}\right), \\ |\beta_k|^2 &= \exp\left(-\pi \frac{k^2}{m'_{\text{eff}}(\tau_0)}\right), \end{aligned} \tag{5.23}$$

where  $m'_{\text{eff}}(\tau_0) = g\bar{\phi}'_0$  is the time derivative of the effective mass evaluated at the moment of production and we set  $a(\tau = \tau_0) = 1$ . We also note that the coefficients respect the normalization  $|\alpha_k|^2 - |\beta_k|^2 = 1$  implying that the Bogolyubov transformation is canonical. The corresponding number density of produced particles is then

---

<sup>7</sup>This explains why it is consistent to use the linearized equation for the graviton in (5.3), whereas we will see that the sources will be quadratic in the created fields.

<sup>8</sup>It was for many of these reasons that within perturbation theory the production of gravitational waves would be negligible [223] (see also [232]).

<sup>9</sup>Within the effective theory, the adiabatic condition can fail either because the particles become massless or simply because the inflaton undergoes non-adiabatic evolution. In the latter case the yield of particles depends on the dynamics of the inflaton and the mass scale of the particles to be produced [238].

$n_\chi \sim \int d^3k n_k$  with  $n_k \sim |\beta_k|^2$  given by (5.23). The most interesting case will be when a number of the locations  $\phi = \phi_0^{(i)}$  occur, as this will lead to a continuous production of gravity waves whereas a single event will lead to an isolated (but perhaps interesting) signature [213].

The amount of gravitational radiation resulting from both single and multiple events has been examined taking two different approaches. In [220] the authors (CS) argued that gravity waves will result from both the production events themselves, as well as from the existence of  $\chi$  particles following production – both sources were found to yield a comparable amount of gravitational radiation. Whereas in [213], the authors (SSZ) performed estimates adapting the methods of Weinberg [239] to the time dependent case of interest here and found that the production event along with gravitational Bremsstrahlung from the inflaton could result in gravity waves. Here we will qualitatively argue that the two approaches yield similar results, but for the majority of our calculations we will primarily follow the approach of [220]. The key will be that in all instances – and independent of the computational method – we find that if particle production for fields coupled directly to the inflaton is to lead to an observable gravity wave signal it presents a tension with existing constraints from Planck on the level of equilateral non-Gaussianity.

To calculate the gravity waves generated from the presence of on-shell  $\chi$  particles following production we can use the result for the Bogolyubov coefficients (5.23) and Green function (5.4) in the correlator (5.18) and we find<sup>10</sup>

$$\langle h_{ij} h_{ij} \rangle = \frac{\delta(\mathbf{k} + \mathbf{k}')}{2\pi^5 k^3} \left( \frac{H}{M_{\text{pl}}} \right)^4 \left( \frac{n_\chi}{H^3} \right) F(k\tau_0) \quad (5.24)$$

with  $n_\chi \sim (m'_{\text{eff}})^{3/2} = (g\bar{\phi}')^{3/2}$  the number density of produced particles in real space

---

<sup>10</sup>This result agrees with the correlators in both the adiabatic and non-adiabatic cases studied in [220].

and

$$F(k\tau_0) \simeq \frac{[k\tau_0 \cos(k\tau_0) - \sin(k\tau_0)]^2}{|k\tau_0|^3} \times \log^2 \left( \frac{n_\chi^{1/3}}{H} \right) \simeq \mathcal{O}(10 - 100), \quad (5.25)$$

the first term results from the two copies of the Green function (5.4) in (5.18) and peaks around  $|k\tau_0| = 2.5$  after which it sharply drops off reflecting both the locality of the production as well as the fact that only gravity waves produced near the horizon have a chance of contributing significantly to the spectrum<sup>11</sup>. The second term in (5.25) is to be evaluated at the time of production and as we will see is typically at most  $\mathcal{O}(100)$ .

Using the definitions (5.5) and (5.6) the contribution to the tensor power spectrum from production is then

$$\Delta_t^2 = \Delta_{\text{vac}}^2 \left[ 1 + 4.8 \times 10^{-4} \left( \frac{n_\chi}{H^3} \right) F(k\tau_0) \left( \frac{H}{M_{\text{pl}}} \right)^2 \right], \quad (5.26)$$

where  $\Delta_{\text{vac}}^2 = 2H^2/(\pi^2 M_{\text{pl}}^2)$  is the standard vacuum contribution coming from (5.6).

Before proceeding, let us compare the result (5.24) (and so also (5.26)) with the estimates found in [213]. From (5.24) we find

$$h_{cs}^2 \sim h(k)^2 k^3 \sim \left( \frac{n_\chi}{H^3} \right) \left( \frac{H}{M_{\text{pl}}} \right)^4 \quad (5.27)$$

where  $h_{cs}$  is the amplitude in real space and  $H$  is the Hubble scale during inflation.

Now let us compare this estimate to the one in [213]. There it was found

$$h_{ssz}^2 \sim \frac{\rho_{\text{GW}}}{\rho_{\text{tot}}} \sim f \frac{H^3}{EM_{\text{pl}}^3}, \quad (5.28)$$

---

<sup>11</sup>Causality requires gravity wave production to occur on near or sub-Hubble scales and gravity waves produced on small length scales will undergo significant red-shifting reducing their effects on observable scales. Thus, production near the Hubble scale will provide the largest contribution to the tensor spectrum.



where  $\rho_{\text{GW}}/\rho_{\text{tot}}$  is the relative energy density in gravity waves,  $E$  is the characteristic energy, and  $f \sim En_\chi/\rho_{\text{tot}}$  is the fraction of waves resulting from the  $n_\chi$  density of particles. Here the frequency of produced waves was taken as  $\omega \sim H$  so no red-shifting occurred (as we also assumed in (5.27)) and plugging in  $f$  we find

$$h_{ssz}^2 \sim f \frac{H^3}{EM_{\text{pl}}^3} \sim \left( \frac{E n_\chi}{H^2 M_{\text{pl}}^2} \right) \left( \frac{H^3}{E M_{\text{pl}}^3} \right) \sim \left( \frac{n_\chi}{H^3} \right) \left( \frac{H}{M_{\text{pl}}} \right)^4 \sim h_{cs}^2, \quad (5.29)$$

and so we see the two approaches agree qualitatively. This result is easily understood – the production events are independent and so proportional to  $n_\chi$  per Hubble volume ( $H^3$ ) and the amplitude of each waves is proportional to  $H^2/M_{\text{pl}}^2$  as expected.

We would now like to see if the new contribution in (5.26) can be competitive with the vacuum contribution  $\Delta_{\text{vac}}^2$ . We define the difference as

$$\Delta P_t \equiv (\Delta_t^2 - \Delta_{\text{vac}}^2)/\Delta_{\text{vac}}^2 \quad (5.30)$$

so that ultimately we are interested in whether  $\Delta P_t \gg 1$  is feasible. Given (5.26) we can already see that a large gravity wave signal is difficult to obtain. In order that the produced particles  $n_\chi$  don't ruin inflation we must have at least  $\rho_\chi = m_\chi n_\chi \ll H^2 M_{\text{pl}}^2$ . Using this in (5.26) we find

$$\Delta P_t \simeq 10^{-2} \left( \frac{H}{M_{\text{pl}}} \right)^2 \left( \frac{n_\chi}{H^3} \right) \ll 10^{-2} \left( \frac{H}{m_\chi} \right), \quad (5.31)$$

where we used that  $F(k\tau_0) \lesssim \mathcal{O}(100)$  and we see that unless the produced scalars remain far lighter than the Hubble scale a competitive signal is simply not possible. This requires that the gravity waves are produced at the time the field is light ( $m_\chi \ll H$ ) and at the time particle production is occurring. But this implies that the gravity waves will actually be a scale-dependent feature in the spectrum, which is manifest from the  $k\tau_0$  dependence in (5.25). Instead we are interested in the continuous generation of gravity waves, which suggests that the multiple production case is

of more interest.

Requiring the inflaton to copiously and continuously produce particles, while also providing an adequate number of e-foldings of slow-roll inflation, requires a delicate approach to model building. However, in models of Trapped Inflation [228] it is precisely this type of balance (and accounting for the backreaction of produced particles) that permits slow-roll inflation in the presence of a steep inflationary potential. Denoting the spacing between the particle production events as  $\Delta \equiv \phi_{i+1} - \phi_i$ , the scalar power spectrum in this model takes the form [228]

$$\frac{k^3}{2\pi^2} P_\zeta^{\text{trap}} = \frac{g^{7/2} H \bar{\phi}'^{1/2}}{2\pi^2 \tilde{m} \Delta}, \quad (5.32)$$

where  $\tilde{m}^2 = \frac{7}{2} \frac{g^{5/2}}{\Delta (2\pi)^3} \bar{\phi}'^{3/2}$ .

In addition, the production events generate non-Gaussianity of the equilateral type, which was estimated in [228] to be

$$f_{\text{NL}}^{\text{equil}} \approx \frac{\tilde{m}^2}{H^2} = \frac{7}{2} \frac{g^{5/2}}{(2\pi)^3} \frac{\bar{\phi}'^{3/2}}{\Delta H^2}. \quad (5.33)$$

Using (5.32) and (5.33) we will be able to place constraints on the level of gravity waves resulting from particle production events.

As before the largest signal will come from gravity waves produced near the Hubble scale (more precisely near  $k\tau_0 = 2.5$ ) as these modes will suffer less red-shifting before freeze-out. In addition, as discussed in [228] the production events are independent and so we can simply add the contributions to the tensor spectrum as

$$\Delta P_t^{\text{tot}} = N_{\text{events}} \Delta P_t, \quad (5.34)$$

with  $\Delta P_t$  the contribution from a single event and the number of events within a Hubble time is roughly  $N_{\text{events}} = H^{-1}/\Delta t = \bar{\phi}'/(H\Delta)$ . Using (5.32) and (5.33) to

eliminate  $\bar{\phi}'$  and  $\Delta$  from the tensor spectrum given by (5.26) and (5.34) and we find

$$\Delta P_t \simeq 2.9 \times 10^{10} N_{\text{events}} g^3 |f_{\text{NL}}^{\text{equil}}|^{3/4} F(k\tau_0) \left( \frac{H}{M_{\text{pl}}^2} \right)^2. \quad (5.35)$$

Here,  $F(k\tau_0)$  is again given by (5.25) and considering the maximum value at  $|k\tau_0| \simeq 2.5$ , we can parametrize it as

$$F^{1/2}(k\tau_0) \simeq 4.5 + \frac{2}{3} \log \left[ \left( \frac{g}{0.01} \right) \left( \frac{|f_{\text{NL}}^{\text{equil}}|}{16} \right)^{1/4} \right], \quad (5.36)$$

where we have again used the constraints (5.32) and (5.33). As written, the level of gravity waves seems to depend sensitively on the model parameters, particularly the coupling  $g$ . However, again using the constraints and noting that the number of events in (5.35) can also be written as

$$N_{\text{events}} = 1.8 \times 10^{-3} \frac{|f_{\text{NL}}^{\text{equil}}|^{3/4}}{g^3} \simeq 1.44 \times 10^4 \left( \frac{0.01}{g} \right)^3 \left( \frac{|f_{\text{NL}}^{\text{equil}}|}{16} \right)^{3/4}, \quad (5.37)$$

we can reexpress (5.35) as

$$\Delta P_t \simeq 1.2 \times 10^{-2} \left( \frac{F}{20} \right) \left( \frac{|f_{\text{NL}}^{\text{equil}}|}{16} \right)^{3/2} \left( \frac{H}{10^{12} \text{ GeV}} \right)^2, \quad (5.38)$$

which is only sensitive to the coupling  $g$  logarithmically through the dependence in (5.36). This result tell us that for the fiducial value  $H = 10^{12} \text{ GeV}$  the tensor vacuum fluctuations are already larger than particle production contribution hence rules out particle production as the primary origin. Contribution from particle production events can be at most made to be at the same order of vacuum fluctuations, e.g  $H \simeq 10^{13} \text{ GeV}$  but the energy scale of inflation (implied by Hubble rate  $H$ ) in this case would not be different than what is inferred from vacuum fluctuations (See equation (5.8)). This can be seen from Figure 5.1 for both single ( $N_{\text{events}} = 1$ ) and multiple production ( $N_{\text{events}} \gg 1$ ) cases. We emphasize that our result (5.38) shows

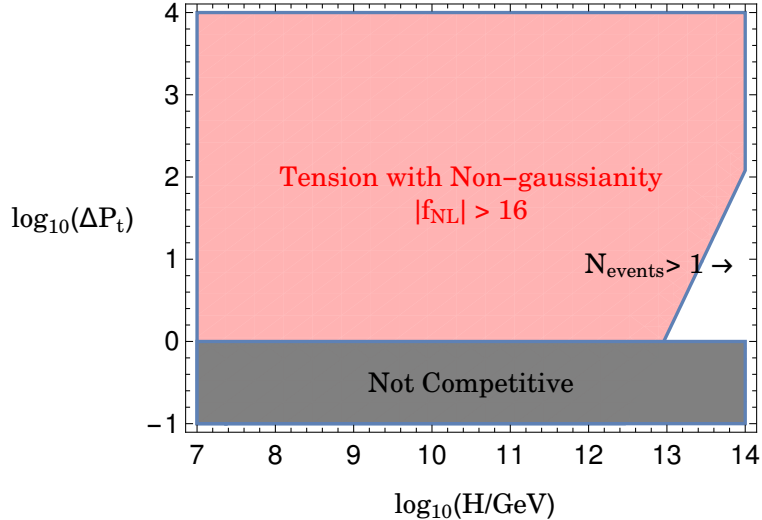


Figure 5.1: Change in the tensor power spectrum due to particle production  $\Delta P_t$  (as defined in the text) vs Hubble rate  $H$  during inflation for both the single ( $N_{\text{events}} = 1$ ) and multiple production cases ( $N_{\text{events}} > 1$ ). The lightly shaded region (red) represents a tension with the Planck upperbound on equilateral type non-Gaussianity ( $|f_{\text{NL}}^{\text{equil}}| < 16$ ), whereas in the dark shaded region particle production is clearly not competitive with the vacuum contribution. We note that even in cases where the signal is competitive, this does not necessarily imply a dominant contribution. Thus, we see that in both cases (single or multiple production) non-Gaussianity puts strong constraints on the tensor contribution. The multiple production case is rather insensitive to the coupling, but in both cases we have plotted results for  $g = 10^{-2}$  and  $|f_{\text{NL}}^{\text{equil}}| < 16$ .

the *tension with non-Gaussianity constraints without even invoking model building constraints within Trapped Inflation*. Moreover, as bounds on non-Gaussianity improve this will strengthen confidence in vacuum fluctuations as the origin of the primordial tensor spectrum.

### 5.3.2 Pseudo-scalar Inflaton and Vector Production

A promising candidate for large field inflation is when the inflaton is realized as a pseudo-Nambu-Goldstone boson (PNGB) associated with the breaking of a global symmetry at some high scale [173, 240]. As discussed above, the UV sensitivity of large field inflation emphasizes the importance of realizing models of inflation within

a high energy framework. Within string theory constructions, PNCB's naturally arise from the compactification of higher dimensional gauge fields to four dimensions [241]. Often the higher dimensional gauge invariance of these fields leads to an approximate shift symmetry  $\phi \rightarrow \phi + \text{const.}$  in the  $4D$  low-energy effective theory. This shift symmetry can be lifted by a number of effects (both tree-level and non-perturbative) that depend on the details of the compactification [241]. One promising class of PNCB inflation models are those arising in models of axion monodromy (see [242] and references within). In these models a large field range for the inflaton is achieved as branes wrapping the same extra dimensions as the gauge fields lift the shift symmetry in a controlled way leading to relevant terms in the inflaton potential but with naturally suppressed coefficients. Other non-perturbative effects can contribute (such as gauge and brane instantons), but in particular constructions its possible to arrange for these effects to be parametrically small yielding a viable inflation model. That is, these string based models realize the idea of natural inflation proposed in [173, 240] in a technically natural way.

In addition to the inflaton sector, it is natural for PNCB inflatons to couple to  $4D$  gauge fields. In fact, for any PNCB of inflation it is natural to consider interactions<sup>12</sup> of the form

$$\mathcal{L}_{\text{int}} = -\frac{1}{4f}\phi F^{\mu\nu}\tilde{F}_{\mu\nu} , \quad (5.39)$$

where  $F_{\mu\nu} = \partial_\mu A_\nu - \partial_\nu A_\mu$  is the field strength tensor,  $\tilde{F}^{\mu\nu} \equiv \eta^{\mu\nu\rho\sigma} F_{\rho\sigma}/(2\sqrt{-g})$  is its dual where alternating symbol  $\eta^{\mu\nu\rho\sigma}$  is 1 for even permutation of its indices,  $-1$  for odd permutations, and zero otherwise. The 'axion' decay constant is denoted by  $f$ . For an exactly constant field  $\phi$  this term is a total derivative (i.e. topological), and so it does not enter the equations of motion. However, during inflation the inflaton slowly evolves and this interaction leads to an effective tachyonic-like mass term for

---

<sup>12</sup>Here we are interested in the case that the inflaton is a pseudo-scalar and so we do not consider couplings of the type  $\sim f(\phi)F_{\mu\nu}F^{\mu\nu}$  – see e.g. [215] for these scalar inflaton models. However, we expect the bounds on the level of gravity waves found in this section and the previous section to be representative of any inflaton coupled to the fields being produced.

the gauge field – thus, particle production is possible. We are interested in whether such a term can lead to significant gravity wave production, while evading the bounds established for the scalar production case in the last section.

Just as in the scalar case of the previous section, the interaction (5.39) can lead to particle production<sup>13</sup> of gauge fields  $\delta A$  when adiabaticity is violated. Analogous to (5.13) we have

$$A''_{\pm} + \omega_k^2(\tau)A_{\pm} = 0 , \quad (5.40)$$

where  $\pm$  denotes the transverse polarization. The time dependent frequency of the field is

$$\omega_k^2(\tau) = k^2 \mp m^2(\tau, k) , \quad (5.41)$$

where the tachyonic-like mass term depends on the wave number as

$$\begin{aligned} m^2(\tau, k) &= \frac{k\dot{\phi}}{H|\tau|f} , \\ &= \frac{1}{2\pi\sqrt{\Delta_s^2}} \left( \frac{kH}{f|\tau|} \right) \simeq 3.2 \times 10^3 k^2 \left( \frac{H}{f} \right) \left( \frac{1}{k|\tau|} \right) \end{aligned} \quad (5.42)$$

where in the last line we have used the normalization of the scalar power spectrum  $\Delta_s^2 = 2.2 \times 10^{-9}$  to eliminate<sup>14</sup>  $\dot{\phi}$ . Assuming  $\dot{\phi} > 0$  without loss of generality, it is easy to see from (5.40),(5.41) and (5.42) that only positive helicity gauge modes  $A_+$  are amplified while  $A_-$  modes stay in the vacuum. For  $\dot{\phi}/(2Hf) \simeq \text{constant}$ , the amplification of the positive helicity modes is given by [217, 243]

$$A_+ \sim e^{(H/f)/(4\sqrt{\Delta_s^2})} \quad \text{for} \quad k|\tau| \lesssim (H/f)/(2\pi\sqrt{\Delta_s^2}) , \quad (5.43)$$

where the exponential dependence here is consistent with the particle production coming from a tachyonic instability. The essential physics is that gauge field modes

<sup>13</sup>See Appendix 5.B for the details of particle production or [216] for a review.

<sup>14</sup>We note that for comparison with the results in [217, 243], here we have used the COBE normalization to simplify the  $\xi \equiv \dot{\phi}/(2Hf)$  parameter of that paper where one would find  $\xi = (H/f)/(4\pi\sqrt{\Delta_s^2})$ .

with  $k|\tau| \lesssim (H/f)/(2\pi\sqrt{\Delta_s^2})$  will become violently excited by the interaction as the tachyonic mass term (5.42) becomes significant in (5.41) in this regime. On the other hand, this growth saturates deep in the IR  $k|\tau| \rightarrow 0$  (See *e.g.* equation (5.131)) causing the “physical”  $\vec{E}$  and  $\vec{B}$  fields to decay sufficiently far outside the horizon. This can be seen by the scaling of the physical fields with the expansion, i.e.  $\vec{B} = (\vec{\nabla} \times \vec{A})/a^2$  and  $\vec{E} = -\vec{A}'/a^2$ . Whereas the gravity waves that result from this process will not decay outside the Hubble radius, but instead become ‘frozen-in’ with this process over time leading to a late time stochastic background of gravity waves. The question is whether this source is competitive with that of the quasi-dS vacuum fluctuations. To answer this question, first we need to take into account the constraints arising on non-Gaussianities and back-reaction produced from the interaction (5.39).

As shown in [217, 243], the NG contribution to cosmological correlators in this model arises due to the inverse decay processes:  $\delta A \delta A \rightarrow \delta \phi$  associated with the interaction (5.39). This new source of inflaton fluctuations leads to curvature perturbations  $\zeta \sim -(H/\dot{\phi})\delta\phi$  and non-Gaussianity of the equilateral type. Following [217] the parameter range of interest implies that the correction to the scalar power spectrum is negligible and the resulting tensor spectrum in our notation is

$$\Delta P_t \simeq (\Delta_s^2)^3 \left(\frac{H}{M_{\text{pl}}}\right)^2 \left(\frac{f}{H}\right)^6 \exp\left(\frac{H}{f\sqrt{\Delta_s^2}}\right), \quad (5.44)$$

Whereas, the equilateral type NG is [217]

$$|f_{\text{NL}}^{\text{equil}}| \simeq 2.2 \times 10^3 (\Delta_s^2)^{11/2} \left(\frac{f}{H}\right)^9 \exp\left(\frac{3H}{2f\sqrt{\Delta_s^2}}\right) \quad (5.45)$$

Thus, combining these results and utilizing the Planck result  $|f_{\text{NL}}^{\text{equil}}| < 16$  we find a

bound on the tensor spectrum

$$\begin{aligned} \Delta P_t &\lesssim 5.5 \times 10^3 |f_{\text{NL}}^{\text{equil}}|^{2/3} \left(\frac{H}{M_{\text{pl}}}\right)^2, \\ &\lesssim 2.3 \times 10^{-8} \left(\frac{|f_{\text{NL}}^{\text{equil}}|}{16}\right)^{2/3} \left(\frac{H}{10^{12} \text{ GeV}}\right)^2, \end{aligned} \quad (5.46)$$

and we see it is difficult for this model to account for the gravity wave spectrum while allowing for a low-scale inflation model.

### 5.3.3 Summary of Direct Coupling Case

In this section, we have considered particle production resulting from a direct coupling of fields to the inflaton and the resulting production of gravitational waves. In particular, we were interested in whether the contribution to the tensor power spectrum from production events could be the leading contribution, since this would imply that an observation of primordial tensors does not necessarily imply the scale at which inflation took place.

However, in both the scalar and gauge field cases we have seen that existing constraints on non-Gaussianity from Planck lead to a tension for model building if the produced tensor signal is to be competitive with the quasi-dS source. Moreover, for gauge field production additional constraints from back-reaction make it very difficult to see how such a source could lead to an alternative origin of gravity waves for any range of the parameters. For scalar production we saw that multiple events can improve the situation, however we are left with a small region of the parameter space near the highest possible inflationary scales. Therefore, even in this special region, if a substantial signal resulted it would still provide us with information on the (high) scale at which inflation took place.

Given the direct coupling of the produced fields to the inflaton in these models a strong level of constraint from non-Gaussianity bounds was anticipated – our results have quantified this. However, we have also argued that the types of couplings and



interactions above are generic expectations from the UV perspective, e.g. in the context of inflationary model building within string theory. One may have asked if such interactions are around, why have we not seen their gravitational signatures? Our results imply that these fields can exist and be produced without leading to a large tensor contribution.

In the next section, we consider gravity wave and particle production in models that contain fields which are only gravitationally coupled to the inflaton.

## 5.4 Particle Production Mechanisms with Gravitational Coupling

In this section we would like to explore whether particle production in a hidden sector which is only gravitationally coupled to the inflaton can lead to a competitive alternative for generating a primordial tensor spectrum. As in the previous section, we will again utilize constraints on the back-reaction and on the level of non-Gaussianity – the latter anticipated to be less stringent since the fields are only gravitationally coupled.

The system is described by the following action [214, 219]

$$S = \int d^4x \sqrt{-g} \left[ \frac{1}{2} M_{\text{pl}}^2 R - \frac{1}{2} (\partial\phi)^2 - V(\phi) + \mathcal{L}_{\text{hid}}[\partial_\mu\chi, \chi, F] \right], \quad (5.47)$$

where the field  $\phi$  is the inflaton and we assume  $V(\phi)$  can support inflation.  $\mathcal{L}_{\text{hid}}$  consists of a pseudoscalar field  $\chi$  with potential  $U(\chi)$  during inflation. It is coupled gravitationally to the inflaton and  $U(1)$  gauge field  $A_\mu$  through an axionic coupling,

$$\mathcal{L}_{\text{hid}} = -\frac{1}{2} (\partial\chi)^2 - U(\chi) - \frac{1}{4} F_{\mu\nu} F^{\mu\nu} - \frac{\chi}{4f} F_{\mu\nu} \tilde{F}^{\mu\nu}. \quad (5.48)$$

The gauge field production is similar to the case in Section 3, except this time the  $\chi$  field is responsible for the amplification of the gauge field fluctuations. The tachyonic

mass term responsible for amplification is now  $m^2(k, \tau) = k^2 \dot{\chi} / (k|\tau|Hf)$  and modes grow as

$$A_+ \sim \exp\left[\pi \sqrt{\frac{\epsilon_\chi}{2}} \left(\frac{M_{\text{pl}}}{f}\right)\right] \quad \text{for} \quad k|\tau| \lesssim \sqrt{2\epsilon_\chi} \left(\frac{M_{\text{pl}}}{f}\right). \quad (5.49)$$

The parameter  $\epsilon_\chi$  is given by  $\epsilon_\chi = \dot{\chi}^2 / (2H^2 M_{\text{pl}}^2)$ .

Successful model building requires the following conditions:

- The field  $\chi$  is to be a spectator field implying that

$$U(\chi) \ll V(\phi), \quad \dot{\chi}^2 \ll \dot{\phi}^2. \quad (5.50)$$

- The energy density of the produced gauge fields must be sub-dominant to the kinetic energy of  $\chi$  and this energy should not back-react on the background evolution of  $\chi$ . It turns out that the former is a stronger condition than latter [214, 244]. Therefore we require,

$$\frac{1}{2} \dot{\chi}^2 \gg \rho_A \equiv \frac{1}{2} \langle \vec{E}^2 + \vec{B}^2 \rangle. \quad (5.51)$$

Using the growing solution of the gauge field mode functions one can show that this condition gives (See the discussion in Appendix 5.B) [214, 244]

$$\dot{\chi}^2 \gg 2.2 \times 10^{-3} H^4 \left(\frac{Hf}{\dot{\chi}}\right)^3 \exp\left(\frac{\pi \dot{\chi}}{Hf}\right) \quad (5.52)$$

- Non-Gaussianity constraints from Planck imply  $|f_{\text{NL}}^{\text{equil}}| < 16$ .

Contrary to the pseudo-scalar inflation case, the inverse decay effects ( $\delta A \delta A \rightarrow \delta \chi$ ) associated with the last term in (5.48) do not necessarily produce strong NG correlations. Moreover, as shown in [214, 219, 244] the scalar power spectrum  $P_\zeta$  gets a negligible contribution from the gauge fields. On the other hand, gravity waves sourced by vector fields  $A_\mu$  can dominate over vacuum ones and hence can contribute significantly to the tensor power spectrum  $P_t$ . We will calculate this contribution

explicitly in Appendix 5.C. The change in the tensor power spectrum is given by [214, 219, 244]

$$\Delta P_t \simeq 2.8 \times 10^{-5} \left( \frac{H}{M_{\text{pl}}} \right)^2 \left( \frac{Hf}{\dot{\chi}} \right)^6 \exp \left( \frac{2\pi\dot{\chi}}{Hf} \right), \quad (5.53)$$

and the NG is

$$f_{\text{NL}}^{\text{equil}} \simeq 2.5 \times 10^5 \left( \frac{H}{M_{\text{pl}}} \right)^6 \left( \frac{Hf}{\dot{\chi}} \right)^9 \exp \left( \frac{3\pi\dot{\chi}}{Hf} \right). \quad (5.54)$$

Combining these we find the constraint

$$\Delta P_t \lesssim 2.2 \times 10^5 \left( \frac{|f_{\text{NL}}^{\text{equil}}|}{16} \right)^{2/3} \left( \frac{10^{12} \text{ GeV}}{H} \right)^2, \quad (5.55)$$

which demonstrates that the tensor signal can be quite large depending on the inflationary scale.

However, we have not yet used the back reaction constraint (5.52). This turns out to be a much more stringent constraint compared to NG and we find

$$\begin{aligned} \Delta P_t &\ll 5.7 \times 10^{14} \left( \frac{\epsilon_\chi}{\epsilon} \right)^2 \left( \frac{H}{M_{\text{pl}}} \right)^2 \\ &\ll 10^2 \left( \frac{\epsilon_\chi}{\epsilon} \right)^2 \left( \frac{H}{10^{12} \text{ GeV}} \right)^2, \end{aligned} \quad (5.56)$$

where  $\epsilon$  is the usual slow-roll parameter of inflaton and we took a fiducial value for the ratio  $\epsilon_\chi/\epsilon$  that is implied by the condition (5.50). In Figure 5.1, we summarize the constraints obtained from (5.55) and (5.56). These constraints can also be used to restrict the axion decay constant  $f$ . The requirement of generating a significant tensor signal implies that the argument of the exponential in (5.49) must satisfy  $\sqrt{\frac{\epsilon_\chi}{2}} \left( \frac{M_{\text{pl}}}{f} \right) \gtrsim 3.5$ . Using this along with the constraint from (5.50) we have

$$\frac{f}{M_{\text{pl}}} \ll 1.8 \times 10^{-2} \left( \frac{\epsilon}{0.008} \right)^{1/2}, \quad (5.57)$$

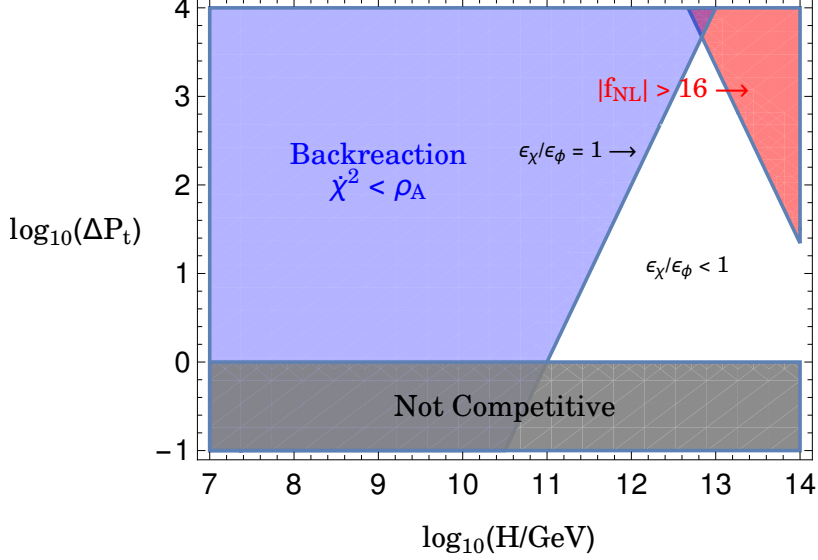


Figure 5.1: Change in the tensor power spectrum  $\Delta P_t$  due to (gravitationally coupled) gauge field production as discussed in the text. The red region represents a tension with the Planck upperbound on equilateral type non-Gaussianity ( $|f_{\text{NL}}^{\text{equil}}| < 16$ ), whereas in the darkest shaded region gauge field production is not competitive with the vacuum contribution. The light Blue region corresponds to the constraint coming from the back reaction of the produced gauge fields on the spectator scalar  $\chi$ . As plotted, the above graph is actually conservative as the real constraint requires the kinetic energy to be *much* greater than the gauge field energy  $\dot{\chi}^2 \gg \langle \vec{E}^2 + \vec{B}^2 \rangle$ . Given this caveat, the two white regions represent the available parameter space for the choices  $\epsilon_\chi = \epsilon$  and the more realistic value  $\epsilon_\chi < \epsilon$  ( $\epsilon_\chi < \epsilon < 1$  is required for  $\chi$  to remain a spectator field.)

where we have chosen a fiducial value for the slow-roll parameter corresponding to a quadratic potential with  $N = 60$  e-foldings. On the other hand, (5.51) implies  $f/M_{\text{pl}} \gg 8.5 \times 10^{-4}(\epsilon/0.008)^{1/2}$  and so we have

$$8.5 \times 10^{-4} \left( \frac{\epsilon}{0.008} \right)^{1/2} \ll \frac{f}{M_{\text{pl}}} \ll 1.8 \times 10^{-2} \left( \frac{\epsilon}{0.008} \right)^{1/2}. \quad (5.58)$$

Thus, we find that this model provides a competitive source of gravity waves for a narrow region of the parameter space. We now turn to the question of whether such a model is UV completable.

## 5.5 Towards a UV Completion and the Resulting Constraints from String Theory

We have seen that the most promising case for observable particle production arises from the gravitationally coupled case. In this section we want to consider the possibility of UV completing such a model and any additional constraints on model building that this might imply. In the next few subsections, we gather the tools that will be required for our analysis.

### 5.5.1 Axions in Type IIB String Theory

As our starting point we will focus on axions arising from compactifications of Type IIB string theory. To see how axions arise in the theory, we consider the dimensional reduction of the theory to four dimensions by starting from the 10D action in the string frame given by [245]

$$S_{10}^{IIB} = \frac{1}{(2\pi)^7 \alpha'^4} \int d^{10}x \sqrt{-G} \left[ \frac{1}{g_s^2} \left( R[G] - \frac{1}{2} |H_3|^2 \right) + \frac{1}{2} |F_3|^2 \right] + \dots \quad (5.59)$$

where  $G_{MN}$  is the ten dimensional string frame metric and  $H_3 = dB_2$  and  $F_3 = dC_2$  are the NS-NS and RR three-form fluxes, respectively, with  $B_2$  and  $C_2$  the corresponding gauge potentials and  $1/(2\pi\alpha')$  is the string tension. The model independent axion  $C_0$  and dilaton are combined as the axio-dilaton  $\tau = C_0 + i/g_s$  where  $g_s = \exp(\phi_0)$  is the string coupling and we will take  $C_0$  to be fixed and instead concentrate on the model dependent axions arising from the compactification of the form fields. The additional terms represented by dots will be discussed in more detail below and include higher form fields such as  $C_4$  (we will concentrate on  $C_2$  axions for now).

The zero modes of  $B_2$  and  $C_2$  are independent of the co-ordinates of the compact dimensions and can be integrated over chosen two-cycles of the internal geometry giving rise to axions in the four dimensional theory. To make this explicit, consider

compactifying on a Calabi-Yau 3-fold (CY<sub>3</sub>) and for the form field  $C_2$  we make the ansatz [241]

$$C_2 = \frac{1}{2\pi} c_I(x) \omega^I, \quad (5.60)$$

where the  $c_I(x)$  are only functions of the four non-compact space-time dimensions and  $I$  labels the two-cycle. We have introduced the basis forms  $\omega^I$  to describe the internal geometry and they obey the normalization condition  $\int_{\Sigma_I} \omega^J = (2\pi)^2 \alpha' \delta_I^J$  with the two cycles  $\Sigma_I$  giving a basis of the dual homology  $H_2(X, \mathbb{Z})$ . The normalization factors of  $2\pi$  are chosen for later convenience. Making a similar ansatz for  $B_2$  and using this in (5.59) we have

$$S = \int \frac{d^{10}x}{(2\pi)^7 \alpha'^4} \sqrt{-G} \left[ g_s^{-2} \left( R[G] - \frac{1}{48\pi^2} G^{mn} G^{lp} \partial_\mu b_I \partial^\mu b_J \omega_{nl}^I \omega_{mp}^J \right) - \frac{1}{48\pi^2} G^{mn} G^{lp} \partial_\mu c_I \partial^\mu c_J \omega_{nl}^I \omega_{mp}^J \right], \quad (5.61)$$

where Greek indices run over the four non-compact dimensions and lower-case latin indices denote the compact dimensions. At the classical level, the gauge invariance of the higher dimensional gauge potential implies that the axions can only be derivatively coupled and so we have a shift-symmetric pseudo-scalar in the low energy theory. This symmetry can be broken in a number of ways, which we will discuss shortly. Denoting both types of axions as  $a_I$ , upon dimensional reduction we find

$$S_4 = \int d^4x \sqrt{-g} \left( \frac{M_{\text{pl}}^2}{2} R[g] - \frac{1}{2} \gamma^{IJ} \partial_\mu a_I \partial^\mu a_J \right) \quad (5.62)$$

where  $g$  is the 4D Einstein frame metric and the 4D reduced Planck mass is

$$M_{\text{pl}}^2 = \frac{2\mathcal{V}}{(2\pi)^7 g_s^2 \alpha'}, \quad (5.63)$$

with  $\mathcal{V} = V_6/\alpha'^3$  the string frame volume of CY<sub>3</sub>. Another common convention is to instead work with the Einstein frame volume. The 10D string frame is related to the

Einstein frame by the Weyl rescaling  $G_{MN}^{string} = \exp(\phi/2)G_{MN}^{Einstein}$  and working in units of the string length  $l_s = 2\pi\sqrt{\alpha'}$  the two volumes are related by  $\mathcal{V}_E = (2\pi)^6\mathcal{V}/g_s^{3/2}$ .

For the RR axion the  $\gamma^{IJ}$  provide the axion decay constants and depend on the internal geometry as [241]

$$\gamma_{\text{RR}}^{IJ} = \frac{1}{6(2\pi)^9\alpha'^4} \int \omega_I \wedge \star \omega_J, \quad (5.64)$$

whereas for the NS axion one gets the same result multiplied by an extra factor of  $g_s^{-2}$ . However, for the remainder of this paper we will restrict our attention to the RR axion, since (as shown in [246]) the NS axions will suffer an  $\eta$  problem when moduli stabilization proceeds through non-perturbative effects<sup>15</sup>. Alternatively, one could work in perturbative (Large Volume) stabilization scenarios [247].

Once the specifics of the internal geometry are known one can calculate the  $\gamma^{IJ}$  to find the corresponding axion decay constants. This is a non-trivial task, which requires a full specification of the compactification geometry in a Calabi-Yau manifold. Mostly, we will be interested in order-of-magnitude estimates of this quantity. This is the project taken up in [241], where the quantity  $\gamma^{IJ}$  was calculated in a variety of string models assuming compactifications sufficiently symmetric to be amenable to estimates.

## 5.5.2 Orientifold Compactification Data and Axion Decay Constant

In order to proceed with concrete estimates of the axion decay constant and the axion potential, it is best to locate oneself within a orientifold compactification in which these quantities can be given in terms of the compactification data.

We will consider an  $N = 2$  IIB compactification on  $\text{CY}_3$ , which has a moduli space

---

<sup>15</sup>This is because the NS axion appears explicitly in the Kahler potential and leads to a Hubble scale mass for the field in the models we will consider. For recent progress on this issue in a different class of models we refer the reader to [242].

$\mathcal{M}_h \times \mathcal{M}_v$  of exactly flat directions. Here,  $\mathcal{M}_h$  denotes the hypermultiplet moduli space while  $\mathcal{M}_v$  is the vector multiplet moduli space.  $\mathcal{M}_h$  is a quaternionic manifold whereas  $\mathcal{M}_v$  is a special Kähler manifold. The dilaton field is a hypermultiplet component, implying that the geometry of  $\mathcal{M}_h$  receives both  $\alpha'$  and  $g_s$  corrections. The geometry of  $\mathcal{M}_v$ , on the other hand, is exact at tree level in both  $\alpha'$  and  $g_s$ . The hypermultiplet moduli space  $\mathcal{M}_h$  contains a subspace  $\mathcal{M}_h^0$  which is parameterized by vacuum expectation values of NS-NS fields, with the RR moduli being set to zero. At string tree level  $\mathcal{M}_h^0$  has a special Kähler structure that receives nonperturbative  $\alpha'$  corrections which can be exactly summed using mirror symmetry.

From this  $N = 2$  compactification, we can construct a  $N = 1$  theory by gauging a discrete symmetry of the form  $(-1)^{\epsilon F_L} \Omega \sigma$  where  $\Omega$  denotes world-sheet parity,  $F_L$  is left-moving fermion number and  $\epsilon$  takes values 0, 1 depending on the model. Note that  $\sigma : X \rightarrow X$  is a holomorphic involution of the Calabi-Yau manifold  $X$  which preserves the holomorphic three-form  $\Omega_X$  up to sign  $\sigma^* \Omega_X = (-1)^\epsilon \Omega_X$ . For the purposes of this paper, we will take  $\epsilon = 1$ , which corresponds to theories with O3/O7 planes.

The analysis of [248] tells us that the massless spectrum of  $N = 1$  orientifold compactifications is naturally organized in vector and chiral multiplets. For orientifolds with O3/O7 planes, there are  $h_-^{2,1}$  chiral multiplets which correspond to invariant complex structure deformations of  $X$ ,  $h_+^{1,1}$  chiral multiplets that correspond to invariant complexified Kähler deformations of  $X$ , and  $h_-^{1,1}$  chiral multiplets that parameterize the expectation values of the two-form fields  $B_2$  and  $C_2$ . Moreover, there is a dilaton-axion modulus  $\tau$ . The real Kähler deformations of  $X$  pair up with expectation values of the four-form field  $C_4$ , giving rise to the  $h_+^{1,1}$  complexified Kähler moduli.

The moduli space of the  $N = 1$  theory is a Kähler manifold. In the limit of small string coupling and large compactification radius the moduli space is a direct product of the complex structure moduli, complexified Kähler moduli and a dilaton-axion factor. The Kähler geometry of the moduli is determined in this regime by KK reduction of ten dimensional supergravity [248]. For more general values of



parameters, however, the geometry receives both  $\alpha'$  and  $g_s$  corrections which does not preserve the direct product structure. In particular, significant  $\alpha'$  corrections are expected in nongeometric regions of the Kähler moduli space such as the Landau-Ginzburg phase [249, 250].

In this paper, we will stay in the geometric phase. The moduli space of the theory has a direct product structure

$$\mathcal{M} \times \mathcal{K} \tag{5.65}$$

where  $\mathcal{M}$  and  $\mathcal{K}$  are the complex structure and Kähler moduli space respectively of the IIB orientifold  $(X, \sigma)$ .

To further discuss the geometry of  $\mathcal{K}$ , it is necessary to introduce certain geometric data. The Kähler potential is given as  $K_{\mathcal{K}} = -2 \ln \mathcal{V}_E$  in terms of the dimensionless volume  $\mathcal{V}_E$  in the Einstein frame. The Kahler form is given by  $J = v_\alpha \omega^\alpha$  and the volume by  $\mathcal{V}_E = \frac{1}{6} \frac{\int J \wedge J \wedge J}{(2\pi\sqrt{\alpha'})^6} = \frac{1}{6} v^I v^J v^K c_{IJK}$ , where the triple intersection numbers are given by

$$c_{IJK} = \frac{1}{(2\pi\sqrt{\alpha'})^6} \int \omega_I \wedge \omega_J \wedge \omega_K . \tag{5.66}$$

The  $\omega_I$  are the basis of the cohomology of  $H^2(X, \mathbb{Z})$  with normalization  $\int_{\Sigma_I} \omega_J = (2\pi)^2 \alpha' \delta_J^I$ . The two-cycle volumes  $v^i$  are functions of the appropriately defined Kähler coordinates  $T_i = (3i/2)\rho_i + (3/4)c_{ijk}v^jv^k - (3/2)\zeta_i$  and  $G^i = (1/2\pi)(c^i - i(b^i/g_s))$ . Here,  $\zeta_i = -(i/2(\tau - \bar{\tau}))c_{ijk}G^j(G - \bar{G})^k$  and the  $c_i$  have been defined in (5.60), with similar expressions for  $b_i$ .

The axion decay constant can now be extracted in terms of the orientifold data by noticing that  $\gamma_{IJ}$  given in (5.64) is the Kähler metric  $K_{G\bar{G}}$  along the axion direction. For an axion wrapped on the two-cycle  $\Sigma$  we have [248, 251]

$$\frac{1}{l_s^6} \int \omega_I \wedge \star \omega_J = \frac{2}{3} c_{\alpha\Sigma\Sigma} v^\alpha \tag{5.67}$$

where  $v^\alpha$  is the dimensionless volume of the two-cycle in string units, the  $\alpha$  index runs over the number of two-cycles surviving the orientifold projection,  $\Sigma$  is the two-cycle

wrapped by the axion. Using this and (5.64) the axion decay constants are then

$$\left(\frac{f_\Sigma}{M_{\text{pl}}}\right)^2 = \frac{g_s}{8\pi^2} \left(\frac{c_{\alpha\Sigma\Sigma} v^\alpha}{\mathcal{V}_E}\right) \quad (5.68)$$

As a simple example, if we consider an internal geometry that is highly symmetric with all two-cycles of equal size  $Ll_s$  then using (5.63) we have  $(f/M_{\text{pl}})^2 \sim g_s \mathcal{V}_E^{-2/3}$ . Thus, we see that requiring the string theory completion of the axion model explicitly connects the compactification scale  $\mathcal{V}_E$ , the string coupling  $g_s$ , and the axion decay constant to the Planck scale. As we will see, theoretical consistency will lead to requirements such as  $\mathcal{V}_E > 1$  and  $g_s < 1$  (for validity of the geometric regime) leading to additional constraints on model building.

### 5.5.3 Stable Five-brane-Anti-brane Systems and Axion Potentials

Given the axion decay constants (5.68), we now turn to the question of their potential energy. Classically the axions descending from the compactification enjoy a shift symmetry, however there are a number of ways the symmetry can be broken.

Crucial to our construction will be the presence of either  $D5$  branes or  $NS5$  branes in the geometry. In this subsection, we discuss various aspects of such geometric constructions.

The D-brane configuration will consist of a 5-brane wrapping a holomorphic curve  $\Sigma$  and an anti-5-brane wrapping the image curve  $\Sigma'$  under the orientifold projection. We will take  $\Sigma$  and  $\Sigma'$  to be rigid cycles that do not intersect each other. Under the orientifold action, the modulus  $T_+$  of the even combination  $\Sigma_+$  and the modulus  $G_-$  of the odd combination  $\Sigma_-$  are projected in. The sizes of the cycles are equal in the covering space:  $v_\Sigma = v_{\Sigma'} = \frac{1}{2}v_+$ , while the odd volume modulus  $v_-$  is projected out. By abuse of notation, we will continue to use  $v_\Sigma$  to denote the even volume modulus.

In general, one has to be careful about open string fields in the brane / anti-brane

sector which may destabilize the system. In flat space one would expect the system to decay and give a supersymmetric configuration of space-filling  $D3$  branes. On a  $CY_3$ , the curves  $\Sigma$  and  $\Sigma'$  can be chosen to be rigid, meaning that the corresponding wrapped branes have no moduli. For branes that are sufficiently far apart, the open string spectrum is not expected to contain tachyons. The attractive force will be weak, resulting in a metastable state which can only decay through tunnelling effects <sup>16</sup>.

The situation is best studied by taking a simple potential for the system. We will be interested in the case where  $\Sigma$  and  $\Sigma'$  are part of a one parameter family of holomorphic curves  $\mathcal{E}$ . The effective dynamics of the brane system can be described by a single chiral superfield  $\zeta$ , which corresponds to normal deformations of the brane wrapping  $\Sigma$ . This can also be identified as the normal deformations of the anti-brane wrapping  $\Sigma'$ . The effective dynamics of the system can be described by a potential of the form

$$V(r) = m(r - r_0)^2 + c \ln \left( \frac{r}{r_0} \right), \quad (5.69)$$

where  $r$  is the distance between the two branes. The first term is a quadratic mass term corresponding to normal deformations of the brane in the ambient  $CY_3$ . The second term is a typical two dimensional brane / anti-brane attractive potential. We expect  $m, r_0$  to be approximately the string scale. Then, if  $c \sim 10^{-2}$  the attractive force will be negligible. The well-known logarithmic attractive potential has been previously pointed out in the case of axion monodromy inflation in [253].

We will not aim for a greater degree of precision than the above arguments, and assume that there is a region in configuration space where the destabilization is small. From the perspective of the string landscape, this makes sense; by scanning over fluxes, one can explore all regions of configuration space, and the vacuum solutions

---

<sup>16</sup>There is an added layer of complication for branes with magnetic fluxes. There is a tachyonic contribution to the mass of the lightest open string modes that is proportional to the supersymmetry breaking parameter, which is given by the relative phase between the central charges of the  $D5$  and the induced  $D3$  [252]. However, this tachyonic contribution is usually small. We will explore these issues soon for the brane construction of the  $\chi$  sector.

which are in the regime of instability are discarded.

Branes wrapping the corresponding cycle of the axions can induce monodromies, which leads to a mechanism realizing theoretically self-consistent, large field, slow-roll inflation (see [242] and references within). Let us consider the potential generated by axion monodromy, again focusing on RR axions descending from  $C_2$ . For these axions the symmetry can be broken by considering a NS5-brane with two directions wrapping the two cycle  $\Sigma$  associated with the axion. The resulting potential is given by the Born-Infeld action [246]

$$V(c_a) = \frac{\epsilon_{warp}}{(2\pi)^5 g_s^2 \alpha'^2} \sqrt{l^4 + (2\pi g_s c_a)^2}, \quad (5.70)$$

where  $\epsilon_{warp}$  captures the possible effects of warping,  $l\sqrt{\alpha'}$  is the size of the two-cycle and we see for  $c_a \gg l^2/(2\pi g_s)$  the potential is linear in  $c_a$  – the shift symmetry has been broken by the presence of the wrapped brane leading to a linear potential for the axion.

In addition to the monodromy effect, D-brane and world sheet instantons can break the shift symmetry of the axion. Such corrections should be generically expected and imply a contribution to the potential

$$\Delta V(\chi_a) = \sum_i \Lambda_i^4 \cos(\chi_a/f_a), \quad (5.71)$$

where we introduce the canonically normalized field  $\chi_a = c_a f_a$  and we must sum over all such contributions that give a significant contribution to the potential. These contributions break the continuous shift symmetries to discrete ones with  $\chi_a \rightarrow \chi_a + 2\pi f_a$ , and such terms can lead to additional important contributions to the potential and so must be checked against (5.70) and the slow-roll conditions.

We now turn to the question of  $D3$  charge and tadpole cancellation in these

models. The induced  $D3$  charge on the  $NS5$ -brane is given by

$$N_{D3,induced} = \frac{1}{(2\pi)^2 \alpha'} \int_{\Sigma} C_2 . \quad (5.72)$$

This quantity turns out to be given by  $N_{D3,induced} = \frac{\phi}{2\pi f}$ , where  $\phi$  denotes a generic field that may be the inflaton. Thus,  $N_{D3,induced}$  can be quite large in the case when  $\phi$  is the inflaton and  $\frac{\phi}{f} \gg 1$ .

Suppressing the energy density of the wrapped brane to match observations will force us to place the branes in warped throats. Thus, there is a  $D3$  charge contribution coming from the warping. We will denote the  $D3$  charge of the throat by  $N_{D3,throat}$ . The total  $D3$  charge of the system is then given by

$$N_{D3,total} = N_{D3,induced} + N_{D3,throat} . \quad (5.73)$$

This will be cancelled by the orientifold action that wraps an anti-5-brane on the cycle  $\Sigma'$  in a throat with anti- $D3$  charge given by  $-N_{D3,throat}$ .

## 5.6 A String Model of Gauge Field Production

In the last Section, we have gathered all the tools required for our construction. In this Section, we will give a string construction that realizes the model of gravity wave production discussed in Section 5.4.

We will begin by sketching how such a setup is achieved within the string compactification and the model building constraints that result. Crucial to gauge field production (for the purposes of our model, and more generally for realistic reheating in these classes of models) will be the introduction of magnetized 5-branes in the  $CY_3$  geometry. In the next subsection, we will discuss this topic. We will then describe the inflaton and spectator field dynamics in terms of UV data, and give the UV constraints that appear in our construction.

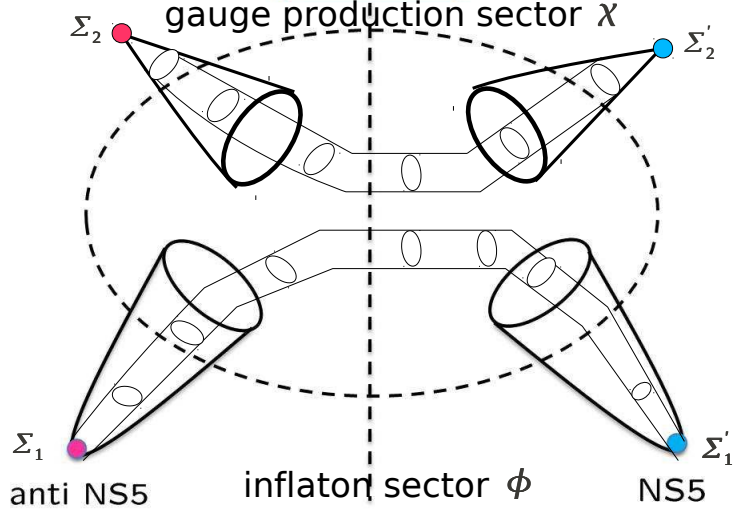


Figure 5.1: A cartoon of the model for gauge field production from a sector  $\chi$  that is gravitationally coupled to the inflaton  $\phi$ .

Recall from Section 5.4 that we are interested in an inflationary sector that successfully provides at least 60 e-folds of inflation, coupled only gravitationally to spectator fields. The action was

$$S = \int d^4x \sqrt{-g} \left[ \frac{1}{2} M_{\text{pl}}^2 R - \frac{1}{2} (\partial\phi)^2 - V(\phi) + \mathcal{L}_{\text{hid}}[\partial_\mu \chi, \chi, F] \right], \quad (5.74)$$

$$\mathcal{L}_{\text{hid}} = -\frac{1}{2} (\partial\chi)^2 - U(\chi) - \frac{1}{4} F_{\mu\nu} F^{\mu\nu} - \frac{\chi}{4f} F_{\mu\nu} \tilde{F}^{\mu\nu}, \quad (5.75)$$

where  $\phi$  was the inflaton and  $\chi$  and  $F_{\mu\nu}$  were spectator fields.

Given both the axion decay constant (5.68) and potential energy (5.70) and ensuring that the oscillating contribution (5.71) is subdominant, we can construct a slow-roll inflation model as done in [246, 251].

A sketch of our construction is provided in Figure 5.1. We will be interested in a

compactification with

$$h_-^{1,1} \geq 2. \tag{5.76}$$

The inflaton sector is engineered by wrapping an *NS5*-brane on a cycle  $\Sigma_1$  that supports the axion  $\phi$ . Under the orientifold action, an anti-*NS5*-brane wraps a cycle  $\Sigma'_1$  for tadpole cancellation.

We note that placing the cycles  $\Sigma_1$  and  $\Sigma'_1$  in warped throats is necessary to suppress the inflationary potential energy coming from the wrapped *NS5*-brane and match the COBE normalization. The curves  $\Sigma_1$  and  $\Sigma'_1$  are thus members of a one parameter family of holomorphic curves  $\mathcal{E}_1$  which extends down a warped throat (we denote this throat by T1).

Similarly, the sector  $\chi$  responsible for gauge field production is engineered on cycles  $\Sigma_2$  and  $\Sigma'_2$  that are members of a one-parameter family of holomorphic curves  $\mathcal{E}_2$ . This family extends down a different warped throat T2, and we assume that  $\mathcal{E}_1$  and  $\mathcal{E}_2$  do not intersect. This enables our system to satisfy the requirement that the two sectors are only gravitationally coupled. One can ask how generic such a set-up is. Such multi-axion models that are coupled only gravitationally can be generically anticipated given the large number of two-cycles within a typical  $CY_3$  geometry. Indeed, this fact helps motivate the notion that monodromy inflation could proceed via two or more axions – an idea first pursued in [254].

We need to couple the  $\chi$  field to gauge fields in our low energy Lagrangian. Given a gauge field  $F$  on the brane, the desired operator descends from a Chern-Simon's term

$$\int C_2 \wedge F \wedge F \tag{5.77}$$

upon compactification to 4D [241]. In the context of axion monodromy model building such a term has already been considered for; gauge field production associated with the inflaton sector<sup>17</sup> [216], as a way to reheat at the end of inflation [255], and as a

---

<sup>17</sup>In [216] the authors considered gauge field production in the case where inflaton is coupled directly to gauge fields, which as discussed in Section 5.3 is in tension with existing bounds on

possible constraint from CMB rotation when the axion corresponds to a quintessence field [256].

We note that phenomenological requirements such as a visible sector with chiral matter (and/or obtaining acceptable reheating into visible sector fields) will in general require us to turn on fluxes on the branes supporting the inflaton and the gravitationally coupled field  $\chi$ . To illustrate this, we consider an example where  $\chi$  couples to an appropriately constructed visible sector, and turn on magnetic flux on the 5-branes wrapping  $\Sigma_2$  and  $\Sigma'_2$ . We will prefer to turn on an effective  $D3$ -brane charge  $p$ :

$$\frac{1}{2\pi} \int_{\Sigma} F = p - 1 .$$

It is important to perform a number of checks when introducing brane fluxes into the system. We now turn to a discussion of the subtleties that arise.

### 5.6.1 Magnetized 5-Branes in Orientifold Compactifications

Magnetized branes in type IIB have a long history in the context of building semirealistic string vacua with chiral matter. These models are  $T$ -dual to models of intersecting  $D6$ -branes in type IIA. Chiral matter is vital in any phenomenological construction of low-energy physics, as well as any realistic reheating model based on axion monodromy inflation. We refer to [257] for a review of the  $T$ -dual intersecting brane models, and to [258] for the type IIB picture in toroidal models <sup>18</sup>.

For our purposes, we will require magnetized 5-branes in  $CY_3$ , going beyond the simple toroidal picture. We will mainly follow [252] in our treatment. Although we will be describing everything in the language of  $D5$ -branes, it can be adapted to the case of  $NS$ -branes as well.

Starting with the  $N = 2$  theory, it is clear that the system breaks tree level non-Gaussianity from Planck.

---

<sup>18</sup>We also refer to [259], [260], [261], [262] for a sample of the literature on toroidal magnetized brane models.



supersymmetry since the brane and anti-brane preserve different fractions of the bulk  $N = 2$ . The  $N = 1$  supersymmetry preserved is determined by the central charge of a brane. For the brane and anti-brane, the central charges are respectively

$$Z_+ = Z_{D5} + pZ_{D3}, \quad Z_- = -Z_{D5} + pZ_{D3} . \quad (5.78)$$

The phases of  $Z_+$  and  $Z_-$  are not aligned for any deformation of the bulk Kahler structure away from the  $Z_{D5} = 0$  locus, leading to breaking of brane world-volume supersymmetry. This breaking can be described by supergravity  $D$ -terms at weak string coupling and in a small neighborhood of the marginal stability locus  $Z_{D5} = 0$  in the Kahler moduli space<sup>19</sup>. The Fayet-Iliopoulos couplings in the low energy gauge theory have been used to construct de-Sitter vacua in for example [263], where background fluxes and non-perturbative superpotential contributions fix moduli, followed by an uplift utilizing  $D$ -terms from  $D7$ -brane fluxes.

We note that the supersymmetry breaking is best parametrized by the parameter  $\theta$  given by the relative phase between the charge  $Z_+ = Z_{D5} + pZ_{D3}$  and  $Z_{D3}$

$$\theta = \frac{1}{\pi}(Im \ln Z_+ - Im \ln Z_{D3}) . \quad (5.79)$$

The parameter  $\theta$  has a minimum at the Landau-Ginzburg point in the non-geometric phase [252].

In our case, we will not be interested in studying supersymmetry breaking effects. We will remain strictly in the geometric phase for our model for the gauge field production mechanism we are interested in. The supersymmetry breaking induced by the inflaton sector will in any case be more dominant than  $D$ -term contributions from brane flux. However, in a detailed reheating model after the end of inflation based on this class of models, it would be necessary to take into account any supersymmetry

---

<sup>19</sup>For large deformations from the locus of marginal stability, string field theory computations are required to accurately calculate the brane dynamics.

breaking effects carefully. It may be useful then to stay near the large complex structure limit in the complex structure moduli space, and utilize mirror symmetry to situate the calculations in the supergravity limit of the mirror type IIA. We leave these considerations for future work.

As noted before, there is a small subtlety in the brane-anti-brane stability issues we had studied earlier. The dynamics of the brane are encoded by fluctuations of the embedding map  $i : \Sigma \hookrightarrow X$ , which are described by sections  $\zeta$  of the normal bundle  $N_{\Sigma/X}$  of  $\Sigma_+$ . As described in (5.69), a stable system can generally be obtained. However, according to the  $\Pi$ -stability analysis of [252], there is a tachyonic contribution to the mass of the lightest open string modes between the brane-antibrane pair that is proportional to  $\theta$ . Since the curves  $\Sigma_2$  and  $\Sigma'_2$  are isolated, the positive contribution to the mass of the open strings should be typically much larger than the tachyonic contribution  $\theta$ .

We now turn to the issue of moduli stabilization and superpotential terms in the presence of branes with fluxes. In the bulk  $CY_3$ , we will be utilizing a usual background RR flux compactification [264], [265]. However, we now have to take into account the superpotential contribution from the magnetized brane. Brane-flux superpotentials have been studied in [266], [267], and in the context of  $F$ -theory in [268]. For  $D5$ -branes, we refer to the detailed work of [269] and references therein. Here, we summarize the essential points that are relevant for us. The main point is that at the level of the superpotential, one should use a combined brane-RR flux superpotential given by

$$W = \int_X F_3 \wedge \Omega + W_{D5} , \tag{5.80}$$

where  $W_{D5}$  is in general a function of the deformation moduli  $\zeta$ , the complex structure moduli of the  $CY_3$ , and the brane flux  $F$  <sup>20</sup>. For our purposes, we will assume

---

<sup>20</sup>We note that the superpotential is not generally separable in the form given in (5.80). This is possible in special cases, for example if  $X$  contains a connected family of holomorphic curves interpolating between  $\Sigma$  and  $\Sigma'$ . For simplicity, we will assume that this is the case, and refer to [266] for more details.

that tuning the background RR-fluxes and brane flux appropriately in the combined superpotential  $W$  will stabilize the complex structure moduli.

Before moving on, we mention several other caveats to this analysis. We have not explicitly discussed the case of turning on flux on the cycles  $\Sigma_1$  supporting the inflaton, as would ostensibly be required for reheating. It would be interesting to compute the effect of brane flux on the slow-roll conditions. Moreover, our inflaton sector is present in a warped throat with background  $D3$  charge. Generally, the magnetized  $D5$  and background  $D3$  should attract each other and the system should decay to a state where the  $D3$  has been converted to magnetic flux on the  $D5$ . It would be interesting to compute the relevant stability conditions.

In the next subsection, we discuss the microscopic parameters in the inflaton and  $\chi$  sector potentials. We then go on to a discussion of the consistency of the construction.

## 5.6.2 Microscopic Parameters in the Inflaton and Hidden Sector

In this subsection, we write down the potential for the inflaton and  $\chi$  sectors using the microscopic data we have developed till now.

The action of the inflationary sector is

$$S_{\text{inf}} = \int d^4x \sqrt{-g} \left\{ \frac{1}{2} (\partial\phi)^2 - \mu_\phi^3 \phi \right\} + \text{corrections}, \quad (5.81)$$

where we have labeled the canonical inflaton arising from the RR axion as  $\phi = f_\phi c$  with the corresponding decay constant following from (5.68)

$$\left( \frac{f_\phi}{M_{\text{pl}}} \right)^2 = \frac{g_s}{8\pi^2} \left( \frac{c_{\alpha\Sigma_1\Sigma_1} v^\alpha}{\mathcal{V}_E} \right) \quad (5.82)$$

with the sum running over the remaining two-cycles of the compactification. Express-

ing (5.70) in terms of the canonical field  $\phi$  the parameter  $\mu$  is then

$$\mu_\phi^3 = \frac{\epsilon_{(warp,\phi)}}{g_s(2\pi\sqrt{\alpha'})^4 f_\phi}, \quad (5.83)$$

As shown in [246] adequate inflation and accounting for the COBE normalization requires  $\mu \simeq 6.4 \times 10^{-4}$ . Warping in the throat T1 can enable enough suppression of the inflationary energy to match observations.

Given the inflationary sector, we now turn to the spectator field ( $\chi$ ) responsible for the gauge field production. Recall from Section 5.4 that we require this field to be slow-rolling as well. In our construction, we achieve this by introducing an additional axion wrapped around a cycle  $\Sigma_2$  belonging to the non-intersecting family  $\mathcal{E}_2$ . The monodromy term, in conjunction with an appropriate choice of the warping in throat T2, can then be used to ensure that this field is (a) slow-rolling meeting the model building requirement that  $\epsilon_\chi \ll \epsilon \ll 1$  and (b) sub-dominant in energy density to the inflaton sector <sup>21</sup>.

Denoting the warp factor of the spectator by  $\epsilon_{(warp,\chi)}$ , and keeping in mind that we require  $\epsilon_{(warp,\chi)} \ll \epsilon_{(warp,\phi)}$ , the spectator sector is then specified by the decay constant

$$\left(\frac{f_\chi}{M_{\text{pl}}}\right)^2 = \frac{g_s}{8\pi^2} \left(\frac{c_{\alpha\Sigma_2\Sigma_2} v^\alpha}{\mathcal{V}_E}\right) \quad (5.84)$$

with the sum running over the remaining two-cycles of the compactification, and the potential from (5.70) is

$$\mu_\chi^3 = \frac{\epsilon_{(warp,\chi)}}{g_s(2\pi\sqrt{\alpha'})^4 f_\chi}, \quad (5.85)$$

The low-energy description is completed once the brane flux  $F$  is turned on. The

---

<sup>21</sup>Strong warping can lead to additional corrections to the monodromy potential [256], as well as altering expressions like the Planck mass in (5.63). Here we will be interested in *mild* warping and work in the approximation utilized in [270], where it was shown that in the region of interest warping effects can be safely ignored.

Chern Simon's term connects  $\chi$  and  $F$ , with an action given by

$$S_{\text{gauge}} = \int d^4x \sqrt{-g} \left[ -\frac{1}{4} F^2 - \frac{1}{4} \alpha_{\text{brane}} \chi F_{\mu\nu} \tilde{F}^{\mu\nu} \right] \quad (5.86)$$

The coupling  $\alpha$  is given by

$$\alpha_{NS5} = \frac{C_0 g_s^2}{(2\pi)^2 f_\chi}, \quad (5.87)$$

$$\alpha_{D5} = \frac{2\pi g_s^{1/2}}{v_{\Sigma_2} f_\chi}, \quad (5.88)$$

depending on whether we use  $D5$  or  $NS5$  branes.

We note that the coupling matches the notation of [241] up to factors of  $2\pi$  coming from how the four dimensional gauge kinetic term is defined.

### 5.6.3 Consistency Conditions

In this subsection, we will take the most important conditions on the microscopic data required to build the specific model in Section 5.4. We must ensure that the low energy constraints outlined in Section 5.4 are satisfied, and also that the string construction is under control.

The microscopic data that determines the model by fixing the values of the quantities  $(f_\phi, f_\chi, \mu_\phi, \mu_\chi)$  in the low-energy Lagrangian is given by

$$\text{Microscopic data : } (c_{\alpha\Sigma_1\Sigma_1}, c_{\alpha\Sigma_2\Sigma_2}, \epsilon_{(\text{warp},\phi)}, \epsilon_{(\text{warp},\chi)}, v^\alpha, \mathcal{V}_E) \quad (5.89)$$

In the Appendix, we list the possible corrections to slow roll and back-reaction effects on moduli stabilization, and the methods employed in the literature to build consistent inflationary models in these scenarios. These conditions are not particularly specific to the model we are building; rather, they must generally hold in axion monodromy models in type IIB compactifications. Before we proceed, lacking a full-fledged  $\text{CY}_3$

construction, we will make the simplifying assumption that all intersection numbers satisfy

$$c_{\alpha\Sigma_1\Sigma_1}, c_{\alpha\Sigma_2\Sigma_2} \sim \mathcal{O}(1) . \quad (5.90)$$

A statistical analysis following the work of Kreuzer-Skarke is also possible (we refer to [271] for an accessible recent review).

The first condition we require is that the  $\chi$  sector energy density is sub-dominant to the inflaton sector. This can be satisfied by choosing

$$\epsilon_{(warp,\chi)} \ll \epsilon_{(warp,\phi)} \quad (5.91)$$

The second condition that we found in Section 5.4 is that the axion decay constant  $f_\chi$  should lie in the range given by (5.58). As it turns out, the condition on the axion decay constant is intimately connected to the question of keeping  $\alpha'$  corrections under control, so that we remain in the supergravity regime as outlined in Section 5.5.2. This condition reduces to keeping the volume of the  $CY_3$ , and in particular, the volumes of the two-cycles, large enough to remain in the geometric regime.

The issue is not only one of computability in the geometric regime. In principle, one has to check whether  $D5$  and  $D3$  branes are stable BPS states in the non-geometric regime. The stability of BPS states in non-compact  $CY_3$  has been studied in [272], [273], [274]. The situation is less clear in compact  $CY_3$  manifolds. We will avoid this problem by remaining close to the large radius limit. This condition can be placed in a number of ways. For example, following the classic work of [275], the  $\alpha'$  corrections to the volume in the Einstein frame can be obtained in terms of the Hodge numbers of the  $CY_3$ , which will translate into a condition on  $f_\chi$ . We will find it more useful to use the approximation outlined in [251]. Controlling worldsheet instanton corrections, the limit obtained is

$$v^\alpha > \frac{1}{\pi\sqrt{g_s}} . \quad (5.92)$$

This will give a lower bound on  $f_\chi$ , thus giving us

$$\frac{g_s^{1/4}}{(2\pi)^{3/2}\sqrt{\mathcal{V}_E}} < \frac{f_\chi}{M_{\text{pl}}} < 1 . \quad (5.93)$$

We note that there is a constraint on  $f_\chi$  coming from requiring that the induced  $D3$ -brane charge  $N_{D3,\text{induced}}$  (which depends on  $f_\chi$  through (5.72)) be small enough to keep our model local and not distort the throat geometry. This is outlined in the Appendix. However, this condition is milder than (5.93).

To agree with the lower bound in (5.58), we require from (5.93)

$$\mathcal{V}_E > 10^6 \cdot \frac{g_s^{1/2}}{(2\pi)^3} . \quad (5.94)$$

Taking taking  $g_s \sim 0.1$ , one obtains  $\mathcal{V}_E \gtrsim 1000$ . Even without going into the details of moduli stabilization, it is clear that this is a sensible condition which should be easy to satisfy in a typical compactification. We thus reach the conclusion that there is no general obstacle to realizing the model in a string construction.

## 5.7 Conclusions

In this paper we have considered whether particle production and non-adiabaticity during inflation can lead to a competitive source of primordial gravity waves during inflation. In all of the examples we considered, we found that even when these events lead to a detectable level of B-modes that the scale of inflation must be quite high. Stated another way, polarization observations would still be teaching us about the scale of inflation. We identified the most promising case as models where the spectator fields are gravitationally coupled. We then considered the UV completion of these models in the context of Type IIB flux compactifications with Axion Monodromy. The embedding served two purposes. Firstly, although we saw that the range in which the axion decay constant leads to phenomenologically interesting results is quite narrow,

there seems to be no obvious obstruction to realizing the setup in string theory. Indeed, for weakly coupled constructions the primary model building requirements are mild warping and requiring the overall volume to be about a 1000 times the string scale – both conditions easily accommodated in typical compactifications. Secondly, through the UV completion we have argued that it is possible to suppress dangerous sinusoidal terms that are known to spoil the gauge field production. Although a more detailed investigation is needed, this provides further support for the gauge production models that have been considered in the literature. As we note in the text, these models could also provide an interesting approach to reheating at the end of inflation in models of Axion Monodromy.

In summary, we find that although there can be competitive sources to the quasi-deSitter background for the origin of primordial B-modes, it seems challenging to vastly separate the scale of inflation from that implied by CMB polarization measurements. In other words – yes! – we can really determine the scale of inflation.



# Appendix

## 5.A ADM formalism

We focus on the action for the matter Lagrangian minimally coupled to Einstein gravity

$$S = \int d^4x \sqrt{-g} \left[ \frac{M_{\text{pl}}^2}{2} R - \frac{1}{2} (\partial\phi)^2 - V(\phi) - \frac{1}{2} (\partial\chi)^2 - U(\chi) - \frac{1}{4} F^2 - \frac{\chi}{8f} \frac{\eta^{\mu\nu\rho\sigma}}{\sqrt{-g}} F_{\mu\nu} F_{\rho\sigma} \right]. \quad (5.95)$$

The analysis we present in this appendix can be directly applied to direct coupling case we consider in section 5.3.2 by identifying  $\chi \rightarrow \phi$ . In order to study cosmological perturbations, we write the metric in the ADM form,

$$ds^2 = -N^2 dt^2 + \hat{g}_{ij} (dx^i + N^i dt) (dx^j + N^j dt), \quad (5.96)$$

where  $\hat{g}_{ij}$  is the spatial 3-metric defined on constant time surfaces. In this parametrization, the lapse  $N$  and shift vector  $N^i$  appear as Lagrange multipliers and hence can be integrated out from the action (5.95). To study the fluctuations around the infla-

tionary background we consider the following gauge-fixing conditions

$$\begin{aligned}
\phi(t, \vec{x}) &= \bar{\phi}(t) + \delta\phi(t, \vec{x}), \\
\chi(t, \vec{x}) &= \bar{\chi}(t) + \delta\chi(t, \vec{x}), \\
\hat{g}_{ij} &= a^2(t) [\delta_{ij} + h_{ij}], \\
A_0 &= \partial_i A_i = 0
\end{aligned} \tag{5.97}$$

where  $h_{ij}$  is transverse and traceless, *i.e.*  $h_{ii} = \partial_i h_{ij} = 0$ . We can now expand the action at a desired order to solve for  $N$  and  $N^i$  in terms of  $\delta\phi, \delta\chi, h_{ij}$  and  $A_i$  perturbatively. Note that by our gauge choice above and due to the fact that gauge fields do not contribute to the background evolution, solutions to lapse function and the shift vector can not start linear order in  $A_i$  and  $h_{ij}$ . Therefore schematically we expect

$$N = N(\delta\phi, \delta\chi) + \mathcal{O}(h^2, A^2), \tag{5.98}$$

$$N^i = N^i(\delta\phi, \delta\chi) + \mathcal{O}(h^2, A^2). \tag{5.99}$$

In addition, to obtain the action upto third order in fluctuations  $\delta\phi, \delta\chi, h_{ij}, A_i$ , it is enough to solve the lapse and shift to first order in fluctuations [37]. First, we begin by writing the gravity sector in the ADM form

$$S_g = \frac{1}{2} M_{\text{pl}}^2 \int d^4x \sqrt{-g} R = \frac{1}{2} M_{\text{pl}}^2 \int d^4x \sqrt{\hat{g}} N [R^{(3)} + \frac{1}{N^2} (E^{ij} E_{ij} - E^i_i{}^2)], \tag{5.100}$$

where  $R^{(3)}$  is the 3 curvature associated with the spatial metric  $\hat{g}_{ij}$  and  $E_{ij}$  is related to the extrinsic curvature of constant time slices,

$$E_{ij} \equiv NK_{ij} = \frac{1}{2} [\partial_t \hat{g}_{ij} - \hat{\nabla}_i N_j - \hat{\nabla}_j N_i], \tag{5.101}$$

$$R^{(3)} = \hat{g}^{ik} \partial_l \Gamma_{ik}^l - \hat{g}^{ik} \partial_k \Gamma_{il}^l + \hat{g}^{ik} \Gamma_{ik}^l \Gamma_{lm}^m - \hat{g}^{ik} \Gamma_{il}^m \Gamma_{km}^l, \tag{5.102}$$

with the connection

$$\Gamma_{ij}^k = \frac{1}{2} \hat{g}^{kl} (\partial_i \hat{g}_{jl} + \partial_j \hat{g}_{il} - \partial_l \hat{g}_{ij}). \quad (5.103)$$

Here,  $\hat{\nabla}_i$  is the covariant derivative with respect to 3-metric  $\hat{g}_{ij}$ . Noting our gauge choice (5.97) for the spatial metric and its inverse  $\hat{g}^{ij} = a^{-2}[\delta^{ij} - h^{ij}]$ , up to second order in fluctuations we have

$$S_g = M_{\text{pl}}^2 \int d^4x a^3 \left[ 3H^2 \delta N - 3H^2 \delta N^2 - 2H \delta N \partial_i N^i + \frac{1}{8} \left( \dot{h}_{ij} \dot{h}_{ij} - \frac{\partial_k h_{ij} \partial_k h_{ij}}{a^2} \right) \right]. \quad (5.104)$$

We can neglect the higher order terms in the gravity sector as they are slow-roll suppressed compared to the interactions of the form  $\mathcal{O}(hAA)$  in the matter sector.

Next, we focus on the action in the scalar sector neglecting pseudo-scalar coupling in (5.95) for now. As both scalar fields couple gravity minimally, their action will have the same form. Therefore we will refer to both scalar fields collectively using  $X = \{\phi, \chi\}$  with potentials  $V_X = \{V, U\}$ . Expanding the scalar action up to second order in fluctuations, we have

$$S_X = \int d^4x a^3 \left\{ \frac{1}{2} \left[ \delta \dot{X}^2 - \frac{(\partial_i \delta X)^2}{a^2} \right] - \frac{1}{2} V_X''(\bar{X}) \delta X^2 - \dot{X} \delta \dot{X} \delta N \right. \\ \left. + \frac{1}{2} \dot{X}^2 \delta N^2 + \dot{X} N^i \partial_i \delta X - V_X'(\bar{X}) \delta X \delta N \right\} \quad (5.105)$$

Considering  $S = \sum S_X + S_g$ , one can vary the action with respect to  $\delta N$  and  $N^i$  to obtain solutions for lapse and shift in terms of the scalar fields as,

$$2HM_{\text{pl}}^2 \delta N = \sum \dot{X} \delta X, \quad (5.106)$$

$$-2HM_{\text{pl}}^2 \partial_i N^i = \sum \dot{X} \delta \dot{X} + \sum V_X'(\bar{X}) \delta X + \left( 6H^2 M_{\text{pl}}^2 - \sum \dot{X}^2 \right) \delta N. \quad (5.107)$$

Plugging the constraint equation back in the actions (5.100) and (5.105), we obtain

the following second order action for scalar fields,

$$\begin{aligned}
S_X^{(2)} &= \frac{1}{2} \int d^4x a^3 \left\{ \left[ \delta\dot{X}^2 - \frac{(\partial_i \delta X)^2}{a^2} \right] - m_X^2 \delta X^2 \right\}, \\
m_X^2 &= V_X''(X_0) + \left( 3 - \frac{\sum \dot{X}^2}{2H^2 M_{\text{pl}}^2} \right) \frac{\dot{X}^2}{M_{\text{pl}}^2} + \frac{2\dot{X} V_X'(\bar{X})}{H M_{\text{pl}}^2}.
\end{aligned} \tag{5.108}$$

In addition to diagonal mass terms we have mass mixing terms between two sectors at second order in fluctuations. These mixing terms that are induced by the background evolution of the fields can be described by the action,

$$\begin{aligned}
S_{XX'}^{(2)} &= -\frac{1}{2} \int d^4x a^3 \Omega \delta X \delta X', \\
\Omega &= 2 \left( 3 - \frac{\sum \dot{X}^2}{2H^2 M_{\text{pl}}^2} \right) \frac{\dot{X} \dot{X}'}{M_{\text{pl}}^2} + \frac{2 \sum \dot{X} V_X'(\bar{X})}{H M_{\text{pl}}^2}.
\end{aligned} \tag{5.109}$$

Here, pairs of the form  $XX'$  denotes  $\chi\phi$  or  $\phi\chi$ . Also note that in deriving these expression we have used the background equations

$$\ddot{\bar{X}} + 3H\dot{\bar{X}} + V_X'(\bar{X}) = 0, \tag{5.110}$$

$$-2\dot{H}M_{\text{pl}}^2 = \sum \dot{X}^2. \tag{5.111}$$

As far as  $\phi$  and  $\chi$  sector concerned, it is not necessary to consider cubic and higher order interactions as these interactions will be either slow-roll suppressed through the derivative of potentials  $V^{(n)}, U^{(n)}$  with  $n \geq 3$  or via non-linear mixings with gravitational fluctuations  $N$  and  $N^i$  (*e.g.* see (5.106) and (5.107)). Particularly, in the presence of particle production in the gauge field sector, these interaction will be overshadowed by direct couplings to gauge fields  $A_i$  or by the ones induced by gravity, *i.e.* terms of the form  $\mathcal{O}(\delta g AA)$ . Our aim in the next section is to focus on these interactions that arise from the last two terms in the action (5.95).

## Gauge Field Sector

We are interested the part of the action (5.95) that includes gauge fields and its interaction with the spectator sector  $\chi$  and gravitational fluctuations  $\delta N$ ,  $N^i$  and  $h_{ij}$ ,

$$S = \int d^4x \sqrt{-g} \left[ -\frac{1}{4} F_{\mu\nu} F^{\mu\nu} - \frac{\chi}{8f} \frac{\eta^{\mu\nu\rho\sigma}}{\sqrt{-g}} F_{\mu\nu} F_{\rho\sigma} \right]. \quad (5.112)$$

Keeping in mind the gauge fixing conditions  $A_0 = \partial_i A_i = 0$ ,  $h_{ii} = 0$ , we have the following second order and third order actions

$$S_A^{(2)} = \int d^4x a^3 \left\{ \frac{1}{2a^2} \dot{A}_i \dot{A}_i - \frac{1}{2a^4} \partial_j A_i \partial_j A_i + \frac{\dot{\chi}}{a^3 f} \epsilon_{ijk} \partial_j A_k A_i \right\}, \quad (5.113)$$

$$S_{AA\chi} = \int d^4x \left\{ -\frac{\delta\chi}{f} \epsilon_{ijk} \dot{A}_i \partial_j A_k \right\}, \quad (5.114)$$

$$S_{gAA} = \int d^4x a^3 \left\{ -\frac{\delta N}{2a^2} \dot{A}_i \dot{A}_i - \frac{\delta N}{4a^4} F_{ij} F_{ij} - \frac{N^i}{a^2} \dot{A}_j F_{ij} \right\}, \quad (5.115)$$

$$S_{hAA} = \int d^4x a^3 \left\{ -\frac{1}{2a^4} h_{ij} \left[ a^2 \dot{A}_i \dot{A}_j + \epsilon_{ilm} \epsilon_{jnp} \partial_l A_m \partial_n A_p \right] \right\} \quad (5.116)$$

Here, through the terms in the third action above,  $S_{gAA}$ , more interactions between scalar sector and gauge fields arise. First two of these interactions are trivial to write down using (5.106) in (5.115),

$$S_{gAA} \supset \int d^4x a \sum_X \frac{\dot{\chi}}{HM_{\text{pl}}^2} \delta X \left\{ -\frac{1}{4} \dot{A}_i \dot{A}_i - \frac{1}{8a^2} F_{ij} F_{ij} \right\}. \quad (5.117)$$

The last term in (5.115) requires several integration by parts together with usage of background equations (5.110). This procedure leads to

$$S_{gAA} \supset \int d^4x a \sum_X \frac{\dot{\chi}}{2HM_{\text{pl}}^2} \delta X \left\{ \partial^{-2} \partial_i \partial_i \left( \dot{A}_j F_{ij} \right) + H \partial^{-2} \partial_i \left( \dot{A}_j F_{ij} \right) \right\}. \quad (5.118)$$

By switching to conformal time  $d\tau = dt/a$  and using the definitions of Electric and Magnetic fields  $B_i = a^{-2}\epsilon_{ijk}\partial_j A_k$ ,  $E_i = -a^{-1}\dot{A}_i$ , we can re-write the interactions in (5.118), (5.117) and (5.114) in a simpler form

$$S_{gAA} \supset - \int d^3x d\tau \sum_X \frac{\dot{X}}{2HM_{\text{pl}}^2} \delta X \left\{ \partial^{-2} \partial_\tau \left( a^4 \vec{\nabla} \cdot (\vec{E} \times \vec{B}) \right) \right\}, \quad (5.119)$$

$$S_{gAA} \supset - \int d^3x d\tau a^4 \sum_X \frac{\dot{X}}{2HM_{\text{pl}}^2} \delta X \left\{ \frac{\vec{E}^2 + \vec{B}^2}{2} \right\}, \quad (5.120)$$

$$S_{AA\chi} = \int d^3x d\tau a^4 \frac{\delta\chi}{f} \vec{E} \cdot \vec{B}, \quad (5.121)$$

which agrees with [217]

## 5.B Gauge Field Production

Using the gauge field action in Coulomb gauge (5.113), the equation of motion of gauge fields in conformal time can be written as

$$A_i'' - \vec{\nabla}^2 A_i - \frac{a\dot{\chi}}{f} \epsilon_{ijk} \partial_j A_k = 0. \quad (5.122)$$

Following the standard canonical quantization methods, we can promote the gauge field to a quantum field  $\hat{A}_i$  with the following decomposition

$$\hat{A}_i(\tau, \mathbf{x}) = \int \frac{d^3\mathbf{k}}{(2\pi)^{3/2}} e^{i\mathbf{k}\cdot\mathbf{x}} \hat{A}_i(\tau, \mathbf{k}) = \sum_{\lambda=\pm} \int \frac{d^3\mathbf{k}}{(2\pi)^{3/2}} [\epsilon_i^\lambda(\mathbf{k}) A_\lambda(\tau, k) \hat{a}_\mathbf{k}^\lambda e^{i\mathbf{k}\cdot\mathbf{x}} + h.c.], \quad (5.123)$$

where ‘‘h.c.’’ denotes the Hermitian conjugate of the preceding term and the annihilation/creation operators satisfy

$$[\hat{a}_\mathbf{k}^\lambda, \hat{a}_\mathbf{k}'^{\lambda'}] = \delta^{\lambda\lambda'} \delta(\mathbf{k} - \mathbf{k}'). \quad (5.124)$$

We also note the relations helicity vectors are obeying  $k_i \epsilon_i^\pm = 0$ ,  $\epsilon_{ijk} k_j \epsilon_k^\pm = \mp ik \epsilon_i^\pm$ ,  $\epsilon_i^\pm \epsilon_i^\pm = 0$  and  $\epsilon_i^\pm \epsilon_i^\mp = 1$ . Plugging the decomposition in equation (5.123) in (5.122), we write the equation of motion in Fourier space as

$$A_\pm'' + \left( k^2 \pm 2k \frac{\dot{\chi}}{2Hf\tau} \right) A_\pm = 0, \quad (5.125)$$

where we took the scale factor as  $a(\tau) \simeq -(H\tau)^{-1}$  ignoring slow-roll corrections arise in quasi-dS space. For  $-\infty < \tau < 0$  and  $\dot{\chi} > 0$ , positive helicity modes are unstable and the solution that reduced to adiabatic vacuum at early times, *i.e.*  $A_+ \rightarrow \frac{1}{\sqrt{2k}} e^{-ik\tau}$  as  $-k\tau \rightarrow \infty$ , is given in terms of Coulomb functions

$$A_+(\tau, k) \simeq \frac{1}{\sqrt{2k}} [G_0(\xi, -k\tau) + iF_0(\xi, -k\tau)], \quad (5.126)$$

where  $\xi \equiv \dot{\chi}/2Hf$ . The approximate equality in (5.126) above is because we have assumed that the dimensionless measure of field velocity  $\xi$  evolves adiabatically compared to the expansion of space time, *i.e.*  $\dot{\xi}/\xi H \ll 1$ , implying

$$\frac{\ddot{\chi}}{\dot{\chi}H} - \frac{\dot{H}}{H^2} \ll 1. \quad (5.127)$$

Further simplifications on the form of the solution (5.126) arise in the limit where  $\xi \gg -k\tau$ ,

$$A_+ \simeq \sqrt{\frac{-\tau}{2}} \left[ 2e^{\pi\xi} \pi^{-1/2} K_1(\sqrt{-8\xi k\tau}) + ie^{-\pi\xi} \pi^{1/2} I_1(\sqrt{-8\xi k\tau}) \right], \quad (5.128)$$

where  $I_1$  and  $K_1$  are modified Bessel functions of first and second kind. Since interesting phenomenology due to gauge field production arise for  $\xi \gtrsim \mathcal{O}(1)$ , we can further simplify this solution by taking the large argument limit of Bessel function,

$-8\xi k\tau \gg 1$ ,

$$A_+ \simeq \frac{1}{\sqrt{2k}} \left( \frac{-k\tau}{2\xi} \right)^{1/4} e^{\pi\xi - 2\sqrt{-2\xi k\tau}} + \frac{i}{\sqrt{2k}} \left( \frac{-k\tau}{2^5\xi} \right)^{1/4} e^{-\pi\xi + 2\sqrt{-2\xi k\tau}}. \quad (5.129)$$

In order to make these approximations to work simultaneously, it is require that  $\xi > 1/4$ . On the other hand, one can further check that these solutions satisfy the condition

$$A'_+ = \sqrt{\frac{2k\xi}{\tau}} A_+^*, \quad (5.130)$$

corolarly with Wronskian condition  $A_+ A'_+ - c.c. = i$ . We also note that the growth of  $A_+$  modes saturates deep in the IR. This can be seen by taking the limit  $-k\tau \rightarrow 0$  in (5.128), leading to

$$A_+ \rightarrow \frac{e^{\pi\xi}}{2\sqrt{\pi\xi k}} \approx \text{const}. \quad (5.131)$$

We will see this saturation of the particle production from the perspective of energy density contained in the gauge fields which we now turn in the following section.

## Expectation values involving gauge fields

The expressions we are interested in is the energy density contained in gauge fields  $\rho_A$  and the expectation value of the dot product between Electric and Magnetic field  $\langle \vec{E} \cdot \vec{B} \rangle$

$$\begin{aligned} \rho_A \equiv \frac{1}{2} \langle \vec{E}^2 + \vec{B}^2 \rangle &= \frac{1}{4\pi^2 a^4} \int dk \{ k^2 |A'_+|^2 + k^4 |A_+|^2 \}, \\ \langle \vec{E} \cdot \vec{B} \rangle &= -\frac{1}{4\pi^2 a^4} \int dk k^3 \frac{d}{d\tau} |A_+|^2 \end{aligned} \quad (5.132)$$



For convenience we can write-down both integrands as quantities defined per logarithmic wave-number by using  $A_+ = (\sqrt{2k})^{-1}\tilde{A}(x)$  where  $x \equiv -k\tau$ ,

$$\frac{1}{H^4} \frac{d\rho_A}{d \ln x} = \frac{x^4}{8\pi^2} \left\{ \left| \frac{d\tilde{A}}{dx} \right|^2 + |\tilde{A}|^2 \right\}, \quad (5.133)$$

$$\frac{1}{H^4} \langle \vec{E} \cdot \vec{B} \rangle = \frac{x^4}{8\pi^2} \frac{d}{dx} |\tilde{A}|^2 \quad (5.134)$$

Using the approximate solution in (5.128) in the  $(8\xi)^{-1} \ll -k\tau \ll 2\xi$  regime, we can evaluate the integrals in (5.132) analytically. Using the growing Real part of the  $A_+$ , we can write the energy density as

$$\rho_A = \frac{H^4}{8\pi^2(2\xi)^{1/2}} \int_0^{2\xi} dx x^{7/2} \left\{ \frac{2\xi}{x} + 1 \right\} e^{-4\sqrt{2\xi}x}, \quad (5.135)$$

where we have set the lower bound of the integral to zero as the integrands quickly vanishes in this limit. Defining a new variable  $32\xi x = y^2$ , we can re-write the integrals as

$$\rho_A = \frac{H^4}{\xi^3} \frac{e^{2\pi\xi}}{2^{19}\pi^2} \left\{ \int_0^{8\xi} dy y^6 e^{-y} + \frac{1}{2^6\xi^2} \int_0^{8\xi} dy y^8 e^{-y} \right\}. \quad (5.136)$$

Upper boundary of these integrals can be also sent to infinity  $8\xi \rightarrow \infty$  in the  $\xi \gtrsim \mathcal{O}(1)$  regime as the integrand vanishes quickly for large enough  $x$ . This gives the result,

$$\rho_A = \frac{H^4}{\xi^3} e^{2\pi\xi} \frac{\Gamma(7)}{2^{19}\pi^2} \left\{ 1 + \frac{1}{2^6\xi^2} \frac{\Gamma(9)}{\Gamma(7)} \right\}. \quad (5.137)$$

In the  $\xi \gtrsim \mathcal{O}(1)$  regime, the first term in the curly bracket dominates. Following the same steps, one can also obtain the result

$$\langle \vec{E} \cdot \vec{B} \rangle = -\frac{H^4}{\xi^4} e^{2\pi\xi} \frac{\Gamma(8)}{2^{21}\pi^2} \left\{ 1 - \frac{\Gamma(7)}{\Gamma(8)} \right\}. \quad (5.138)$$

## 5.C Gravity Waves sourced by Gauge Fields

In real space, the equation of motion for the canonical graviton field  $\bar{h}_{ij}$  is given by

$$\bar{h}_{ij}'' + \left( \nabla^2 - \frac{a''}{a} \right) \bar{h}_{ij} = \frac{2}{M_{\text{pl}}^2} a T_{ij}^{TT}, \quad (5.139)$$

where the source term on the RHS can be read from the higher dimensional interaction Lagrangian given in (5.116). In fourier space, this source term be written as

$$T_{ij}^{TT}(\mathbf{k}, \tau) = \frac{\Pi_{ij}^{lm}}{a(\tau)^2} \int \frac{d^3x}{(2\pi)^{3/2}} e^{-i\mathbf{k}\cdot\mathbf{x}} \left[ \hat{A}'_l \hat{A}'_m - \epsilon_{lab} \epsilon_{mcd} \partial_a \hat{A}_b \partial_c \hat{A}_d \right]. \quad (5.140)$$

Using the gauge field decomposition in (5.123), it can be expressed as a convolution in momentum space,

$$T_{ij}^{TT} = \frac{\Pi_{ij}^{lm}}{a(\tau)^2} \int \frac{d^3\mathbf{p}}{(2\pi)^{3/2}} \left[ \hat{A}'_l(\mathbf{p}) \hat{A}'_m(\mathbf{k} - \mathbf{p}) - \epsilon_{lab} \epsilon_{mcd} p_a(k-p)_c \hat{A}_b(\mathbf{p}) \hat{A}_d(\mathbf{k} - \mathbf{p}) \right]. \quad (5.141)$$

Now, for each polarization state,  $h_{ij}(\mathbf{k}, \tau)$  can be described in terms of polarization vectors as

$$\bar{h}_{ij}(\mathbf{k}, \tau) = \Pi_{ij,\lambda}(\mathbf{k}) \bar{h}_\lambda(\mathbf{k}, \tau) = \epsilon_i^\lambda(\mathbf{k}) \epsilon_j^\lambda(\mathbf{k}) \bar{h}_\lambda(\mathbf{k}, \tau), \quad (5.142)$$

where we introduced the operator  $\Pi_{ij,\lambda} = \epsilon_i^\lambda(\mathbf{k}) \epsilon_j^\lambda(\mathbf{k})$  [219]. Here it should be understood that there is no summation over the index  $\lambda$ . Using this relation, we apply the projection operator  $\Pi_{ij,\lambda}^*$  to the both hand sides of (5.3) and note  $\Pi_{ij,\lambda}^*(\mathbf{k}) \bar{h}_{ij}(\mathbf{k}, \tau) = \bar{h}_\lambda(\mathbf{k}, \tau)$ ,  $\Pi_{ij,\lambda}^*(\mathbf{k}) \Pi_{ij}^{lm}(\mathbf{k}) = \Pi_{lm,\lambda}^*(\mathbf{k})$ , to obtain the following formula for  $\bar{h}_\lambda(\mathbf{k}, \tau)$ ,

$$\begin{aligned} \bar{h}_\lambda(\mathbf{k}, \tau) &= \frac{2}{M_{\text{pl}}^2} \int d\tau' \frac{G_k(\tau, \tau')}{a(\tau')} \Pi_{lm,\lambda}^*(\mathbf{k}) \\ &\times \int \frac{d^3\mathbf{p}}{(2\pi)^{3/2}} \left[ \hat{A}'_l(\mathbf{p}) \hat{A}'_m(\mathbf{k} - \mathbf{p}) - \epsilon_{lab} \epsilon_{mcd} p_a(k-p)_c \hat{A}_b(\mathbf{p}) \hat{A}_d(\mathbf{k} - \mathbf{p}) \right]. \end{aligned} \quad (5.143)$$

The expression inside the square bracket in the above equation contains both polarization mode functions as can be seen from the expansion (5.B). However, in the models

we consider, only the positive helicity modes of the gauge fields are amplified hence only these modes will enter as a source to the equation (5.143). We are interested in tensor perturbations at late times  $-k\tau \rightarrow 0$  and we also observe that the dominant contribution for the  $\tau'$  integral comes from the modes with  $-k\tau' \lesssim 1/\xi \lesssim 1$ . In this limit, the greens function (See equation (5.4)) in the above expression becomes  $G_k(\tau, \tau') \rightarrow -\tau'^2/3\tau$ . On the other hand, using the solutions for the gauge field mode functions (5.129) and (5.130), one can realize that the “magnetic” contribution (second term in the square brackets above (5.143)) can be neglected compared to the “electric” part in the  $-k\tau' \lesssim 1$  regime. Following these considerations, we can simplify (5.143) as

$$\begin{aligned} \bar{h}_\lambda(\mathbf{k}, \tau) &= -a(\tau) \frac{4H^2}{3M_{\text{pl}}^2} \frac{\xi^{1/2} e^{2\pi\xi}}{2^{1/2}} \int_0^\infty dx x^6 e^{-zx} \\ &\times \int \frac{d^3\mathbf{p}}{(2\pi)^{3/2}} |\mathbf{k} - \mathbf{p}|^{1/4} |\mathbf{p}|^{1/4} \Pi_{lm,\lambda}^*(\mathbf{k}) \hat{\mathcal{O}}_l(\mathbf{k} - \mathbf{p}) \hat{\mathcal{O}}_m(\mathbf{p}), \end{aligned} \quad (5.144)$$

where we defined a new integration variable  $-\tau' \equiv x^2$  together with  $z \equiv 2\sqrt{2\xi}(\sqrt{|\mathbf{p}|} + \sqrt{|\mathbf{k} - \mathbf{p}|})$ . Note that the operators  $\hat{\mathcal{O}}_l(\mathbf{q}) = \epsilon_l^+(\vec{q})[a_{\mathbf{q}}^+ + a_{-\mathbf{q}}^{+\dagger}]$ . The integration over  $x$  can be taken easily to give  $h_\lambda(\mathbf{k}, \tau) = \bar{h}_\lambda(\mathbf{k}, \tau)/a$  as

$$\begin{aligned} h_\lambda(\mathbf{k}, \tau) &= -\frac{\Gamma(7)}{3 \times 2^9 (2\pi)^{3/2}} \frac{H^2}{M_{\text{pl}}^2} \frac{e^{2\pi\xi}}{\xi^3} \\ &\times \int d^3\mathbf{p} \frac{\Pi_{lm,\lambda}^*(\mathbf{k})}{(\sqrt{|\mathbf{p}|} + \sqrt{|\mathbf{k} - \mathbf{p}|})^7} |\mathbf{p}|^{1/4} |\mathbf{k} - \mathbf{p}|^{1/4} \hat{\mathcal{O}}_l(\mathbf{k} - \mathbf{p}) \hat{\mathcal{O}}_m(\mathbf{p}), \end{aligned} \quad (5.145)$$

From (5.145) the sourced two point correlator  $\langle h_\lambda(\mathbf{k}, \tau) h_\lambda(\mathbf{k}', \tau) \rangle$  can be calculated

$$\begin{aligned} \langle h_\lambda h_\lambda \rangle_s &= \frac{\Gamma(7)^2}{9 \times 2^{17} (2\pi)^3} \frac{H^4}{M_{\text{pl}}^4} \frac{e^{4\pi\xi}}{\xi^6} \delta(\mathbf{k} + \mathbf{k}') \\ &\times \int d^3\mathbf{p} |\epsilon_l^{-\lambda}(\mathbf{k}) \epsilon_l^+(\mathbf{p})|^2 |\epsilon_m^{-\lambda}(\mathbf{k}) \epsilon_m^+(\mathbf{k} - \mathbf{p})|^2 \frac{|\mathbf{p}|^{1/2} |\mathbf{k} - \mathbf{p}|^{1/2}}{(\sqrt{|\mathbf{p}|} + \sqrt{|\mathbf{k} - \mathbf{p}|})^7}, \end{aligned} \quad (5.146)$$

where we used the property  $\epsilon_i^\lambda(-\mathbf{k}) = \epsilon_i^{-\lambda}(\mathbf{k}) = \epsilon_i^{\lambda*}(\mathbf{k})$  of the polarization vectors and applied Wick's theorem. The expressions with polarization vectors in the second line of (5.146) can be more explicitly written as

$$|\epsilon_i^{-\lambda}(\mathbf{q}_1)\epsilon_i^+(\mathbf{q}_2)|^2 = \frac{1}{4} \left( 1 + \lambda \frac{\mathbf{q}_1 \mathbf{q}_2}{|\mathbf{q}_1||\mathbf{q}_2|} \right)^2. \quad (5.147)$$

Using the expression (5.147) and making a change of variable  $\mathbf{p}/|\mathbf{k}| \equiv \mathbf{p}_*$ , the three dimensional integral can be integrated numerically. The final result for the dimensionless power spectra of the helicity  $\lambda = \pm$  components of the sourced graviton can be written as

$$\frac{k^3}{2\pi^2} \langle h_+ h_+ \rangle_s = 8.6 \times 10^{-7} \frac{1}{\pi^2} \frac{H^4}{M_{\text{pl}}^4} \frac{e^{4\pi\xi}}{\xi^6}, \quad (5.148)$$

$$\frac{k^3}{2\pi^2} \langle h_- h_- \rangle_s = 1.8 \times 10^{-9} \frac{1}{\pi^2} \frac{H^4}{M_{\text{pl}}^4} \frac{e^{4\pi\xi}}{\xi^6}. \quad (5.149)$$

We therefore see that both helicity modes of tensor spectra are scale invariant. The difference in power of the two spectra is due to violation of parity and originates from the  $|\epsilon_m^{-\lambda}(\mathbf{k})\epsilon_m^+(\mathbf{k} - \mathbf{p})|^2$  term. This situation can be seen more explicitly in the limit of small momentum transfer  $|\mathbf{p}| \ll |\mathbf{k}|$ , as in this case, this term vanishes for  $\lambda = -$  modes but stays finite for  $\lambda = +$  helicity gravitons.

Finally, taking into account the vacuum fluctuations of the tensors in (5.6), the total dimensionless tensor power spectrum can be expressed as

$$\Delta_t^2 \simeq \Delta_{\text{vac}}^2 \left[ 1 + 4.3 \times 10^{-7} \frac{H^2}{M_{\text{pl}}^2} \frac{e^{4\pi\xi}}{\xi^6} \right]. \quad (5.150)$$

## 5.D Microscopic Conditions for Slow Roll and Back Reaction

In this Section, we list the conditions for making sure that the slow roll potential is not ruined during inflation, or that moduli stabilization is not lost due to back-reaction effects. We also list the methods in which these issues are solved in the literature.

- **Possible Correction:** Destabilization of moduli during inflation.

**Resolution:** For the RR axion the shift in the moduli potential during inflation was shown to be negligible as long as one requires  $1 \gg v_+ \gg cg_s$ , where  $v_+$  is the two-cycle volume,  $c$  is the axion and  $g_s$  is the string coupling [246].
- **Possible Correction:** Backreaction of the NS5 brane on the Geometry and Renormalization of Planck Mass by new light species.

**Resolution:** Wrapped NS5 on a two-cycle induces an effect D3-brane charge  $N_{D3}$ . To avoid back-reaction we require  $N_{D3} \ll R_\perp^4 / (4\pi g_s \alpha'^2)$  where  $R_\perp$  is the smallest curvature radius transverse to the brane – this is easily satisfied [246].
- **Possible Correction:** Moduli Stabilizing Fluxes can generate potential for the axions.

**Resolution:** GKP [264] orientifold stabilization in warped Type IIB use imaginary self-dual flux, which do not contribute to the axion potential.
- **Possible Correction:** Inflation could destabilize moduli resulting in run-away to weak coupling or large-volume (Kallosh-Linde problem [276]).

**Resolution:** Focusing on the RR axion allows for  $V_{inf} < V_{moduli}$  where  $V_{moduli}$  sets the height of the barrier for escape. Also, in [246] it was demonstrated that shifts in the moduli from inflation are also benign – this is not the case for the NS axion  $b$ , which suffers an  $\eta$  problem.

- **Possible Correction:** Non-perturbative stabilization of Kahler moduli implies an  $\eta$  problem for  $b$ -type axions since they mix with each other due to the appearance of  $b$  in the Kahler potential.

**Resolution:** One can focus on  $c$ -type axions which do not mix with the volume, alternatively one could use perturbative methods to stabilize the volume [246].
- **Possible Correction:** Moduli stabilization and Euclidean  $D$  brane instanton corrections to the Kahler potential.

**Resolution:** Exponentially suppressed by the size of the two-cycles  $v_\alpha$  if taken larger than string scale.
- **Possible Correction:** Moduli stabilization and Euclidean  $D$  brane instanton corrections to the Super potential.

**Resolution:** One can focus on stabilization of the volume using gaugino condensation on  $D7$  branes. The combined holomorphy of the gauge coupling and the super potential imply that the instanton corrections are exponentially suppressed by the four-cycle volume.
- **Possible Correction:** NS5 brane wrapped on a two-cycle induces a tadpole through an effective  $D3$  brane charge.

**Resolution:** Introduce  $\overline{D3}$  on a nearby two-cycle to cancel (where ‘nearby’ means at a distance small compared to the  $D7$  used to stabilize the Volume via KKL $T$ ).

# Chapter 6

## Toward an Effective Field Theory Approach to Reheating

### 6.1 Introduction

If inflation occurred in the early universe it must have eventually ended resulting in a hot, thermal universe by the time of Big Bang Nucleosynthesis (BBN). The process by which the inflaton’s energy is transferred into other particles – which hopefully, eventually, gave rise to Standard Model particles – is known as inflationary reheating. Reheating can occur perturbatively [277–279], or non-perturbatively in a process known as preheating [25, 280, 281] (see [27, 282] for recent reviews).

Existing investigations into reheating have been rather model dependent, often focusing on constraining the precise regions of the parameter space that lead to successful reheating. Analytic methods for exploring the dynamics still rely on the earliest works mentioned above, and the non-linearities and complexity of the reheating process still require invoking numeric/lattice methods [27, 282–289]. Moreover, the wealth of cosmological observations from the Cosmic Microwave Background (CMB) and Large Scale Structure (LSS) relate to the physics of inflation far before reheating, and so the lack of observational windows on (p)reheating has also made its study far

less compelling than inflation – with the prediction of gravitational waves providing a possible exception.

In this paper, we take steps to address the model dependence of (p)reheating building on motivation from recent works [290–292]. Our approach is to use the Effective Field Theory (EFT) approach to cosmology, which at this point has been applied to all cosmic epochs except for (p)reheating. We will first consider the EFT of the background as developed by Weinberg for inflation in [293] and later adapted to studies of dark energy in [294]. Ultimately, we will find that this approach is not completely satisfactory in generalizing studies of reheating. Instead we find that the different approach of the EFT of cosmological perturbations is more promising.

The EFT of Inflation [168, 295, 296] and generalizations to dark energy [297–302] and structure formation [303] are based on the idea that there is a physical clock corresponding to the Goldstone boson that non-linearly realizes the spontaneously broken time diffeomorphism invariance of the background. In unitary gauge – where the clock is homogeneous – the matter perturbations are encoded within the metric, *i.e.* the would-be Goldstone boson is ‘eaten’ by the metric, since gravity is a gauge theory. After we establish the limitations of the EFT background approach, we then present an EFT of reheating using this EFT of perturbations to develop a more robust approach to studying the end of inflation and reheating.

The rest of the paper is as follows. In Section 6.2, we review some of the important issues and constraints surrounding particular examples of (p)reheating models. In Section 6.3, we consider Weinberg’s approach to the EFT of Inflation, and consider how inflation might end and (p)reheating would proceed. We find that the perturbative approach to the background presents a substantial challenge to this approach, along with the usual problem of knowing the complete inflationary potential. This motivates us to construct an EFT of reheating in Section 6.4 – focusing on the EFT of the perturbations. We analyze the process of particle production, demonstrate how our approach connects to existing preheating models, and discuss ways in which



our EFT can be used to connect to both inflation (and its end) and observations. In Section 6.5, we conclude and discuss the challenges facing our approach and future directions.

## 6.2 Challenges for Inflationary Reheating

Model dependent studies of (p)reheating have raised a number of important questions and issues. From the perspective of inflationary model building within string theory, the requirement to isolate the inflationary sector to achieve an adequate duration of inflation can result in challenges in transferring the energy density to other fields, and eventually the Standard model sector following inflation [304]. The complexity of the string landscape and the large number of moduli fields can exacerbate this problem [305]. In bottom-up approaches, toy models often demonstrate a conflict between the need for the inflaton to have feeble interactions during inflation (so as to be consistent with both successful inflation and constraints on non-Gaussianity), and later having strong enough couplings for the complete decay of the inflaton and the (eventual) successful reheating of the Standard Model. Perturbative decay can also present a challenge depending on the effective mass of the decay channels and the time dependence of the inflaton decay rate [306].

As an example, consider Chaotic inflation with  $V \sim m_\phi^2 \phi^2$  and reheating with a renormalizable coupling to a reheat field,  $\chi$ . We note that this model is in tension with existing CMB constraints, but it presents a simple example of the more general problems one might anticipate with (p)reheating. The Lagrangian we consider is<sup>1</sup>

$$\mathcal{L} = -\frac{1}{2} (\partial\phi)^2 - \frac{1}{2} m_\phi^2 \phi^2 - \frac{1}{2} (\partial\chi)^2 - U(\chi) - \frac{g^2}{2} \phi^2 \chi^2, \quad (6.1)$$

where we assume that initially the reheat field is fixed by its  $U(\chi)$  and remains in

---

<sup>1</sup>We work in reduced Planck units  $m_{\text{pl}} = 1/\sqrt{8\pi G} = 2.4 \times 10^{18}$  GeV with  $\hbar = c = 1$  and with a ‘mostly plus’  $(-, +, +, +)$  sign convention for the metric. Our conventions for curvature tensors are those of Weinberg.

its vacuum during inflation. The mass of the inflaton is fixed by the power spectrum [38],

$$\Delta_{\mathcal{R}}^2 = \frac{1}{96\pi^2} \left( \frac{m_\phi}{m_{\text{pl}}} \right)^2 (4N_*)^2 \equiv 2.2 \times 10^{-9} \quad (6.2)$$

where  $N_*$  is the number of e-folds before the end of inflation and with  $N_* = 60$  we have  $m_\phi \simeq 6.4 \times 10^{-6} m_{\text{pl}}$ . The inflaton will begin to oscillate around the minimum of its potential when its mass becomes comparable to the Hubble scale,  $m_\phi \approx H(t_{\text{osc}})$ , with a profile given by the expression  $\phi_0(t) = \Phi(t) \sin(\phi t)$  [25]. The amplitude of the oscillations,  $\Phi(t)$ , is a monotonic function of cosmic time given by  $\Phi = \sqrt{8/3} (m_{\text{pl}}/2\pi N_{\text{osc}})$ , where  $N_{\text{osc}}$  is the number of oscillations after the end of inflation. Setting  $N_{\text{osc}} = 1$  gives  $\Phi \approx 0.3 m_{\text{pl}}$ , which we take as the initial amplitude of the inflaton oscillations.

If the direct coupling in (6.1) presents the only decay channel for the inflaton the expansion of the universe will prevent the complete perturbative decay of the inflaton [25]. This is because the decay rate,  $\Gamma$ , scales as  $\Gamma \propto \Phi^2 \sim 1/t^2$  whereas the expansion rate during reheating scales as  $H \sim 1/t$ . Instead, in this case decay must proceed non-perturbatively through preheating [25, 280, 281], where parametric resonance can lead to enhanced decay of the inflaton condensate. The mode equation for  $\chi$  fluctuations resulting from (6.1) in the presence of the oscillating condensate  $\phi_0(t)$  is

$$\ddot{\chi}_k + [k^2 + m_\chi^2 + g^2\phi_0^2] \chi_k = 0, \quad (6.3)$$

where we have neglected the expansion of the universe ( $a = 1$ ) and note that including gravitational effects would act to strengthen the main conclusion below. If the field begins in its Bunch-Davies vacuum the corresponding WKB solution is  $\chi_k \sim \exp(-i \int \omega_k(t') dt')$ , where  $\omega_k$  is time-dependent frequency corresponding to the terms inside the brackets in (6.3). Particle production occurs if the adiabatic conditions fail corresponding to  $\dot{\omega}_k \gg \omega_k^2$  or  $\ddot{\omega}_k \gg \omega_k^3$ , etc... Thus, a necessary condition for preheating is

$$\frac{\dot{\omega}_k}{\omega_k^2} \simeq \frac{g^2 \phi \dot{\phi}}{(k^2 + m_\chi^2 + g^2 \phi^2)^{3/2}} > 1, \quad (6.4)$$

corresponding to the production of modes with their momenta satisfying

$$k^2 \lesssim \left(g^2 \phi \dot{\phi}\right)^{2/3} - g^2 \phi^2 - m_\chi^2. \quad (6.5)$$

The ratio in (6.4) is maximal when the inflaton is near the bottom of the potential, where we can approximate  $\dot{\phi}_0 \simeq m_\phi \Phi$ . Broad resonance [25] will assure us that preheating is successful. This corresponds to a restriction on the range of wave numbers in the resonance band  $\Delta k \gg m_\phi$ . Maximizing the right side of (6.5) with respect to  $\phi$ , we find the maximum value of  $\phi_*^2 \simeq 0.2 \dot{\phi}/g$  corresponding to a maximum value of resonant momentum  $k_*^2 = 0.4 g \dot{\phi} - m_\chi^2$ . Therefore the condition for broad resonance  $\Delta k \simeq k_* \gg m_\phi$  can be written as a condition on the coupling constant  $g$ ,

$$g \gg \frac{m_\phi^2 + m_\chi^2}{\dot{\phi}} \simeq \frac{m_\phi^2 + m_\chi^2}{m_\phi \Phi}. \quad (6.6)$$

Taking  $\Phi \simeq 0.3 m_{\text{pl}}$  and assuming  $m_\chi \ll m_\phi$  we find  $g \gg 3.8 \times 10^{-5}$  for efficient preheating in the broad resonance regime.

On the other hand, we can obtain a lower bound on the strength of the coupling by requiring the one-loop correction induced by the  $g^2 \phi^2 \chi^2$  interaction to not to spoil the flatness of the potential during inflation. That is, we require  $\delta m_\phi \lesssim m_\phi \simeq 6.4 \times 10^{-6} m_{\text{pl}}$ , whereas the loop correction is  $\delta m_\phi^2 = (g^2 \Lambda_{\text{uv}}^2)/(16\pi^2)$ . The cut-off is expected to be Planckian  $\Lambda_{\text{uv}} \approx m_{\text{pl}}$ , implying  $g < 10^{-5}$ . Clearly, this result implies that the required value of the coupling,  $g$ , to obtain efficient preheating is inconsistent with having a naturally light inflaton during inflation. In other words, in general it is expected that heavy  $\chi$  fields running in the loops induced by the direct coupling  $g^2 \phi^2 \chi^2$  tends to de-stabilize parameters of the inflationary sector if we insist on the effective particle production at the end of inflation.

We have a good understanding of the limitations to the approximations we have used above to constrain preheating in chaotic inflation models, especially since these toy models have been well-studied over the years to establish when they lead to

successful reheating. At the same time, it is clear that we are seeing tension in analytic expectations for finding reliable preheating models. It is also clear that doing a full non-linear analysis for all parameters in all models of preheating is not an efficient way to do model analysis. Can one always establish a connection between the parameters during inflation and those same parameters during reheating? What is the expected mass of the reheat fields during inflation? Can't the inflaton just decay through higher dimensional operators present at the time of reheating? These are some of the questions we hope to address by developing a more systematic approach to reheating below.

## 6.3 Reheating in Weinberg's Covariant formulation of the EFT of Inflation

In this section, we extend Weinberg's EFT approach to inflation [293] to include the end of inflation and the beginning of (p)reheating. Focusing on a two-field scalar field model for simplicity, we present both analytic and numeric results from our investigation into the background evolution and the resulting particle production. We find that consistency of the background EFT within this approach limits its applicability and how well it can be used to successfully describe (p)reheating. This will motivate us to consider a different approach in Section 6.4.

### 6.3.1 Construction of the EFT

Following [293] we consider the most general EFT of a scalar field in General Relativity which can be written as

$$\mathcal{L}_{\text{inf}} = -\frac{1}{2}m_{\text{pl}}^2 R - \frac{1}{2}(\partial\phi)^2 - V(\phi) + \frac{c_1}{\Lambda^4}(\partial\phi)^4, \quad (6.7)$$

where  $\Lambda$  is the UV cutoff of the theory, in general  $c_1 = c_1(\phi)$  is an arbitrary function of the scalar, and we have neglected terms involving the Weyl tensor which are suppressed relative to the leading correction [293]. Assuming that the equations of motion admit inflationary solutions it was shown in [293] that this is also the most general EFT for the inflationary background (to be contrasted to the EFT for the perturbations which we will discuss in Section 6.4).

CMB observations imply that the power spectrum of scalar fluctuations is nearly scale-invariant, which can be realized through an approximate shift symmetry for the inflaton. This allows us to approximate  $c_1(\phi)$  as nearly constant during inflation (its time evolution is slow-roll suppressed). When the EFT expansion is applicable, *i.e.*  $\Lambda > \dot{\phi}^{1/2}$ , self-interactions of the inflaton are small and non-Gaussianity is negligible [37].

We now introduce an additional scalar that will play the role of the reheat field after inflation. For simplicity, we will focus on the situation where the reheat field has an effective mass of at least the Hubble-scale during inflation to avoid considering multi-field inflation. However, the reheat field's mass during inflation is an important consideration which we comment on later. Given these assumptions the starting point of our analysis is similar in spirit to that of [307], where those authors considered the EFT of the inflationary background coupled to an additional scalar sector during inflation. Again working to next-to-leading order in the derivative expansion we can introduce the Lagrangian for the additional scalar  $\chi$ ,

$$\mathcal{L}_\chi = -\frac{1}{2}(\partial\chi)^2 - U(\chi) + \frac{c_2}{\Lambda^4}(\partial\chi)^4, \quad (6.8)$$

where  $c_2$  and  $U(\chi)$  are arbitrary functions of  $\chi$ , but can not contain the inflaton due to its approximate shift symmetry<sup>2</sup>.

Finally, we can introduce the interactions between the two sectors that respect

---

<sup>2</sup>The spontaneous or explicit breaking of the shift symmetry at the time of reheating can be important and creates an additional limitation of this approach.

the inflaton's shift symmetry – implying that terms of the form  $\phi^p \chi^q$  are forbidden. At the level of dimension five operators it was shown in [307] that the shift symmetry can be used to forbid the operators  $\partial_\mu \phi \partial^\mu \chi$  and  $\chi \partial_\mu \phi \partial^\mu \chi$ . Similar arguments can be used at the level of dimension six operators and we find the two leading interactions<sup>3</sup>

$$\mathcal{L}_{\text{mix}} = -c_3 (\partial\phi)^2 \frac{\chi}{\Lambda} - c_4 (\partial\phi)^2 \frac{\chi^2}{\Lambda^2} + \mathcal{O}\left(\frac{1}{\Lambda^3}\right), \quad (6.9)$$

where  $c_3$  and  $c_4$  are expected to be order one constants and positive (for a UV completable EFT [308] and to avoid pathological instabilities [309]). Given our discussion and assumptions above, the EFT of Inflation with an additional to-be reheat field is then given by,  $\mathcal{L} = \mathcal{L}_{\text{inf}} + \mathcal{L}_\chi + \mathcal{L}_{\text{mix}}$ . Focusing on the leading interactions we have

$$\mathcal{L} = \frac{1}{2} m_{\text{pl}}^2 R - \frac{1}{2} f\left(\frac{\chi}{\Lambda}\right) (\partial\phi)^2 - \frac{1}{2} (\partial\chi)^2 - V(\phi) - U(\chi), \quad (6.10)$$

where

$$f\left(\frac{\chi}{\Lambda}\right) = 1 + 2c_3 \frac{\chi}{\Lambda} + 2c_4 \frac{\chi^2}{\Lambda^2}. \quad (6.11)$$

The dynamics of fluctuations that arise from (6.10) have been studied extensively in the context of inflation. In particular, there can be interesting signatures for both the power spectrum and higher point correlation functions (*e.g.* non-gaussianity) depending on the mass of  $\chi$  [310], its stabilization [238, 311–315], and whether the  $\chi$  and  $\phi$  sectors are strongly or weakly mixed [316].

In this work we are interested in connecting this system to the end of inflation and reheating. In particular, we would like to investigate if (p)reheating of the  $\chi$  sector can be achieved through the derivative couplings in (6.11) as these are the leading interactions allowed by the shift symmetry of the inflaton.

We note that (p)reheating with derivative couplings has been considered before.

---

<sup>3</sup>We have taken the cutoff of the EFT to be the same for both the inflationary and hidden sector for simplicity, although this need not be the case. We expect our main conclusions in this section to be insensitive to this assumption.

The authors of [317] have studied a particular realization of the EFT we are considering in this work. In their case the approximate shift symmetry of the EFT resulted from a specific UV completion motivated by Natural Inflation [240], where the spontaneous (and explicit) breaking of a  $U(1)$  symmetry of a complex scalar resulted in an inflaton associated with the pseudo-Nambu-Goldstone Boson (pNGB) and the reheat field corresponded to the excitation of the radial direction. The UV theory took the form

$$\mathcal{L} = -(\partial_\mu \Phi)(\partial^\mu \Phi^*) - \lambda(F^2 - \Phi^* \Phi), \quad (6.12)$$

where the  $U(1)$  symmetry is broken by the vacuum solution  $\langle |\Phi| \rangle = F$ . The inflaton potential results from the explicit breaking term

$$V(\phi) = \mu^4 \left[ 1 - \cos \left( \frac{\phi}{F} \right) \right]. \quad (6.13)$$

Expanding around the vacuum solution using

$$\Phi = (F + \chi) e^{i\phi/F}, \quad (6.14)$$

one can easily see that this particular model can be recast as the EFT of the matter sector given by the Lagrangian (6.10) with the replacement  $\Lambda \rightarrow F$ . We note that in this particular class of models, adequate inflation unfortunately requires  $F \gg m_{\text{pl}}$ , which seems to be at odds with additional non-perturbative corrections and expectations from quantum gravity [318, 319]. However, we emphasize that the (bottom-up) EFT approach we are taking here is more general than this particular class of models. In particular, we emphasize (see also [307]) that the symmetries resulting in (6.10) may be the result of a fundamental symmetry of the UV theory (as in the example of [317]), but they can also be the result of an accidental symmetry in the IR, or the result of fine-tuning of the effective potential. In this way, the model of [317] provides a particular UV completion of the more general EFT approach we consider here. This

is analogous to the way in which EFT methods can capture phenomenology near the scale of Electroweak symmetry breaking, without one having a precise description of the UV physics and mechanism responsible for breaking Electroweak symmetry.

In general, the inflaton potential  $V(\phi)$  in our EFT is arbitrary and does not need to take the specific form given in (6.13). We also have that the scale  $\Lambda$  can be taken as  $\Lambda < m_{\text{pl}}$  without raising any immediate issues about the consistency of inflation. We will see the importance of this observation when we consider the dynamics of the background and fluctuations in the following sections.

### 6.3.2 Analysis of Reheating in the EFT

To justify using an EFT at the end of inflation, we need to ensure that the model is self-consistent, i.e. we have to check that there is a consistent background solution to the equations of motion for the fields,

$$\ddot{\phi} + 3H\dot{\phi} + \partial_{\chi}(\ln f)\dot{\phi}\dot{\chi} + f^{-1}\partial_{\phi}V = 0, \quad (6.15)$$

and

$$\ddot{\chi} + 3H\dot{\chi} - \frac{1}{2}(\partial_{\chi}f)\dot{\phi}^2 + \partial_{\chi}U = 0, \quad (6.16)$$

and that the background also admits a perturbative description. This procedure will allow us to study the existence (or non-existence) of resonant phenomena, and establish when viable preheating occurs.

We begin by studying the behavior of the background fields  $\phi_0$  and  $\chi_0$ . These are described by the following equations of motion,

$$\ddot{\phi}_0 + 3H\dot{\phi}_0 + \partial_{\chi}(\ln f)\dot{\phi}_0\dot{\chi}_0 + f^{-1}\partial_{\phi}V = 0, \quad (6.17)$$

and

$$\ddot{\chi}_0 + 3H\dot{\chi}_0 - \frac{1}{2}(\partial_{\chi}f)\dot{\phi}_0^2 + \partial_{\chi}U = 0. \quad (6.18)$$



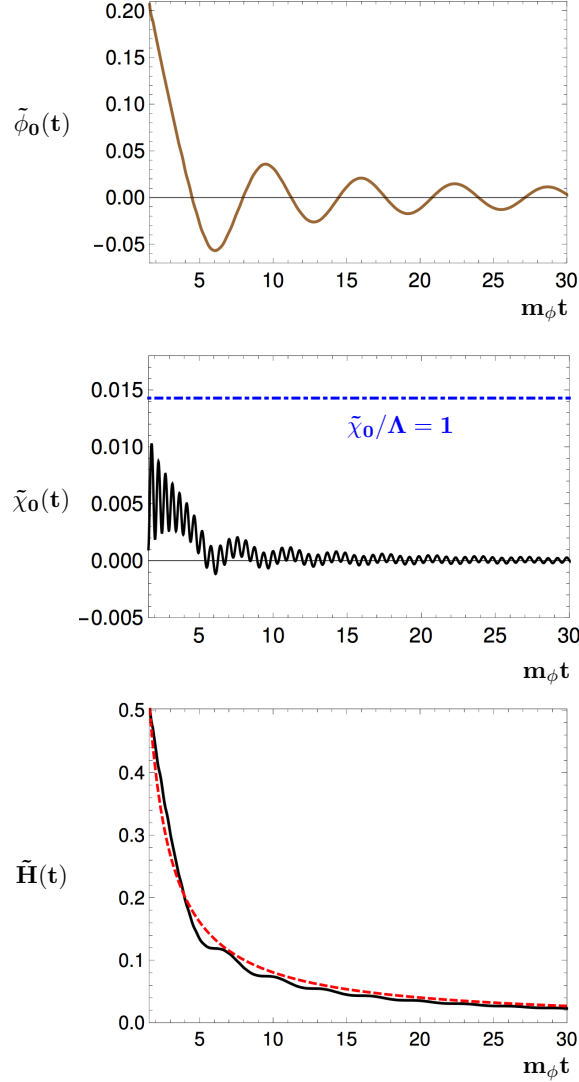


Figure 6.1: This figure gives the evolution of the background fields and Hubble parameter, where tildes imply we have normalized these quantities by  $\sqrt{8\pi}m_{\text{pl}}$ , and time is in units of the inflaton mass. For this realization we take  $m_\chi/m_\phi = 10$ ,  $m_{\text{pl}}/\Lambda = 14$  and initial conditions  $\phi_0 = 1.038 m_{\text{pl}}$ ,  $\dot{\phi}_0 = -0.662 m_{\text{pl}}$ ,  $\chi_0 = \dot{\chi}_0 = 0.005 m_{\text{pl}}$ . The top panel gives the evolution of the inflaton. In the middle panel the solid black curve is  $\tilde{\chi}_0(t)$  and below the dot-dashed blue horizontal line marks the region where the EFT of the background is valid. The bottom plot gives the Hubble rate where the red-dashed line represents a strictly matter dominated evolution.

If we further assume that the zero-mode dominates the energy density (and pressure) of the universe in the linear regime, then we can write down the evolution equations for the scale factor,

$$H^2 = \frac{1}{3m_{\text{pl}}^2} \left( \frac{1}{2} f \dot{\phi}_0^2 + \frac{1}{2} \dot{\chi}_0^2 + V(\phi_0) + U(\chi_0) \right), \quad (6.19)$$

and the Hubble parameter,

$$\dot{H} = -\frac{1}{2m_{\text{pl}}^2} \left( f \dot{\phi}_0^2 + \dot{\chi}_0^2 \right). \quad (6.20)$$

The first question that we need to address is whether the zero-mode of the reheat field acquires a significant displacement from zero. Using (6.11), and taking  $c_3$  and  $c_4$  to be order-one constants then (6.18) becomes

$$\ddot{\chi}_0 + 3H\dot{\chi}_0 + \partial_\chi U - \frac{\dot{\phi}_0^2}{\Lambda^2} \chi_0 - \frac{\dot{\phi}_0^2}{\Lambda} = 0, \quad (6.21)$$

The last two terms in (6.21) come from the EFT expansion – *i.e.* we have dropped terms in the Lagrangian of order  $\sim \dot{\phi}_0^2 \chi_0^3 / \Lambda^3$  and higher. Therefore, if either of these terms become large (e.g. if  $\chi_0 / \Lambda > 1$ ) then the EFT expansion of the background is not justified. Equation (6.21) is that of a harmonic oscillator with time-dependent frequency, where the last term resembles an external force, which we also require to be small compared to the restoring force from the effective potential. Assuming that  $U(\chi_0) \approx m_\chi^2 \chi_0^2 / 2$ , which is self consistent with our small-displacement assumption, we can find the stable minimum of the effective potential,

$$U_{\text{eff}} = U(\chi_0) - \frac{1}{2} \dot{\phi}_0^2 f \left( \frac{\chi_0}{\Lambda} \right). \quad (6.22)$$

to be

$$\chi_0(t) \simeq \frac{\dot{\phi}_0^2}{m_\chi^2 \Lambda} + \mathcal{O} \left( \frac{\dot{\phi}_0^4}{m_\chi^4 \Lambda^2} \right). \quad (6.23)$$

The velocity of the inflaton at the end of inflation is roughly  $\dot{\phi} \sim m_\phi m_{\text{pl}}$ , which allows us to write down an approximate condition on the size of  $\chi_0$ ,

$$\frac{\chi_0}{\Lambda} < 1 \tag{6.24}$$

implies that

$$\frac{m_\phi^2}{m_\chi^2} < \left( \frac{\Lambda}{m_{\text{pl}}} \right)^2 \tag{6.25}$$

That is, we find that we are free to lower the cutoff of the EFT below the Planck scale ( $\Lambda \ll m_{\text{pl}}$ ), but at the cost of increasing the mass of the reheat field above that of the inflaton. The fact that particle production is still possible in the  $m_\chi \gg m_\phi$  regime emphasizes the importance of preheating versus reheating, since in this situation perturbative decays are kinematically forbidden. It is also interesting that this condition is *independently* required so that the reheat field does not interfere with the the inflationary dynamics prior to reheating (constraints from non-Gaussianity could also be imposed). That is, even for  $m_\phi < m_\chi \simeq 3H_I$  such heavy fields can have a dramatic impact on inflation [238, 310–316]. We also note that the presence of a discrete  $Z_2$  symmetry could be used to forbid the dimension five operator leading to the tadpole in (6.21), and our stability condition (6.25) would still hold due to the presence of the dimension six operator.

We have numerically verified the result (6.25) by solving the system (6.17)-(6.19) for a range of masses, initial conditions, and the cutoff  $\Lambda$ . In Figure 6.1, we plot a particular realization of a consistent configuration for the background fields together with the evolution of the cosmological background. In the plot, we take  $m_{\text{pl}}/\Lambda = 14$  and  $m_\chi/m_\phi = 10$  consistent with (6.25). We see that the background value  $\chi_0$  stays consistent within the EFT regime, while inflaton oscillations proceed as in the case of a quadratic potential. On the other hand, it can be seen that the expansion of the universe is slightly faster than  $H(t) \propto t^{-1}$  initially, and then asymptotes to this behavior at late times  $m_\phi t \gg 1$ . We conclude this section by emphasizing that in

order to have a stable, well-behaved background solution within the regime of validity of the EFT, one requires the condition, (6.25) to be satisfied.

### Non-perturbative Dynamics and Limitations of the Background EFT

We now consider whether resonant particle production is possible around the background we analyzed in the previous section. Expanding both scalar fields to first order around their background values,  $\phi = \phi_0 + \delta\phi$ ,  $\chi = \chi_0 + \delta\chi$  in the Lagrangian (6.10), we write the equation of motion for the linearized fluctuations of the reheating field in Fourier space as

$$\delta\ddot{\chi}_k + 3H\delta\dot{\chi}_k + \left[ \left(\frac{k}{a}\right)^2 + m_\chi^2 - \frac{\dot{\phi}_0^2}{\Lambda^2} \right] \delta\chi_k = 2\frac{\dot{\phi}_0}{\Lambda} \left[ 1 + \frac{\chi_0}{\Lambda} \right] \delta\dot{\phi}_k, \quad (6.26)$$

where the terms on the right side are due to the mixing with inflaton fluctuations. These terms can source  $\delta\chi_k$  fluctuations whenever  $\delta\dot{\phi}_k$  is large. In the initial stage of (p)reheating the effect of this term will be negligible. Neglecting these terms, we focus on sub-Hubble scales first neglecting the cosmological expansion (we take  $a(t) \rightarrow 1$ ,  $H(t) \rightarrow 0$ ). In this approximation, (6.26) becomes

$$\delta\ddot{\chi}_k + \left[ k^2 + m_\chi^2 - \frac{\dot{\phi}_0^2}{\Lambda^2} \right] \delta\chi_k = 0, \quad (6.27)$$

where we define the frequency of the modes as  $\omega_k^2(t) = k^2 + m_\chi^2 - \dot{\phi}_0^2/\Lambda^2$ . Given a coherently oscillating inflaton,  $\phi_0 = \Phi(t) \sin(m_\phi t)$ , we can map this mode equation to the Mathieu equation

$$\delta\chi_k'' + [A_k - 2q \cos(2z)] \delta\chi_k = 0, \quad (6.28)$$

where we have defined the dimensionless time  $z = m_\phi t$  and  $A_k = (k^2 + m_\chi^2)/m_\phi^2 - 2q$  with  $q = \Phi^2/4\Lambda^2$ . Floquet's theorem [320] states that for a given wave-number, (6.26)

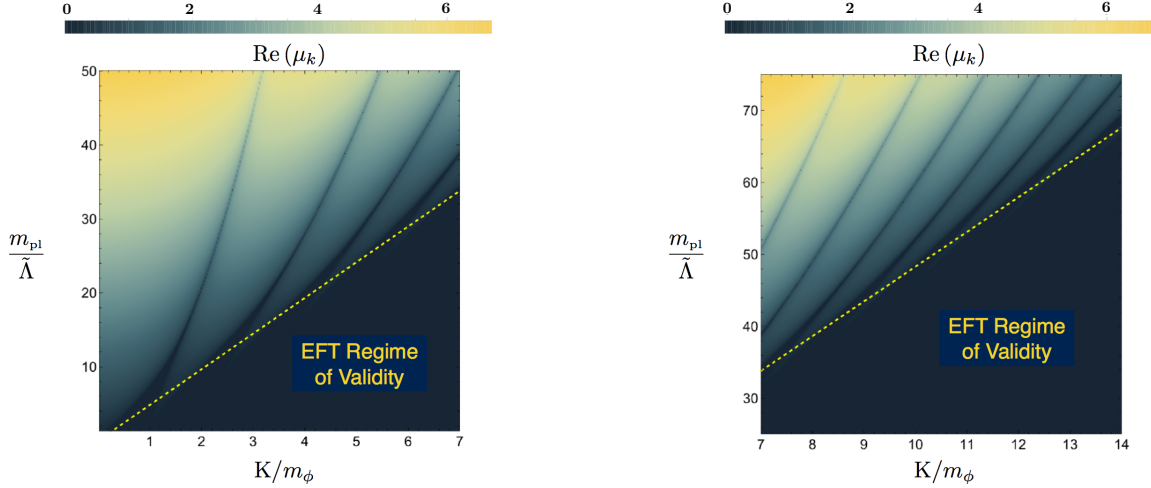


Figure 6.2: Instability band structure for the model  $V_{\text{tot}} = \frac{1}{2}m_\phi^2\phi^2 + \frac{1}{2}m_\chi^2\chi^2 - \frac{1}{2}\dot{\phi}_0^2 f\left(\frac{\chi}{\Lambda}\right)$ , where  $f$  is given by (6.11). This density plot represents the real part of the scaled Floquet exponent,  $\text{Re}(\mu_k)$ , where lighter regions represent larger values. The y-axis is the hierarchy between the Planck mass and the rescaled cut-off of the EFT,  $\tilde{\Lambda} = \Lambda/\sqrt{8\pi}$ , while the x-axis corresponds to  $K = \sqrt{k^2 + m_\chi^2}$  in units of  $m_\phi$ .

has solutions of the form

$$\delta\chi_k = e^{\mu_k z} g_1(z) + e^{-\mu_k z} g_2(z), \quad (6.29)$$

where  $g_1$  and  $g_2$  are periodic functions and  $\mu_k$  is the Floquet exponent. In general, the Floquet exponent  $\mu_k$  depends on the wave number  $k$ , the mass of the reheat field  $m_\chi$ , and the ratio  $\Phi/\Lambda$ . For cases where the real part of the exponent is non-zero, we have exponentially growing modes of  $\delta\chi_k$ .

The structure of (6.28) tells us that the resonant momenta are grouped into bands in parameter space. Since  $k^2 > 0$ , and hence,  $A_k > -2q$ , there are also meaningful statements one can make about the regions of the Mathieu parameter space that are probed by our reheating models. One interesting case is when some modes satisfy  $-2q < A_k < 0$ ; in this case, (6.28) assures us that there's a time when the mass-squared of these modes is negative (analogous to the cases explored in [321]) and

the Floquet exponent can be very large,  $\mu_k \simeq (4/\pi) q^{1/2}$  for  $q \gg 1$ . There's another case in which  $0 < A_k < 2q$ , where the mass-squared of some of the  $\delta\chi_k$  modes become tachyonic for certain time intervals and is also very efficient (analogous to [286].)

On the other hand,  $A_k$  is frequently larger than  $2q$ . While these models have parametric instabilities, the resonance structure requires us to be more careful. For our purposes here, the consistency of the background EFT requires the mass of the reheat field to satisfy  $m_\chi^2 > \dot{\phi}_0^2/\Lambda^2$ , which requires avoiding the regions of the parameter space that guarantee strong, broad, resonance. While the inflaton undergoes periodic oscillations this condition implies

$$m_\chi^2 > m_\phi^2 \frac{\Phi^2}{\Lambda^2}, \quad (6.30)$$

which is exactly what we have found in equation (6.25) with  $\Phi = m_{\text{pl}}$ . Here, we have used  $\phi(t) = \Phi \sin(m_\phi t)$  considering the maximum value of  $\dot{\phi}_0^2/\Lambda^2$ . We have also studied this system numerically, using FloqEx [322], with our results appearing in Figure 6.2. The figure shows the magnitude of the Floquet exponent as a function of cutoff and wave number. One can see the broad (and tachyonic) resonance regimes mostly live outside of those probed by the EFT. We must keep in mind, though, that these estimates could still produce some particles through parametric resonance, and should be studied through full lattice methods – we leave this to future work.

Our main conclusion thus far is that if we require the reheat field to respect the shift symmetry of the inflationary sector (implying adequate inflation consistent with CMB observations), successful reheating suggests considering an EFT cutoff far below the Planck scale  $\Lambda \ll m_{\text{pl}}$ . We saw that having such a sub-Planckian cutoff can quickly lead to the breakdown of the background EFT expansion when we require efficient reheating in the EFT.

As another example of when the EFT expansion may breakdown, consider the corrections we have thus far neglected in (6.7). When evaluated on the background

the operator contains a term

$$\frac{c_1}{\Lambda^4} (\partial\phi)^4 \supset \frac{c_1}{\Lambda^4} \dot{\phi}_0^2 (\partial\phi)^2. \quad (6.31)$$

During inflation this term will be slow-roll suppressed  $\dot{\phi}_0^2/\Lambda^4 \sim \epsilon H^2 m_{\text{pl}}^2/\Lambda^4$  and higher order terms will be even further suppressed as long as  $\Lambda$  is not far below  $m_{\text{pl}}$  during inflation<sup>4</sup>. However, for smaller values of the cutoff this corresponds to strong coupling of the background and our EFT approach breaks down – this would also lead to a large level of non-Gaussianity [316]. Assuming the background remains weakly coupled at the end of inflation we have

$$\frac{c_1}{\Lambda^4} \dot{\phi}_0^2 \sim \frac{m_\phi^2 \phi_e^2}{\Lambda^4} \sim \left(\frac{m_\phi}{m_{\text{pl}}}\right)^2 \left(\frac{\phi_e}{m_{\text{pl}}}\right)^2 \left(\frac{m_{\text{pl}}}{\Lambda}\right)^4, \quad (6.32)$$

so for  $\Lambda$  far below the Planck scale the EFT would again fail as this term would be as important as the kinetic term (and terms even higher in derivatives that we neglected would also be important). For example, in chaotic inflation where the inflaton mass is fixed by the COBE normalization this implies  $\Lambda \gtrsim 10^{-3} m_{\text{pl}}$ . We emphasize that this constraint has nothing to do with requiring adequate inflation and is an added constraint for the consistency of the derivative expansion of the EFT during reheating. We now turn to a different EFT approach where the challenges discussed in this section can be addressed.

## 6.4 The EFT of (p)Reheating

We have seen that using an EFT approach to the background has limited utility in simultaneously describing inflation and reheating. Indeed, in addition to the challenges discussed at the end of Section 6.3, an additional concern is that there could be terms

---

<sup>4</sup>Using the power spectrum normalization one can also show the condition  $\dot{\phi}_0^2/\Lambda^4 < 1$  implies a lower bound  $\Lambda/m_p \gtrsim \sqrt{\epsilon} 10^{-2}$ , where  $\epsilon = d(H^{-1})/dt$  is the slow-roll parameter.

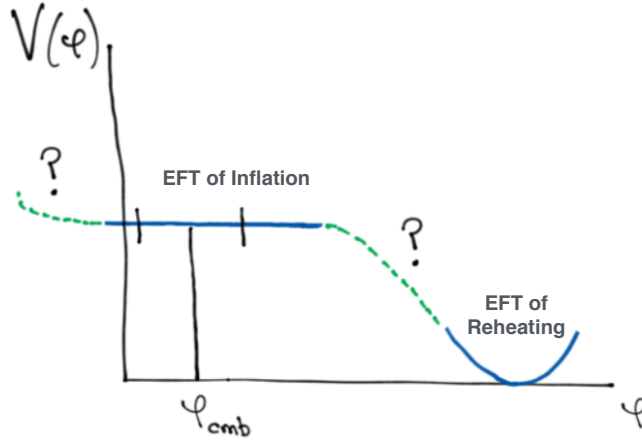


Figure 6.1: Obtaining adequate inflation, ending inflation and then successful reheating in the EFT requires a complete knowledge of the inflationary potential. This presents a challenge when using Weinberg’s EFT approach to capture reheating in many classes of models.

that badly break the shift symmetry at the time of reheating. Such terms could be small during inflation (suppressed by the breaking scale), but could be important at the time of reheating. Alternatively, there are many reheating models in which the shape of the potential during inflation is vastly different than it is during reheating (and could include additional fields like in hybrid models) and the background EFT approach requires a knowledge of the complete potential. This is illustrated in Figure 6.1.

In particular, the terms arising from the breaking of the shift symmetry of the inflaton (which would include thus far forbidden terms of the form  $g_i \phi^p \chi^q$ ) could become as important as the other terms we have considered in (6.26). As another example consider the potential

$$V = \frac{m^2 M^2}{2\alpha} \left[ \left( 1 + \frac{\phi^2}{M^2} \right)^\alpha - 1 \right]. \quad (6.33)$$

where  $\alpha < 1$ . This toy model captures many important inflationary models including axion monodromy [323]. During the inflationary phase this potential scales as  $V \sim$



$\phi^{2\alpha}$  and is sensitive to the scale  $M$ , whereas the behavior during reheating ( $\phi < M$ ) is independent of  $M$  and  $V \sim m^2\phi^2$ . So in our EFT approach expanding the field in powers of  $\phi/\Lambda$  is causing us to miss these types of theories.

In addition, new degrees of freedom could appear at the time of reheating that were heavy during inflation and could have been integrated out – in other words the EFT during inflation and the EFT during reheating can correspond to two distinct EFTs. This is not to say our approach doesn't capture many models. In particular, we've seen that the model of [317] is captured by our approach, and most chaotic inflation models would be as well. But even focusing only on the inflationary epoch we know that Weinberg's EFT is not capable of capturing a large number of interesting models. For example, in DBI type models where the background is in some sense strongly coupled one needs a non-perturbative expression for the background as it is a resummed expression where each derivative in the derivative expansion must be kept, e.g.  $V \sim \sqrt{1 - \dot{\phi}^2/\Lambda^4}$ . Such models are not captured by the Lagrangian of (6.7). One may also anticipate reheating models where the background of the reheat field could also exhibit such non-linear behavior and then the derivative expansion of the Lagrangian (6.8) would be inadequate – as well as the expansion of the mixing terms stopping at dimension six in (6.9). One final objection is that we have only concentrated on scalar reheat fields. Reheating to fermions and gauge fields is also important, and the way in which this proceeds is not only model dependent, but the spin statistics can also make important differences in the efficiency of reheating [324].

Given these shortcomings of the EFT of the background we now turn to construct an EFT for reheating along the lines of the EFT of Inflation [168]. As we will discuss, this approach can overcome many of the obstacles established in this Section. In the remainder of this section, we first begin by constructing an EFT focusing on the fluctuations directly at the end of inflation. This theory will share many similarities with the EFT of multi-field inflation [296, 316]. However there will be important differences which we will discuss. We then demonstrate how the approach

can reproduce both the results of self resonant reheating and multi-field reheating. We also discuss some new models that arise from considering the symmetries of the EFT.

### 6.4.1 Construction of the EFT of Fluctuations

The EFT expansion in fluctuations (rather than the background) relies on the fact that the background expansion of the universe spontaneously breaks time-translation invariance. Over the history of the universe there have been many different dominant forms of matter and energy, and so many different sources of time-translation breaking including; inflatons, post-inflation / pre-BBN fields, radiation, dark matter, and eventually dark energy today. As the universe passed through these phases the energy density changed its composition many times, but the scale factor continued to monotonically increase. The EFT approach takes this background evolution as given *a priori* (as specified by the background functions  $a(t)$ ,  $H(t)$ , and  $\dot{H}(t)$ ) and focuses directly on the most general EFT for the fluctuations around this background.

In taking this approach we give up on realizing explicit models for the background, and instead focus on implications and observations associated with the fluctuations. In regards to connecting with observations this approach is adequate<sup>5</sup>, since physical observables correspond to fluctuations and not background quantities [326]. The approach also has the advantage that the underlying physics responsible for driving the background expansion can be non-perturbative, in the sense that the background doesn't need to admit an EFT expansion (as we required in Section 6.3). Instead, this EFT approach is more general and models are classified by their symmetry breaking properties and the allowed operators in the Lagrangian correspond to cosmological perturbations. In many cases the symmetries alone can be used to establish rigid constraints on the theory of the fluctuations and associated observables. For example, it is well known that inflation requires that de Sitter symmetry must be non-linearly

---

<sup>5</sup>Although the connection to observables is not necessarily always straightforward [325].

realized and this leads to constraints on inflaton correlation functions. This fact is manifest in the EFT of Inflation approach using the corresponding Goldstone boson [326]. This EFT approach has also been shown to be useful when the cosmological background changes its behavior, e.g. in the EFT of dark energy [298–302], where one is primarily interested in observations during matter domination, but also must account for observations during dark energy domination.

The generality of the EFT approach when applied to cosmological backgrounds was first established in [295], where the authors were investigating violations of the Null Energy Condition in non-standard cosmologies. In that paper, referencing earlier work of Weinberg [327], it was pointed out that on long wavelengths there is always an adiabatic mode corresponding to the Goldstone boson of spontaneously broken time diffeomorphism invariance. Whenever a decoupling limit exists – in which the Goldstone decouples from gravity – this broken symmetry is then realized as spontaneously broken time translation invariance (the gauge symmetry effectively becomes a global symmetry). Thus, for any FRW spacetime it is possible to utilize the EFT approach and it is in this vain that we will construct our EFT for reheating following the initial ideas presented in [292].

As an example, suitable for studying the dynamics at the end of inflation, we can consider a decelerated FRW expansion with the background metric

$$ds^2 = -dt^2 + a^2(t)\delta_{ij}dx^i dx^j, \quad \ddot{a}(t) < 0. \quad (6.34)$$

We can think of this background as generated by the evolution of a set of homogeneous scalars<sup>6</sup> fields, *i.e.*  $\{\phi_0, \chi_0, \dots\}$ . In this work, to study dynamics at the end of inflation, we may consider only one of the scalars, *e.g.* the inflaton  $\phi_0$ , that contributes significantly to the evolution of scale factor,  $a(t)$ . This FRW evolution has a preferred time slicing described by the homogeneous scalar which can also be consid-

---

<sup>6</sup>In general, we are not restricted to scalar fields, *e.g.* another example can be a set of perfect fluids.

ered a clock. In order to describe the theory of fluctuations around this background, we can go to a co-moving frame (unitary gauge) where the vacuum expectation value of the scalar coincides with this privileged time slicing, corresponding to distinct values of  $\langle\phi\rangle = \phi_0$ . As we have fixed the slicing of space-time, general time diffs<sup>7</sup> are no longer a symmetry and the fluctuations of the scalar are hidden in the metric perturbations, which now describe three degrees of freedom: two transverse for the graviton and one for the scalar. We can always re-introduce inflaton fluctuations by a common local shift in time, *i.e.*  $t \rightarrow t + \pi(x)$ . By definition, such a fluctuation corresponds to an adiabatic fluctuation, proportional to Goldstone mode  $\delta\phi = \dot{\phi}_0\pi$  associated with the broken symmetry. In this work, apart from the adiabatic fluctuations, we will consider an additional degree of freedom  $X(t, x) = \chi_0(t) + \chi(t, x)$ , which will play the role of the (p)reheat field. As is standard in the literature we will take this field to be a subdominant source of background evolution during the first stages of preheating (*i.e.*  $\rho_\phi \gg \rho_\chi$ ) since before particle creation  $\langle X \rangle \simeq 0$ .

### The Action in Unitary Gauge

The procedure for constructing the EFT of fluctuations for the inflationary sector coupled to a reheat field *at the time of reheating* is similar to the case of quasi-single field inflation considered in [329]. Those authors considered the effects of particle production during inflation, whereas here we consider reheating and important differences will be discussed below. Nevertheless, the action can be constructed analogously and working in unitary gauge the action for the fluctuations is

$$S = \int d^4x \sqrt{-g} \left[ \frac{m_{\text{pl}}^2}{2} R - f_1(t) - f_2(t)g^{00} + F^{(2)}(\delta g^{00}, \chi, \delta R_{\mu\nu\rho\sigma}, \delta K_{\mu\nu}; \nabla_\mu; t) \right], \quad (6.35)$$

where  $f_1$  and  $f_2$  are arbitrary functions of time,  $F^{(2)}$  starts quadratic in operators which must be covariant in spatial indices but not in time,  $\nabla_\mu$  is the covariant deriva-

---

<sup>7</sup>As we mentioned before our main interest is the global part of time diffs, *i.e.* time translations. See [328] for more discussion on this matter.

tive, and  $\delta R_{\mu\nu\rho\sigma}$  and  $\delta K_{\mu\nu}$  are the fluctuations in the Riemann tensor and extrinsic curvature, respectively. Careful readers might wonder why we did not consider sums of terms that are linear in  $\chi$  and hence allowed in the unitary gauge,

$$\int d^4x \sqrt{-g} [f_3(t)\chi + f_4(t)\partial^0\chi], \quad (6.36)$$

where  $f_3$  and  $f_4$  are generic time dependent functions. We will work out these terms in Appendix 6.A and show that they can be re-written as second and higher order in terms of  $\delta g^{00}$ ,  $\chi$  and  $\delta K_\mu^\mu$  by taking into account background equation of motion for  $\chi$ . So the second and third terms in the above action are the only ones that contain linear perturbations. Requiring that terms linear in the fluctuations vanish (*i.e.* tadpole cancelation) follows from enforcing the background equations of motion in an FRW background [168],

$$3H^2 m_{\text{pl}}^2 = f_1(t) + f_2(t), \quad (6.37)$$

and

$$-2\dot{H} m_{\text{pl}}^2 = 2f_2(t). \quad (6.38)$$

As a simple example of tadpole cancelation, consider the end of inflation where the inflaton begins oscillating with a potential  $V(\phi)$  and where derivative interactions and the density of other fields are negligible. In this case the functions in (6.38) are given by  $f_1 = V(\phi_0)$  and  $f_2 = \dot{\phi}_0^2/2$ . However, more generally,  $f_1$  and  $f_2$  can take any form as long as the background corresponds to the (p)reheating period, *i.e.* an FRW universe with possibly small corrections due to oscillations. For example, we could have a preheating model corresponding to DBI-like models of inflation where a large number of derivative self-interactions could play an important role [330]. In that case the functions  $f_1$  and  $f_2$  would contain terms with an infinite number of derivatives at the level of the background. The key is that the behavior of the matter sector will be

captured by the functions  $f_1$  and  $f_2$ , and once we cancel the tadpoles, the background is then given (by the equations of motion) by  $H(t)$  and its derivatives. Then, we can focus on the EFT of the fluctuations about this background – just as in the case of the EFT of Inflation or DE [168, 298, 299]. Thus, the problem we encountered in the previous section, where we would need to keep all the terms in the  $\chi/\Lambda$  expansion is not an issue here. Instead, these terms are captured by  $H$  and  $\dot{H}$  and could represent re-summed, non-perturbative expressions for the background<sup>8</sup>. Moreover, because we are *not* performing a perturbative expansion of the background, we work under the assumption that we have a complete knowledge of the potential overcoming the problems associated with Figure 6.1.

The most general action is found by expanding the function  $F^{(2)}$  in (6.35) in terms of fluctuations  $\{\delta g^{00}, \chi, \delta K_{\mu\nu}, \delta R_{\mu\nu\rho\sigma}\}$  and their derivatives. We emphasize that this EFT expansion is one in perturbations and derivatives. During reheating, the fluctuations are also assumed to be initially small, however significant particle production can change this (as we will discuss). Whereas the derivative expansion follows from locality, causality and unitarity in an FRW universe. In the gravity sector,  $\delta g^{00}$  is a zero derivative object, whereas  $\delta K_{\mu\nu}$  corresponds to one derivative and  $\delta R_{\mu\nu\rho\sigma}$  to two, as they contain first and second order derivatives of the metric, respectively. When we introduce the Goldstone boson in the next section, it will be clear that terms with  $\delta K$  and  $\delta R$  will include higher derivatives of the Goldstone boson. Finally, we find it convenient to split the action in (6.35) into three parts

$$S = S_g + S_\chi + S_{g\chi}, \quad (6.39)$$

where the action  $S_g$  contains only terms build out of  $\{\delta g^{00}, \delta K_{\mu\nu}, \delta R_{\mu\nu\rho\sigma}\}$ ,  $S_\chi$  contains those purely from  $\chi$  and the action  $S_{g\chi}$  is due to mixing between gravity sector and

---

<sup>8</sup>The importance of strong coupling and resummation appears in many areas of physics including QCD and theories of modified gravity. See e.g. [331]. An approach to strong coupling during preheating, using methods of holography, appeared in [332, 333].

$\chi$ . Following our discussion above, we then have

$$S_g = \int d^4x \sqrt{-g} \left[ \frac{m_{\text{pl}}^2}{2} R - m_{\text{pl}}^2 \left( 3H^2(t) + \dot{H}(t) \right) + m_{\text{pl}}^2 \dot{H}(t) g^{00} + \frac{m_2^4(t)}{2!} (\delta g^{00})^2 + \dots \right], \quad (6.40)$$

$$S_\chi = \int d^4x \sqrt{-g} \left[ -\frac{\alpha_1(t)}{2} g^{\mu\nu} \partial_\mu \chi \partial_\nu \chi + \frac{\alpha_2(t)}{2} (\partial^0 \chi)^2 - \frac{\alpha_3(t)}{2} \chi^2 + \alpha_4(t) \chi \partial^0 \chi \right], \quad (6.41)$$

$$S_{g\chi} = \int d^4x \sqrt{-g} \left[ \beta_1(t) \delta g^{00} \chi + \beta_2(t) \delta g^{00} \partial^0 \chi + \beta_3(t) \partial^0 \chi - (\dot{\beta}_3(t) + 3H(t) \beta_3(t)) \chi \right], \quad (6.42)$$

where  $g^{00} = -1 + \delta g^{00}$  and the dots represent terms higher order in fluctuations and derivatives. Here,  $\{m_2(t), \alpha_i(t), \beta_i(t)\}$  are thus far arbitrary functions of time that are permitted in the unitary gauge as time diffs have been spontaneously broken by the background. We note that the coefficient of the  $\delta g^{00}$  operator is fixed by the background, implying that it is *universal* in the sense that all preheating models with the same background evolution will have the same coefficient (specified by  $H(t)$  and its derivatives). Whereas, the operator  $(\delta g^{00})^2$  is an example of a *non-universal* operator, because  $m_2$  is not fixed by the symmetries of the FRW background. Instead its value corresponds to a specific class of models (those with a non-unity sound speed). Similarly, broken time diffs generally allow for a term proportional to  $\alpha_2$  that leads to non-trivial sound speed  $c_\chi = \alpha_1 / (\alpha_1 + \alpha_2)$  in the reheat sector  $\chi$ . In (6.42), the functions  $\beta_i$  can be seen as a measure of the strength of mixing with gravitational fluctuations (including one scalar d.o.f). At this stage, the usefulness of this approach might be in question, given the large number of free parameters. However, as we will see in the following sections, even though this is the most general theory to quadratic order, in practice many of the terms in (6.40)-(6.42) are not important for elementary processes within reheating. Finally, we can further simplify the action by performing a field re-definition of  $\chi$ , using that  $\chi = 0$  on the background trajectory and using time reparametrization invariance to set  $\alpha_4 = \beta_3 = 0$  in the actions (6.41) and (6.42).

The form of (6.40), (6.41) and (6.42) are not particularly useful in studying the

dynamics as the scalar fluctuation representing inflaton is not manifest. We can re-introduce diffeomorphism invariance and the Goldstone mode related to inflaton by the Stückelberg trick, which will be our main focus in the following section.

### Introducing the Goldstone Boson

To introduce the Goldstone boson along with time diffs, we first perform the broken time diffs  $t \rightarrow t + \xi^0(t, \vec{x})$  in the actions (6.40)-(6.42). Since the cosmological background (*i.e.*  $H, \dot{H}$ ) as well as the free functions  $\{\alpha_i, \beta_i\}$  depend on cosmic time,  $t$ . The gauge function,  $\xi^0$ , will appear explicitly in the actions for the perturbations. We then replace  $\xi^0 \rightarrow \pi(t, \vec{x})$  everywhere it appears in the action and require that the Goldstone transforms non-linearly,  $\pi \rightarrow \pi - \xi^0$  under diffs. In this way, clearly full diffeomorphism invariance can be restored in (6.40)-(6.42). In order to find the explicit form of the actions including the Goldstone  $\pi$ , we need to know the transformation rule for the remaining operators appearing in (6.40)-(6.42) under  $t \rightarrow t + \pi$ . Under the transformation we have

$$\begin{aligned}
 g^{00} &\rightarrow g^{00} + 2g^{0\mu}\partial_\mu\pi + g^{\mu\nu}\partial_\mu\pi\partial_\nu\pi, \\
 g^{i0} &\rightarrow g^{i0} + g^{i\nu}\partial_\nu\pi, \\
 \partial^0\chi &\rightarrow \partial^0\chi + g^{\mu\nu}\partial_\mu\chi\partial_\nu\pi, \\
 f(t) &\rightarrow f(t + \pi)
 \end{aligned} \tag{6.43}$$

$$\begin{aligned}
 R_{\mu\nu\lambda\sigma} &\rightarrow R_{\mu\nu\lambda\sigma} \\
 \int d^4x\sqrt{-g} &\rightarrow \int d^4x\sqrt{-g}
 \end{aligned} \tag{6.44}$$



where  $f(t)$  represents any time-dependent function appearing in the action. Carrying out this procedure on the action (6.40) we find

$$\begin{aligned}
S_g = \int d^4x \sqrt{-g} & \left[ \frac{m_{\text{pl}}^2}{2} R - m_{\text{pl}}^2 \left( 3H(t+\pi)^2 + \dot{H}(t+\pi) \right) \right. \\
& + m_{\text{pl}}^2 \dot{H}(t+\pi) (g^{00} + 2g^{0\mu} \partial_\mu \pi + g^{\mu\nu} \partial_\mu \pi \partial_\nu \pi) \\
& \left. + \frac{m_2^4(t+\pi)}{2!} (\delta g^{00} + 2g^{0\mu} \partial_\mu \pi + g^{\mu\nu} \partial_\mu \pi \partial_\nu \pi)^2 \right]. \quad (6.45)
\end{aligned}$$

We see that this action is invariant under time diffs if we require the Goldstone to transform as  $\pi \rightarrow \pi - \xi^0(t, \vec{x})$ , *i.e.* the symmetry is non-linearly realized [296]. We also note that requiring the symmetry be realized in the UV has forced relationships between the various operators (all the terms in parentheses must have the same coefficients). Following the same steps, (6.41) and (6.42) become

$$\begin{aligned}
S_\chi = \int d^4x \sqrt{-g} & \left[ -\frac{\alpha_1(t+\pi)}{2} g^{\mu\nu} \partial_\mu \chi \partial_\nu \chi + \frac{\alpha_2(t+\pi)}{2} (\partial^0 \chi + \partial_\mu \pi \partial^\mu \chi)^2 \right. \\
& \left. - \frac{\alpha_3(t+\pi)}{2} \chi^2 \right], \quad (6.46)
\end{aligned}$$

$$\begin{aligned}
S_{g\chi} = \int d^4x \sqrt{-g} & \left[ \beta_1(t+\pi) (\delta g^{00} + 2\partial^0 \pi + \partial_\mu \pi \partial^\mu \pi) \chi \right. \\
& \left. + \beta_2(t+\pi) (\delta g^{00} + 2\partial^0 \pi + \partial_\mu \pi \partial^\mu \pi) (\partial^0 \chi + \partial_\mu \pi \partial^\mu \chi) \right]. \quad (6.47)
\end{aligned}$$

Similar to the discussion above, the non-linearly realized symmetry introduces interactions between  $\chi$  and the Goldstone,  $\pi$ .

To describe the dynamics at the end of inflation, working with the full action given by  $S_g + S_\chi + S_{g\chi}$  in complete generality is a difficult task. First of all, we need to have some input for the time-dependent functions, *i.e.*  $\{H(t), \alpha_i(t), \beta_i(t)\}$  appearing in the Lagrangian. However, as we will see, an investigation on the background dynamics during reheating along with the associated symmetries and scales of interest will allow us to obtain generic information on the form of these functions. This will be our main

focus in the next section.

## 6.4.2 Background Evolution During Reheating and Symmetries of the Action

### Background Evolution and Symmetries

In parametrizing the background expansion we have assumed a decelerating FRW universe. A simple example is provided by a perfect fluid with an equation of state  $w$  and with corresponding scale factor  $a(t) \propto t^{2/3(1+w)}$  and expansion rate  $H(t) = \dot{a}/a \propto t^{-1}$  with  $H^{-1}$  setting the cosmic time scale. On the other hand, in studies of the dynamics at the end of inflation the frequency of inflaton oscillations introduce another important time scale. For example, if the inflaton oscillates in a power-law potential,  $V \propto \phi_0^n$ , the period of oscillations will be  $2\pi\omega^{-1} = 4 \int_0^{\phi_i} d\phi_0 (V(\phi_i) - V(\phi_0))^{-1/2}$ , which for general  $n$  depends on the initial amplitude,  $\phi_i$  [334]. In the limit that the period of oscillations is much smaller than the expansion time scale,  $\omega^{-1} \ll H^{-1}$ , coherent scalar field oscillations behave like a perfect fluid with an average equation of state,  $\langle w \rangle_a = (n - 2)/n + 2$  [93].

The presence of two different time scales leads to interesting symmetry breaking patterns within the EFT, and whether a symmetry is realized will depend on the dynamics under investigation. At high energies (or small wavelengths) the energy being probed  $E_{\text{probed}}$  exceeds both the oscillation and expansion energy *i.e.*  $E_{\text{probed}} \gg \omega \gg H$  and so the time evolution of the oscillator and the cosmic expansion is negligible – time-translations are a good symmetry. As we lower the energy scale to  $E_{\text{probed}} \lesssim \omega$  we first break time-translation invariance down to a discrete symmetry  $t \rightarrow t + 2\pi\omega^{-1}$ . Then as we further lower the energy to  $E_{\text{probed}} \lesssim H \ll \omega$  this discrete symmetry is further broken by the cosmic expansion. This symmetry breaking reflects that on large scales (low-energy) we have an expanding universe, but on sub-Hubble scales the only time dependence results from the oscillating scalar field and the effect

of the expansion can be ignored. And at even higher energies (smaller distances / faster time scales) the scalar oscillations would not be probed.

This hierarchy in scales can be captured by parameterizing the background behavior by a Hubble rate that is a sum of a monotonically evolving part and a small rapidly oscillating component,

$$H(t) = H_{\text{FRW}}(t) + H_{\text{osc}}(t)P(\omega t), \quad (6.48)$$

where the first term is adiabatically evolving  $H_{\text{FRW}}(t) \propto t^{-1}$  and monotonically decreasing, whereas the second term leads to an oscillatory correction described by a general periodic function  $P(\omega t)$  with period  $T = 2\pi\omega^{-1}$ . In order to ensure an overall monotonic FRW evolution we take the first term to be dominant,  $H_{\text{FRW}} \gg H_{\text{osc}}$ . This implies our clock is always monotonically increasing – as exemplified by the monotonic evolution of the scale factor  $a(t)$  in an FRW universe. This situation is to be contrasted with models where the universe itself is oscillating [335], which can exhibit a number of pathologies [309]. We also note that the time dependence of  $H_{\text{FRW}}$  and  $H_{\text{osc}}$  is slow compared with the time scale of oscillations  $\omega^{-1}$ , *i.e.*  $\dot{H}_{\text{FRW}}/(H_{\text{FRW}}\omega) \sim \dot{H}_{\text{osc}}/(H_{\text{osc}}\omega) \ll 1$ . This corresponds to our earlier statement that on short time scales (larger energies) there is an approximate discrete symmetry.

An important question is whether we can generalize the symmetry arguments above for the time-dependent functions associated with the non-universal operators in (6.45)-(6.47), *i.e.*  $\{m_2, \alpha_i, \beta_i\}$ . On general grounds, in an FRW background described by (6.48) we expect that the functions  $m_2, \alpha_i, \beta_i$  – which describe the self-couplings, and couplings/mixings between the Goldstone and the reheat sector  $\chi$  – to be a generic function of the Hubble rate in (6.48) and its derivatives. Depending on the couplings between these sectors this suggests that in general we can write these functions in the form

$$F_i(t) = M_i^P(t)P'(\omega' t), \quad (6.49)$$

where in general the periodic function  $P'$  is different from the one in (6.48) as is the frequency  $\omega' \neq \omega$ . Here, the index  $i$  collectively represents time-dependent functions  $\{m_2, \alpha_i, \beta_i\}$  and  $p$  denotes the mass dimension of these functions. Suggested by the symmetry breaking pattern we discussed above, we can similarly take  $\dot{M}_i/(M_i\omega) \ll 1$ .

## Symmetries of the Action and Implications

An important consequence of the discrete symmetry of the Goldstone is that non-derivative interactions can appear in the action. When this is a good symmetry we can expand the background and non-universal parameters  $\{H, \dot{H}, m_2, \alpha_i, \beta_i\}$  in the form

$$F_i(t + \pi) = F_i(t) + \dot{F}_i(t)\pi + \frac{1}{2}\ddot{F}_i(t)\pi^2 + \dots \quad (6.50)$$

This breaking is similar in spirit to the work of [336], where those authors considered resonant non-Gaussianity induced through small-scale oscillations in  $H$  and  $\dot{H}$  during single-field inflation. In the two-sector EFT we are considering here we can extend that study to dynamics that arise in the presence of interactions between the Goldstone  $\pi$  and reheating  $\chi$  sectors. Moreover, contrary to the situation during inflation, where there is a fixed energy scale corresponding to horizon crossing, [168], to study dynamics at the *end* of inflation we are often interested in the dynamics at sub-Hubble scales. For sub-Hubble scales with  $E_{\text{probe}} > \omega$  we expect interactions induced by expanding the time-dependent functions in (6.50), which parametrize important contributions to the dynamics. Such interactions can induce large loop corrections for the parameters of the EFT, and additionally back-reaction effects can become large and the perturbative expansion of the EFT of fluctuations will fail. In typical studies of preheating, the importance of such contributions correspond to the end of ‘stage one’, which can be followed by turbulence and chaotic behavior [25]. We leave an investigation of these stages to future work. In the following, we will focus on the first stages of preheating and establish how our framework captures existing models. We will also explore new models and their connection to observations during the first

stages of preheating.

### 6.4.3 Capturing Existing Models

#### Reheating Through Self-Resonance

In this section, we focus on the Goldstone sector in (6.45) to construct models of reheating through self-resonance. That is, we want to establish how the EFT reproduces self-resonant models of reheating where inflaton ‘particles’ (here corresponding to the Goldstone  $\pi \sim \delta\phi$ ) are created from oscillations of the background condensate  $\phi_0(t)$ . We will also consider when gravitational fluctuations can be shown to decouple. To begin we expand the time-dependent functions in (6.45) and use the ADM decomposition<sup>9</sup> of the metric in spatially flat gauge working to second order in fluctuations  $\delta N, N^i$  and  $\pi$ . We have

$$\begin{aligned} \mathcal{L}_{\pi_c} &= \frac{1}{2} \left( \dot{\pi}_c^2 - c_\pi^2 \frac{(\partial_i \pi_c)^2}{a^2} \right) - \frac{1}{2} m_\pi^2(t) \pi_c^2 - \frac{(-2\dot{H})^{1/2}}{c_\pi} \left( \dot{\pi}_c \delta N_c - \frac{1}{2} \left( \frac{\ddot{H}}{\dot{H}} - 2 \frac{\dot{c}_\pi}{c_\pi} \right) \pi_c \delta N_c \right) \\ &+ (-2\dot{H})^{1/2} c_\pi (3H \delta N_c + \partial_i N_c^i) \pi_c + \dots \end{aligned} \quad (6.51)$$

where we introduced the canonical fields  $\pi_c = \sqrt{-2\dot{H}m_{\text{pl}}^2} c_\pi^{-1} \pi$ ,  $\delta N_c = m_{\text{pl}} \delta N$ ,  $N_c^i = m_{\text{pl}} N^i$ , the sound speed of the fluctuations is  $c_\pi^2 = m_{\text{pl}}^2 \dot{H} / (m_{\text{pl}}^2 \dot{H} - m_2^4)$ , and we neglect terms involving the scalar curvature as they are sub-leading.

An important consequence of the background evolution and time-dependent sound speed is that it induces a time-dependent mass<sup>10</sup> for the Goldstone

$$m_\pi^2 = -3\dot{H}c_\pi^2 - \frac{1}{4} \left( \frac{\ddot{H}}{\dot{H}} - 2 \frac{\dot{c}_\pi}{c_\pi} \right)^2 - \frac{3H}{2} \left( \frac{\ddot{H}}{\dot{H}} - 2 \frac{\dot{c}_\pi}{c_\pi} \right) - \frac{1}{2} \partial_t \left( \frac{\ddot{H}}{\dot{H}} - 2 \frac{\dot{c}_\pi}{c_\pi} \right), \quad (6.52)$$

which we note would vanish in a strictly de Sitter limit with constant sound speed (fa-

<sup>9</sup>Details appear in Appendix A

<sup>10</sup>This is the mass term in the absence of mixing terms given in the second and third lines of (6.51).

miliar from the EFT of Inflation). Resonant effects induced by such time dependence of  $c_\pi$  is an interesting possibility that we will explore in future work. For simplicity, here we will focus on the time-dependence of the background and assume that the time dependence of the sound speed is negligible.

To understand the Goldstone dynamics we first identify the energy scales at which different phenomena become important. An important scale is the symmetry breaking scale below which we are able to focus on the EFT of the perturbations (we can ‘integrate out the background’) and the Goldstone description can be useful. Following closely the example of [316], we can identify the Noether current associated with the broken symmetry by introducing ‘fake’ Lorentz invariance in (6.51) by rescaling the spatial coordinates

$$\tilde{\mathcal{L}}_g = -\frac{1}{2}(\tilde{\partial}\tilde{\pi}_c)^2 + \dots, \quad (6.53)$$

where  $\tilde{x} \equiv c_\pi^{-1}x$ ,  $\tilde{\mathcal{L}}_g \equiv c_\pi^3\mathcal{L}_g$  and  $\tilde{\pi}_c = (-2\dot{H}m_{\text{pl}}^2c_\pi)^{1/2}\pi_c$ . The Noether current associated with (6.53) is then  $\tilde{J}^\mu = -\Lambda_{\text{sb}}^2\partial^\mu\tilde{\pi}_c$ , and the symmetry breaking scale is given by<sup>11</sup>  $\Lambda_{\text{sb}}^2 = (-2\dot{H}m_{\text{pl}}^2c_\pi)^{1/2}$ .

For the simplest models, with unity sound speed, we have  $\Lambda_{\text{sb}}^2 = (-2\dot{H}m_{\text{pl}}^2)^{1/2}$ , and this agrees with expectations that the time evolution of the background is responsible for breaking the time translation symmetry ( $H(t)$  is changing in time). In particular, given the background evolution in (6.48) we are interested in the time averaged value  $\Lambda_{\text{sb}}^2 \equiv \langle(-2\dot{H}m_{\text{pl}}^2c_\pi)^{1/2}\rangle_T \approx H_{\text{FRW}}m_{\text{pl}}c_\pi^{1/2}$ . For energy scales where  $E < \Lambda_{\text{sb}}$  the Goldstone description of (6.51) is valid. We emphasize that we are focusing on fluctuations around a decelerating FRW background, and so the symmetry breaking scale is more dependent on time<sup>12</sup> than the inflationary case *i.e.*  $\Lambda_{\text{sb}}^2 \propto t^{-1}$ . However, in the presence of resonance and with strong enough couplings to the reheating sector to make reheating efficient, it is justified to take a decoupling limit

---

<sup>11</sup>We present the scale in terms of energy, but it is important to remember that since Lorentz invariance is spontaneously broken energy scales do not necessarily coincide with momenta [168].

<sup>12</sup>This raises the interesting issue of ‘level crossing’, which is ubiquitous when applying EFT to gravitational systems [337].

$H_{\text{FRW}} \rightarrow 0$  and  $m_{\text{pl}} \rightarrow \infty$ , such that the combination  $H_{\text{FRW}}m_{\text{pl}}$  remains fixed. In this case, an evolving symmetry breaking scale is unimportant for the validity of the Goldstone description – all that is required is a hierarchy of scales  $\Lambda_{\text{sb}} \gg \omega$  where  $\omega$  is the oscillation time scale associated with the background evolution that appeared in (6.48).

Another important scale in understanding the Goldstone dynamics is the energy scale where mixing with gravitational fluctuations becomes important ( $E_{\text{mix}}$ ). Consider the frequency of the Goldstone  $\pi_c$  in Fourier space and in the absence of mixing terms

$$\omega_\pi^2 = \frac{c_\pi^2 k^2}{a^2} + m_\pi^2(t) + \dots, \quad (6.54)$$

where dots represent sub-leading contributions of order  $H^2$ . We emphasize that  $\omega_\pi$  is the frequency of the Goldstone, whereas the inflaton oscillations have a frequency we continue to denote by  $\omega$  which is often comparable to the Goldstone mass  $\omega \sim m_\pi$  as follows from (6.48) and (6.52). Remembering this distinction, we note that contrary to the inflationary case, we are not interested in the dynamics at a fixed energy scale, and in general whether mixing with gravity is important will depend on the scales one is interested in. For example, we can separate the Goldstone modes into relativistic  $\omega \lesssim c_\pi k/a$  (or equivalently  $m_\pi \lesssim c_\pi k/a$ ) and non-relativistic  $\omega > (c_\pi k)/a$  modes. For relativistic modes, time derivatives scale the same as spatial ones in (6.51), *i.e.*  $\dot{\pi}_c^2 \sim c_\pi^2 (\partial_i \pi_c/a)^2 \sim \omega_\pi^2 \pi_c$ . On the other hand, for non-relativistic modes, spatial derivatives are less important than time derivatives and terms involving the spatial kinetic terms can be compared with the mixing terms in (6.51). The most relevant mixing term<sup>13</sup> between  $\pi_c$  and gravitational fluctuations is given by

$$\mathcal{L}_{\text{mix}} \supset \frac{(-2\dot{H})^{1/2}}{2c_\pi} \frac{\ddot{H}}{\dot{H}} \pi_c \delta N_c. \quad (6.55)$$

---

<sup>13</sup>Another equally important term is the one proportional to  $\dot{\pi}_c \delta N_c$ . When we solve for  $\delta N_c$  in terms of  $\pi_c$  and use this solution in (6.51), we can integrate by parts the time derivative on  $\pi_c$  leading to a term comparable to (6.55).

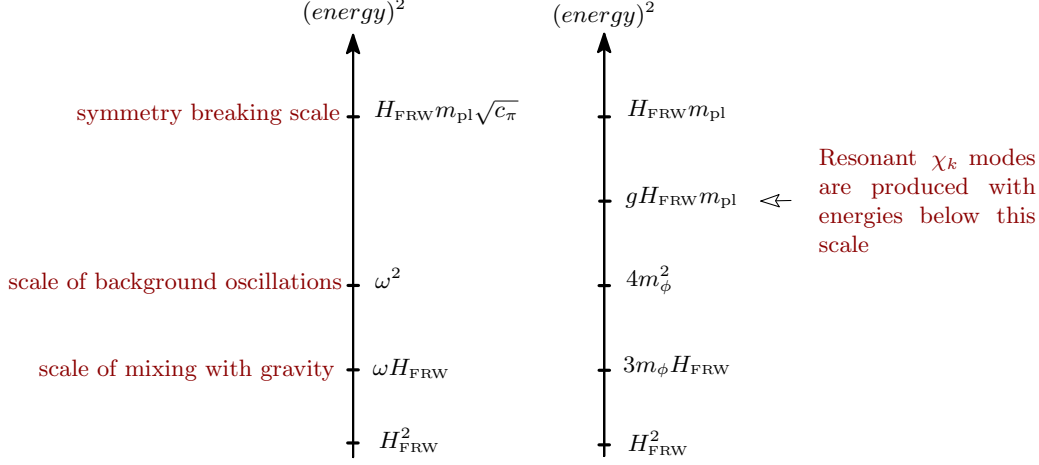


Figure 6.2: Relevant energy scales for the preheating models considered in Section 6.4.3. On the left, we have the hierarchy in energy scales associated with the dynamics of the Goldstone boson with a sound speed  $c_\pi$  following our general discussion of self-resonant models. The right diagram shows the hierarchy of scales for the example of canonical two-field preheating models.

From Appendix A, we use the solution  $\delta N_c \approx c_\pi \pi_c$  in (6.55) and note that  $\dot{H} \approx H^2$ ,  $\ddot{H} \approx \omega H^2$  (where we keep the leading terms). This leads to  $\mathcal{L}_{\text{mix}} \approx \omega H \pi_c^2$  from which we can see the energy scale at which mixing with gravity becomes important is  $E_{\text{mix}} \approx (\omega H)^{1/2}$ . For relativistic modes, mixing with gravity is always irrelevant as  $\omega_\pi^2 > \omega^2 \gg \omega H$ . For non-relativistic modes, we compare the mixing term with the spatial kinetic term in (6.51). This leads to the conclusion that mixing with gravity will be important for modes with momenta satisfying the following condition,

$$\frac{k}{a} \lesssim \frac{\sqrt{\omega H}}{c_\pi} \quad (6.56)$$

**An explicit example:** The generic construction above is useful in studying models of inflaton self-resonance. Consider an example where mixing with gravity at the end of inflation leads to resonant effects for  $\pi_c$ . For this purpose, we consider a simple limit of the unitary gauge action in (6.40) where  $m_2 = 0$ ,  $m_{\text{pl}}^2(3H^2 + \dot{H}) = V(\phi_0) = m_\phi^2 \phi_0^2 / 2$ , and  $\dot{H} m_{\text{pl}}^2 = -\dot{\phi}_0^2 / 2$ . These choices correspond to a cosmology dominated by a single scalar field – the inflaton. In the regime where  $m_\phi \gg H$ , the



background condensate oscillates around the minimum of its potential  $V = m_\phi^2 \phi_0^2/2$ , and in this case we can solve for the background evolution [338]

$$H(t) = H_{\text{FRW}}(t) - \frac{3H_{\text{FRW}}(t)^2}{4m_\phi} \sin(2m_\phi t) + \dots, \quad (6.57)$$

where  $H_{\text{FRW}} = 2/(3t)$  is the Hubble rate in a matter dominated universe with scale factor  $a(t) \propto t^{2/3}$  and dots represent terms suppressed by higher powers of  $H_m/m_\phi$ . This solution has exactly the form proposed in (6.48) with  $H_{\text{osc}} \equiv -3H_{\text{FRW}}^2/4m_\phi$ ,  $\omega \equiv 2m_\phi$ , and we also have  $H_{\text{FRW}} \ll m_\phi$ .

Given the background evolution in (6.57), we can now consider the dynamics of  $\pi_c$ . To reproduce this class of models we take the  $c_\pi \rightarrow 1$  limit, and solve for the constraints  $\delta N_c$  and  $N_c^i$ . Using our results from Appendix A, along with (6.51) we have

$$\mathcal{L}_{\pi_c} = -\frac{1}{2}(\partial\pi_c)^2 - \frac{1}{2}\left(m_\pi^2(t) + m_{\text{mix}}^2(t)\right)\pi_c^2, \quad (6.58)$$

where the mass mixing induced by  $\delta N_c$  and  $N_c^i$  is

$$m_{\text{mix}}^2 = 6\dot{H} + 2\frac{\ddot{H}}{H} - 2\frac{\dot{H}^2}{H^2}. \quad (6.59)$$

Using the background evolution given by (6.57) and (6.59) the mode equation for the re-scaled field variable  $\tilde{\pi}_c = a^{3/2}\pi_c$  can be written as

$$\ddot{\tilde{\pi}}_c + \left[ \frac{k^2}{a^2} + m_\phi^2 \left( 1 + 6\frac{H_{\text{FRW}}}{m_\phi} \sin(2m_\phi t) \right) \right] \tilde{\pi}_c = 0, \quad (6.60)$$

where we have dropped additional terms further suppressed by  $H_{\text{FRW}}^2/m_\phi^2$  and  $m_\pi^2 \rightarrow V''(\phi_0) = m_\phi^2$  which follows from relating derivatives of the potential to the time derivatives of the Hubble rate given in (6.57) (See Appendix B).

To establish whether self-resonance results in particle production we can recast (6.60) in the form of a Mathieu equation by re-defining the time variable  $z = m_\phi t + \pi/4$  with  $A_k = 1 + k^2/(a^2 m_\phi^2)$  and  $q = 3H_{\text{FRW}}/m_\phi$ . As the background evolution implies

the hierarchy  $H_{\text{FRW}} \ll m_\phi$ , this implies modes in equation (6.60) will be in the narrow resonance regime,  $q \ll 1$ . The first instability corresponds to the condition  $A_k < 1 + q$  implying modes with momenta

$$\frac{k}{a} < \sqrt{3H_{\text{FRW}}m_\phi} \quad (6.61)$$

will be amplified [25]. This result matches well with our previous estimate on the momentum scales where mixing with gravitational fluctuations is important in (6.56) (recalling we have  $c_\pi = 1$  here).

Such resonant effects due to mixing with gravity have been considered previously in the literature [109, 339], where those authors studied the growth of the density perturbations and the onset of non-linear effects arising during oscillations of the background. Here, we can use the EFT to reproduce their results

$$\delta_k \equiv \frac{\delta\rho_k}{\bar{\rho}(t)} = \frac{\delta\rho_k}{3H^2m_{\text{pl}}^2} \propto \left(\frac{k}{aH_{\text{FRW}}}\right)^2, \quad \text{for } \frac{k}{a} < \sqrt{3H_{\text{FRW}}m_\phi}, \quad (6.62)$$

where  $\delta\rho_k$  is defined as

$$\delta\rho_k = (-2\dot{H})^{1/2}m_{\text{pl}} \left[ \dot{\pi}_c - \frac{1}{2} \left( 3 + \frac{\ddot{H}}{\dot{H}} - 2\frac{\dot{H}}{H} \right) \pi_c \right]. \quad (6.63)$$

We now consider how the EFT captures models where the reheat sector results from the inflaton resonance given by the time-dependent functions in (6.46) and (6.47). If any of these couplings are stronger than gravitational strength the resonance in the reheat sector will typically dominate over the gravitationally induced effects discussed above.

## Reheating in a Two-Field Model

In this section, we explicitly demonstrate how the EFT approach reproduces models of two-field reheating, taking as a concrete example the specific class of models given

by (6.1). In the early stages of preheating the inflaton will dominate the energy density. We take the reheat field to be initially in its vacuum<sup>14</sup> with  $\chi_0 = 0$ , and we consider production of  $\chi$  quanta in the presence of the oscillating inflaton condensate  $\phi_0(t)$ . In the unitary gauge with  $\phi = \phi_0(t)$  and  $\chi_0 = 0$ , we have the following matter Lagrangian

$$S_m = \int d^4x \sqrt{-g} \left[ -\frac{1}{2} \dot{\phi}_0^2 g^{00} - V(\phi_0) - \frac{1}{2} g^{\mu\nu} \partial_\mu \chi \partial_\nu \chi - \frac{1}{2} (U''(\chi_0) + g^2 \phi_0^2) \chi^2 \right]. \quad (6.64)$$

Using the background equations of motion we can cancel the tadpole terms,  $m_{\text{pl}}^2(3H^2 + \dot{H}) = V(\phi_0) = m_\phi^2 \phi_0^2/2$ ,  $\dot{H} m_{\text{pl}}^2 = -\dot{\phi}_0^2/2$ , and the unitary gauge matter Lagrangian is then given by

$$\mathcal{L}_m = m_{\text{pl}}^2 \dot{H} g^{00} - m_{\text{pl}}^2 (3H^2 + \dot{H}) - \frac{1}{2} g^{\mu\nu} \partial_\mu \chi \partial_\nu \chi - \frac{1}{2} \left( m_\chi^2 + 2 \frac{g^2 m_{\text{pl}}^2}{m_\phi^2} (3H^2 + \dot{H}) \right) \chi^2, \quad (6.65)$$

where we defined  $U''(\chi_0) \equiv m_\chi^2$ . Comparing with the unitary gauge action (6.40) – (6.42), the matter Lagrangian (6.65) corresponds to the following choice for non-universal parameters in the EFT framework,

$$\alpha_1 = 1, \quad \alpha_3 = m_\chi^2 + 2 \frac{g^2 m_{\text{pl}}^2}{m_\phi^2} (3H^2 + \dot{H}), \quad \{m_2, \alpha_2, \alpha_4, \beta_1, \beta_2\} = 0. \quad (6.66)$$

We emphasize that in this model the linear mixing between the  $\chi$  sector and gravitational sector (which includes the Goldstone in the unitary gauge) vanishes automatically since  $\beta_1, \beta_2 = 0$  in (6.42). As before, we can introduce the Goldstone sector in (6.65) following the transformation<sup>15</sup> rules in (6.43). However, in the presence of strong resonance in the  $\chi$  sector, *i.e.* if  $\dot{\alpha}_3/\alpha_3^2 > \mathcal{O}(1)$  during any time in the linear stage of preheating, Goldstone fluctuations will be negligible compared to the

<sup>14</sup>We saw in Section 6.3 that it was a challenge for the background EFT model, but this is natural here as the shift symmetry of the background has been badly broken by the interactions.

<sup>15</sup>It is important to note that the transformation  $t \rightarrow t + \pi$  that introduces the Goldstone also induces non-linear interactions between the Goldstone and reheat sectors – we will elaborate on this below.

$\chi$ 's that are amplified through the strong resonance. In general, the validity of this argument relies on the strength of the coupling between the background and the  $\chi$  sector through the mass term. For example, in the model we are considering here, introducing  $\pi$  via  $t \rightarrow t + \pi$  (See also (6.43)) will lead to the Goldstone sector we have discussed in the previous section, where mixing with gravity leads to weak resonance  $q \approx H_{\text{FRW}}/m_\phi \ll 1$  (c.f. (6.60) and the discussion that follows). On the other hand, the strength of the resonance in the  $\chi$  sector depends on the ratio  $gm_{\text{pl}}/m_\phi$  which can be quite large unless  $g \ll 1$ . To see this in detail, it is enough to compare the scales in our EFT. The strength of the resonance in  $\chi$  can be read from (6.66) and compared to the strength  $\approx m_\phi H_{\text{FRW}}$  of the resonance in the Goldstone sector in equation (6.60). The following condition is sufficient to neglect the Goldstone dynamics

$$g^2 \left( \frac{m_{\text{pl}}}{m_\phi} \right) \left( \frac{\Lambda_{\text{sb}}}{m_\phi} \right)^2 > 1. \quad (6.67)$$

It is clear from this expression that unless the coupling constant is tiny  $g \ll 1$  we can neglect the mild amplification of Goldstone due to mixing with gravity.

Another simplification we can make in this case is to consider the decoupling limit in the EFT where  $|\dot{H}| \approx H_{\text{FRW}}^2 \rightarrow 0$  and  $m_{\text{pl}}^2 \rightarrow \infty$ , while keeping the combinations  $\dot{H}m_{\text{pl}}^2$  and  $H^2m_{\text{pl}}^2$  as constant. In this limit, it is clear that  $\pi$  fluctuations will stay in their vacuum as the terms leading to narrow resonance vanishes ( $H_{\text{FRW}} \rightarrow 0$ ). We also note that the decoupling limit corresponds to taking the rigid space-time limit,  $a \rightarrow 1$  that is commonly discussed in the preheating literature<sup>16</sup> [25, 27].

To study particle production, we can focus on the decoupling limit of the Lagrangian (6.65), and consider the mode equation for  $\chi$  as,

$$\ddot{\chi}_k + \omega_\chi^2(t)\chi_k = 0 \quad (6.68)$$

---

<sup>16</sup>An additional and important point on the decoupling limit is that in this limit the time-dependent functions such as  $\alpha_3$  we are considering will be purely periodic functions. This can be seen by using (6.57) in equation (6.66) and taking the decoupling limit. This implies that EFT should respect an exact discrete symmetry in this limit.

where the time dependent frequency is given by

$$\omega_\chi^2 = k^2 + m_\chi^2 + \frac{g^2 m_{\text{pl}}^2}{m_\phi^2} (3H^2 + \dot{H}). \quad (6.69)$$

In the decoupling limit, the time dependent mass induced by the background evolution stays intact, which is crucial for particle production. As we have mentioned before, particle production corresponds to the breakdown of the adiabaticity in the frequency, *i.e.*  $|\dot{\omega}_\chi/\omega_\chi^2| > \mathcal{O}(1)$ . Using (6.57) and the relations with the potential and Hubble rate in Appendix B, this condition translates into

$$K^2 \lesssim g H_{\text{FRW}} m_{\text{pl}} \approx g \Lambda_{\text{sb}}^2, \quad (6.70)$$

where  $K = \sqrt{k^2 + m_\chi^2}$  is the rescaled momenta. In the example we are considering, we see that this condition justifies the use of the EFT formalism as the resonant modes have a momenta much smaller than the symmetry breaking scale for small enough coupling, *i.e.*  $H_{\text{FRW}} m_{\text{pl}} \equiv \Lambda_{\text{sb}}^2 \gg g \Lambda_{\text{sb}}^2$  for  $g \ll 1$ . The structure of the instability band along with the exponentially growing solutions in the  $\chi$  sector have been studied many times in the literature [27]. Here, our main purpose is to show the connection of the EFT approach to well established two-field reheating models.

Another potential use of EFT formalism is to capture the effects of backreaction. This can be achieved by realizing that once we introduce the Goldstone mode in the unitary gauge Lagrangian (6.65) the time dependent mass (and for general models other time dependent functions) of  $\chi$  becomes  $\alpha_3(t + \pi)$ . As  $\alpha_3$  is a rapidly varying function of time in the presence of particle production in the  $\chi$  sector, this term will induce higher order interactions between  $\pi$  and  $\chi$  upon expanding the function,

$$\mathcal{L}_{\text{int}} = -\frac{1}{2} \left( \dot{\alpha}_3 \pi + \frac{1}{2} \ddot{\alpha}_3 \pi^2 \right) \chi^2. \quad (6.71)$$

In particular, in the current example the first term in (6.71) will lead to a tadpole

term for  $\pi_c = (-2\dot{H})^{1/2}m_{\text{pl}}\pi$ . In the Hartree approximation [25] this gives

$$\mathcal{L}_{\text{int}} \supset -\frac{1}{2} \frac{\dot{\alpha}_3}{(-2\dot{H}m_{\text{pl}}^2)^{1/2}} \langle \chi^2 \rangle \pi_c, \quad (6.72)$$

where

$$\langle \chi^2(t) \rangle = \frac{1}{2\pi^2} \int_0^\infty dk k^2 |\chi_k(t)|^2. \quad (6.73)$$

The existence of such a tadpole term can be considered as an indication of backreaction effects. For example, as we produce  $\chi$  particles the coefficient in front of  $\pi_c$  will grow and may eventually disturb the background evolution. In particular they can increase the frequency of the background oscillations of the condensate [25],

$$m_\phi^2 \rightarrow m_\phi^2 + \frac{\dot{\alpha}_3}{(-2\dot{H}m_{\text{pl}}^2)^{1/2}} \langle \chi^2 \rangle \quad (6.74)$$

In order to understand the onset of the backreaction effects in the presence of particle production, we can compare the second term in (6.74) with  $m_\phi^2$ . We refer to this time where the backreaction becomes important as  $t_b$  and the condition reads

$$m_\phi^2 = \frac{\dot{\alpha}_3(t_b)}{(-2\dot{H}(t_b)m_{\text{pl}}^2)^{1/2}} \langle \chi^2(t_b) \rangle \quad (6.75)$$

Knowing the solutions for  $\chi_k$ , the background evolution (6.57) and the couplings  $\alpha_3$  one can calculate  $t_b$ .

We emphasize that our discussion in this section is not limited to the example given by (6.66). Using the EFT formalism, we can in principle capture models that belong to the same “universality class”, *i.e.* direct coupling models with interactions including  $\mathcal{L}_m \propto \mu\phi\chi^2$  and non-renormalizable couplings  $\mathcal{L}_m \propto \phi^n\chi^2/M^{n-2}$  where  $n > 2$  and  $M, \mu$  are energy scales [340].

### 6.4.4 A New Class of Reheating Models

In the previous section, we showed how the EFT captures resonance effects in two-field reheating models. We now reconsider particle production in the presence of a reduced sound speed for the reheat field,  $c_\chi \neq 1$ . Familiar from the EFT of Inflation and Dark Energy, there is no symmetry protecting  $c_\chi = 1$  in the EFT of reheating. This gives rise to a new class of models for preheating where the produced particles can have  $c_\chi \ll 1$ .

We follow our previous discussion in Section 6.4.2 and consider the time-dependent functions associated with the reheat sector  $\{\alpha_i, \beta_i\}$ . The terms proportional to  $\beta_1$  and  $\beta_2$  in (6.47) lead to mixing of  $\chi$  with both gravity and the Goldstone sector. We will ignore these terms here, leaving a discussion of them to Appendix A. In the absence of these mixing terms we focus on the action (6.46). Defining the canonical field  $\chi_c = \alpha_\chi(t)\chi$  where  $\alpha_\chi^2(t) = \alpha_1(t) + \alpha_2(t)$ , we have the following second order Lagrangian for the canonical reheat field

$$\mathcal{L}_{\chi_c} = \frac{1}{2} \left[ \dot{\chi}_c^2 - c_\chi^2(t) \frac{(\partial_i \chi_c)^2}{a^2} \right] - \frac{1}{2} m_\chi^2(t) \chi_c^2, \quad (6.76)$$

where we have defined the sound speed  $c_\chi^2 = \alpha_1/(\alpha_1 + \alpha_2)$  and the time-dependent mass term is

$$m_\chi^2(t) = \frac{\alpha_3(t)}{\alpha_\chi^2(t)} - \left( \frac{\dot{\alpha}_\chi}{\alpha_\chi} \right)^2 + 3H \left( \frac{\dot{\alpha}_\chi}{\alpha_\chi} \right) + \partial_t \left( \frac{\dot{\alpha}_\chi}{\alpha_\chi} \right). \quad (6.77)$$

Similar to the Goldstone case in Section 6.4.3, we have a time-dependent mass  $m_\chi(t)$  induced by the time dependence of the sound speed  $c_\chi$  and  $\alpha_1$ <sup>17</sup>. We will concentrate on strong resonant effects due to non-adiabaticity in the time-dependent coefficient  $\alpha_3$  and assume that the time variation of  $\alpha_\chi$  is slow compared to  $\alpha_3$ , so that the sound speed is nearly constant<sup>18</sup> (where  $\alpha_1, \alpha_2 \approx \text{constant}$ ). We can then neglect the last three terms in (6.77) and the mode equation for the re-scaled field variable

---

<sup>17</sup>Recall that  $c_\chi^2 = \alpha_1/\alpha_\chi^2$

<sup>18</sup>Again, we leave the interesting case of strong time dependence of the sound speed to future work.

$\tilde{\chi}_c = a^{3/2}\chi_c$  in Fourier space is

$$\ddot{\tilde{\chi}}_c^k + \left[ c_\chi^2 \frac{k^2}{a^2} + \alpha_3 + \Delta \right] \tilde{\chi}_c^k = 0, \quad (6.78)$$

where  $\Delta = -3(3H^2 + 2\dot{H})/4 \approx \mathcal{O}(H^2)$  are gravitational terms resulting from the rescaling  $\chi_c \rightarrow \tilde{\chi}_c$  and we have absorbed the constants  $\alpha_1, \alpha_2$  into the definition of  $\alpha_3$ . Following our discussion in Section 6.4.2, it is convenient to parameterize  $\alpha_3$  as  $\alpha_3 = M^2(t)F(\omega t)$ , where  $M(t)$  is always adiabatic so that  $\dot{M}/M^2 \ll 1$  and  $F$  is a periodic function which must violate adiabaticity so that preheating occurs. That is, at some point adequate particle production requires the so-far arbitrary function to satisfy  $\dot{F}/F^2 > 1$ . In many models the periodicity of the function will be set by the background evolution in (6.48). We focus on the strong resonance regime where  $M \gg H$  and  $M/\omega \gg 1$  and hence drop  $\mathcal{O}(H^2)$  terms in the frequency  $\omega_\chi^2$ ,

$$\omega_\chi^2 = c_\chi^2 \frac{k^2}{a^2} + M^2 F(\omega t). \quad (6.79)$$

The non-adiabaticity in  $\alpha_3$  will lead to non-adiabaticity in the frequency  $\omega_\chi^2$ , *i.e.*  $\dot{\omega}_\chi/\omega_\chi^2 > \mathcal{O}(1)$ . We take this to occur as times  $t_j$  when  $\omega_\chi^2$  is at its minimum<sup>19</sup>. This suggests that we can expand the frequency around the times  $t_j$  as

$$\omega_\chi^2 \simeq c_\chi^2 \frac{k^2}{a^2} + \frac{1}{2} M^2 \omega^2 (t - t_j)^2 + \dots \quad (6.80)$$

where we have used  $\ddot{F} \approx \omega^2 F$  and dots represent higher order terms in the  $t - t_j$  expansion. This allows us to re-write the mode equation in a simpler form

$$\ddot{\tilde{\chi}}_c^k + \left[ c_\chi^2 \frac{k^2}{a^2} + \frac{M^2 \omega^2}{2} (t - t_j)^2 \right] \tilde{\chi}_c^k = 0 \quad (6.81)$$

---

<sup>19</sup>Note that here we are focusing on non-tachyonic resonance, for tachyonic resonance this situation will be different, see *e.g.* [340].



and the typical momenta when adiabaticity is violated  $\dot{\omega}_\chi > \omega_\chi^2$  corresponds to

$$k_*^2 \equiv \frac{M\omega}{c_\chi^2} \gtrsim \frac{k^2}{a^2}, \quad (6.82)$$

We see that for  $c_\chi < 1$ , the physical wave numbers inside the resonant regime are further enhanced (the resonance band is broadened) compared to the standard cases that have been studied in the literature. It is customary to map the mode equation (6.81) to a scattering problem described by a Schrödinger equation with a negative parabolic potential by defining a new time variable  $\tau \equiv c_\chi k_*(t-t_j)$  and a dimensionless physical momentum  $\kappa \equiv k/(ak_*)$ ,

$$\frac{d^2 \tilde{\chi}_c^k}{d\tau^2} + (\kappa^2 + \tau^2) \tilde{\chi}_c^k = 0. \quad (6.83)$$

The solution to the scattering problem and the resulting number density of particles between scattering events has appeared in the literature many times [25, 176] (See also [291]). In real space, the growth of the number density of particles can be described by the following expression [25],

$$n_\chi(t) = \frac{1}{2\pi a^3} \int d^3k n_\chi^k(t) \sim \frac{k_*^3}{\sqrt{\pi\mu m_\phi t}} e^{2\mu m_\phi t}, \quad (6.84)$$

where (for simplicity) we have assumed that the background is given by the quadratic potential we considered before, *i.e.*  $\omega \sim m_\phi$ . Here  $\mu$  is the maximum value of the Floquet index at  $k_{\max} \approx k_*/2$  [25]. It is clear from this expression that there will be an enhancement in the number of produced particles due to the small sound speed in the  $\chi$  sector,  $k_* \propto c_\chi^{-1}$ . This also agrees with our intuition as equation (6.82) tells us that resonant bands are wider for  $c_\chi < 1$  and thus the contribution to the integral in (6.84) over resonant modes will be enhanced by factors of  $c_\chi^{-1}$ . In the next section we will consider observational consequences of the EFT of reheating, focusing on this new class of models with non-standard sound speed. We also discuss additional challenges

and future directions for the approach.

## 6.5 Challenges and Outlook

In this paper we have presented an EFT approach to reheating that overcomes the challenges of the background evolution discussed in Section 6.3 and is adequate to capture all existing reheating models in the literature. Guided by symmetries, our approach is also useful for finding new models of reheating, *e.g.* we found a new class of models where the reheating sector has  $c_\chi \neq 1$ . However, there are many challenges remaining for our EFT approach.

One of the more serious concerns is the lack of a direct connection to observations. This problem is not specific to our approach, with the lack of direct observational constraints on reheating being an important reason that far less is known about this epoch than inflation. In our EFT framework, symmetries help to alleviate more of the theoretical uncertainties associated with reheating than a toy model approach. For example, the need to non-linearly realize time translations demonstrated that many of the unknown coefficients are related, and the need to violate non-adiabaticity (required for particle production) also placed some level of theoretical constraint on the reheating sector. Nevertheless, we saw in Section 6.4 there are a large number of free functions that must be further restricted by observations. Unlike the situation for inflation, where non-Gaussianity and features in the primordial power spectrum are a rich source of observational constraints, direct observational constraints on reheating are lacking. One possibility to remedy this is gravitation wave (GW) signatures.

Once particles are produced during reheating<sup>20</sup> they can scatter off each other creating a background of GWs [284, 287]. The scattering leads to a transverse-

---

<sup>20</sup>This should not be confused with sourcing a gravity perturbation with a second order scalar perturbation. Here we are considering on-shell particles that are classically scattering off of each other and generating a GW spectrum. We refer the reader to [232] for more details.

traceless source for the gravitons

$$\ddot{h}_{ij} + 3H\dot{h}_{ij} - \frac{1}{a^2}\partial^2 h_{ij} = \frac{2}{m_{\text{pl}}^2} T_{ij}^{TT} \quad (6.85)$$

Following the methods of [232] we can then estimate the critical density of gravitational waves today<sup>21</sup>

$$\Omega_{\text{gw}} = \frac{S_k(t_f)}{a_J^4 \rho_J} \left( \frac{a_J}{a_{\text{rh}}} \right)^{1-3w} \left( \frac{g_{\text{rh}}}{g_0} \right)^{-1/3} \Omega_{r,0}, \quad (6.86)$$

where subscript ‘‘0’’ denotes a quantity evaluated today, ‘ $J$ ’ represents the time when the universe becomes radiation dominated and ‘rh’ denotes the beginning of reheating. Here,  $w$  is the average equation of state of the universe between the time interval  $t_J < t < t_{\text{rh}}$  and  $g_i$  is the effective relativistic degrees of freedom. Finally, the source term  $S_k$  encodes the predictions for different classes of models in the EFT.

For example, let us consider the new class of models discussed in Section 6.4.4. In that case the source term  $S_k$  is given by

$$S_k(t_f) = \frac{c_\chi^4 k^3}{4\pi^2 m_{\text{pl}}^2} \int dp \int_{-1}^1 d(\cos \theta) p^6 \sin^4 \theta \times \left[ \left| \int_{t_i}^{t_f} dt \cos(kt) \chi_c(p, t) \chi_c(|\vec{k} - \vec{p}|, t) \right|^2 + \left| \int_{t_i}^{t_f} dt \sin(kt) \chi_c(p, t) \chi_c(|\vec{k} - \vec{p}|, t) \right|^2 \right] \quad (6.87)$$

where we focus on two-body scattering,  $\theta$  is the scattering angle, and we assume that scattering happens at a fast enough rate that we can neglect the Hubble expansion. To get an order of magnitude estimate we can focus on the low momenta. In this case, the contribution of the mode functions to time integrals will be maximal for

---

<sup>21</sup>For a different approach we refer the reader to [341].

$p_* = \sqrt{M\omega}/c_\chi$  and defining a dimensionless momentum  $P = p/p_*$  we have

$$S_k^{j+1} \sim \frac{1}{c_\chi^3} \frac{(M\omega)^{3/2} k^3}{m_{\text{pl}}^2} \int_{-1}^1 d(\cos\theta) \sin^4\theta \int dP P^6 \times [Time\ integrals], \quad (6.88)$$

where we recall that  $\alpha_3$  is parameterized by  $M$  and  $\omega$  as in (6.81), and so the EFT parameters are determining the strength of the GW signal. Moreover, the gravitational waves will be amplified by a factor of  $c_\chi^{-3}$ . This scaling may be counter-intuitive to the reader. The prefactor in (6.87) results from the two-to-two scattering of the particles as their momenta is now  $p \rightarrow c_\chi p$ . However, the lower sound speed implies it costs less energy to produce the particles leading to an enhancement of the particle production rate, and more particles scattering leads to more gravity waves. Thus, the GW signal is enhanced compared to the  $c_\chi = 1$  case. Assuming this signal survives the later stages of reheating the detectability will depend on the peak frequency [284, 287, 341]

$$f = \frac{\sqrt{M\omega}}{a_j \rho_j^{1/4} c_\chi} 4 \times 10^{10} \text{ Hz}, \quad (6.89)$$

which again depends explicitly on the EFT parameters and the sound speed. We see that by reducing the sound speed we can increase the frequency in the new class of reheating models.

GWs provide one way to constrain the EFT parameters. However, we leave a more complete analysis, which requires following the signal through all the stages of reheating<sup>22</sup>, to future work. Primordial Black Hole constraints and the matching of inflationary perturbations to late time observables lead to additional ways in which the EFT parameters may be restricted. In regards to the latter, we have stressed that direct observables correspond to perturbations, however the subtle ways in which we match inflationary predictions to CMB and LSS observations does depend implicitly on the background dynamics, particularly through the equation of state. Recently,

---

<sup>22</sup>One interesting approach would be to see if we could combine the EFT framework here with the recent fitting analysis of [342].

it has been shown that the physics of reheating (including non-linearities and back-reaction) can have subtle and interesting effects on the equation of state and the dynamics of thermalization [343]. We hope to return to these issues and interesting possibilities in future work.

In addition to the challenge to connect with observations, a number of theoretical issues remain to be addressed. In particular, in this paper we have primarily focused on connecting the EFT to scalar field driven models of reheating. However, the spectator field  $\chi$  can be thought of as an additional clock field, which can also represent reheat fields beyond spin zero. Extending our framework to other spins is an important consideration. We have also primarily focused on the first stage of reheating in the EFT. However, one of the most useful applications of our approach could be to gain a better understanding of the rescattering and back-reaction effects that happen following the first stage. These are stages that usually require lattice simulations, and the Goldstone approach could be a fruitful way to get a better analytical understanding. There is also the issue of when the produced particles become significant enough that they contribute to the energy density. At this point the Goldstone boson (related to the matter sector responsible for time-translations being broken) can change its nature from inflatons to the reheat field. How this transition proceeds is important for establishing the connection between the Goldstone and the background fields. This is similar to the situation in studies of dissipation in the EFT of Inflation (see *e.g.* [344]), and we expect many of the techniques there could prove useful for the case of reheating as well.

# Appendix

## 6.A Terms proportional to $\chi$ in the unitary gauge action

We make use of the unit 4-vector,  $n_\mu = -\delta_\mu^0/\sqrt{-g^{00}}$  that is orthogonal to constant time hyper-surfaces  $\Sigma_t$  and the definition of extrinsic curvature,  $K_{\mu\nu} = h_\mu^\sigma \nabla_\sigma n_\nu$ , where  $h_\mu^\sigma \equiv \delta_\mu^\sigma + n^\sigma n_\mu$  to tackle the term that linear in  $\chi$ . In this appendix, first we focus on the tadpole terms in  $\chi$  that are of the following form

$$\int d^4x \sqrt{-g} f_4(t) \partial^0 \chi = \int d^4x \sqrt{-g} f_2(t) \sqrt{-g^{00}} n^\mu \nabla_\mu \chi, \quad (6.90)$$

where we have used  $g^{\mu\nu} n_\mu \equiv n^\nu = g^{\nu 0}(-g^{00})^{-1/2}$ . Making an integration by parts in the relation (6.90) above and realizing  $K_\mu^\mu = \nabla_\mu n^\mu$ , we have

$$- \int d^4x \sqrt{-g} \left[ g^{00} \dot{f}_4(t) \chi + \frac{f_4(t)}{2} \partial^0 (\ln(-g^{00})) + f_4(t) \sqrt{-g^{00}} K_\mu^\mu \right] \chi. \quad (6.91)$$

Now expanding the fluctuations in the metric and trace of the extrinsic curvature as  $g^{00} = -1 + \delta g^{00} + \dots$  and  $K_\mu^\mu = K^{(0)} + \delta K + \dots$  by noting  $K^{(0)} = -3H(t)$  and including the term  $\int d^4x \sqrt{-g} f_3(t) \chi$  to (6.91) we have

$$\int d^4x \sqrt{-g} \left\{ \left[ f_3(t) + \dot{f}_4(t) + 3H(t) f_4(t) \right] \chi + \mathcal{O}(\delta g^{00}, \delta K) \chi \right\} \quad (6.92)$$

Therefore, imposing the background equation of motion  $f_3(t) + \dot{f}_4(t) + 3H(t)f_4(t) = 0$ , we see that all the other terms are second and higher order in fluctuations as claimed in the text.

## 6.B ADM Formalism and Mixing with Gravity

To account for gravitational fluctuations and discuss the regime where they are irrelevant to the dynamics of the Goldstone we decompose the metric in the ADM form. In the spatially flat gauge we have

$$ds^2 = -(N^2 - N_i N^i) dt^2 + 2N_i dx^i dt + \hat{g}_{ij} dx^i dx^j, \quad (6.93)$$

where  $\hat{g}_{ij} = a^2(\delta_{ij} + h_{ij})$  is the spatial metric and our gauge choice implies  $h_{ii} = \partial_i h_{ij} = 0$ . Inverse metric elements can be written as

$$g^{00} = -\frac{1}{N^2}, \quad g^{0i} = g^{i0} = \frac{N^i}{N^2}, \quad g^{ij} = h^{ij} - \frac{N^i N^j}{N^2}. \quad (6.94)$$

To find the relevant terms in the gravitational sector, we expand the Einstein Hilbert term as

$$S_g \supset \frac{m_{\text{pl}}^2}{2} \int d^4x \sqrt{-g} R = \frac{m_{\text{pl}}^2}{2} \int d^4x \sqrt{\hat{g}} [NR^{(3)} + \frac{1}{N}(E^{ij}E_{ij} - E^i_i{}^2)], \quad (6.95)$$

where  $R^{(3)}$  is the three curvature associated with spatial metric  $\hat{g}_{ij}$  and  $E_{ij}$  is related to the extrinsic curvature of constant time slices through

$$E_{ij} \equiv NK_{ij} = \frac{1}{2}[\partial_t \hat{g}_{ij} - \hat{\nabla}_i N_j - \hat{\nabla}_j N_i], \quad (6.96)$$

where  $\hat{\nabla}_i$  is the covariant derivative with respect to spatial metric  $\hat{g}_{ij}$ . Using the

above expressions, we can expand (6.45) up to second order in scalar fluctuations

$$\begin{aligned} \mathcal{L}_g = & -\frac{m_{\text{pl}}^2 \dot{H}}{c_\pi^2} \left( \dot{\pi}^2 - c_\pi^2 \frac{(\partial_i \pi)^2}{a^2} \right) - 3m_{\text{pl}}^2 \dot{H}^2 \pi^2 + m_{\text{pl}}^2 (2c_\pi^{-2} \dot{H} \dot{\pi} - 6H \dot{H} \pi) \delta N \\ & + 2m_{\text{pl}}^2 \dot{H} N^i \partial_i \pi - m_{\text{pl}}^2 (3H^2 + c_\pi^{-2} \dot{H}) \delta N^2 - 2m_{\text{pl}}^2 H \delta N \partial_i N^i \end{aligned} \quad (6.97)$$

where the speed of sound is defined as  $c_\pi^2 = m_{\text{pl}}^2 \dot{H} / (m_{\text{pl}}^2 \dot{H} - m_2^4)$ . Defining the canonical fields,  $\pi_c = \sqrt{-2\dot{H}m_{\text{pl}}^2} c_\pi^{-1} \pi$ ,  $\delta N_c = m_{\text{pl}} \delta N$ ,  $N_c^i = m_{\text{pl}} N^i$ , one can re-write the Lagrangian as in (6.51).

Focusing on the Goldstone sector for now, we can solve for the Lagrange multipliers  $\delta N$  and  $N^i$  in terms of  $\pi$ . To linear order in  $\pi$  we have,

$$\delta N = -\frac{\dot{H}}{H} \pi, \quad \partial_i N^i = c_\pi^{-2} \frac{\dot{H}}{H^2} \partial_t (H \pi). \quad (6.98)$$

Using the canonical field definitions above we may write

$$\delta N_c = \frac{(-2\dot{H})^{1/2}}{2H} \pi_c, \quad \partial_i N_c^i = c_\pi^{-2} \frac{\dot{H}}{H^2} \partial_t \left( \frac{c_\pi H \pi_c}{(-2\dot{H})^{1/2}} \right). \quad (6.99)$$

Using these solutions for the gravitational fluctuations  $\delta N_c$   $N_c^i$  in (6.51) (while taking the  $c_\pi \rightarrow 1$  limit) we recover the result of (6.58).

In the presence of a reheat sector  $\chi$ , we need to take into account the mixing between  $\chi$  and gravitational fluctuations, as well as  $\pi - \chi$  mixings. Considering the mixings at second order we need to take into account the action in (6.47). Expanding up to second order in  $\delta N$ ,  $N^i$ ,  $\pi$  and  $\chi$ , we have

$$S_{\text{mix}}^{(2)} = \int d^4x a^3 \left[ 2\beta_1 (\delta N - \dot{\pi}) \chi - 2\beta_2 (\delta N - \dot{\pi}) \dot{\chi} \right]. \quad (6.100)$$

We note that the action (6.46) does not lead to any second order mixing therefore it is enough to consider the mixing action above. Combining (6.97) and (6.100) in the



presence of mixing we have the following solutions for the constraints,

$$\delta N = -\frac{\dot{H}}{H}\pi, \quad \partial_i N^i = c_\pi^{-2} \frac{\dot{H}}{H^2} \partial_t (H\pi) + \frac{\beta_1}{m_{\text{pl}}^2 H} \chi - \frac{\beta_2}{m_{\text{pl}}^2 H} \dot{\chi}. \quad (6.101)$$

We see that inclusion of reheat sector does not change the solution for  $\delta N$ , but we have additional contributions to  $N^i$  proportional to the time-dependent parameters  $\beta_1, \beta_2$ . To illustrate the decoupling of  $\chi$ , we consider a simple  $\pi_c$  sector with  $c_\pi = 1$  and note that time derivatives of canonically normalized fields  $\chi_c$  and  $\pi_c$  have the approximate scalings in the WKB approximation,

$$\dot{\pi}_c \approx \omega_\pi \pi_c \sim \omega \pi_c, \quad \dot{\chi}_c \approx \omega_\chi \chi_c \sim \sqrt{\alpha_3} \chi_c \sim M \chi_c, \quad (6.102)$$

where we take  $|\alpha_3| = M^2$  following our discussion in the main text and focused on the non-relativistic modes for both fields. Following our discussion in section 6.4.2, we assume that the strength of the couplings  $\beta_1$  and  $\beta_2$  is as strong as the time-dependent parameter  $\alpha_3$  responsible for the resonance. By dimensional analysis, we therefore take  $|\beta_1| \sim M^3$  and  $|\beta_2| \sim M^2$ . Canonically normalizing the fields as before we find from (6.100) that for resonant modes mixing between  $\chi_c$  and gravitational fluctuations can be neglected in the following range of momenta

$$\left( \frac{M}{\Lambda_{\text{sb}}} \right) \sqrt{MH} < \frac{c_\chi k}{a} < \sqrt{M\omega}. \quad (6.103)$$

Similarly we have the following range where we can neglect direct mixing between  $\pi_c$  and  $\chi_c$ ,

$$\left( \frac{M}{\Lambda_{\text{sb}}} \right) \sqrt{M\omega} < \frac{c_\chi k}{a} < \sqrt{M\omega}. \quad (6.104)$$

Consistency of the EFT picture requires  $M/\Lambda_{\text{sb}} \ll 1$  and we see that within this regime we can neglect both types of mixing for a wide range of momenta. In particular, with some mild assumptions, we showed that in the presence of strong resonance, we can neglect the mixings between  $\pi_c$  and  $\chi_c$ . This finding is similar in spirit to the

discussion presented in the recent works [291, 345] where those authors pointed out that it is technically natural to assume a flat field space metric in the presence of strong disorder/resonance.

We conclude this appendix by giving the second order action for tensor perturbations and their interaction with  $\pi_c$  and  $\chi_c$  that we used in the main text. Using the gravitational part of the action in (6.95) with (6.96) and noting the Ricci curvature  $R^{(3)}$  on spatial hyper-surfaces,

$$R^{(3)} = \hat{g}^{ik} \partial_l \Gamma_{ik}^l - \hat{g}^{ik} \partial_k \Gamma_{il}^l + \hat{g}^{ik} \Gamma_{ik}^l \Gamma_{lm}^m - \hat{g}^{ik} \Gamma_{il}^m \Gamma_{km}^l, \quad (6.105)$$

$$\Gamma_{ij}^k = \frac{1}{2} \hat{g}^{kl} (\partial_i \hat{g}_{jl} + \partial_j \hat{g}_{il} - \partial_l \hat{g}_{ij}), \quad (6.106)$$

we have the following second order action for the tensor part of the metric fluctuations

$$S_g = \frac{m_{\text{pl}}^2}{8} \int d^4x a^3 \left( \dot{h}_{ij} \dot{h}_{ij} - \frac{\partial_k h_{ij} \partial_k h_{ij}}{a^2} \right). \quad (6.107)$$

On the other hand, expanding the actions (6.45) and (6.46) we find the following cubic order interactions between  $\pi_c$  and  $\chi_c$

$$S_{hXX} \supset \int d^4x a^3 \left( \frac{c_\chi^2}{2} h_{ij} \frac{\partial_i \chi_c \partial_j \chi_c}{a^2} + \frac{c_\pi^2}{2} h_{ij} \frac{\partial_i \pi_c \partial_j \pi_c}{a^2} \right). \quad (6.108)$$

## 6.C Relating Unitary Gauge to the Scalar Potential

In cosmologies dominated by a scalar field, we can map the time-dependent background quantities in our Unitary gauge Lagrangian (6.40) to the explicit scalar field models with a given potential  $V(\phi_0)$ . A simple example we provided in the main text was

$$V(\phi_0) = m_{\text{pl}}^2 (3H^2(t) + \dot{H}(t)), \quad -2\dot{H}m_{\text{pl}}^2 = \dot{\phi}_0^2 \quad (6.109)$$

Using  $d\phi_0 = \dot{\phi}_0 dt$  and time derivatives of expressions in (6.109), we can relate the derivatives of the potential with respect to  $\phi$  to the time derivatives of the Hubble rate  $H(t)$ . Here, we list some of these expressions,

$$V'(\phi_0) = \frac{m_{\text{pl}}^2}{(-2\dot{H})^{1/2}} (6H\dot{H} + \ddot{H}), \quad (6.110)$$

$$V''(\phi_0) = -3\dot{H} - \frac{1}{4} \left( \frac{\ddot{H}}{\dot{H}} \right)^2 - \frac{3H}{2} \left( \frac{\ddot{H}}{\dot{H}} \right) - \frac{1}{2} \partial_t \left( \frac{\ddot{H}}{\dot{H}} \right), \quad (6.111)$$

$$V'''(\phi_0) = \frac{1}{(-2\dot{H}m_{\text{pl}}^2)^{1/2}} \left[ -\frac{H^{(4)}}{2\dot{H}} - \frac{9\ddot{H}}{2} + \frac{\ddot{H}^3}{2\dot{H}^3} - \frac{3H}{2} \partial_t \left( \frac{\ddot{H}}{\dot{H}} \right) + \frac{1}{2} \partial_t \left( \frac{\ddot{H}^2}{\dot{H}^2} \right) \right]$$

# Bibliography

- [1] P. A. R. Ade et al. (Planck), *Astron. Astrophys.* **571**, A15 (2014), [1303.5075](#).
- [2] M. Ackermann et al. (Fermi-LAT), *Phys. Rev. Lett.* **107**, 241302 (2011), [1108.3546](#).
- [3] P. Gondolo, J. Edsjo, P. Ullio, L. Bergstrom, M. Schelke, and E. A. Baltz, *JCAP* **0407**, 008 (2004), [astro-ph/0406204](#).
- [4] F. Iocco, M. Pato, G. Bertone, and P. Jetzer, *JCAP* **1111**, 029 (2011), [1107.5810](#).
- [5] V. M. Slipher, *Proceedings of the American Philosophical Society* **56**, 403 (1917).
- [6] E. Hubble, *Proceedings of the National Academy of Science* **15**, 168 (1929).
- [7] A. A. Penzias and R. W. Wilson, *Astrophys.J* **142**, 419 (1965).
- [8] G. Gamow, *Physical Review* **74**, 505 (1948).
- [9] A. G. Doroshkevich and I. D. Novikov, *Soviet Physics Doklady* **9**, 111 (1964).
- [10] K. K. Wu, O. Lahav, and M. J. Rees, *Nature* **397**, 225 (1999).
- [11] J. Yadav, S. Bharadwaj, B. Pandey, and T. Seshadri, *Monthly Notices of the Royal Astronomical Society* **364**, 601 (2005).

- [12] A. Friedmann, *Zeitschrift für Physik* **10**, 377 (1922).
- [13] A. Friedmann, *Zeitschrift für Physik* **21**, 326 (1924).
- [14] G. Lemaitre, *Annales Soc.Sci.Brux.Ser.I Sci.Math.Astron.Phys.* pp. 49–55 (1927).
- [15] H. P. Robertson, *Astrophys.J* **82**, 284 (1935).
- [16] A. G. Walker, *Proceedings of the London Mathematical Society* **s2-42**, 90 (1937).
- [17] R. A. Alpher, H. Bethe, and G. Gamow, *Phys. Rev.* **73**, 803 (1948), URL <http://link.aps.org/doi/10.1103/PhysRev.73.803>.
- [18] P. A. R. Ade et al. (Planck), *Astron. Astrophys.* **571**, A16 (2014), [1303.5076](https://arxiv.org/abs/1303.5076).
- [19] J. Preskill, *Annual Review of Nuclear and Particle Science* **34**, 461 (1984).
- [20] G. Steigman, *Int. J. Mod. Phys.* **E15**, 1 (2006), [astro-ph/0511534](https://arxiv.org/abs/astro-ph/0511534).
- [21] E. Komatsu et al. (WMAP), *Astrophys. J. Suppl.* **192**, 18 (2011), [1001.4538](https://arxiv.org/abs/1001.4538).
- [22] L. Abbott, E. Farhi, and M. B. Wise, *Physics Letters B* **117**, 29 (1982), ISSN 0370-2693, URL <http://www.sciencedirect.com/science/article/pii/037026938290867X>.
- [23] A. Albrecht, P. J. Steinhardt, M. S. Turner, and F. Wilczek, *Physical Review Letters* **48**, 1437 (1982).
- [24] J. H. Traschen and R. H. Brandenberger, *Physical Review D* **42**, 2491 (1990).
- [25] L. Kofman, A. D. Linde, and A. A. Starobinsky, *Phys. Rev.* **D56**, 3258 (1997), [hep-ph/9704452](https://arxiv.org/abs/hep-ph/9704452).
- [26] D. I. Podolsky, G. N. Felder, L. Kofman, and M. Peloso, *Phys. Rev.* **D73**, 023501 (2006), [hep-ph/0507096](https://arxiv.org/abs/hep-ph/0507096).

- [27] M. A. Amin, M. P. Hertzberg, D. I. Kaiser, and J. Karouby, *Int. J. Mod. Phys. D* **24**, 1530003 (2014), [1410.3808](#).
- [28] A. R. Liddle and S. M. Leach, *Physical Review D* **68**, 103503 (2003).
- [29] G. F. Smoot et al. (COBE), *Astrophys. J.* **396**, L1 (1992).
- [30] V. F. Mukhanov and G. V. Chibisov, *JETP Lett.* **33**, 532 (1981), [*Pisma Zh. Eksp. Teor. Fiz.*33,549(1981)].
- [31] V. F. Mukhanov, H. A. Feldman, and R. H. Brandenberger, *Phys. Rept.* **215**, 203 (1992).
- [32] D. Baumann, in *Physics of the large and the small, TASI 09, proceedings of the Theoretical Advanced Study Institute in Elementary Particle Physics, Boulder, Colorado, USA, 1-26 June 2009* (2011), pp. 523–686, [0907.5424](#), URL <http://inspirehep.net/record/827549/files/arXiv:0907.5424.pdf>.
- [33] J. M. Bardeen, *Phys. Rev.* **D22**, 1882 (1980).
- [34] J. M. Bardeen, P. J. Steinhardt, and M. S. Turner, *Phys. Rev.* **D28**, 679 (1983).
- [35] D. Wands, K. A. Malik, D. H. Lyth, and A. R. Liddle, *Phys. Rev.* **D62**, 043527 (2000), [astro-ph/0003278](#).
- [36] R. L. Arnowitt, S. Deser, and C. W. Misner, *Gen. Rel. Grav.* **40**, 1997 (2008), [gr-qc/0405109](#).
- [37] J. M. Maldacena, *JHEP* **05**, 013 (2003), [astro-ph/0210603](#).
- [38] P. A. R. Ade et al. (Planck), *Astron. Astrophys.* **594**, A20 (2016), [1502.02114](#).
- [39] V. F. Mukhanov, *Sov. Phys. JETP* **67**, 1297 (1988), [*Zh. Eksp. Teor. Fiz.*94N7,1(1988)].

- [40] A. A. Starobinsky, JETP Lett. **30**, 682 (1979), [Pisma Zh. Eksp. Teor. Fiz.30,719(1979)].
- [41] M. Kamionkowski, A. Kosowsky, and A. Stebbins, Phys. Rev. Lett. **78**, 2058 (1997), [astro-ph/9609132](#).
- [42] K. N. Abazajian et al. (CMB-S4) (2016), [1610.02743](#).
- [43] E. Komatsu et al. (2009), [0902.4759](#).
- [44] X. Chen, Adv. Astron. **2010**, 638979 (2010), [1002.1416](#).
- [45] P. A. R. Ade et al. (Planck), Astron. Astrophys. **594**, A17 (2016), [1502.01592](#).
- [46] P. Creminelli and M. Zaldarriaga, JCAP **0410**, 006 (2004), [astro-ph/0407059](#).
- [47] F. Zwicky, Helv. Phys. Acta **6**, 110 (1933).
- [48] G. Bertone, D. Hooper, and J. Silk, Phys. Rept. **405**, 279 (2005), [hep-ph/0404175](#).
- [49] W. Bernreuther, Lect. Notes Phys. **591**, 237 (2002), [237(2002)], [hep-ph/0205279](#).
- [50] A. R. Liddle and S. M. Leach, Phys. Rev. **D68**, 103503 (2003), [astro-ph/0305263](#).
- [51] W. H. Kinney and A. Riotto, JCAP **0603**, 011 (2006), [astro-ph/0511127](#).
- [52] H. V. Peiris and R. Easther, JCAP **0807**, 024 (2008), [0805.2154](#).
- [53] P. Adshead, R. Easther, J. Pritchard, and A. Loeb, JCAP **1102**, 021 (2011), [1007.3748](#).
- [54] M. J. Mortonson, H. V. Peiris, and R. Easther, Phys. Rev. **D83**, 043505 (2011), [1007.4205](#).

- [55] R. Easther and H. V. Peiris, Phys. Rev. **D85**, 103533 (2012), [1112.0326](#).
- [56] J. Norena, C. Wagner, L. Verde, H. V. Peiris, and R. Easther, Phys. Rev. **D86**, 023505 (2012), [1202.0304](#).
- [57] J. Martin and C. Ringeval, Phys. Rev. **D82**, 023511 (2010), [1004.5525](#).
- [58] J. Martin and C. Ringeval, JCAP **0608**, 009 (2006), [astro-ph/0605367](#).
- [59] D. J. H. Chung, E. W. Kolb, and A. Riotto, Phys. Rev. **D60**, 063504 (1999), [hep-ph/9809453](#).
- [60] N. Fornengo, A. Riotto, and S. Scopel, Phys. Rev. **D67**, 023514 (2003), [hep-ph/0208072](#).
- [61] C. Pallis, Astropart. Phys. **21**, 689 (2004), [hep-ph/0402033](#).
- [62] G. B. Gelmini and P. Gondolo, Phys. Rev. **D74**, 023510 (2006), [hep-ph/0602230](#).
- [63] G. Gelmini, P. Gondolo, A. Soldatenko, and C. E. Yaguna, Phys. Rev. **D74**, 083514 (2006), [hep-ph/0605016](#).
- [64] S. Watson, Adv. Ser. Direct. High Energy Phys. **21**, 305 (2010), [0912.3003](#).
- [65] R. Allahverdi, B. Dutta, R. N. Mohapatra, and K. Sinha, Phys. Rev. Lett. **111**, 051302 (2013), [1305.0287](#).
- [66] D. Hooper, F. S. Queiroz, and N. Y. Gnedin, Phys. Rev. **D85**, 063513 (2012), [1111.6599](#).
- [67] C. Kelso, S. Profumo, and F. S. Queiroz, Phys. Rev. **D88**, 023511 (2013), [1304.5243](#).
- [68] G. B. Gelmini and P. Gondolo, JCAP **0810**, 002 (2008), [0803.2349](#).



- [69] P. Grajek, G. Kane, D. Phalen, A. Pierce, and S. Watson, Phys. Rev. **D79**, 043506 (2009), [0812.4555](#).
- [70] P. Grajek, G. Kane, D. J. Phalen, A. Pierce, and S. Watson (2008), [0807.1508](#).
- [71] B. Dutta, L. Leblond, and K. Sinha, Phys. Rev. **D80**, 035014 (2009), [0904.3773](#).
- [72] G. Kane, R. Lu, and S. Watson, Phys. Lett. **B681**, 151 (2009), [0906.4765](#).
- [73] P. Sandick and S. Watson, Phys. Rev. **D84**, 023507 (2011), [1102.2897](#).
- [74] J. L. Feng, P. Kant, S. Profumo, and D. Sanford, Phys. Rev. Lett. **111**, 131802 (2013), [1306.2318](#).
- [75] M. R. Douglas, in *Strings, gauge fields, and the geometry behind: The legacy of Maximilian Kreuzer*, edited by A. Rebhan, L. Katzarkov, J. Knapp, R. Rashkov, and E. Scheidegger (2012), pp. 261–288, [1204.6626](#), URL <https://inspirehep.net/record/1112865/files/arXiv:1204.6626.pdf>.
- [76] N. Arkani-Hamed, A. Gupta, D. E. Kaplan, N. Weiner, and T. Zorawski (2012), [1212.6971](#).
- [77] T. Moroi and L. Randall, Nucl. Phys. **B570**, 455 (2000), [hep-ph/9906527](#).
- [78] B. S. Acharya, G. Kane, S. Watson, and P. Kumar, Phys. Rev. **D80**, 083529 (2009), [0908.2430](#).
- [79] B. S. Acharya, P. Kumar, K. Bobkov, G. Kane, J. Shao, and S. Watson, JHEP **06**, 064 (2008), [0804.0863](#).
- [80] E. Dudas, A. Linde, Y. Mambrini, A. Mustafayev, and K. A. Olive, Eur. Phys. J. **C73**, 2268 (2013), [1209.0499](#).

- [81] J. L. Evans, M. Ibe, K. A. Olive, and T. T. Yanagida, Eur. Phys. J. **C73**, 2468 (2013), [1302.5346](#).
- [82] M. B. Hoffman and M. S. Turner, Phys. Rev. **D64**, 023506 (2001), [astro-ph/0006321](#).
- [83] D. J. Schwarz, C. A. Terrero-Escalante, and A. A. Garcia, Phys. Lett. **B517**, 243 (2001), [astro-ph/0106020](#).
- [84] W. H. Kinney, Phys. Rev. **D66**, 083508 (2002), [astro-ph/0206032](#).
- [85] P. A. R. Ade et al. (Planck), Astron. Astrophys. **571**, A22 (2014), [1303.5082](#).
- [86] E. W. Kolb and M. S. Turner, Front. Phys. **69**, 1 (1990).
- [87] J. Beringer et al. (Particle Data Group), Phys. Rev. **D86**, 010001 (2012).
- [88] H. Baer, V. Barger, and A. Mustafayev, Phys. Rev. **D85**, 075010 (2012), [1112.3017](#).
- [89] D. H. Lyth and E. D. Stewart, Phys. Rev. **D53**, 1784 (1996), [hep-ph/9510204](#).
- [90] G. D. Coughlan, W. Fischler, E. W. Kolb, S. Raby, and G. G. Ross, Phys. Lett. **B131**, 59 (1983).
- [91] B. de Carlos, J. A. Casas, F. Quevedo, and E. Roulet, Phys. Lett. **B318**, 447 (1993), [hep-ph/9308325](#).
- [92] T. Banks, D. B. Kaplan, and A. E. Nelson, Phys. Rev. **D49**, 779 (1994), [hep-ph/9308292](#).
- [93] M. S. Turner, Phys. Rev. **D28**, 1243 (1983).
- [94] S. Hannestad, Phys. Rev. **D70**, 043506 (2004), [astro-ph/0403291](#).
- [95] M. Kawasaki, K. Kohri, and N. Sugiyama, Phys. Rev. **D62**, 023506 (2000), [astro-ph/0002127](#).

- [96] M. Kawasaki, K. Kohri, and N. Sugiyama, Phys. Rev. Lett. **82**, 4168 (1999), [astro-ph/9811437](#).
- [97] F. De Bernardis, L. Pagano, and A. Melchiorri, Astropart. Phys. **30**, 192 (2008).
- [98] O. Loaiza-Brito, J. Martin, H. P. Nilles, and M. Ratz, AIP Conf. Proc. **805**, 198 (2006), [198(2005)], [hep-th/0509158](#).
- [99] G. Jungman, M. Kamionkowski, and K. Griest, Phys. Rept. **267**, 195 (1996), [hep-ph/9506380](#).
- [100] N. Arkani-Hamed, A. Delgado, and G. F. Giudice, Nucl. Phys. **B741**, 108 (2006), [hep-ph/0601041](#).
- [101] T. Moroi, M. Nagai, and M. Takimoto, JHEP **07**, 066 (2013), [1303.0948](#).
- [102] G. Kane, Nature **480**, 415 (2011).
- [103] D. Feldman and P. Sandick, Phys. Lett. **B724**, 241 (2013), [1303.0329](#).
- [104] C. Cheung, L. J. Hall, D. Pinner, and J. T. Ruderman, JHEP **05**, 100 (2013), [1211.4873](#).
- [105] S. Chatrchyan et al. (CMS), JHEP **11**, 147 (2012), [1209.6620](#).
- [106] E. Aprile et al. (XENON100), Phys. Rev. Lett. **109**, 181301 (2012), [1207.5988](#).
- [107] P. Beltrame (XENON), in *Proceedings, 48th Rencontres de Moriond on Electroweak Interactions and Unified Theories: La Thuile, Italy, March 2-9, 2013* (2013), pp. 143–148, [1305.2719](#), URL <https://inspirehep.net/record/1233051/files/arXiv:1305.2719.pdf>.
- [108] D. Hooper, C. Kelso, P. Sandick, and W. Xue, Phys. Rev. **D88**, 015010 (2013), [1304.2417](#).
- [109] R. Easther, R. Flauger, and J. B. Gilmore, JCAP **1104**, 027 (2011), [1003.3011](#).

- [110] J. Fan and M. Reece, JHEP **10**, 124 (2013), [1307.4400](#).
- [111] A. Abramowski et al. (H.E.S.S.), Phys. Rev. Lett. **106**, 161301 (2011), [1103.3266](#).
- [112] G. F. Giudice, M. A. Luty, H. Murayama, and R. Rattazzi, JHEP **12**, 027 (1998), [hep-ph/9810442](#).
- [113] L. Randall and R. Sundrum, Nucl. Phys. **B557**, 79 (1999), [hep-th/9810155](#).
- [114] K. Choi, A. Falkowski, H. P. Nilles, and M. Olechowski, Nucl. Phys. **B718**, 113 (2005), [hep-th/0503216](#).
- [115] K. Choi, K. S. Jeong, and K.-i. Okumura, JHEP **09**, 039 (2005), [hep-ph/0504037](#).
- [116] J. P. Conlon and F. Quevedo, JHEP **06**, 029 (2006), [hep-th/0605141](#).
- [117] J. P. Conlon, S. S. Abdussalam, F. Quevedo, and K. Suruliz, JHEP **01**, 032 (2007), [hep-th/0610129](#).
- [118] B. S. Acharya, K. Bobkov, G. L. Kane, P. Kumar, and J. Shao, Phys. Rev. **D76**, 126010 (2007), [hep-th/0701034](#).
- [119] B. S. Acharya, K. Bobkov, G. L. Kane, J. Shao, and P. Kumar, Phys. Rev. **D78**, 065038 (2008), [0801.0478](#).
- [120] J. D. Wells, in *11th International Conference on Supersymmetry and the Unification of Fundamental Interactions (SUSY 2003) Tucson, Arizona, June 5-10, 2003* (2003), [hep-ph/0306127](#).
- [121] N. Arkani-Hamed and S. Dimopoulos, JHEP **06**, 073 (2005), [hep-th/0405159](#).
- [122] N. Arkani-Hamed, S. Dimopoulos, G. F. Giudice, and A. Romanino, Nucl. Phys. **B709**, 3 (2005), [hep-ph/0409232](#).

- [123] G. F. Giudice and A. Romanino, Nucl. Phys. **B699**, 65 (2004), [Erratum: Nucl. Phys. **B706**, 487(2005)], [hep-ph/0406088](#).
- [124] L. J. Hall and Y. Nomura, JHEP **01**, 082 (2012), [1111.4519](#).
- [125] M. Ibe and T. T. Yanagida, Phys. Lett. **B709**, 374 (2012), [1112.2462](#).
- [126] A. Arvanitaki, N. Craig, S. Dimopoulos, and G. Villadoro, JHEP **02**, 126 (2013), [1210.0555](#).
- [127] L. J. Hall, Y. Nomura, and S. Shirai, JHEP **01**, 036 (2013), [1210.2395](#).
- [128] L. J. Hall and Y. Nomura, JHEP **02**, 129 (2014), [1312.6695](#).
- [129] W. Altmannshofer, R. Harnik, and J. Zupan, JHEP **11**, 202 (2013), [1308.3653](#).
- [130] M. Baumgart, D. Stolarski, and T. Zorawski, Phys. Rev. **D90**, 055001 (2014), [1403.6118](#).
- [131] M. Dhuria and A. Misra, Nucl. Phys. **B867**, 636 (2013), [1207.2774](#).
- [132] T. Cohen, M. Lisanti, A. Pierce, and T. R. Slatyer, JCAP **1310**, 061 (2013), [1307.4082](#).
- [133] P. A. R. Ade et al. (BICEP2), Phys. Rev. Lett. **112**, 241101 (2014), [1403.3985](#).
- [134] K. Harigaya and T. T. Yanagida, Phys. Lett. **B734**, 13 (2014), [1403.4729](#).
- [135] C. Pallis, JCAP **1408**, 057 (2014), [1403.5486](#).
- [136] K. Harigaya, M. Ibe, K. Ichikawa, K. Kaneta, and S. Matsumoto, JHEP **07**, 093 (2014), [1403.5880](#).
- [137] L. E. Ibanez and I. Valenzuela, Phys. Lett. **B734**, 354 (2014), [1403.6081](#).
- [138] N. Craig and D. Green, JHEP **07**, 102 (2014), [1403.7193](#).

- [139] J. Ellis, M. A. G. Garcia, D. V. Nanopoulos, and K. A. Olive, JCAP **1405**, 037 (2014), [1403.7518](#).
- [140] D. H. Lyth, JCAP **1411**, 003 (2014), [1403.7323](#).
- [141] K. Hamaguchi, T. Moroi, and T. Terada, Phys. Lett. **B733**, 305 (2014), [1403.7521](#).
- [142] L. J. Hall, Y. Nomura, and S. Shirai, JHEP **06**, 137 (2014), [1403.8138](#).
- [143] J. Pradler and F. D. Steffen, Phys. Lett. **B648**, 224 (2007), [hep-ph/0612291](#).
- [144] V. S. Rychkov and A. Strumia, Phys. Rev. **D75**, 075011 (2007), [hep-ph/0701104](#).
- [145] R. Allahverdi, A. Jokinen, and A. Mazumdar, Phys. Rev. **D71**, 043505 (2005), [hep-ph/0410169](#).
- [146] C. Cheung, G. Elor, and L. Hall, Phys. Rev. **D84**, 115021 (2011), [1103.4394](#).
- [147] L. J. Hall, K. Jedamzik, J. March-Russell, and S. M. West, JHEP **03**, 080 (2010), [0911.1120](#).
- [148] C. Cheung, G. Elor, L. J. Hall, and P. Kumar, JHEP **03**, 042 (2011), [1010.0022](#).
- [149] M. Kawasaki, F. Takahashi, and T. T. Yanagida, Phys. Lett. **B638**, 8 (2006), [hep-ph/0603265](#).
- [150] M. Kawasaki, F. Takahashi, and T. T. Yanagida, Phys. Rev. **D74**, 043519 (2006), [hep-ph/0605297](#).
- [151] M. Dine, R. Kitano, A. Morisse, and Y. Shirman, Phys. Rev. **D73**, 123518 (2006), [hep-ph/0604140](#).
- [152] K. Nakayama, F. Takahashi, and T. T. Yanagida, Phys. Lett. **B718**, 526 (2012), [1209.2583](#).

- [153] M. Kawasaki, K. Kohri, T. Moroi, and A. Yotsuyanagi, Phys. Rev. **D78**, 065011 (2008), [0804.3745](#).
- [154] J. Hisano, S. Matsumoto, M. Nagai, O. Saito, and M. Senami, Phys. Lett. **B646**, 34 (2007), [hep-ph/0610249](#).
- [155] A. Hryczuk and R. Iengo, JHEP **01**, 163 (2012), [Erratum: JHEP06,137(2012)], [1111.2916](#).
- [156] A. Hryczuk, Phys. Lett. **B699**, 271 (2011), [1102.4295](#).
- [157] M. Ibe, S. Matsumoto, and R. Sato, Phys. Lett. **B721**, 252 (2013), [1212.5989](#).
- [158] R. Kallosh, A. Linde, K. A. Olive, and T. Rube, Phys. Rev. **D84**, 083519 (2011), [1106.6025](#).
- [159] M. Ackermann et al. (Fermi-LAT), Astrophys. J. Suppl. **203**, 4 (2012), [1206.1896](#).
- [160] M. Ackermann et al. (Fermi-LAT), Phys. Rev. **D88**, 082002 (2013), [1305.5597](#).
- [161] A. Hryczuk, I. Cholis, R. Iengo, M. Tavakoli, and P. Ullio, JCAP **1407**, 031 (2014), [1401.6212](#).
- [162] D. Hooper, C. Kelso, and F. S. Queiroz, Astropart. Phys. **46**, 55 (2013), [1209.3015](#).
- [163] A. Abramowski et al. (H.E.S.S.), Phys. Rev. Lett. **110**, 041301 (2013), [1301.1173](#).
- [164] M. Cirelli, A. Strumia, and M. Tamburini, Nucl. Phys. **B787**, 152 (2007), [0706.4071](#).
- [165] R. Easther, R. Galvez, O. Ozsoy, and S. Watson, Phys. Rev. **D89**, 023522 (2014), [1307.2453](#).

- [166] R. Allahverdi, M. Cicoli, B. Dutta, and K. Sinha, Phys. Rev. **D88**, 095015 (2013), [1307.5086](#).
- [167] V. F. Mukhanov, JETP Lett. **41**, 493 (1985), [Pisma Zh. Eksp. Teor. Fiz.41,402(1985)].
- [168] C. Cheung, P. Creminelli, A. L. Fitzpatrick, J. Kaplan, and L. Senatore, JHEP **03**, 014 (2008), [0709.0293](#).
- [169] D. N. Spergel et al. (WMAP), Astrophys. J. Suppl. **170**, 377 (2007), [astro-ph/0603449](#).
- [170] D. H. Lyth, Phys. Rev. Lett. **78**, 1861 (1997), [hep-ph/9606387](#).
- [171] A. D. Linde, Mod. Phys. Lett. **A1**, 81 (1986).
- [172] A. D. Linde, Phys. Lett. **B175**, 395 (1986).
- [173] K. Freese, J. A. Frieman, and A. V. Olinto, Phys. Rev. Lett. **65**, 3233 (1990).
- [174] K. Harigaya, M. Ibe, K. Schmitz, and T. T. Yanagida, Phys. Lett. **B733**, 283 (2014), [1403.4536](#).
- [175] K. Freese and W. H. Kinney, JCAP **1503**, 044 (2015), [1403.5277](#).
- [176] B. A. Bassett, S. Tsujikawa, and D. Wands, Rev. Mod. Phys. **78**, 537 (2006), [astro-ph/0507632](#).
- [177] R. Kallosh, L. Kofman, A. D. Linde, and A. Van Proeyen, Phys. Rev. **D61**, 103503 (2000), [hep-th/9907124](#).
- [178] G. F. Giudice, A. Riotto, and I. Tkachev, JHEP **11**, 036 (1999), [hep-ph/9911302](#).



- [179] R. Kallosh, L. Kofman, A. D. Linde, and A. Van Proeyen, *Class. Quant. Grav.* **17**, 4269 (2000), [Erratum: *Class. Quant. Grav.*21,5017(2004)], [hep-th/0006179](#).
- [180] A. L. Maroto and A. Mazumdar, *Phys. Rev. Lett.* **84**, 1655 (2000), [hep-ph/9904206](#).
- [181] H. P. Nilles, M. Peloso, and L. Sorbo, *JHEP* **04**, 004 (2001), [hep-th/0103202](#).
- [182] H. P. Nilles, M. Peloso, and L. Sorbo, *Phys. Rev. Lett.* **87**, 051302 (2001), [hep-ph/0102264](#).
- [183] P. B. Greene, K. Kadota, and H. Murayama, *Phys. Rev.* **D68**, 043502 (2003), [hep-ph/0208276](#).
- [184] J. R. Ellis, C. Kounnas, and D. V. Nanopoulos, *Nucl. Phys.* **B247**, 373 (1984).
- [185] J. Scherk and J. H. Schwarz, *Nucl. Phys.* **B153**, 61 (1979).
- [186] G. F. Giudice, A. Notari, M. Raidal, A. Riotto, and A. Strumia, *Nucl. Phys.* **B685**, 89 (2004), [hep-ph/0310123](#).
- [187] M. Kamionkowski and J. March-Russell, *Phys. Lett.* **B282**, 137 (1992), [hep-th/9202003](#).
- [188] G. D. Kribs, A. Martin, and A. Menon, *Phys. Rev.* **D88**, 035025 (2013), [1305.1313](#).
- [189] A. Arvanitaki, M. Baryakhtar, X. Huang, K. van Tilburg, and G. Villadoro, *JHEP* **03**, 022 (2014), [1309.3568](#).
- [190] J. A. Evans, Y. Kats, D. Shih, and M. J. Strassler, *JHEP* **07**, 101 (2014), [1310.5758](#).
- [191] J. Fan and M. Reece, *JHEP* **06**, 031 (2014), [1401.7671](#).

- [192] T. Gherghetta, B. von Harling, A. D. Medina, and M. A. Schmidt, JHEP **04**, 180 (2014), [1401.8291](#).
- [193] L. Iliesiu, D. J. E. Marsh, K. Moodley, and S. Watson, Phys. Rev. **D89**, 103513 (2014), [1312.3636](#).
- [194] A. L. Erickcek and K. Sigurdson, Phys. Rev. **D84**, 083503 (2011), [1106.0536](#).
- [195] G. Arcadi and P. Ullio, Phys. Rev. **D84**, 043520 (2011), [1104.3591](#).
- [196] G. F. Giudice, E. W. Kolb, and A. Riotto, Phys. Rev. **D64**, 023508 (2001), [hep-ph/0005123](#).
- [197] M. Lemoine, J. Martin, and J. Yokoyama, Phys. Rev. **D80**, 123514 (2009), [0904.0126](#).
- [198] R. H. Brandenberger, H. Feldman, V. F. Mukhanov, and T. Prokopec, in *The Origin of Structure in the Universe Chateau de Pont d'Oye, Belgium, April 27-May 2, 1992* (1992), pp. 0013–32.
- [199] A. Loeb and M. Zaldarriaga, Phys. Rev. **D71**, 103520 (2005), [astro-ph/0504112](#).
- [200] C. Boehm, P. Fayet, and R. Schaeffer, Phys. Lett. **B518**, 8 (2001), [astro-ph/0012504](#).
- [201] X.-l. Chen, M. Kamionkowski, and X.-m. Zhang, Phys. Rev. **D64**, 021302 (2001), [astro-ph/0103452](#).
- [202] S. Hofmann, D. J. Schwarz, and H. Stoecker, Phys. Rev. **D64**, 083507 (2001), [astro-ph/0104173](#).
- [203] E. Bertschinger, Phys. Rev. **D74**, 063509 (2006), [astro-ph/0607319](#).

- [204] A. M. Green, S. Hofmann, and D. J. Schwarz, *Mon. Not. Roy. Astron. Soc.* **353**, L23 (2004), [astro-ph/0309621](#).
- [205] A. M. Green, S. Hofmann, and D. J. Schwarz, *JCAP* **0508**, 003 (2005), [astro-ph/0503387](#).
- [206] A. Boyarsky, J. Lesgourgues, O. Ruchayskiy, and M. Viel, *JCAP* **0905**, 012 (2009), [0812.0010](#).
- [207] W. B. Lin, D. H. Huang, X. Zhang, and R. H. Brandenberger, *Phys. Rev. Lett.* **86**, 954 (2001), [astro-ph/0009003](#).
- [208] B. Bhattacharjee, M. Ibe, K. Ichikawa, S. Matsumoto, and K. Nishiyama, *JHEP* **07**, 080 (2014), [1405.4914](#).
- [209] J. Hisano, K. Kohri, and M. M. Nojiri, *Phys. Lett.* **B505**, 169 (2001), [hep-ph/0011216](#).
- [210] A. D. Linde, *Contemp. Concepts Phys.* **5**, 1 (1990), [hep-th/0503203](#).
- [211] K. A. Malik and D. Wands, *JCAP* **0502**, 007 (2005), [astro-ph/0411703](#).
- [212] D. Baumann et al. (CMBPol Study Team), *AIP Conf. Proc.* **1141**, 10 (2009), [0811.3919](#).
- [213] L. Senatore, E. Silverstein, and M. Zaldarriaga, *JCAP* **1408**, 016 (2014), [1109.0542](#).
- [214] N. Barnaby, J. Moxon, R. Namba, M. Peloso, G. Shiu, and P. Zhou, *Phys. Rev.* **D86**, 103508 (2012), [1206.6117](#).
- [215] N. Barnaby, R. Namba, and M. Peloso, *Phys. Rev.* **D85**, 123523 (2012), [1202.1469](#).

- [216] N. Barnaby, E. Pajer, and M. Peloso, Phys. Rev. **D85**, 023525 (2012), [1110.3327](#).
- [217] N. Barnaby, R. Namba, and M. Peloso, JCAP **1104**, 009 (2011), [1102.4333](#).
- [218] N. Barnaby and Z. Huang, Phys. Rev. **D80**, 126018 (2009), [0909.0751](#).
- [219] J. L. Cook and L. Sorbo, JCAP **1311**, 047 (2013), [1307.7077](#).
- [220] J. L. Cook and L. Sorbo, Phys. Rev. **D85**, 023534 (2012), [Erratum: Phys. Rev.D86,069901(2012)], [1109.0022](#).
- [221] C. Caprini and L. Sorbo, JCAP **1410**, 056 (2014), [1407.2809](#).
- [222] L. Sorbo, JCAP **1106**, 003 (2011), [1101.1525](#).
- [223] D. Carney, W. Fischler, E. D. Kovetz, D. Lorshbough, and S. Paban, JHEP **11**, 042 (2012), [1209.3848](#).
- [224] E. Pajer and M. Peloso, Class. Quant. Grav. **30**, 214002 (2013), [1305.3557](#).
- [225] M. A. Fedderke, E. W. Kolb, and M. Wyman, Phys. Rev. **D91**, 063505 (2015), [1409.1584](#).
- [226] L. Kofman, A. D. Linde, X. Liu, A. Maloney, L. McAllister, and E. Silverstein, JHEP **05**, 030 (2004), [hep-th/0403001](#).
- [227] S. Watson, Phys. Rev. **D70**, 066005 (2004), [hep-th/0404177](#).
- [228] D. Green, B. Horn, L. Senatore, and E. Silverstein, Phys. Rev. **D80**, 063533 (2009), [0902.1006](#).
- [229] R. Z. Ferreira and M. S. Sloth, JHEP **12**, 139 (2014), [1409.5799](#).
- [230] C. W. Misner, K. S. Thorne, and J. A. Wheeler, *Gravitation* (W. H. Freeman, San Francisco, 1973).

- [231] D. Baumann and L. McAllister, *Inflation and String Theory* (Cambridge University Press, 2015), ISBN 9781107089693, 9781316237182, [1404.2601](#), URL <https://inspirehep.net/record/1289899/files/arXiv:1404.2601.pdf>.
- [232] J. F. Dufaux, A. Bergman, G. N. Felder, L. Kofman, and J.-P. Uzan, *Phys. Rev.* **D76**, 123517 (2007), [0707.0875](#).
- [233] S. S. Gubser, *Phys. Rev.* **D69**, 123507 (2004), [hep-th/0305099](#).
- [234] S. Cremonini and S. Watson, *Phys. Rev.* **D73**, 086007 (2006), [hep-th/0601082](#).
- [235] B. Greene, S. Judes, J. Levin, S. Watson, and A. Weltman, *JHEP* **07**, 060 (2007), [hep-th/0702220](#).
- [236] X. Dong, B. Horn, E. Silverstein, and A. Westphal, *Phys. Rev.* **D84**, 026011 (2011), [1011.4521](#).
- [237] E. Silverstein and D. Tong, *Phys. Rev.* **D70**, 103505 (2004), [hep-th/0310221](#).
- [238] A. Avgoustidis, S. Cremonini, A.-C. Davis, R. H. Ribeiro, K. Turzynski, and S. Watson, *JCAP* **1206**, 025 (2012), [1203.0016](#).
- [239] S. Weinberg, *Gravitation and Cosmology* (John Wiley and Sons, New York, 1972), ISBN 0471925675, 9780471925675, URL <http://www-spines.fnal.gov/spines/find/books/www?cl=QC6.W431>.
- [240] F. C. Adams, J. R. Bond, K. Freese, J. A. Frieman, and A. V. Olinto, *Phys. Rev.* **D47**, 426 (1993), [hep-ph/9207245](#).
- [241] P. Svrcek and E. Witten, *JHEP* **06**, 051 (2006), [hep-th/0605206](#).
- [242] L. McAllister, E. Silverstein, A. Westphal, and T. Wrase, *JHEP* **09**, 123 (2014), [1405.3652](#).
- [243] N. Barnaby and M. Peloso, *Phys. Rev. Lett.* **106**, 181301 (2011), [1011.1500](#).

- [244] S. Mukohyama, R. Namba, M. Peloso, and G. Shiu, JCAP **1408**, 036 (2014), [1405.0346](#).
- [245] J. Polchinski, *String theory. Vol. 2: Superstring theory and beyond* (Cambridge University Press, 2007), ISBN 9780511252280, 9780521633048, 9780521672283.
- [246] L. McAllister, E. Silverstein, and A. Westphal, Phys. Rev. **D82**, 046003 (2010), [0808.0706](#).
- [247] M. Cicoli, M. Goodsell, and A. Ringwald, JHEP **10**, 146 (2012), [1206.0819](#).
- [248] T. W. Grimm and J. Louis, Nucl. Phys. **B699**, 387 (2004), [hep-th/0403067](#).
- [249] E. Witten, Nucl. Phys. **B403**, 159 (1993), [AMS/IP Stud. Adv. Math.1,143(1996)], [hep-th/9301042](#).
- [250] D.-E. Diaconescu, A. Garcia-Raboso, R. L. Karp, and K. Sinha, Adv. Theor. Math. Phys. **11**, 471 (2007), [hep-th/0606180](#).
- [251] R. Flauger, L. McAllister, E. Pajer, A. Westphal, and G. Xu, JCAP **1006**, 009 (2010), [0907.2916](#).
- [252] D.-E. Diaconescu, A. Garcia-Raboso, and K. Sinha, JHEP **06**, 058 (2006), [hep-th/0602138](#).
- [253] J. P. Conlon, JCAP **1201**, 033 (2012), [1110.6454](#).
- [254] M. Berg, E. Pajer, and S. Sjors, Phys. Rev. **D81**, 103535 (2010), [0912.1341](#).
- [255] R. Blumenhagen and E. Plauschinn, Phys. Lett. **B736**, 482 (2014), [1404.3542](#).
- [256] S. Panda, Y. Sumitomo, and S. P. Trivedi, Phys. Rev. **D83**, 083506 (2011), [1011.5877](#).
- [257] R. Blumenhagen, M. Cvetič, P. Langacker, and G. Shiu, Ann. Rev. Nucl. Part. Sci. **55**, 71 (2005), [hep-th/0502005](#).

- [258] R. Blumenhagen, D. Lust, and T. R. Taylor, Nucl. Phys. **B663**, 319 (2003), [hep-th/0303016](#).
- [259] J. F. G. Cascales and A. M. Uranga, JHEP **05**, 011 (2003), [hep-th/0303024](#).
- [260] A. Font and L. E. Ibanez, JHEP **03**, 040 (2005), [hep-th/0412150](#).
- [261] M. Cvetič, T. Li, and T. Liu, Phys. Rev. **D71**, 106008 (2005), [hep-th/0501041](#).
- [262] F. Marchesano and G. Shiu, JHEP **11**, 041 (2004), [hep-th/0409132](#).
- [263] C. P. Burgess, R. Kallosh, and F. Quevedo, JHEP **10**, 056 (2003), [hep-th/0309187](#).
- [264] S. B. Giddings, S. Kachru, and J. Polchinski, Phys. Rev. **D66**, 106006 (2002), [hep-th/0105097](#).
- [265] S. Kachru, R. Kallosh, A. D. Linde, and S. P. Trivedi, Phys. Rev. **D68**, 046005 (2003), [hep-th/0301240](#).
- [266] W. Lerche, P. Mayr, and N. Warner (2002), [hep-th/0208039](#).
- [267] W. Lerche, P. Mayr, and N. Warner (2002), [hep-th/0207259](#).
- [268] T. W. Grimm, T.-W. Ha, A. Klemm, and D. Klevers, JHEP **04**, 015 (2010), [0909.2025](#).
- [269] T. W. Grimm, T.-W. Ha, A. Klemm, and D. Klevers, Nucl. Phys. **B816**, 139 (2009), [0811.2996](#).
- [270] S. Kachru, R. Kallosh, A. D. Linde, J. M. Maldacena, L. P. McAllister, and S. P. Trivedi, JCAP **0310**, 013 (2003), [hep-th/0308055](#).
- [271] Y.-H. He, Int. J. Mod. Phys. **A28**, 1330032 (2013), [1308.0186](#).
- [272] M. R. Douglas, B. Fiol, and C. Romelsberger, JHEP **09**, 057 (2005), [hep-th/0003263](#).

- [273] T. Bridgeland, *Annals of Mathematics* pp. 317–345 (2007).
- [274] T. Bridgeland, *Communications in mathematical physics* **266**, 715 (2006).
- [275] K. Becker, M. Becker, M. Haack, and J. Louis, *JHEP* **06**, 060 (2002), [hep-th/0204254](#).
- [276] R. Kallosh and A. D. Linde, *JHEP* **12**, 004 (2004), [hep-th/0411011](#).
- [277] L. F. Abbott, E. Farhi, and M. B. Wise, *Phys. Lett.* **B117**, 29 (1982).
- [278] A. Albrecht, P. J. Steinhardt, M. S. Turner, and F. Wilczek, *Phys. Rev. Lett.* **48**, 1437 (1982).
- [279] A. D. Dolgov and A. D. Linde, *Phys. Lett.* **B116**, 329 (1982).
- [280] A. D. Dolgov and D. P. Kirilova, *Sov. J. Nucl. Phys.* **51**, 172 (1990), [*Yad. Fiz.*51,273(1990)].
- [281] J. H. Traschen and R. H. Brandenberger, *Phys. Rev.* **D42**, 2491 (1990).
- [282] R. Allahverdi, R. Brandenberger, F.-Y. Cyr-Racine, and A. Mazumdar, *Ann. Rev. Nucl. Part. Sci.* **60**, 27 (2010), [1001.2600](#).
- [283] S. Yu. Khlebnikov and I. I. Tkachev, *Phys. Rev. Lett.* **77**, 219 (1996), [hep-ph/9603378](#).
- [284] R. Easther and E. A. Lim, *JCAP* **0604**, 010 (2006), [astro-ph/0601617](#).
- [285] J. Garcia-Bellido and A. D. Linde, *Phys. Rev.* **D57**, 6075 (1998), [hep-ph/9711360](#).
- [286] G. N. Felder, J. Garcia-Bellido, P. B. Greene, L. Kofman, A. D. Linde, and I. Tkachev, *Phys. Rev. Lett.* **87**, 011601 (2001), [hep-ph/0012142](#).
- [287] R. Easther, J. T. Giblin, Jr., and E. A. Lim, *Phys. Rev. Lett.* **99**, 221301 (2007), [astro-ph/0612294](#).



- [288] L. R. Price and X. Siemens, Phys. Rev. **D78**, 063541 (2008), [0805.3570](#).
- [289] R. Easther, H. Finkel, and N. Roth, JCAP **1010**, 025 (2010), [1005.1921](#).
- [290] M. P. Hertzberg, J. Karouby, W. G. Spitzer, J. C. Becerra, and L. Li, Phys. Rev. **D90**, 123528 (2014), [1408.1396](#).
- [291] M. A. Amin and D. Baumann, JCAP **1602**, 045 (2016), [1512.02637](#).
- [292] O. Ozsoy, G. Sengor, K. Sinha, and S. Watson (2015), [1507.06651](#).
- [293] S. Weinberg, Phys. Rev. **D77**, 123541 (2008), [0804.4291](#).
- [294] M. Park, K. M. Zurek, and S. Watson, Phys. Rev. **D81**, 124008 (2010), [1003.1722](#).
- [295] P. Creminelli, M. A. Luty, A. Nicolis, and L. Senatore, JHEP **12**, 080 (2006), [hep-th/0606090](#).
- [296] L. Senatore and M. Zaldarriaga, JHEP **04**, 024 (2012), [1009.2093](#).
- [297] P. Creminelli, G. D'Amico, J. Norena, and F. Vernizzi, JCAP **0902**, 018 (2009), [0811.0827](#).
- [298] J. K. Bloomfield, . . Flanagan, M. Park, and S. Watson, JCAP **1308**, 010 (2013), [1211.7054](#).
- [299] G. Gubitosi, F. Piazza, and F. Vernizzi, JCAP **1302**, 032 (2013), [JCAP1302,032(2013)], [1210.0201](#).
- [300] M. Fasiello and Z. Vlah, Phys. Rev. **D94**, 063516 (2016), [1604.04612](#).
- [301] M. Fasiello and Z. Vlah (2016), [1611.00542](#).
- [302] M. Lewandowski, A. Maleknejad, and L. Senatore (2016), [1611.07966](#).

- [303] D. Baumann, A. Nicolis, L. Senatore, and M. Zaldarriaga, JCAP **1207**, 051 (2012), [1004.2488](#).
- [304] L. Kofman and P. Yi, Phys. Rev. **D72**, 106001 (2005), [hep-th/0507257](#).
- [305] D. R. Green, Phys. Rev. **D76**, 103504 (2007), [0707.3832](#).
- [306] G. N. Felder, L. Kofman, and A. D. Linde, Phys. Rev. **D59**, 123523 (1999), [hep-ph/9812289](#).
- [307] V. Assassi, D. Baumann, D. Green, and L. McAllister, JCAP **1401**, 033 (2014), [1304.5226](#).
- [308] A. Adams, N. Arkani-Hamed, S. Dubovsky, A. Nicolis, and R. Rattazzi, JHEP **10**, 014 (2006), [hep-th/0602178](#).
- [309] D. A. Easson and A. Vikman (2016), [1607.00996](#).
- [310] X. Chen and Y. Wang, JCAP **1004**, 027 (2010), [0911.3380](#).
- [311] S. Cremonini, Z. Lalak, and K. Turzynski, JCAP **1103**, 016 (2011), [1010.3021](#).
- [312] A. Achucarro, J.-O. Gong, S. Hardeman, G. A. Palma, and S. P. Patil, JCAP **1101**, 030 (2011), [1010.3693](#).
- [313] A. J. Tolley and M. Wyman, Phys. Rev. **D81**, 043502 (2010), [0910.1853](#).
- [314] G. Shiu and J. Xu, Phys. Rev. **D84**, 103509 (2011), [1108.0981](#).
- [315] C. P. Burgess, M. W. Horbatsch, and S. Patil, JHEP **01**, 133 (2013), [1209.5701](#).
- [316] D. Baumann and D. Green, JCAP **1109**, 014 (2011), [1102.5343](#).
- [317] C. Armendariz-Picon, M. Trodden, and E. J. West, JCAP **0804**, 036 (2008), [0707.2177](#).

- [318] N. Arkani-Hamed, H.-C. Cheng, P. Creminelli, and L. Randall, JCAP **0307**, 003 (2003), [hep-th/0302034](#).
- [319] S. Dimopoulos, S. Kachru, J. McGreevy, and J. G. Wacker, JCAP **0808**, 003 (2008), [hep-th/0507205](#).
- [320] N. Vogt-Nilsen, Tech. Rep., Illinois. Univ., Urbana; Midwestern Universities Research Assn., Urbana, Ill. (1956).
- [321] B. R. Greene, T. Prokopec, and T. G. Roos, Phys. Rev. **D56**, 6484 (1997).
- [322] M. Amin, *FloqEx*, <http://mustafa-amin.com/home/codes/>.
- [323] M. A. Amin, R. Easther, H. Finkel, R. Flauger, and M. P. Hertzberg, Phys. Rev. Lett. **108**, 241302 (2012), [1106.3335](#).
- [324] P. Adshead, Y. Cui, and J. Shelton, JHEP **06**, 016 (2016), [1604.02458](#).
- [325] E. V. Linder, G. Sengr, and S. Watson, JCAP **1605**, 053 (2016), [1512.06180](#).
- [326] C. Cheung, A. L. Fitzpatrick, J. Kaplan, and L. Senatore, JCAP **0802**, 021 (2008), [0709.0295](#).
- [327] S. Weinberg, Phys. Rev. **D67**, 123504 (2003), [astro-ph/0302326](#).
- [328] F. Piazza and F. Vernizzi, Class. Quant. Grav. **30**, 214007 (2013), [1307.4350](#).
- [329] T. Noumi, M. Yamaguchi, and D. Yokoyama, JHEP **06**, 051 (2013), [1211.1624](#).
- [330] H. L. Child, J. T. Giblin, Jr, R. H. Ribeiro, and D. Seery, Phys. Rev. Lett. **111**, 051301 (2013), [1305.0561](#).
- [331] C. de Rham, Living Rev. Rel. **17**, 7 (2014), [1401.4173](#).
- [332] Y.-F. Cai, S. Lin, J. Liu, and J.-R. Sun (2016), [1612.04394](#).
- [333] Y.-F. Cai, S. Lin, J. Liu, and J.-R. Sun (2016), [1612.04377](#).

- [334] M. C. Johnson and M. Kamionkowski, Phys. Rev. **D78**, 063010 (2008), [0805.1748](#).
- [335] J. S. Bains, M. P. Hertzberg, and F. Wilczek (2015), [1512.02304](#).
- [336] S. R. Behbahani, A. Dymarsky, M. Mirbabayi, and L. Senatore, JCAP **1212**, 036 (2012), [1111.3373](#).
- [337] C. P. Burgess, Living Rev. Rel. **7**, 5 (2004), [gr-qc/0311082](#).
- [338] V. Mukhanov, *Physical Foundations of Cosmology* (Cambridge University Press, Oxford, 2005), ISBN 0521563984, 9780521563987, URL <http://www-spires.fnal.gov/spires/find/books/www?cl=QB981.M89::2005>.
- [339] K. Jedamzik, M. Lemoine, and J. Martin, JCAP **1004**, 021 (2010), [1002.3278](#).
- [340] J. F. Dufaux, G. N. Felder, L. Kofman, M. Peloso, and D. Podolsky, JCAP **0607**, 006 (2006), [hep-ph/0602144](#).
- [341] J. T. Giblin and E. Thrane, Phys. Rev. **D90**, 107502 (2014), [1410.4779](#).
- [342] D. G. Figueroa and F. Torrenti, JCAP **1702**, 001 (2017), [1609.05197](#).
- [343] K. D. Lozanov and M. A. Amin (2016), [1608.01213](#).
- [344] D. Lopez Nacir, R. A. Porto, L. Senatore, and M. Zaldarriaga, JHEP **01**, 075 (2012), [1109.4192](#).
- [345] D. Green, JCAP **1503**, 020 (2015), [1409.6698](#).

# Curriculum Vitae

## Ogan Ozsoy

Department of Physics, Syracuse University,  
Physics Building, Room: 363, Syracuse, NY 13244

*Phone:* (315) 380-9075 *Fax:* (315) 443-9103

*Email:* oozsoy@syr.edu

*Homepage:* oozsoy.expressions.syr.edu

---

### Education

---

- Ph.D. Candidate in Physics, Syracuse University, Expected Date: May 2017  
Advisor: Prof. Scott Watson
- Master of Science in Physics, Bogazici University, Istanbul, Turkey, 2011  
Dissertation: *Cosmological Perturbations in String Gas Cosmology*  
Advisor : Prof. Ali Kaya
- Bachelor of Science in Physics with distinction,  
Istanbul Technical University, Istanbul, Turkey, 2009  
Dissertation: *Solar System Tests of General Relativity*

---

### Awards and Honors

---

- Visiting Graduate Fellows Award, Fall 2015  
*Delta Institute of Theoretical Physics (D-ITP), University of Amsterdam, Amsterdam, Netherlands*

- Best Student Talk on High Energy Frontiers  
*Phenomenology Symposium, 2014, Pittsburgh University, Pittsburgh, PA*
  - Dean's Honor List for excellence in undergraduate studies, 2005-2009  
*Istanbul Technical University, Istanbul, Turkey*
- 

## Invited Seminars

---

- Bogazici University, July 2016, Theoretical Cosmology and High Energy Seminar, Istanbul, Turkey  
*Title: "Alternative Sources of Gravitational Waves"*
- 

## Talks at Conferences and Workshops

---

- New Frontiers in Fields and Strings (TASI 2015), June 2015, Boulder, CO  
*Title : Primordial Gravitational Waves and the Scale of Inflation*
- Phenomenology Symposium 2015, University of Pittsburgh, Pittsburgh, PA  
*Title : Synthetic Gravitational Waves and the Scale of Inflation*
- Neighborhood Workshop on Astrophysics and Cosmology 2015, Penn State University, State College, PA  
*Title: How Well Can We Really Determine the Scale of Inflation ?*
- Summer School on Cosmology 2014, ICTP, Trieste, Italy  
*Title: Towards establishing the post-inflationary Universe*
- Phenomenology Symposium 2014, University of Pittsburgh, Pittsburgh, PA  
*Title: Heavy Gravitino and Split SUSY in the light of BICEP2*

- High Energy and Cosmology Seminar, November 2013, Syracuse University, Syracuse, NY

*Title: Non-thermal histories and implications for sub-structure formation*

- 15th East Coast Gravity Meeting, April 2012, Syracuse University, Syracuse, NY

*Title: Alternatives of Inflation*

---

## **Schools, Workshops, Conferences, and Extended Visits**

---

- Utrecht Cosmology Symposium (UCoS) 2016, June 27-July 1, Utrecht, Netherlands
- Visitor, Delta ITP, University of Amsterdam, Amsterdam, Netherlands
- Visitor, Bogazici University, Istanbul, Turkey
- New Frontiers in Fields and Strings (TASI 2015), June 2015, Boulder, CO
- Phenomenology Symposium 2015, University of Pittsburgh, Pittsburgh, PA
- Neighborhood Workshop on Astrophysics and Cosmology 2015, Penn State University, State College, PA
- Summer School on Cosmology 2014, ICTP, Trieste, Italy
- Phenomenology Symposium 2014, University of Pittsburgh, Pittsburgh, PA
- 15th East Coast Gravity Meeting, April 2012, Syracuse University, Syracuse, NY
- Northeast Cosmology Meeting, McGill University, Montreal, QC, Canada

---

## Other Academic Experience

---

### **Teaching Assistant, Syracuse University, Syracuse, NY, 2011-Present**

*Courses included: Electricity and Magnetism, Stars, Galaxies and Universe, Introduction to Modern Physics*

Graded all written work, assisted with labs and held problem solving sessions.

### **Teaching Assistant, Bogazici University, Istanbul, Turkey, 2010-2011**

*Courses included: Introduction to Physics, Advanced Statistical Mechanics*

Graded all written work including final exams and assisted with labs.

---

## Programming Skills

---

- *Numerical:* Experience in Boltzmann codes in Python and Fortran.  
Experience with GABE: A C++ code based on lattice field theory methods to simulate the dynamics at the end of inflation
  - *Analytical:* Extensive Experience in Mathematica
- 

## Outreach

---

**Undergraduate Research Day, 2015, Syracuse University,**

*Participated in the organization of an important undergraduate recruitment event.*

**Quora Writer, 2017-,**

*Occasionally, I wrote answers in quora.com for physics related questions*



---

## Professional References

---

**Scott Watson**, Associate Professor, Syracuse University, Syracuse, NY, 13244

*E-mail:* gswatson@syr.edu

**JiJi Fan**, Assistant Professor, Brown University, Providence, RI, 02912

*E-mail:* jiji\_fan@brown.edu

**Jan Pieter van der Schaar**, Assistant Professor, University of Amsterdam, Amsterdam, Netherlands

*E-mail:* j.p.vanderschaar@uva.nl

**Cristian Armendariz-Picon**, Associate Professor, St. Lawrence University, Canton, NY, 13617

*E-mail:* carmendarizpicon@syr.edu

**Jay Hubisz**, Assistant Professor, Syracuse University, Syracuse, NY, 13244

*E-mail:* jhubisz@syr.edu

---

## Publications

---

1. O. Ozsoy, J.T. Giblin, E. Nesbit, G. Sengor and S. Watson, “Toward an Effective Field Theory Approach to Reheating,” [arXiv:1701.01456 [hep-ph]].
2. O. Ozsoy, G. Sengor, K. Sinha and S. Watson, “A Model Independent Approach to (p)Reheating,” [arXiv:1507.06651 [hep-th]].
3. O. Ozsoy, K. Sinha and S. Watson, “How Well Can We Really Determine the Scale of Inflation?,” *Phys. Rev. D* **91**, no. 10, 103509 (2015), [arXiv:1410.0016 [hep-th]].
4. J. Fan, O. Ozsoy and S. Watson, “Nonthermal histories and implications for

structure formation,” Phys. Rev. D **90** (2014) no.4, 043536, [arXiv:1405.7373 [hep-ph]].

5. J. Fan, B. Jain and O. Ozsoy, “Heavy Gravitino and Split SUSY in the Light of BICEP2,” JHEP **1407**, 073 (2014), [arXiv:1404.1914 [hep-ph]]
6. R. Easther, R. Galvez, O. Ozsoy and S. Watson, “Supersymmetry, Nonthermal Dark Matter and Precision Cosmology,” Phys. Rev. D **89**, no. 2, 023522 (2014), [arXiv:1307.2453 [hep-ph]].